Modelling Biota-Sediment Interactions in Estuarine Environments

This research was developed in the context of the innovation program Building with Nature, aimed to integrate the functionality of wet infrastructure with the creation of opportunities for nature and society. Building with Nature is founded from different sources, among which the Subsidieregeling Innovatieketen Water (sponsored by the Netherlands Ministry of Infrastructure and Environment), the Ecoshape consortium, the European Fund for Regional Development and the Municipality of Dordrecht.

Cover design: Proefschriftmaken.nl - Uitgeverij BOXPress
Printed by: Proefschriftmaken.nl - Uitgeverij BOXPress
Published by: Uitgeverij BOXPress, 's-Hertogenbosch

Cover illustration: Gurzo playing on the mudflat, by Fabrizio De Tommaso

ISBN: 978-94-6295-433-5

Copyright © 2016 Francesco Cozzoli. All rights reserved.

Modelling Biota-Sediment Interactions in Estuarine Environments

(met een samenvatting in het Nederlands)

Proefschrift

ter verkrijging van de graad van doctor
aan de Radboud Universiteit Nijmegen
op gezag van de rector magnificus
volgens besluit van het college van decanen
in het openbaar te verdedigen op
vrijdag 12 februari 2016
om 10.30 uur precies

door

Francesco Cozzoli

geboren op 9 september 1985
Brindisi, Italië

De promotiecommissie bestaat uit:

Fungerend rector:
prof. dr. A.M. Breure

Promotor:
prof. dr. P.M.J. Herman

Copromotoren:
dr. T.Y. Ysebaert
prof. dr. T. Bouma

Leden manuscriptcommissie:
prof. dr. ir. A.J. Hendriks
prof. dr. P. Meire
prof. dr. J.C. Winterwerp

Overige leden:
prof. dr. J.H. de Vriend
dr. C. Van Colen
dr. M. Baptist
prof. dr. Z.B. Wang

“It is probably true that in the history of human thinking the most fruitful developments frequently take place at those points where two different lines of thought meet. These lines may have their roots in quite different parts of human culture, in different times or different cultural environments or different religious traditions: hence if they actually meet, that is, if they are at least so much related to each other that a real interaction can take place, then one may hope that new and interesting developments may follow."

Werner Heisenberg

Contents

List of Tables xi

List of Figures xv

1 Introduction 1

- 1.1 The estuarine environment 1
  - 1.1.1 The physical environment: tides, salt and sediment . . . 2
  - 1.1.2 The biotic environment 3
  - 1.1.3 Humans and estuaries 5
  - 1.1.4 BwN: Thinking, Acting and Interacting differently . . . 8
- 1.2 Niche filtering *vs.* Ecosystem engineering 8
- 1.3 Sediment transport as biotic-physical feedback 10
- 1.4 Thesis Outline 12
  - 1.4.1 Rationale 12
  - 1.4.2 Structure 13

2 An application of non-linear quantile regression to macrozoobenthic species distribution modeling: comparing two contrasting basins 15

- 2.1 Introduction 16
- 2.2 Material and methods 19
  - 2.2.1 Study area 19
  - 2.2.2 Sampling and data processing 21
  - 2.2.3 Data analysis 21
- 2.3 Results 23
  - 2.3.1 Abiotic variables 23
  - 2.3.2 Biotic variables: 24
  - 2.3.3 Non-linear quantile regression 26
- 2.4 Discussion 30
  - 2.4.1 Considerations about the statistical method 30
  - 2.4.2 Community responses across basins 31

2.4.3 Individual taxa responses across basins 32
2.4.4 Management considerations 33
2.5 Conclusions 34

3 A mixed modeling approach to predict the effect of environmental modification on species distributions 37
3.1 Introduction 38
3.2 Material and methods 40
3.2.1 Study area 40
3.2.2 Environmental variables 42
3.2.3 Biotic variables 42
3.2.4 Model fitting and validation 44
3.3 Results 46
3.4 Discussion 50
3.4.1 Considerations about the modeling methodology 51
3.4.2 Comparison with previous estimates 53
3.4.3 Temporal trends in the Oosterschelde 56
3.5 Conclusion 57

4 Coastal defense *vs.* Enhanced navigability: how management affects benthic habitat quality. 59
4.1 Introduction 60
4.2 Material and methods 63
4.2.1 Study area 63
4.2.2 Hydrodynamic variables 64
4.2.3 Ecological variables 65
4.2.4 Predicting benthic communities: upper boundary regression models 66
4.3 Results 67
4.4 Discussion 68

5 Modeling benthic habitat suitability to evaluate ecological benefits of a new sediment disposal strategy in shallow tidal waters 73
5.1 Introduction 74
5.2 Material and methods 76
5.2.1 Study area 76
5.2.2 Evaluating a new disposal strategy aiming at ecological benefits 76
5.2.3 TELEMAC model 78
5.2.4 Macrozoobenthos habitat suitability model 81
5.3 Results 84
5.3.1 Physical variables 84
5.3.2 Benthic community responses 84
5.3.3 Specific responses 85
5.4 Discussion 90

5.5 Conclusions 92

6 Ecosystem Engineering, aiming to generalization 95
6.1 Introduction 96
  6.1.1 Conceptual framework: allometry in ecosystem engineering 96
  6.1.2 Model system: bioturbation 97
6.2 Material and methods 98
  6.2.1 Target organisms 98
  6.2.2 Experimental devices 99
  6.2.3 Experimental protocol 99
  6.2.4 Data analysis 102
6.3 Results 102
6.4 Discussion 106

7 Ecosystem engineering, extrapolation to a realistic context 111
7.1 Introduction 112
7.2 Material & Methods 113
  7.2.1 Study area 113
  7.2.2 Target organisms 115
7.3 Modeling sediment-biota interactions 115
  7.3.1 Step 1: Prognostic model of the physical environment . 115
  7.3.2 Step 2: Ecosystem engineers distribution model 116
  7.3.3 Step 3: Allometric model of ecosystem engineers effect . 119
  7.3.4 Step 4: Integration 126
7.4 Results 127
7.5 Discussion 130
  7.5.1 Modeling sediment-biota interactions 130
  7.5.2 Recommendations for future research 134
7.6 Conclusion 135

8 Outlook 137

Appendices 141

Summary 159

Samenvatting 161

Sommario 165

Curriculum vitae 167

Acknowledgments 169

Bibliography 171

List of Tables

2.1 **Some characteristics (year average) of the Westerschelde and the Oosterschelde.** The Westerschelde values separated by a dash are referring to the mouth (right) and to 80 km upstream (left) 20

3.1 **Areas of the total, subtidal and intertidal surface for the different scenarios.** Values are in km^2. NDW (No Delta Works) indicates the results of the scenarios simulated removing the major coastal defense infrastructures 41

3.2 **Number of samples included into analysis** 43

3.3 **Target species characteristics** 44

3.4 **Target species occurrences.** Observed occurrence are expressed in percentage of occupied samples on the overall dataset. For each modeled scenarios, predicted occurrences were calculated as the percentage of cells for which the model forecast a biomass >= of the lowest value observed in nature. The predicted occurrence values reported in the table are the average of all the scenarios modeled between 1968 and 2010 46

6.1 **Table of treatments.** According to the availability of experimental organisms, we tested several combinations of individual abundances and individual body sizes of different bioturbators. 100

6.2 **Summary table of the multivariate models $EE_{pop} = aM^bA^c$.** Explanatory and response variables were log-transformed, centered and scaled to make coefficients directly comparable. 95% CI were calculated by bootstrapping the dataset 50000 times. R^2 values were adjusted to account for the effect of multiple explanatory variables 104

6.3 **Summary table of the univariate models $EE_{pop} = aB^d$.** Explanatory and response variables were log-transformed, centered and scaled to make coefficients directly comparable. 95% CI were calculated by bootstrapping the dataset 50000 times . 105

6.4 **Model comparison.** The AIC-scores of the different models are shown in the first and the second line. The p-values in the third line result from analysis of variance between the multivariate and the univariate model 105

7.1 **Table of treatments.** According to the availability of experimental organisms, we tested several combinations of individual abundances and individual body sizes of *Cerastoderma edule* and *Arenicola marina* 123

7.2 **Summary table of the multivariate models $EE_{lan} = aM^bA^cX^z$.** Explanatory and response variables were log-transformed, centered and scaled to make coefficients directly comparable. 95% CI were calculated by bootstrapping the dataset 50000 times. . 124

7.3 **Summary table of the multivariate models $EE_{lan} = aB^dX^z$.** Explanatory and response variables were log-transformed, centered and scaled to make coefficients directly comparable. 95% CI were calculated by bootstrapping the dataset 50000 times . 125

7.4 **Summary table of the abiotic model $SSC = aX^z$.** Explanatory and response variables were log-transformed, centered and scaled to make coefficients directly comparable. 95% CI were calculated by bootstrapping the dataset 50000 times 125

A.1 **AIC scores for different models (average of the AIC scores of all the fitted quantiles)** 143

A.2 ***Scoloplos armiger*, summary of the 0.975 quantile (upper boundary) model** 143

A.3 ***Peringia ulvae*, summary of the 0.975 quantile (upper boundary) model** 143

A.4 ***C. edule*, summary of the 0.975 quantile (upper boundary) model** 143

A.5 ***Lanice conchilega*, summary of the 0.975 quantile (upper boundary) model** 144

B.1 **Summary of the analyzed benthic dataset.** For the Westerschelde only the present time scenarios can be used to extrapolate the abiotic condition for a larger number of benthic samples. For the Oosterschelde, several intermediate year-scenario were modeled, thus it was possible to include in the analysis a large number of observation collected in the past. The use of a large and long-term dataset allow to include the complete span of possible combinations between environmental conditions and biomasses/densities. 148

B.2 **Total biomass, summary of the 95^{th} quantile regression model.** Standard errors were calculated by an inverted rank test. *vel= current velocity; salmean = average salinity, salrange= daily salinity range, em=inundation time* 149

B.3 **Density of inidividuals, summary of the 95^{th} quantile regression model.** Standard errors were calculated by an inverted rank test. *vel= current velocity; salmean = average salinity, salrange= daily salinity range, em=inundation time* 149

B.4 **Per capita body mass, summary of the 95^{th} quantile regression model.** Standard errors were calculated by an inverted rank test. *vel= current velocity; salmean = average salinity, salrange= daily salinity range, em=inundation time* 150

B.5 **Shannon diversity, summary of the 95^{th} quantile regression model.** Standard errors were calculated by an inverted rank test. *vel= current velocity; salmean = average salinity, salrange= daily salinity range, em=inundation time* 150

List of Figures

1.1 **Different levels of spatial organization in estuaries.** Larger landscape patterns are determined from smaller scale processes 2

1.2 **Estuarine sediment** A) Relative sizes of sand, silt, clay; B) Shepard's ternary diagram, including textural fields for naming siliciclastic sediment (after Shephard 1954). Numbers on the axis indicates the percentage of the different sediment fractions in the matrix 4

1.3 **Some endobenthic species:** the bivalves A) *Cerastoderma edule*, B) *Macoma balthica*, C) *Scrobicularia plana* D) *Abra alba* and the Polychaeta E) *Arenicola marina.* These organisms live into the sediment at different depths: from very shallow (*C. edule*, shells usually emerge from the sediment surface) to intermediate (other bivalves, from 3 to 10 cm) and relatively deep (*A. marina*, below 10 cm) [Degraer et al., 2006, Holtmann et al., 1996]. In association, their feeding mode change from obliged suspension feeding (*C. edule*) to a mixture of suspension and deposit feeding (other bivalves) to obliged deposit feeding (*A. marina*). *A. marina* swallow sediment from the surface and expel it in form of pseudo-faeces, forming characteristics feeding funnels and pseudofaeces casts [Zebe and Schiedek, 1996]. *Illustration cured by Fabrizio De Tommaso* 6

1.4 **Coastal Anthropocene.** A large part of the human populations is nowadays endangered by storm surge risks (coastlines enlighten in red). In the northern hemisphere (particularly in Europe) this led to the construction of coastal defense infrastructures like open surge barriers. In the map we show the largest existent (red circles), in realization (yellow circles) or proposed (green circle) storm surge barriers. Other smaller storm surge barriers exist, mostly on tributaries rivers (*e.g.* along the Elbe, the Humber, the Hull). Contextually, the increasing exchange of goods through sea routes is pushing to a more extensive dredging of the waterways to harbors (main dredging operations in estuaries, embayments or straits are reported on the map with orange asterisks). Sources for flood risk: World Bank; ship transit: NCEAS , population density: FAO; key dredging projects 2012 in estuaries, lagoons, embayments or straits: International Dredger Association and China Dredger Association. 7

1.5 **Niche filters** (after Zobel 1997). Realized assemblages of species are the result of different hierarchic levels of environmental filters acting on the individual traits 9

1.6 **Feedbacks in EE** (after Gutiérrez and Jones 2008). By modifying the abiotic environment, ecosystem engineers induce changes in their population structure and abundance, that in turn are reflected in the ecosystem engineering activity. 10

1.7 **Pictorial model of the feedback between biotic and physical components in structuring the sedimentary landscape.** The local sediment structure influences the composition of the benthic community (niche filtering). At the same time the benthic community is able to modify the sediment structure (ecosystem engineering). On a large scale, the ecosystem state is determined from the dynamic interactions of physical and biological agents 11

2.1 **Map of the study area.** Note the back-barrier dams and the sea-side storm surge barrier in the Oosterschelde 20

2.3 **Correlograms of d50 and different sediment fractions in the Oosterschelde and Westerschelde.** Histograms show the number of observations 24

2.4 **Boxplot of sediment d50 distribution across basins** for the overall dataset and for intertidal samples only 25

2.5 **Correlation of sediment d50 with measured depth and modeled Bed Shear Stress** 26

2.6 **Boxplot of community indices distribution across basins** 27

2.7 **Bar plot of mean biomass and occurrence of the 25 most common taxa in the Westerschelde and the Oosterschelde.** Stars show the significance of Fisher's test and ANOVA on differences between basins 27

2.8 **Distribution of species richness, total biomass and ecological diversity along the sediment d50 gradient.** The expected distributions are sketched using the 25^{th}, 50^{th} and 75^{th} quantiles 28

2.9 **Predicted d50-conditioned cumulative probability functions** for the biomass distribution of the 25 most common taxa in the Oosterschelde (black) and Westerschelde (white) basins. Bars show the maximal biomass predicted for the sediment compositions indicated on the x axis. Tick marks along the bars are drawn at intervals of 0.05 (1 tick mark from the top, then in the 5% of the cases is expected to found a biomass superior to that value at the given d50) 29

2.10 **Relationship between the sediment d50 optima detected separately for the two basins.** Optima are calculated as average of the optimal d50 values detected for each quantile of the forecasted distributions (from τ=0.01 to τ=0.99). The line shows the 1:1 ratio. Error bars are representative of the standard error of optima distribution around the mean value. Abbreviations refer to the first three letter of the generic name of the species. For species belonging to the same genus, also the first letter of the specific name is reported 34

3.1 **The Oosterschelde basin.** In the boxes are reported the name and the realization date of the major dikes 41

3.2 **Models validation. Ratio between observed and predicted values.** To validate our forecast for each of the modeled quantiles, the whole dataset was sampled with replacement. Due to sampling with replacement, some observations are repeated and others remain unpicked. The model was fitted on the sampled observation (training dataset) and used to predict the unpicked ones (validation dataset). The random sampling-fitting-predicting procedure was iterated 5000 times and repeated for each one of the forecast quantiles. To make predicted (quantiles) and realized values comparable each other, we discretized them in 10 homogeneous classes based on the predicted values. For each of the classes, the correspondent sample quantile of the observed data was calculated. To finally asses the validity of the model, observed and predicted quantiles were plotted against each other and checked for linear correlation. The four quantiles for species showed as examples in the graphs were selected among those predicting occurrence (*e.g.*, up to the 35^{th} quantile for *S. armiger*, up to the 78^{th} quantile for *L. conchilega* Table 3.4). The other quantiles generally follow the same trends. The black broken line represent the 1:1 ratio 48

3.3 **Models of the $\mathbf{0.975}^{th}$ quantile, response surfaces.** Models of the maximal biomass, when extrapolated in the explanatory variable space, give a description of the species potential niche consistent with the Liebig's Law 49

3.4 **Median values of the explanatory variables on different year-scenarios.** Circles represent the median values predicted for the available years-scenarios by the hydrodynamic model. Triangles represent the values predicted for the years 2010 and 2100 removing the Delta Works (NDW) 50

3.5 **Models of the $\mathbf{0.975}^{th}$ quantile, habitat suitability.** Once extrapolated to realistic scenarios, the response surface shown in Figure 3.3 are useful to produce clearly interpretable habitat suitability maps. In the figure we show as example the output for the 1968, 2010 and 2100 scenarios 51

3.6 **Complete distribution model *vs* Model of the maxima.** Example for *C. edule*, year 2010. Map produced by sampling from the complete quantile distribution models (A) are able to represent the realistic scatter around (mainly below) the response surface shown in (B). To help the reader in appreciating the fine mosaic of points in (A) we restricted the map to a smaller portion of the basin and we used a logarithmic scale for plotting the estimated values 52

3.7 **Biomass standing stocks, time series.** Colored bar show the intertidal (green) and subtidal (blue) realized biomass stock estimated from the different scenarios for the present extension of the basin. Broken-line bars on the years 1968 and 1983 include the area that was cut-off from the beginning of the Oesterdam works in 1979 (25 km^2 between 1968 and 1983 and 12 km^2 between 1983 and 1986). Empty bars on the years 2010 and 2100 show the result of the scenarios simulated removing the Delta Works 54

3.8 **Potential** *vs* **Realized stocks.** The graphs show the ratio between potential (τ=0.975) and realized (sampling from the complete cumulative distribution) intertidal (green) and subtidal (blue) biomass stocks estimated for different year/scenarios. The black dotted line represent the 1:5 ratio. The black broken line represent the 1:10 ratio 55

4.1 **Coastal Anthropocene.** A large part of the human populations is nowadays endangered by storm surge risks (coastlines enlighten in red). In the northern hemisphere (particularly in Europe) this led to the construction of coastal defense infrastructures like open surge barriers. In the map we show the largest existent (red circles), under construction (yellow circles) or proposed (green circle) storm surge barriers. Other smaller storm surge barriers exist, mostly on tributaries rivers (*e.g.* along the Elbe, the Humber, the Hull). Contextually, the increasing exchange of goods through sea routes is pushing to a more extensive dredging of the waterways to harbors (main dredging operations in estuaries, embayments or straits are reported on the map with orange asterisks). Sources for flood risk: World Bank; ship transit: NCEAS , population density: FAO; key dredging projects 2012 in estuaries, lagoons, embayments or straits: International Dredger Association and China Dredger Association (representative of ca. 70% of the global dredging market) . . . 61

4.2 **The Oosterschelde and Westerschelde basins.** A-D: main dams in the Oosterschelde; 1-9: main dredging sites in the Westerschelde. Intertidal areas are marked with a black line. Channels deeper than 10 m are enclosed by a with a gray line (bathymetry of 2010). Global trends in coastal development are well represented in the SW Delta of The Netherlands. On the one hand, the Oosterschelde was disconnected from the previous freshwater network (dams B & C) and embanked from the seaside by a storm surge barrier (Oostercheldekering, A). During the last decades,the maximal size of commercial vessels almost doubled. As consequence, channels in the Westerschelde were locally deepened (1-9) to enhance the shipping route capacity to the port of Antwerp (bottom right) 63

4.3 **Changes in abiotic variables between 1960 and 2010.** Maps show the absolute changes in hydrodynamic variables, as predicted from the hydrodynamic models. Intertidal areas are marked with a black line. Boxplots show the distribution of the variables in 1960 and 2010 for the Westerschelde (Wes) and Oosterschelde (Oos). Intertidal (green) and subtidal (blue) data are presented separately in the box plots. The realization of the Oosterscheldkering in 1986 strongly dampened the tidal currents in the Oosterschelde, while deepening of the Westerschelde had the opposite effect, especially in the subtidal (A). Local decreases in intertidal current strength and high suspended sediment loads are promoting sedimentation on the Westerschelde intertidal mudflats. In the Oosterschelde some signs of intertidal erosion are visible on the edges of the mudflats (B). The increased tidal flux in the Westerschelde led to a deeper penetration of the saltwater in the estuary (C) and, in general, to wider daily salinity fluctuations (D) 70

4.4 **Changes in habitat suitability between 1960 and 2010.** Maps show the absolute changes in potential benthic communities responses, as predicted from the 95th quantile regression models. Intertidal areas are marked with a black line. Boxplots show the distribution of the predicted variables in 1960 and 2010 for the Westerschelde (Wes) and Oosterschelde (Oos). Prediction for the intertidal (green) and subtidal (blue) habitats are presented separately in the box plots. Compared to 1960, benthic habitat suitability has strongly improved in the subtidal part of the Oosterschelde, especially in terms of potential biomass (A), per capita body size (C) and species diversity (D). Changes are less relevant in the intertidal part of the basin, mostly involving a slightly decrease in individual density (B). For the Westerschelde, we modeled a generalized decrease in habitat suitability. Increases in intertidal potential density associated with decreases in potential per capita body size (B & C) are indicative of the proliferation of small sized opportunistic deposit feeders. Increased hydrodynamic and salinity stress had a detrimental effect on species richness, especially in the most marine part of the estuary (D) 71

5.1 **The Schelde Estuary.** A) Location of the Westerschelde in Europe. B) The Westerschelde with tide gauges (red dots), discharge transects (red lines). C) Detail of shoal of Walsoorden with discharge transects (red lines) and locations of ADCP flow velocity measurements (black dots). The black arrows indicate the flood channel, the white arrows the ebb channel 77

5.2 **Walsoorden nourishment.** Bathymetry of the tip of the shoal of Walsoorden (more detailed than Figure 5.1 C) for 2003, 2009, 2012 and an hypothetical scenario (addition of 340000 m^3 of sediment in the downstream tip of the shoal) 78

5.3 **Cost function.** The cost function results of different calibration steps (1-10) for high water levels (HW), the standard deviation on HW, low water levels (LW), standard deviation on LW . . . 80

5.4 **Calibration of discharges.** For a neap spring tidal cycle the total discharge volumes over the transect 'Schaar van Waarde' are given in function of their respective tidal range. The distance between the measured total discharge volume and the models linear regression line evaluates the calibration effort 80

5.5 **Calibration of flow velocities.** For a neap-spring tidal cycle the maximum flow velocity is given as a function of the high water level (dots) for an ADCP measurement location on the shoal of Walsoorden. Measurements are shown as dark symbols and trend line, simulations as light symbols and trend line . . . 81

5.6 **Calibration of salinity level.** Comparison of measured and modeled salinity values (g L^{-1}) for the locations Overloop van Hansweert (OVHA) and Baalhoek (locations see Figure 5.1 B) 82

5.7 **Modeled area.** The subtidal area investigated for benthos at shoal of Walsoorden is comprised between between blue and red line. The intertidal area is inside the red polygon 84

5.8 **Changes in maximum flow velocity.** The year 2003, before the sediment disposal, is taken as the reference for all scenarios. Positive values denote an increase and negative values a decrease in maximum flow velocities (m sec^{-1}). The full line indicates the border of the intertidal area. The thick red line indicates where sediment was disposed 85

5.9 **Subtidal community responses.** Averages of benthic community maximal parameters (Biomass, Abundance, Per capita body mass and Shannon diversity) for the four scenarios for the subtidal zone around the downstream tip of the shoal of Walsoorden. Error bars indicate standard deviation 86

5.10 **Intertidal community.** Averages of benthic community maximal parameters (Biomass, Abundance, Per capita body mass and Shannon diversity) for the four scenarios for the intertidal zone around the downstream tip of the shoal of Walsoorden. Error bars indicate standard deviation 86

5.11 **Community responses.** Difference maps for the benthic community maximal parameters: Total biomass, Abundance, Per capita body mass and Shannon diversity 87

5.12 **Specific subtidal responses.** Averages of four benthic species maximal biomass (*C. edule*, *Macoma balthica*, *Hediste diversicolor*, *Heteromastus filiformis*) for the four scenarios for the subtidal zone around the downstream tip of the shoal of Walsoorden. Error bars indicate standard deviation. 88

5.13 **Specific intertidal responses.** Averages of four benthic species maximal biomass (*C. edule*, *M. balthica*, *H. diversicolor*, *H. filiformis*) for the four scenarios for the intertidal zone around the downstream tip of the shoal of Walsoorden. Error bars indicate standard deviation 88

5.14 **Specific responses.** Difference maps for the benthic species maximal biomass: *C. edule*, *M. balthica*, *H. diversicolor*, *H. filiformis* and *Bathyporeia pilosa*. 89

6.1 **Target organisms.** Three different archetypes of bioturbators were used in our experiments: shallow (A, *Cerastoderma edule*), intermediate (B *Macoma balthica*, C *Scrobicularia plana*, D *Abra alba*, *Venerupsis philippinarum*) and deep burrowers (E, *Arenicola marina*). *C. edule* reworking of sediment is mostly related to biodeposition, vertical and horizontal movements and valves adduction . The other species of bivalves are generally less motile than *C. edule*, but they can disrupt the sediment surface by inhaling the sediment with their siphons to graze on benthic diatoms [Zwarts et al., 1994]. *A. marina* swallow sediment from the surface and expel it in form of pseudo-faeces, forming characteristics feeding funnels and pseudofaeces casts [Zebe and Schiedek, 1996]. *Illustration cured by Fabrizio De Tommaso* 101

7.1 **The Oosterschelde and Westerschelde basins.** A-D: main dams in the Oosterschelde; 1-9: main dredging sites in the Westerschelde. Intertidal areas are marked with a black line. Channels deeper than 10 m are enclosed by a with a gray line (bathymetry of 2010). Global trends in coastal development are well represented in the SW Delta of The Netherlands. On the one hand, the Oosterschelde was disconnected from the previous freshwater network (dams B & C) and embanked from the seaside by a storm surge barrier (Oostercheldekering, A). During the last decades,the maximal size of commercial vessels almost doubled. As consequence, channels in the Westerschelde were locally deepened (1-9) to enhance the shipping route capacity to the port of Antwerp (bottom right) 114

7.2 **Physical variables.** The 2010 scenario is shown as example . 117

7.3 **Potential ecosystem engineering.** A-B) Maximal expected biomass of *C. edule* and *A. marina* (as estimated from a 0.9 quantile distribution model, [Cozzoli et al., 2014]; D-C) Maximal increase in sediment erodability due to *C. edule* and *A. marina* bioturbation. Estimates are expressed as factor of increment in sediment resuspension with respect to what predicted from the abiotic erosion model (Figure 7.3); E-F) Changes in maximal EE from 1960 to 2010 129

7.4 **Potential ecosystem engineering, changes between 1960 and 2010.** Correlation between changes in maximal current velocity, maximal bioturbators biomass and potential ecosystem engineering for the Westerschelde and Oosterschelde (one point each 400 m^2). Broken lines indicates the linear relationships between variables 130

7.5 **Realized ecosystem engineering, summary of changes between 1960 and 2010.** Each block of bars shows (from left to right), for the Westerschelde (green) and Oosterschelde (blue) 1960 and 2010 scenarios, the average values predicted for the upper (submerged for less than the 50% of a tidal cycle), intermediate (submerged between 50% and 75% of a tidal cycle) and lower (submerged for more than the 75% of a tidal cycle) intertidal areas. Error bars represent standard errors. A) Average intertidal current velocity as estimated from the prognostic environmental model (Figure 7.2); B) Average realized intertidal biomass of *C. edule* and *A. marina* as estimated from a full quantile distribution model; C) Average realized increment of sediment resuspension due to bioturbation from *C. edule* and *A. marina* 132

A.1 **Cluster analysis** on biomass distributions (g AFDW m^{-2}) of the 10 most common species in the Oosterschelde between 1963 and 2010 144
A.2 **Variations of the coefficients with respect to modeled quantile for *S. armiger*.** vel = current velocity, em = emersion time 145
A.3 **Variations of the coefficients with respect to modeled quantile for *P. ulvae*.** vel = current velocity, em = emersion time 145
A.4 **Variations of the coefficients with respect to modeled quantile for *C. edule*.** vel = current velocity, em = emersion time 146
A.5 **Variations of the coefficients with respect to modeled quantile for *L. conchilega*.** vel = current velocity, em = emersion time 146
B.1 **Validation, Observed vs Predicted values.** Red lines and R^2 coeffiecnts were obtained by linear regression. Dashed lines indicates the 1:1 ratio 151
B.2 **Oosterschelde, benthic observations**. The black vertical dashed line marked the finalization year of the Oosterscheldekering (1986). Before than 1975, only individuals density and taxonomical records were take. Average body size and total biomass values were obtained by multiplying the numerical density of each species for the average body size registered in later years (dahsed boxes). Coherently with our forecast, observed data show a decrease in intertidal habitat suitability and an increase in subtidal habitat suitability after the realization of the Oosterscheldekering. Not enough observation are available for plotting a similar time series for the Westerschelde (Table B.1) 152
B.3 **Potential community parameters distribution in 1960.** . 153

B.4 **Potential community parameters distribution in 2010.** . 154
C.1 **Experimental devices**. The annular flumes used are a variation of the design described by [Widdows et al., 1998]. For each experiment, we used standard, wet, fine-sand sediment (median grain size = 120 μm). 155
C.2 Annular flumes, 40 cm height model 156
C.3 Annular flumes, 80 cm height model 157

CHAPTER 1

Introduction

1.1 The estuarine environment

Wherever a river flows into a sea with a relevant tidal regime, tides will penetrate inland along the river valley. Following Fairbridge [1980], an estuary (from the latin *aestus*, tide) is the part of the river subjected to tidal fluctuations. Estuaries can be referred to by many different names, such as bays, harbors, lagoons, inlets, or sounds. On a geological time scale, they have an ephemeral life. Their physical location is related to the fluctuation of the sea-level [Day et al., 1989]. Present-day estuaries have been formed during the last inter-glacial period (from 15000 to 5000 years ago) when the sea level rose to the actual level [Day et al., 1989].

Estuaries are heterogeneous and dynamic systems with strong spatial and temporal gradients in environmental conditions [McLusky, 1993, 2004]. Mega-scale (10 - 10^3 km^2) geophysical processes (sandbanks and gullies migration, glacial water level fluctuation) typically act on long time (10 - 10^4 years). Faster processes (10^{-1} - 10^1 years) govern spatial gradients (bottom elevation, sediment granulometry) at a smaller scale (10^{-2} - 10 km^2) [De Vriend, 1991]. Finally, local environmental properties are determined by micro-scale processes like advective and diffusive fluxes of sediment and interstitial media, particle interactions and geochemical reactions [Winterwerp and van Kesteren, 2004]. The cross-scale interactions between processes (Figure 1.1) generates non-linearity in landscape evolution and make long-term morphological changes difficult to predict [De Vriend, 2001].

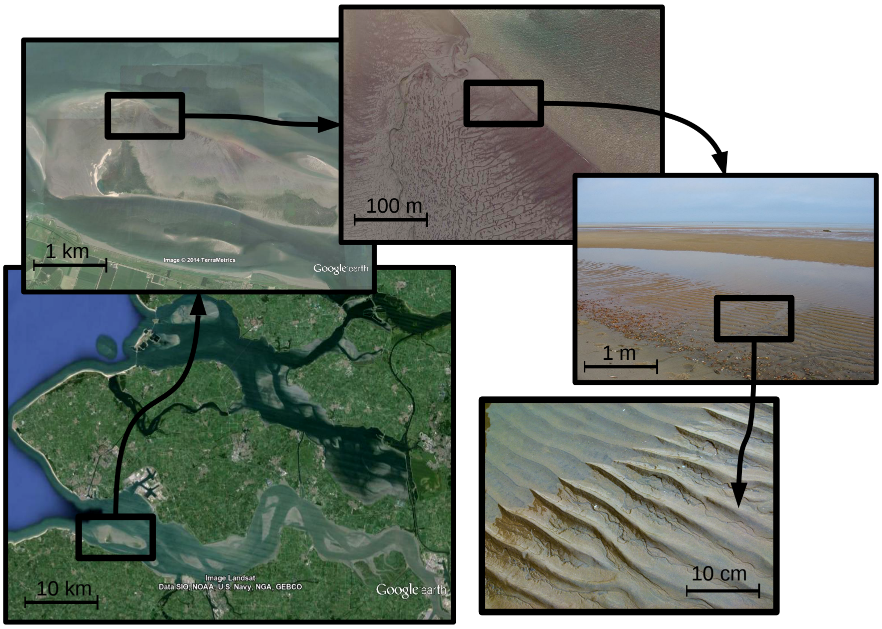
100 m
1 km
Image © 2014 TerraMetrics
Google earth
1 m
10 km
Image Landsat
Data SIO, NOAA, U.S. Navy, NGA, GEBCO
Google earth
10 cm

Figure 1.1: **Different levels of spatial organization in estuaries.** Larger landscape patterns are determined from smaller scale processes

1.1.1 The physical environment: tides, salt and sediment

The sea water enters in estuaries with the rhythm of the tides and it mixes with the fresh water flowing from rivers and streams. The tidal influence causes daily variations in the morphological, hydrological and chemical characteristics of the estuarine environment [Day et al., 1989]. The fluctuation of high and low water levels causes part of the shore to be drained and exposed at low tide, while it is submerged during high tide. The current velocities generated by the water flux are largely heterogeneous in space and time, depending on the bottom elevation and on the phase of the tidal wave (*i.e.*, mounting, stationary, retreating). Variations in the tidal regime can be related to (predictable) astronomic cycles or to the (more stochastic) effect of wind, that can push or contrast the water mass movement. Exposure to wave action can further increase the intensity of the hydrodynamic stress on the bottom [Le Hir et al., 2000].

One of the principal characteristics of estuaries is the increasing gradient in salinity along the longitudinal (river-sea) axis, with a range of near zero at the tidal propagation limit to the marine level (30-35 PSU unit) at the estuary mouth. Within the main river-sea gradient, the tidal water movements generate regular daily fluctuations in local salinity. Further variability can derive from seasonal dynamics, especially related to changes in the freshwater discharge [Day et al., 1989].

Differential erosion and deposition of sediment are the main processes shaping the estuarine landscape [McLusky, 2004]. Although sediment transport can affect broad areas of space, it is the cumulative result of micro - scale interactions between the bed shear stress exerted by the water flux on the bottom and the sediment particles. In certain areas the bed shear stress is low enough so that sediment can settle and accrete, forming intertidal flats upon which coastal wetlands can build. Other areas, characterized by stronger current velocities, are occupied by a complex net of submerged channels. Estuaries can collect sediment from both marine and riverine inputs. Estuarine sediments are typically composed of a mixture of sand, silt and clay particles (Figure 1.2 A) of siliciclastic origin. A sediment matrix composed mainly of sand (Figure 1.2 B) behaves granularly and is called a non-cohesive bed. Because of the relatively large grain size, the medium occupying the interstitial spaces between sand grains (porewater) has high degree of exchange with the external environment [Huettel and Gust, 1992]. Silt and clay particles, due to their smaller size and the flattened shape, can occupy interstices between larger particles causing pore water flow to decrease. Clay particles develop an asymmetric electrical charge distribution on their surfaces [Winterwerp and van Kesteren, 2004]. This generates a net attractive force between the particles, called cohesion, that confers plastic behavior to the sediment. Cohesive behavior often arises once the volume content (Figure 1.2 B) of clay in sediment exceed 10 % [Winterwerp and van Kesteren, 2004]. While sandy sediment is often associated with intense hydrodynamic stress and physical mixing, silt and clay bottoms usually can be found in shallow and quiet areas [Allen, 1985].

1.1.2 The biotic environment

Estuaries are among the richest natural habitats in the world [McLusky, 2004] and their major ecological and economical value is widely recognized [Adger et al., 2005, Barbier et al., 2011, Costanza et al., 1997, Matthews et al., 2011]. The estuarine ecosystem is tightly coupled to processes on the surrounding land, the adjacent coastal sea and the river(s) that feed it. The high level of nutrients from both marine and terrestrial sources allows high primary production rates [Heip et al., 1995]. The environmental variability occurring at different spatial and temporal scales, generates well developed spatial and temporal patterns in estuarine species distribution both along the longitudinal (river-sea) and latitudinal (mudflat-gully) axes of the estuary [Wolff, 1983].

Microphytoplankton and microphytobenthos (mainly diatoms and dinoflagellates) are key primary producers [Stal, 2003, Underwood and Kromkamp, 1999]. Their productivity is largely dependent on the turbidity of the water [Heip et al., 1995]. Large numbers of autotrophic bacteria are also found within the sediment. Their activity boosts the mineralization rate of organic material

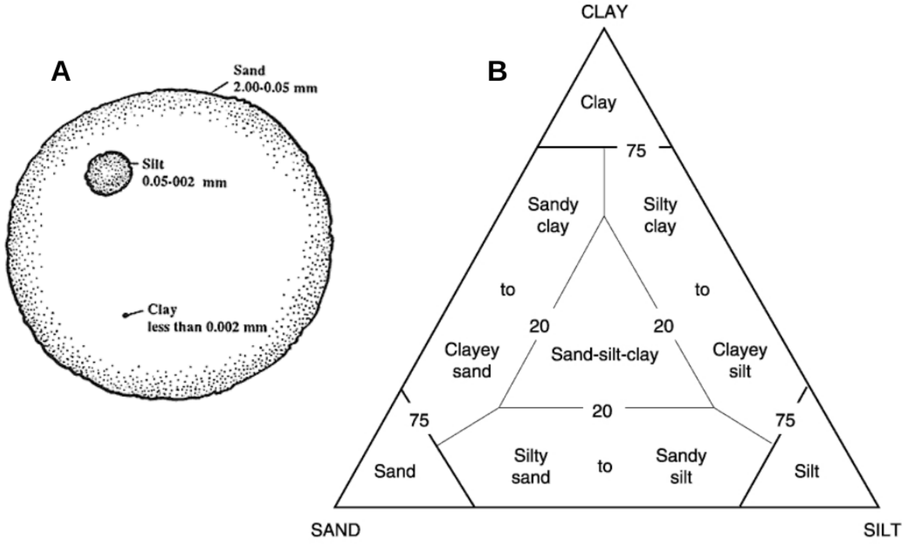
A
Sand
2.00-0.05 mm
Silt
0.05-002 mm
Clay
less than 0.002 mm
B
CLAY
Clay
75
Sandy clay
Silty clay
to
to
20
20
Clayey sand
Sand-silt-clay
Clayey silt
75
20
75
Sand
Silty sand
to
Sandy silt
Silt
SAND
SILT

Figure 1.2: **Estuarine sediment** A) Relative sizes of sand, silt, clay; B) Shepard's ternary diagram, including textural fields for naming siliciclastic sediment (after Shephard 1954). Numbers on the axis indicates the percentage of the different sediment fractions in the matrix

and denitrification processes [Christensen et al., 2000]. This implies a very high oxygen demand and reduces the levels of oxygen within the sediment [Sutherland et al., 1998]. Organically rich sediments are often in partially anoxic conditions, which can be further exacerbated by limited water flux [Pearson and Rosenberg, 1978].

Macrophyta can form dense submerged canopies and in the intertidal zone they can develop into salt marshes. By doing so, they play a large role in the aquatic food web and the delivery of nutrients to coastal water [Jones et al., 1994, 1997]. The shallowness of estuaries provides a relatively safe habitat for a wide range of organisms [McLusky, 2004]. A large number of fish species spend their entire life cycle in estuaries, while others use these environments as breeding and nursery habitat [Jackson et al., 2001]. The abundance of preys attracts many consumers (flagship species) like birds and sea mammals [McLusky, 2004].

Life at the bottom: the macrozoobenthos

Benthic macrofauna or macrozoobenthos are all benthic invertebrate animals that live in or on the bottom substrate of a water body. Although macrozoobenthos individuals are small (usually from 1 mm to a max of 20 cm), they may occur in very high densities and exert strong influences on their environment.

Within the macrozoobenthos, all types of taxonomic and functional diversity can be found [Snelgrove, 1998]. Despite the lack of oxygen, many animals burrow into the sediment (*endobentos*, Figure 1.3) to feed or to avoid predation; they have special adaptation to resist to anoxia [Sutherland et al., 1998]. Other animals live on the surface of the sediment (*epibenthos*) and can form persistent reefs (*e.g.* oysters, mussels, sandmasons). Common taxa are Polychaeta (worms), Crustacea (shrimps, crabs, lobsters) and Mollusca (snails, slugs and shellfish). Most macrozoobenthic organisms are either suspension feeders that filter the overlying water and retain phytoplankton and Suspended Particulate Matter (SPM) or deposit feeders that ingest sediment particles and organic material associated with these particles. Herbivores graze on mycrophytes on the surface of the sediment substrate. Predators and scavengers respectively use live or dead animal tissue for their sustenance.

Benthic organisms are usually the link between primary producers (phytobenthos and phytoplankton) and higher trophic levels, such as fish, birds, aquatic mammals and humans [Herman et al., 1999]. By processing the organic material present at the water-sediment interface, macrozoobenthos provide a conduit for trophic transfers into and from the water column [Carlson et al., 1997, Newell, 1998]. Deposit feeders bioturbate sediments as they feed, resulting in increased sediment oxygenation [Rhoads and Young, 1970]. Because organic matter and oxygen are so important to microbial activities in sediment that contribute to nutrient cycling [Heip et al., 2001], macrozoobenthos can impact nitrogen, carbon, and sulfur cycling at a global scale.

1.1.3 Humans and estuaries

Humans have lived in or near estuaries for tens of thousand of years [Small and Nicholls, 2003]. These environments guarantee high protein yields through fishing, shellfish harvesting and bird-hunting. Given their accessibility from the sea, river and land, early human settlements in proximity of estuaries have grown out to become important trade hubs and centers of cultural exchange. At the present time, a great part of the human population live in proximity of the coast (Figure 1.4) and 22 of the 32 biggest cities in the world are located on or near estuaries [Small and Nicholls, 2003]. In order to make estuarine environments more livable and safe, the growing human communities developed a long tradition of hydraulic engineering and realization of wet infrastructure (dikes, storm surge barriers, piers, artificial channels) [Temmerman et al., 2013]. The continuously growing global trade network and the ongoing increase of the size of commercial ships are also pushing toward a more intensive dredging of the waterways to the harbors (Figure 1.4). Coastal infrastructures are so ubiquitously diffused that they have been proposed as a main driver of change in marine environments [Bulleri and Chapman, 2010].

The estuarine areas are highly valuable environments for the economic activities that take place within (fisheries, aquaculture, sand extraction, transport of goods and people, recreation) and for the services they provide to the

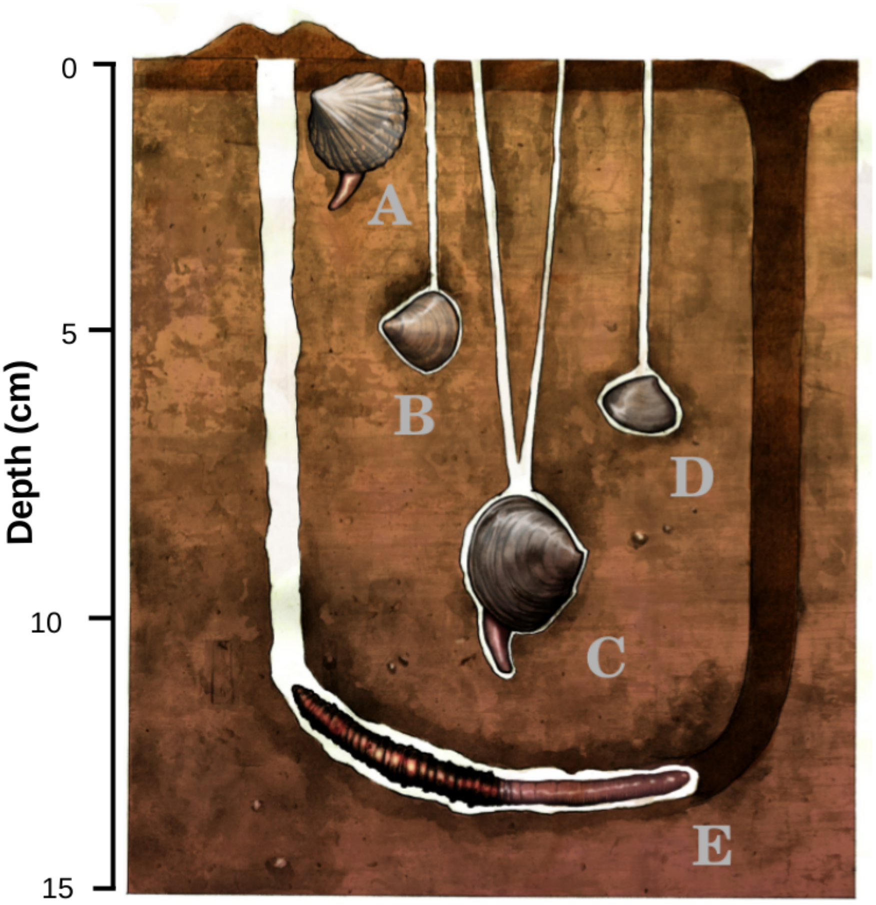

Figure 1.3: **Some endobenthic species:** the bivalves A) *Cerastoderma edule*, B) *Macoma balthica*, C) *Scrobicularia plana* D) *Abra alba* and the Polychaeta E) *Arenicola marina*. These organisms live into the sediment at different depths: from very shallow (*C. edule*, shells usually emerge from the sediment surface) to intermediate (other bivalves, from 3 to 10 cm) and relatively deep (*A. marina*, below 10 cm) [Degraer et al., 2006, Holtmann et al., 1996]. In association, their feeding mode change from obliged suspension feeding (*C. edule*) to a mixture of suspension and deposit feeding (other bivalves) to obliged deposit feeding (*A. marina*). *A. marina* swallow sediment from the surface and expel it in form of pseudo-faeces, forming characteristics feeding funnels and pseudofaeces casts [Zebe and Schiedek, 1996]. *Illustration cured by Fabrizio De Tommaso*

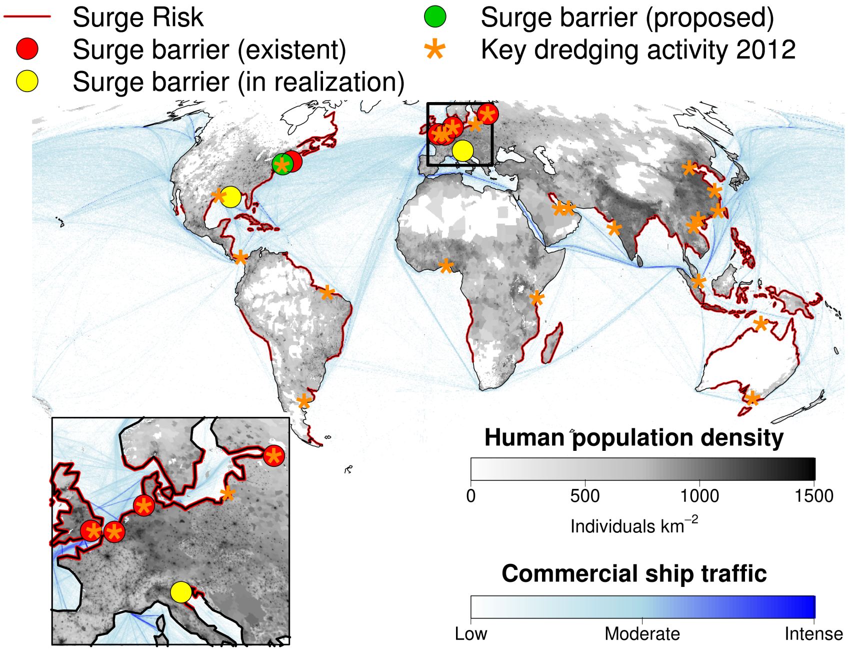
Surge Risk
Surge barrier (existent)
Surge barrier (in realization)
Surge barrier (proposed)
Key dredging activity 2012
Human population density
0
500
1000
1500
Individuals km^{-2}
Commercial ship traffic
Low
Moderate
Intense

Figure 1.4: **Coastal Anthropocene.** A large part of the human populations is nowadays endangered by storm surge risks (coastlines enlighten in red). In the northern hemisphere (particularly in Europe) this led to the construction of coastal defense infrastructures like open surge barriers. In the map we show the largest existent (red circles), in realization (yellow circles) or proposed (green circle) storm surge barriers. Other smaller storm surge barriers exist, mostly on tributaries rivers (*e.g.* along the Elbe, the Humber, the Hull). Contextually, the increasing exchange of goods through sea routes is pushing to a more extensive dredging of the waterways to harbors (main dredging operations in estuaries, embayments or straits are reported on the map with orange asterisks). Sources for flood risk: World Bank; ship transit: NCEAS , population density: FAO; key dredging projects 2012 in estuaries, lagoons, embayments or straits: International Dredger Association and China Dredger Association.

human communities (processing of water and pollutants, recycling of nutrients) [Costanza et al., 1997]. However, the extensive human exploitation and modification of these environments leads to habitat deterioration and consequent loss of functionality [Barbier et al., 2011]. Alterations of the eco-hydromorphological environment can have negative, or even catastrophic, social consequences when they affect essential ecological services [Adger et al., 2005, Danielsen et al., 2005, Diaz et al., 2006]. Future plans on estuarine management should reconcile the human development and the protection of the natural patrimony [Leschine et al., 2003]. Ecological forecast must be included into dynamic infrastructure design to maintain operational efficiency and reduce ecological impacts [Matthews et al., 2011]. A public debate is needed on whether nature conservation goals can and should be brought closer in line with other management objectives, and to what degree natural values should be constraining other management options.

1.1.4 BwN: Thinking, Acting and Interacting differently

Traditional approaches to morphological management focus on minimizing negative impacts in the project phase and compensating for any residual negative effects. These procedures have usually high costs in terms of limitations of economic activities and compensation measurements are often inadequate or fail completely [Roni et al., 2002]. A more innovative way of thinking is to include natural processes as an active component of the infrastructure development process. The Building with Nature (BwN) [Ecoshape, 2014] project has the main goal to integrate the functionality of wet infrastructure with the creation of opportunities for nature and society. A pivotal concept in the BwN philosophy is that natural components should be considered, rather than as just passively influenced by human activities, as an operational part of the infrastructure functional design. BwN is widely supported within the Dutch water sector and embraced by a number of government institutions in the field of infrastructure and ecosystem development. Examples of BwN designs are the Delfland Sand Engine [van Slobbe et al., 2013], the use of oyster reefs to prevent intertidal erosion in the Oosterschelde [Ysebaert et al., 2012], the revitalization of the Ijsselmeer [Lammens et al., 2008], and the design of ecosystem-based management of tropical coastlines such as coral reefs, seagrass meadows and mangrove forests [Gillis et al., 2014].

1.2 Niche filtering *vs.* Ecosystem engineering

The niche concept describes how an organism or population responds to the distribution of resources and competitors. Hutchinson [1957] define the niche as an n-dimensional space where the dimensions are environmental conditions and the resources that define the requirements of an individual or a species. Realized assemblages of species are the result of different hierarchic levels of environmental filters acting on the individual traits (Zobel 1997, Figure 1.5). The physical habitat conditions have a primary role in determining the fundamental niche and physical descriptors can be used to forecast potential species distributions [Franklin, 2010]. The realized niche is a sub-portion of the potential one, delimited by biological interactions. While physical niche filtering generally prevents co-occurent species to be too dissimilar in their function and behavior (they need to fulfill the same environmental requirements), a certain degree of functional heterogeneity is often maintained in realized assemblages to reduce competition [Mouillot, 2007].

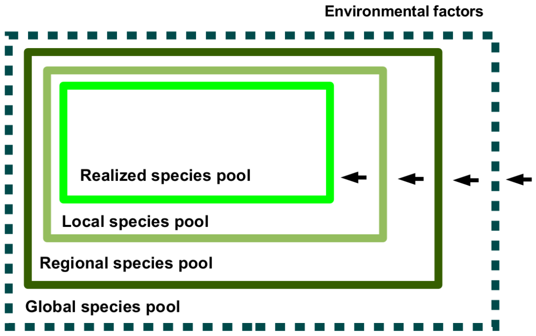

Figure 1.5: **Niche filters** (after Zobel 1997). Realized assemblages of species are the result of different hierarchic levels of environmental filters acting on the individual traits

The ecosystem engineering framework focuses on how organisms physically change the abiotic environment, either by their structures (*i.e.*, autogenic engineers) or by their activity (*i.e.*, allogenic engineers) [Jones et al., 1994, 1997]. Ecosystem engineering happens almost ubiquitously on Earth, performed by different organisms, with different modalities, at different scales [Hastings et al., 2007]. It both influences biogeomorphic landscape development [Raynaud et al., 2013] as well as the structure and fate of entire communities [Bruno et al., 2003, Jones et al., 1994, 1997]. Descriptions of ecosystem engineering are important to the understanding of the patterns and dynamics of diverse species interactions in nature [Kefi et al., 2012]. The role of ecosystem engineering is often essential to understanding ecological successions [Bouma et al., 2005, Bruno, 2000] and landscape evolution [Pearce, 2011].

Niche filtering and ecosystem engineering are not strictly alternative mechanisms, but they coexist in a dynamic equilibrium [Rietkerk et al., 2004, van de Koppel et al., 2001], *i.e.* ecosystem engineers are often able to modify the same environmental conditions (niche axes) that are relevant for their fitness or for the fitness of co-occurring species. By doing so, ecosystem engineers induce changes in their population structure and abundance, that in turn are reflected in the ecosystem engineering activity (Gutiérrez and Jones 2008, Figure 1.6). The interdependence between abiotic and biotic components in ecosystem engineering induces strong environmental feedbacks, potentially causing the emergence of multiple stable states, sudden regime shifts and chaos [Cuddington et al., 2009, Rietkerk et al., 2004, Scheffer and Carpenter, 2003, van de Koppel et al., 2001]. By means of ecosystem engineering, changes in the spatial distribution of organisms (shift in areas, invasion, local extinction) can exacerbate or dampen ongoing physical trends [Crooks, 2002].

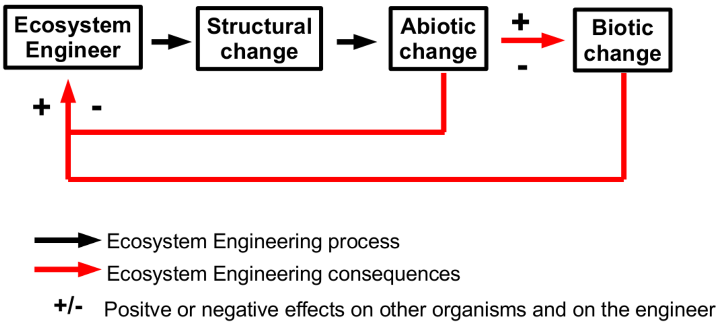
Ecosystem Engineer
Structural change
Abiotic change
Biotic change
+
-
+
-
Ecosystem Engineering process
Ecosystem Engineering consequences
+/- Positve or negative effects on other organisms and on the engineer

Figure 1.6: **Feedbacks in EE** (after Gutiérrez and Jones 2008). By modifying the abiotic environment, ecosystem engineers induce changes in their population structure and abundance, that in turn are reflected in the ecosystem engineering activity.

1.3 Sediment transport as biotic-physical feedback

Biotic elements are tightly coupled with the physical processes shaping the sedimentary landscape. On one hand, the environmental factors involved in sediment dynamics are important drivers for the spatial distribution of organisms. For example, high bed shear stress can inhibit the majority of benthic organisms to establish [Snelgrove and Butman, 1994], or the sediment composition can drive the species distribution on intertidal flats [Gray, 1974]. On the other hand, many benthic organisms act as ecosystem engineers in the sense that they typically modify the interactions between physical elements in sediment dynamics. Benthic organisms generally increase the bottom roughness, changing the bottom boundary layer locally, and increasing the small-scale variability in bottom shear stress [Friedrichs et al., 2000]. The microphytobenthos can armor and stabilize the sediment surface [Stal, 2003]. Biogenic reefs can trap sediment and shelter the underlying sediment from bed shear stress [Borsje et al., 2008].Conversely, endobenthic macrozoobenthos decreases sediment stability and increases the erodability by bioturbating activities [Le Hir et al., 2007, van Prooijen et al., 2011, Willows et al., 1998]. Suspension feeders can increase sedimentation rates by deposition of pseudofaeces [Bruschetti et al., 2011].

Although macrozoobenthic organisms can functionally affect sediment dynamics only on micro to meso scale, their long-term action, exerted on large areas, can influence the development of these intertidal flats as a whole [Borsje et al., 2008, Orvain et al., 2012, Rhoads and Young, 1970, Volkenborn et al., 2007] and have a direct impact on sediment transport and nearshore geology [Widdows and Brinsley, 2002]. By modifying the bottom topography, elevation and composition, the benthic biota affect those environmental conditions that are in turn relevant for their own fitness (Figure 1.7). Such interdependence between physical and biological factors can generate complex feedbacks and non linear dynamics [Rietkerk et al., 2004, van de Koppel et al., 2001, 2005]. While numerical models are available for simulating sediment transport driven by physical factors, the interaction between biological elements and physical factors and their impact on sediment dynamics are still hard to predict [van Prooijen et al., 2011, Winterwerp and van Kesteren, 2004].

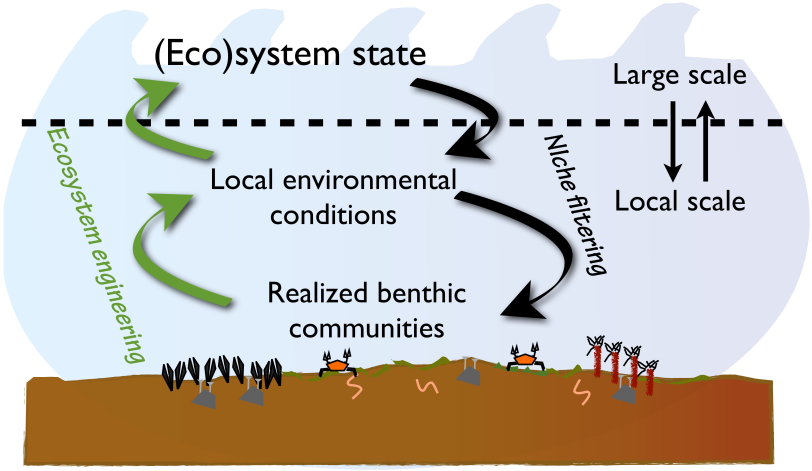

Figure 1.7: **Pictorial model of the feedback between biotic and physical components in structuring the sedimentary landscape.** The local sediment structure influences the composition of the benthic community (niche filtering). At the same time the benthic community is able to modify the sediment structure (ecosystem engineering). On a large scale, the ecosystem state is determined from the dynamic interactions of physical and biological agents

1.4 Thesis Outline

1.4.1 Rationale

The macrozoobenthos potentially constitutes a hinge point between the morphological and the ecological state of the estuarine environments: on the one hand, it constitutes a fundamental element of estuarine food webs, the alteration of which can have strong repercussion on higher trophic levels (fishes, birds, humans). On the other hand, it has a broad and differentiated influence on sediment dynamics and geochemistry. Future choices about habitat and landscape management 1) should be based on solid forecasts about the changes they will generate in the physical environment; 2) should be able to adaptively cope with the interested natural processes [Ecoshape, 2014]. Along this line, forecasts on infrastructure impacts cannot neglect the influence of biological elements in medium to long term landscape evolution. The integration of ecological insights in sediment transport models presents the double advantage of 1) providing simultaneous forecasts about the ecological and morphological evolution of sedimentary basins; 2) including explicitly the effect of macrozoobenthos on sediment dynamics, thus accounting for the biotic-induced deviations from purely physical expectations. Two main points need to be addressed to include biological elements in realistic sediment transport scenarios:

1. How are benthic ecosystem engineers distributed in relation to the physical variables involved in sediment transport? How do benthic EEs respond to alterations of estuarine habitats following wet infrastructure realization?

2. How do benthic ecosystem engineers modify the outcome of physical interactions involved in sediment transport? How can their effect be described in general terms?

During this PhD project I investigated both sides of the sediment-biota interaction. As a first step, I modeled macrozoobenthic distributional responses as function of those environmental variables that are relevant for sediment transport (Chapters 2 - 5). In this phase, I devoted particular attention to the effect of large (Chapters 3 & 4) and local scale (Chapter 5) anthropogenic alterations of the hydromorphological habitat. As a second step, I measured in laboratory conditions the effect of several macrozoobenthic species on sediment erodability (Chapters 6 - 7). I chose to relate the ecosystem engineering activity to general individual (body size) and population (abundance of individuals, total biomass) ecological descriptors. This approach allows generalization of interactions mediated by ecosystem engineering, thus providing a framework for extrapolation and application to a wide range of environments. Finally (Chapter 8), I integrated the two steps in a unitary framework. Once 'fueled' with semi-empirical descriptions of the ecological processes, numerical models of sediment dynamics can be used to upscale the quantification of the interactions between biota and sediment transport to a whole-estuary context. While this work is specifically aimed to forecast estuarine geomorphological dynamics, the proposed framework can be generalized to quantify the realized impact of any kind of ecosystem engineering on landscape evolution and ecosystem functionality.

1.4.2 Structure

- **Chapter 2**: Measured environmental explanatory variables for species distribution models are inevitably a restrict subset of those which really matter in a realistic environment. When the aim is to predict species distribution on the base of a limited subset of explanatory variables, it should not been forget that different environmental contexts can modulate the species distributional responses. To investigate this point in estuarine environments, I compared the relationships between sediment granulometry and macrozoobenthos in two neighboring but differing temperate coastal ecosystems (SW Delta area, Oosterschelde and Westerschelde, The Netherlands).

- **Chapter 3**: Large infrastructures can have a broad and long-term impact on benthic habitats by affecting hydrological habitat characteristics on a whole-basin scale. Sustainable development requires the ability to predict responses of species to anthropogenic pressures. Novel modeling techniques can be useful to explore the effects of anthropic modification of habitats. In this chapter I focused our analysis on the effects of recent morphological and hydrological alteration of the Oosterschelde basin, which was partially embanked by a storm surge barrier (Oosterscheldekering, 1986).

- **Chapter 4**: The comparison of the Oosterschelde and Westerschelde basins offers the opportunity to identify the ecological consequences of two main anthropogenic impacts on estuaries: intensification of global maritime trades and need of coastal defense. By multidisciplinary integration of empirical data and modeling of estuarine morphology, hydrodynamics and benthic ecology, I investigated the long term effect on benthic habitats of two contrasting management strategies: deepening of estuarine channels to enhance navigability *vs.* realization of a storm surge barrier to enhance coastal safety. The integration of hydrological and ecological modeling allow us to investigate the effects of habitat alterations on a whole-basin scale and over a time span that is relevant compared to intrinsic morphodynamic time scales.

- **Chapter 5**: This chapter focuses on an evaluation method to optimize the disposal of dredged sediment with the preservation or improvement of benthic habitat suitability (essential for the ecological functioning). The macrozoobenthic community SDMs presented in the previous chapters were used to evaluate the impacts of sediment disposal on an intertidal shoal. The model proves it usefulness not only for the impact assessment for morphological changes, but also in the design of these changes.

- **Chapter 6**: Semi-empirical descriptions of the behavior of organisms (like that one I present) are needed for integrated modeling of biota-mediated physical processes. I propose an empirical framework to scale ecosystem engineering activity in term of fundamental ecological descriptors: individual body size and abundance of individuals. To test the framework, I perform a large series of experiments to measure and compare the body-size and individual abundance scaling of the ecosystem engineers activity performed from different archetypes of wet sediment engineers.

- **Chapter 7**: In this chapter, I joined the points previously addressed to produce an integrated physics-biota model of sediment erosion. As a first step, numerical models were used to predict the Westerschelde and Oosterschelde hydraulic habitat conditions. As a second step, the environmental conditions forecasted from the hydrodynamic models were used to estimate the composition and abundance of benthic community (Chapters 2-5). As a third step, I extend the framework proposed in Chapter 6 to account for the physical context in which the ecosystem engineers activity (*i.e.* bioturbation) is performed. Finally, hydrodynamic, species distribution and ecosystem engineers activity models were integrated to estimate the effect of bioturbators in a realistic environmental context.

CHAPTER 2

An application of non-linear quantile regression to macrozoobenthic species distribution modeling: comparing two contrasting basins

Francesco Cozzoli, Tjeerd J. Bouma, Tom Ysebaert and Peter M. J. Herman

Published as: Cozzoli, F., Bouma, T.J., Ysebaert, T. and Herman, P.M.J. (2013). Application of non-linear quantile regression to macrozoobenthic species distribution modeling: comparing two contrasting basins. MARINE ECOLOGY PROGRESS SERIES, 475, 119+

Abstract

The occurrence and distribution of macrozoobenthos in estuaries are strongly related to sediment grain-size characteristics. However, statistical prediction of the distribution of benthic populations as a response to a single environmental gradient has proven to be difficult, because the focal variable may set upper limits to the abundance, but other (partly uncorrelated) variables may cause considerable deviation from the maximum. A multi-quantile regression approach is better suited to characterize biota-environment relationships than a single (average or boundary) estimation, because it shows the variation in responses and quantifies the relative importance of other unmeasured factors. Here, a univariate application of non-linear quantile regression is proposed to account for heteroskedasticity and non-linearity in the biological response to sediment grain size. The analysis was applied to a large macrozoobenthic dataset from the SW Delta area (The Netherlands) to compare the relationships between sediment granulometry and macrozoobenthos in two neighboring but differing temperate coastal ecosystems (Oosterschelde and Westerschelde). Preference of individual species for grain-size was consistent between both systems, although in general a slightly higher median grain size (ca. + 60 % in grain diameter) was preferred in the Oosterschelde than in the Westerschelde. The major difference in the community was, however, that mud-fitted species dominated the assemblage in the Westerschelde, and sand-preferring species in the Oosterschelde. Although the prevalence of muddy and sandy sediments in both systems is similar, in the Westerschelde, strong hydrodynamic stress is correlated with sandy habitats, causing impoverishment of assemblages at sandy sites. In the Oosterschelde, sandy sediments are usually associated with much more benign conditions and have the richest species assemblage.

2.1 Introduction

Macrozoobenthic organisms play a fundamental role in estuarine ecosystem dynamics. They are central components of estuarine food webs [Herman et al., 1999] and they affect sediment biogeochemistry [Heip et al., 2001]. The importance of estuaries for human activities (fisheries, aquaculture, sand extraction, transport of goods and people, recreation) leads to changes in habitats [Kraufvelin et al., 2001] and directs research towards the study of the relationships between environmental conditions and distribution of macrozoobenthic organisms [Degraer et al., 2008, Herman et al., 2001, Snelgrove and Butman, 1994, Thrush et al., 2004]. Among the environmental factors directly delimiting the potential niche of macrozoobenthic species, the sediment composition is of great relevance [Gray, 1974]. On the one hand, the sediment composition is a proxy for typically covarying stressors, such as the hydrodynamic regime [Allen, 1985, Snelgrove and Butman, 1994], depth (or emersion time) and resource distribution [Heip et al., 1995, Herman et al., 1999, van der Wal et al., 2008]. On the other hand, it influences benthic biota directly as it constitutes the physical matrix in which benthic organisms live, gather food and construct burrows [Gray, 1974]. Sediment granulometry correlates with hydrodynamic stress [van Prooijen and Winterwerp, 2010], water permeability [van Ledden et al., 2004], organic matter content [Curry et al., 2007, Mayer, 1994] and microbial oxygen consumption [Sutherland et al., 1998]. Degraer et al. [2008] found that sediment median granulometry and mud percentage are the most important environmental variables in determining macrozoobenthos spatial distribution in the Belgian North Sea. The influence of sediment composition on macrozoobenthic distributions is evident also in estuarine environments, where the salinity gradient can have a major relevance [Ysebaert et al., 2002]. The variability in the morphological, hydrological and chemical characteristics [Day et al., 1989] of estuarine environments generates spatial and temporal patterns in species distribution [Wolff, 1983, Ysebaert et al., 2003]. The accurate statistical prediction of these patterns as a response to an environmental gradient has proven to be extremely difficult [Butman, 1987, Chapman et al., 2010, Snelgrove and Butman, 1994] as the observed distributions are the outcome of complex interactions between hydrodynamics, sediment dynamics and benthic biology [Herman et al., 2001]. When unmeasured factors interact with the measured factor, they generate an error distribution with respect to the variables included in the model. Complicated forms of non-linear and heterogeneous response distributions can be expected in observational studies where many important processes interact [Cade et al., 2005]. Stochastic factors also contribute to variability in the response of individual sample densities. Commonly univariate species-environment relationships show heteroskedastic error distributions: variances are smaller in limiting conditions, but they increase for more suitable sites [Anderson, 2008, Cade et al., 1999, Terrell et al., 1996, Thomson et al., 1996]. The local spatial and temporal covariance structures between environmental factors may differ from one system to another, thereby decreasing the predictability of species' responses across different scales of observations [Chapman et al., 2010, Kraufvelin et al., 2001, Thrush et al., 2005]. Traditional regression methods like Ordinary Least Squares focus exclusively on changes in the means. They assume that the response variable has constant variance in its errors, regardless of the value of the predictor variable. Thus, central estimators are not able to account for the variance-mean relationship. In a regime of limitation by subsidiary factors (high prevalence of zero observations along the entire gradient), they are not representative of the higher densities and they may fail to distinguish real non-zero changes [Cade and Noon, 2003, Terrell et al., 1996]. To overcome these confounding effects, recent studies on species distribution models have focused on models that predict the likelihood of species presence [Franklin, 2010]. Presence/absence observations minimize variation by emphasizing the lower threshold (one specimen per sample) in the observations. They give as output a measure of habitat suitability expressed as the frequency of positive observations (presence) given the environmental conditions. Habitat suitability models have been often used to describe and compare relationships between macrozoobenthic species distribution and different environmental factors, including sediment texture [Degraer et al., 2008, Ysebaert et al., 2002]. A second approach to heteroskedasticity is by applying a regression analysis through the 'ceiling' of the distribution. Upper boundary regression emphasizes the upper limit (maximum attainable abundance), consistent with the ecological theory of the minimum [Cade et al., 1999, Cade and Noon, 2003, Cade et al., 2005, Downes, 2010]. While all lower observations are constrained by subsidiary factors, the upper edge of the multivariate data cloud is mostly representative of the (potential, maximal) response of the species to the measured variable. Examples of upper boundary regression applied to benthic species distribution modeling along the sediment granulometry gradient can be found in Anderson [2008], Ellis et al. [2006], Thrush et al. [2005, 2003]. The methodologies mentioned above offer only an inaccurate (OLS) or partial (occurrence and maxima models) description of heteroskedastic distribution. While habitat suitability is more stable through time compared to abundances and is generally considered as highly important for management strategies [Degraer et al., 2008], the magnitude of the effect organisms have on ecosystem processes is often influenced by the realized size and density rather than the presence or the potential abundance. The estimation of density-related effects of macrozoobenthos (*e.g.* the influence of macrozoobenthos on sediment dynamics or the availability of food for the avifauna) is likely to require extra information about the probability that a density is realized at given environmental conditions. The quantile regression model [Koenker and Bassett, 1978, Koenker and Hallock, 2001, Koenker and Machado, 1999] can solve this problem. Quantile regression is emerging in ecology as a comprehensive approach to the statistical analysis of linear and nonlinear response models [Austin, 2007, Cade and Noon, 2003, Downes, 2010, Franklin, 2010]. This method aims at fitting any desired quantile of a response variable distribution to an independent variable. Regression quantile estimates can be used to construct predictions without assuming any parametric error distribution and without specifying how variance heterogeneity is linked to changes in means. The effect of the error distribution to parameters is indexed by a family of quantiles. By representing the regressions of different quantiles simultaneously, the quantile regression model expresses the expected variation in the form of a conditional probability density distribution. The multi-quantile regression models permit to estimate the expected distribution of observations as (co-) determined by all other factors affecting occurrence and abundance [Cade et al., 1999, Cade and Noon, 2003]. Compared to presence/absence and maxima analysis, they offer not only a measure of habitat suitability (occurrence or potential maximum) but also a more complete view of biotic distributions along single gradients. Under this point of view, a multi-quantile regression approach can be preferable to a single rate models not because it “fits better”, but because it provides better insights on observed distributions. The full method, including the simultaneous estimation of regression models for all quantiles, has been suggested by Cade et al. [2005] to be the best solution when the interactions between measured and unmeasured environmental variables are unknown, and one has no a priori basis for the selection of one of the quantiles as the most representative.

In this paper we propose the use of non-linear quantile regression to estimate the entire cumulative distribution of common macrozoobenthic species as a function of granulometry in temperate coastal basins. The primary aim of the analysis is to accurately describe how the biomass is distributed along a gradient of sediment composition. This description is fairly complete, as it yields a predicted probability distribution of the response variable for all values of the independent variable. To be properly validated, the predicted probability distribution should be compared with a complete population of values from an independent dataset. It was not possible to find, within a single basin, two or more sufficiently large and independent data sets. We therefore approached the validation problem from a different angle, by comparing two neighboring coastal ecosystems: the Oosterschelde and the Westerschelde (Figure 2.1). The sediment grain size composition is per se similar in both basins (Figure 2.3). Due to the different anthropogenic impacts there is a different covariance structure between sediment composition, water salinity and local hydrodynamic forcing (Table 2.1). The basins share a common pool of macrozoobenthic species, but abundances and dominances often differ. The comparison of the Westerschelde and the Oosterschelde allows evaluating the consistency of the predicted responses despite different covariance structures with other variables. Apart from the statistical validation of the method, it also allows formulating hypotheses on causal factors (covariance structure within environmental variables) explaining the differences in the response of macrozoobenthic community to a similarly distributed gradient in sediment composition.

2.2 Material and methods

2.2.1 Study area

The Scheldt estuary, a macrotidal, turbid, nutrient-rich, coastal plain estuary is situated near the border between The Netherlands and Belgium (Figure 2.1). It was originally composed of two aligned and interconnected water bodies called Westerschelde and Oosterschelde. The present geomorphology and functioning of these basins has been deeply affected by human interference [Louters et al., 1998]. Due to land reclamation, the Oosterschelde was progressively separated from the Westerschelde. The freshwater input from the Schelde river was definitively interrupted in 1903, transforming the estuary in an enclosed sea-arm with stable (marine) salinity (Table 2.1). The construction of two back-barrier dams in 1965 and 1969 had a significant impact on the Oosterschelde tidal hydrodynamics and sediment transport. The effects of these interventions were still ongoing when in 1986 the basin was partly closed off from the sea by a storm surge barrier (Delta Works, Eelkema et al. 2012). After the Delta Works the tidal prism of the Oosterschelde basin has been reduced by approximately 30%. Current velocities have declined by 20-40% in the tidal channels and by over 40% around the tidal shoals and salt-marshes [Louters et al., 1998]. Simultaneously the import of sediment from the coastal sea has been cut off by the storm surge barrier. As a consequence, the channels tend to fill up using sediment eroded from the tidal flats. The availability of suspended mud for deposition on the flats has decreased considerably, with present suspended particulate matter concentrations being only half those of the pre-barrier situation [Louters et al., 1998]. The erosive trend of the Oosterschelde's tidal flats has increased to a warning level for coastal defense and habitat preservation, putting new challenges for the Oosterschelde management [Bijker, 2002]. The Westerschelde, due to its importance as a shipping route to the Antwerp port, kept its open connection to the sea. It is, however, subject to extensive dredging in order to enhance its function as a shipping route. The estuary is character-

Table 2.1: **Some characteristics (year average) of the Westerschelde and the Oosterschelde.** The Westerschelde values separated by a dash are referring to the mouth (right) and to 80 km upstream (left)

Variable	Westerschelde	Oosterschelde
Water surface (km)	310	351
Depth (m)	9.7 - 13.7	8
Tidal range (m)	5.20 - 3.82	3.25
Tidal volume (m^3 10^9)	1	0.88
Salinity (PSU)	2.5 - 29	30
Freshwater load (m sec^{-1})	104	25
Suspended sediment (mg l^{-1})	101	25

ized by a fully developed salinity gradient and a complex network of channels surrounding several large intertidal flats and salt marshes. Current velocities, especially in the gullies, are high [De Vriend et al., 2011]. The suspended particulate matter concentrations are on average 4 times higher in the Westerschelde compared to the Oosterschelde.

`Figures/Chapter_2/Map_Study_area.pdf`

Figure 2.1: **Map of the study area.** Note the back-barrier dams and the sea-side storm surge barrier in the Oosterschelde

2.2.2 Sampling and data processing

A total of 3926 macrozoobenthic samples, taken between 2000 and 2008, were used in the analysis. Samples were collected by Netherlands Institute of Sea Research (NIOZ) - Yerseke and Rijkswaterstaat (RWS). The use of such a large and multi-year dataset accounts for most of the spatiotemporal variability of environmental conditions and biotic responses. Data collection was carried out in spring and autumn (except for spring 2006, for which no data are available). While in the Westerschelde samples were randomly collected within four depth strata, in the Oosterschelde the sampling was repeated at the same sites across years in similar depth strata as used for the Westerschelde sampling. In both basins, 25% of the records come from intertidal sites, 50% of the records were collected above a depth of 5 m NAP (Normaal Amsterdams Peil, the Dutch height datum, 0 m NAP = mean sea level in Amsterdam) and 95% above 20 m NAP. From each site, three cores of 8 cm diameter were taken and lumped. Sediment was sieved through 1 mm mesh. Subtidal sites were sampled using a large (30 cm diameter cylinder) box-corer, from which the three 8 cm sub-cores were extracted. The collected animals were weighted and classified at the lowest practical taxonomic level. Abundances are expressed as number of individuals m^{-2}; biomass as mg m^{-2} of ash-free dry weight. Rare or occasional species (less than 6 observations) were removed from the dataset (see at Ysebaert 2002). After this skimming, the dataset comprised 194 taxa. Sediment samples were analyzed for grain size distribution by laser diffraction performed with a Malvern Mastersizer 2000. For each sample, the median sediment grain size (d50), expressed in μm, and the % of different granulometric size-classes (mud < 63 μm $<$ very fine sand < 125 μm $<$ fine sand < 250 μm) were reported. In this analysis mostly d50 is used. Depth (m NAP) was measured on site. Tidal-averaged Bed Shear Stress (BSS, N m^{-2}) and daily-averaged salinity (spring) were calculated using the DELFT3D FLOW model (version 3.55.05.00) with tidal forcing only [Lesser et al., 2004]. The spatial resolution of the grid varies from more than 2000 m at the seaward boundary to around 100 m at the Oosterschelde inlet. For the Westerschelde, 25% of the records were collected at a salinity higher than 25 PSU unit, 50% of the records at a salinity between 25 and 18 PSU unit.

2.2.3 Data analysis

Quantile regression was developed as an extension of the linear regression model [Koenker and Bassett, 1978]. The τ-th sample quantile of any random variable Y, $Q(\tau)$, is that value splitting the distribution in a *tau* portion $Y \leq Q(\tau)$ and a $(1 - tau)$ portion $Y > Q(\tau)$. It can be calculated by by minimizing the expectation of the loss function $\rho_\tau(y_i - \xi)$:

$$\underset{\xi \in \Re}{\operatorname{argmin}} \sum_{i=1}^{n} (\rho_\tau(y_i - \xi)) = \underset{\xi \in \Re}{\operatorname{argmin}} \left[(\tau - 1) \sum_{y_i \leq \xi} (y_i - \xi) + \tau \sum_{y_i > \xi} (y_i - \xi) \right] \tag{2.1}$$

with respect to $\xi(\tau)$ possible solutions, the smallest of which is $Q_Y(\tau)$. The simultaneous estimation of several quantiles permits to characterize the distribution of the variable Y by its quantiles $Q_Y(\tau)$. By extension, the linear conditional quantile $Q_Y(\tau|X = x)$ linearly depending on an independent variable X can be estimated by replacing the term ξ in Equation 2.1 with the term $x_i\beta$:

$$\hat{\beta}(\tau) = \underset{\beta \in \Re^p}{\operatorname{argmin}} \sum \rho_\tau(y_i - x_i'\beta) \tag{2.2}$$

where $\hat{\beta}(\tau)$ is the unknown regression coefficient for the τ-th quantile and β are the possible solutions with respect to x (Equation 2.2). With $\tau = 1$, $Q_\tau(y|x_i)$ is the expected maximal response at x_i; in case of biomass or abundance distributions this value represents the expected response when (unmeasured) disturbance is at a minimum, or (unmeasured) facilitation at a maximum. The succession of the underlying quantiles represents the expected distribution of responses given the actual distribution in the habitat of the unmeasured facilitating or inhibiting variables. We extend the use of quantile regression to the non-linear case by the use of spline transformations [Koenker, 1994, Thompson et al., 2010]. The B-spline smoothing of the explanatory variable produces flexible curves without linking the response shape to a predetermined function. Regression splines produce a similar output to general additive models, but they are computationally faster and better suited for the analysis of large spatio-temporal datasets [Elith and Leathwick, 2007]. Quantile regression can easily be coupled with a spline transformation of the independent variable. A B-spline function is a piecewise polynomial of given order satisfying second-order continuity conditions between the pieces. Breakpoints are automatically selected by an iterative calculation [Barsky and Thomas, 1981]. Because of its property of continuity, the polynomial resulting from a B-spline expansion of the explanatory variable forms a smooth and flexible curve. B-spline quantile regression analysis is particularly suited for describing the heterogeneous responses of species abundances to environmental factors [Anderson, 2008]. The main variable to control the flexibility of the spline shape is the degree of the polynomial, resulting in the number of parameters for the regression model. As suggested from previous studies [Anderson, 2008, Cade et al., 2005] we select the spline degree from 2 to 5. Measurements of goodness of fitness like the R^2 and its equivalent for quantile regression [Koenker and Machado, 1999] cannot decrease with increasing number of parameters, thus they are not useful to select the most appropriate spline degree. Conversely, the Akaike Information Criterion [Akaike, 1980] offers a relative measurement of the goodness of fit based on the trade-off between the accuracy and the complexity of the model: the lowest AIC value provide a summary measure of the best fit with the fewest number of parameters. In this analysis we used a small sample size corrected version of the Akaike Information Criterion (AICc). Non-linear multi-quantile regression models are able not only to reproduce the asymmetry of the distributions along the x axis but also the asymmetry along the y axis (*i.e.*, the rate at which the abundances drop to zero beyond the upper boundary of the distribution). In this study B-spline quantile regression was used to characterize relationships between the median sediment grain size (d50 μm) and the principal community descriptors total biomass (mg m^{-2}), abundance (m^{-2}), number of taxa (S) and Shannon diversity index. The method was also used to regress the biomass of the 25 most frequently observed (relative number of occupied samples) taxa on sediment d50. We analyzed the distribution of the most abundant taxa irrespectively to the level of taxonomic accuracy at which they were identified. We made this choice to offer an as complete and realistic as possible overview of the overall benthic assemblages. Focusing the analysis only at specific level would force us to reduce the numbers of groups accounted for in the analysis due to scarcity of data available for single species. Species optimal d50 were assessed as the average of the optimum predicted by each quantile of the biomass distributions predicting occurrence. Environmental variables were significantly affected by spatial autocorrelation (Moran's I p-value$< 10^{-10}$ in both basins). However the spatial trend was not removed from the dataset as Cade et al. [2005] showed that quantile regression models have high performance in explaining the observed variance also in the presence of spatial autocorrelation of environmental variables. Data scarcity at the extremes of the (long-tailed) d50 distributions can affect the behavior of the spline function, leading to overestimation of the expected densities. In order to avoid this effect, the analysis was limited between the 1^{st} (42 μm) to the 99^{th} (358 μm) percentile of the Oosterschelde range of median grain size. To make the analysis still more resistant, the regression was 'shrank' by computing the fit with a lasso algorithm [Tibshirani, 1996] using as threshold parameter $\lambda =$ 10 for analysis of community indices and $\lambda = 1$ for single taxa analysis. The full quantile range from $\tau = 0.01$ to $\tau = 0.99$, with increments of 0.005, was fitted. All the statistical analyses were implemented in R [R Development Core Team, 2011] using the packages 'splines' and 'quantreg' (Koenker, 2010).

2.3 Results

2.3.1 Abiotic variables

The Oosterschelde and Westerschelde sampling sites show similar sediment composition and distribution (Figure 2.3). Also the ratios between the different granulometric classes of sediment appear similar across basins. Measures of sediment composition related to the percentage of different granulometric size-classes are truncated to 0 or 100 % at the extreme of the gradient, while sediment median grain size is more continuously distributed (Figure 2.3). For this reason the latter variable was preferred in this study.

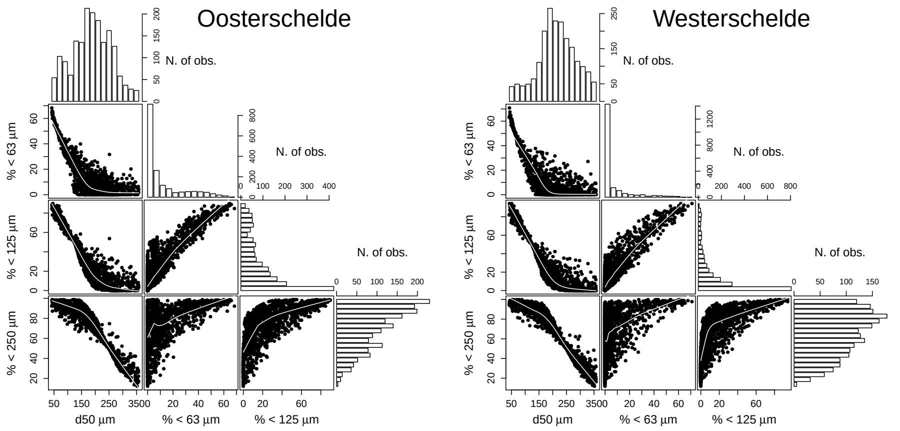

Figure 2.3: **Correlograms of d50 and different sediment fractions in the Oosterschelde and Westerschelde.** Histograms show the number of observations

On average, the sediment in the Oosterschelde was slightly but significantly (p-value $< 1^{-10}$) finer than in the Westerschelde (Figure 2.4). In the intertidal samples the d50 distribution was wider in the Westerschelde than in the Oosterschelde. The relationships between sediment d50, bottom shear stress and depth differ across basins (Figure 2.5). In the Westerschelde fine sediments are rare at deeper sites and at higher hydrodynamic stress values. In the Oosterschelde the relations with depth and hydrodynamic stress are less significant than in the Westerschelde. In the case of bottom shear stress, the distribution of the explanatory variable was very different between the two systems: in the Oosterschelde the maximal tide-averaged BSS is 0.92 N m^{-2} , while in the Westerschelde BSS is over 3 N m^{-2}. Sediment composition in the Westerschelde is not correlated with the average salinity gradient (p-value=0.1107).

2.3.2 Biotic variables:

Total biomass, abundance, number of taxa per sample and Shannon diversity were different between the basins (Figure 2.6). Comparing the median values, the benthic communities of the Westerschelde reached only 11% of the biomass (Westerschelde 435 mg m^{-2} *vs.* Oosterschelde 3832 mg m^{-2}) , 13% of the abundance (266 *vs.* 2000 individuals m^{-2}), 28% of the number of taxa (2 *vs.* 7 taxa for site), and 42% of the diversity (0.53 *vs.* 1.27 for site) realized in the Oosterschelde. The total biomass and abundance distributions are positively skewed, indicating a prevalence of sites with low benthic abundance and biomass. Based on the 25 most frequent (relative number of occupied samples) taxa, clear differ-

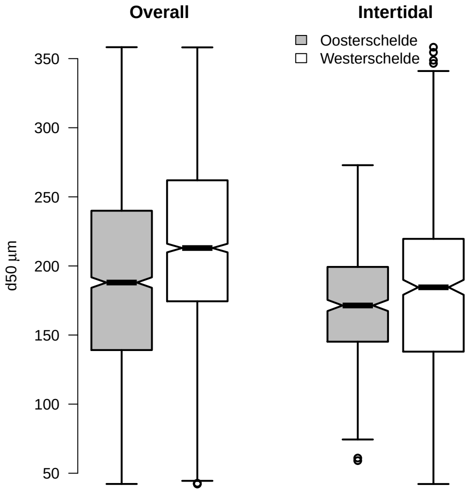

Figure 2.4: **Boxplot of sediment d50 distribution across basins** for the overall dataset and for intertidal samples only

ences in taxonomic composition were found between the benthic assemblages in both basins (Figure 7). Only few taxa, *i.e. Arenicola marina* and *Corophium arenarium*, reached similar biomass and frequency in the Oosterschelde and the Westerschelde, while the majority were abundant in one basin and scarcely present in the other. The Westerschelde was dominated by the Polychaeta *Heteromastus filiformis* (avg. biomass 457 mg m^{-2}, frequency 48%) and *Hediste diversicolor* (avg. biomass 201 mg m^{-2}, frequency 11%), and the bivalve *Macoma balthica* (avg. biomass 636 mg m^{-2}, frequency 27%), all deposit-feeding. In contrast to other tube-building worms, *Pygospio elegans* (avg. biomass 36 mg m^{-2}, frequency 22%) attained 6 times higher biomass in the Westerschelde than in the Oosterschelde (Figure 2.7).

Most of the dominant taxa in the Westerschelde were almost absent in the Oosterschelde. The most common species in this basin were the scavenger-predator *Nepthys hombergii* (avg. biomass 427 mg m^{-2}, frequency 44%) and the burrower-deposit feeder *S. armiger* (avg. biomass 308 mg m^{-2}, frequency 59%). High biomass values were observed in the Oosterschelde for the small herbivorous gastropod *Peringia ulvae* (avg. biomass 829 mg m^{-2}, frequency 26%). In the Oosterschelde we also recorded high biomass and frequency of the tube-dwelling worms *Lanice conchilega* (avg. biomass 1014 mg m^{-2}, frequency 23%), *Spiophanes bombyx* (avg. biomass 36 mg m^{-2}, frequency 31%) and *Notomastus latericeus* (avg. biomass 254 mg m^{-2}, frequency 15%) and for the deposit-feeding worms *Streblospio shrubsolii* (avg. biomass 17 mg m^{-2},

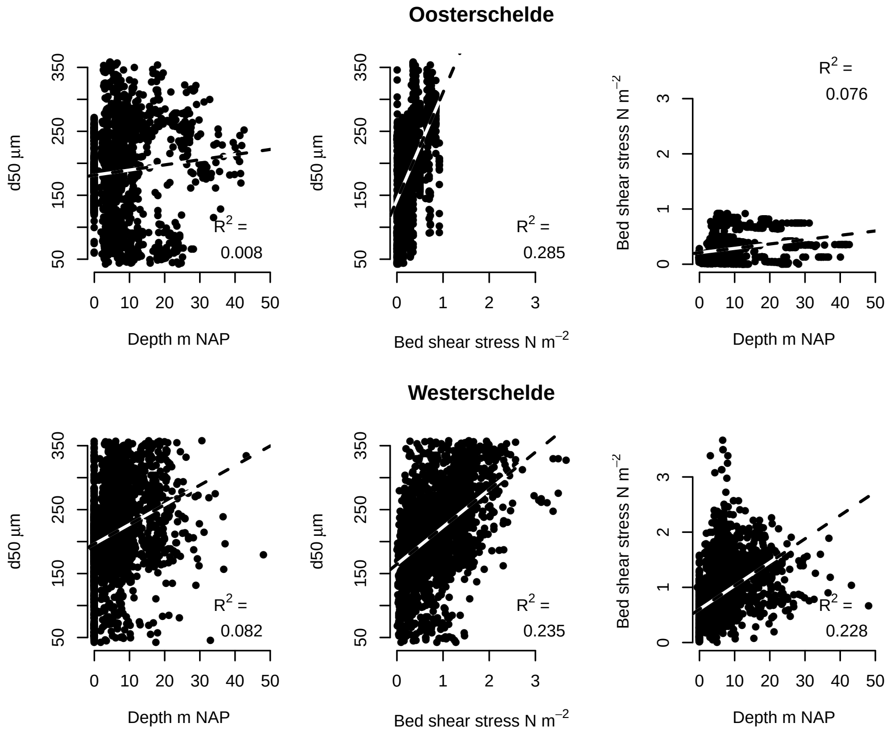

Figure 2.5: **Correlation of sediment d50 with measured depth and modeled Bed Shear Stress**

frequency 39%) and *Capitella capitata* (avg. biomass 45 mg m^{-2}, frequency 33%).

2.3.3 Non-linear quantile regression

Community indices:

Total biomass, total abundance, number of taxa and Shannon diversity index showed relevant variations along the sediment d50 gradient (Figure 2.8). For each point along the sediment d50 gradient, the total biomass and abundance were asymmetrically distributed around the median value (the fitted median curve is closer to the 25^{th} than to the 75^{th} quantile curve). As effect of data heteroskedasticity the distance between quantiles is not constant along the gradient, but decreases at less suitable conditions. The number of taxa and the Shannon diversity distributions are homoskedastic in both basins. In the Westerschelde, the maximum expected biomass and diversity peaked at d50

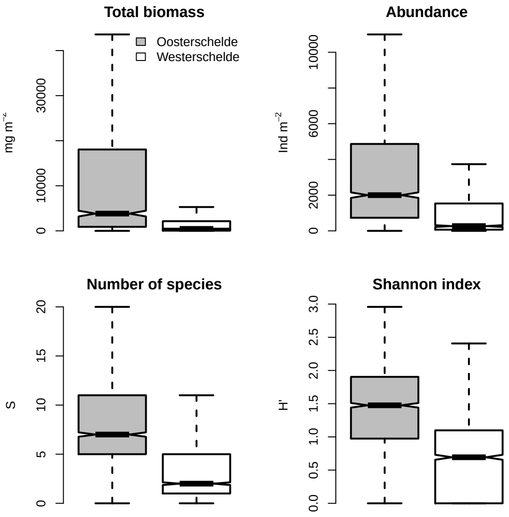

Figure 2.6: **Boxplot of community indices distribution across basins**

Figure 2.7: **Bar plot of mean biomass and occurrence of the 25 most common taxa in the Westerschelde and the Oosterschelde.** Stars show the significance of Fisher's test and ANOVA on differences between basins

of ca. 55 μm. High abundance, richness and diversity were only observed in samples with small median grain size. In the Oosterschelde, the community indices had a unimodal shape, reaching their highest values at an average d50 of around 170 μm. In contrast to the Westerschelde, benthic assemblages in very coarse sediments (d50 of 350 μm) still conserved 56% of the maximal diversity and 26% of the maximal biomass. At the lower range of d50, the Oosterschelde presented similar diversity but lower biomass and abundance than the Westerschelde. For a d50 up to 100 μm, the probability to measure an elevated abundance in the Oosterschelde was consistently lower than in the Westerschelde, while the differences between the lower quantiles (observations around the 25^{th} quantile) were less pronounced.

Individual taxa:

Predictions from nonlinear quantile regression of the biomass distribution of the 25 most common taxa in the Westerschelde and Oosterschelde basins are shown in Figure 2.9. Forecasted biomass distributions tended to be unimodally distributed along the gradient. Only *Abra alba* and *Eteone spec.* (Oosterschelde)

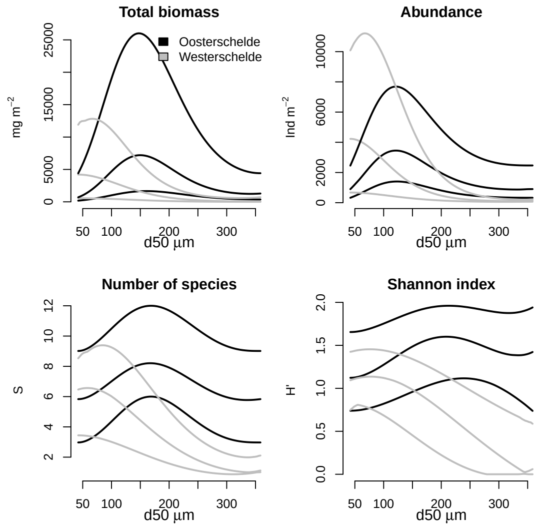

Figure 2.8: **Distribution of species richness, total biomass and ecological diversity along the sediment d50 gradient.** The expected distributions are sketched using the 25^{th}, 50^{th} and 75^{th} quantiles

seemed to be unaffected by sediment grain size. Optima in the distributions of the different quantiles generally coincided well at approximately the same d50. The order of species preference along the sediment d50 gradient was similar in both systems (Figure 10). The estimated optimal values of d50 covered the full range of observed d50 values in the samples, between a minimum of 44 μm (*Streblospio shrubsolii*) to a maximum of 319 μm (*Nepthys cirrosa*). These extremophile species did not change preference for sediment granulometry across basins. In the Westerschelde, d50 optima were concentrated at fine granulometry. The 80% of the taxa had their peak abundance in the first quarter of the d50 gradient. In the Oosterschelde, the taxa were spread out much wider over the gradient. With the exception of four taxa (*S. shrubsolii*, *A. marina*, *Capitella capitata*, *Nepthys cirrosa*), all taxa that occurred in both basins realized their peak at smaller grain size in the Westerschelde than in the Oosterschelde (Figure 10). The order of species preference is roughly preserved across basins, with the exception of the broad taxonomic group of Oligochaeta, and three taxa that almost exclusively occurred in one of the basins and were consequently badly estimated in the other: *H. diversicolor*, *Ensis spec.* and *L. conchilega*.

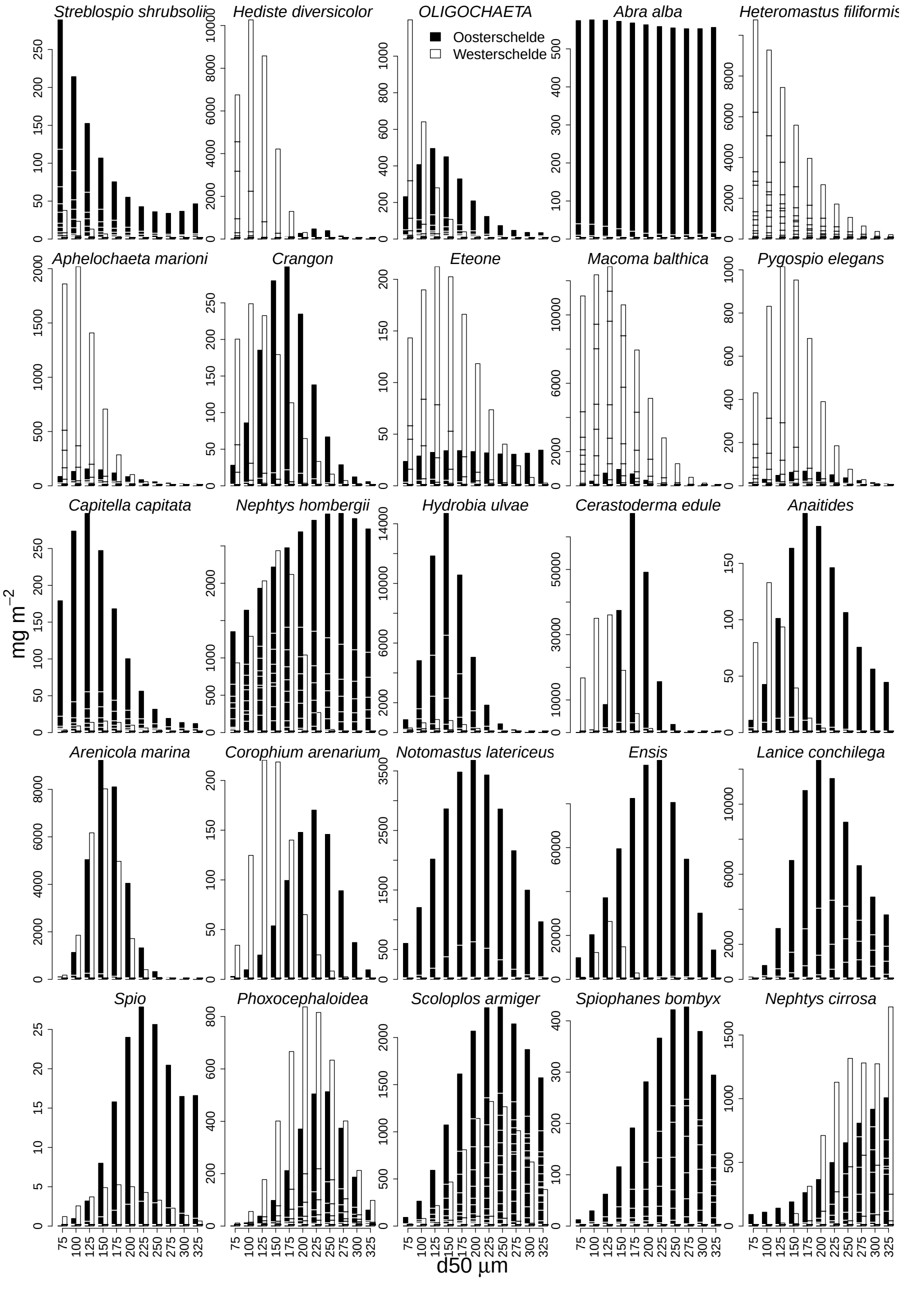

Figure 2.9: **Predicted d50-conditioned cumulative probability functions** for the biomass distribution of the 25 most common taxa in the Oosterschelde (black) and Westerschelde (white) basins. Bars show the maximal biomass predicted for the sediment compositions indicated on the x axis. Tick marks along the bars are drawn at intervals of 0.05 (1 tick mark from the top, then in the 5% of the cases is expected to found a biomass superior to that value at the given d50)

2.4 Discussion

2.4.1 Considerations about the statistical method

In this paper we use quantile regression to study the effect of a single environmental variable (sediment grain size) in two systems where the covariance structure with other environmental variables is very different. There is a significant spatial gradient in salinity in the Westerschelde, which is almost completely absent in the Oosterschelde. Furthermore, the correlation structure between depth, bottom shear stress and sediment grain size composition is very different between the two systems (Figure 2.4). This comparison shows that the models can only partly be considered as validated by the systems comparison. For several of the species, the maximum biomass modeled (τ=0.99) differs largely between the two systems. Although the first interpretation of the maximum is that it shows the value to be reached at this grain size when all other conditions are optimal, it is clear that for many species the conditions are never near optimal in at least one of the two systems. Thus, the maxima estimated for a particular grain size, when only using data from a single estuary, are not unconstrained. As argued before by [Thrush et al., 2005], there is a strong scale dependency in species-environment relations in estuaries. In order to estimate real optimal biomass values for a particular grain size, a large number of ecosystems will have to be sampled in order to ensure that optimal conditions for all other variables have been realized. Factors may vary considerably between ecosystems but hardly within each of the systems. It is impossible to estimate the influence of such factors when restricting the analysis (or the validation) to a single system. With the exception of a few species for which the comparison is difficult, the fitted models do yield consistent estimates of the optimal grain size of a species over the two systems. Often the estimate for the Westerschelde is for a somewhat lower optimal grain size, but the general ordering of the species remains the same (Figure 2.10). Therefore, the relative predictions by the model (where will the species occur if it does occur at all) are much better validated by the systems comparison than the absolute predictions.

Our examples show that the response curves for the different quantiles are similar and the range of optima of the different quantile regression models is limited (Figure 2.8). This can be ascribed to correlations (Figure 2.5) and interactions between measured and unmeasured environmental variables, that have the effect to increase the non-linearity and decrease the heterogeneity of the responses [Cade et al., 2005]. The similitude between quantiles is indicative of a strong correlation between the percentage of occurrence, the average and maximal biomass. This lead to the considerations that both occurrences, central and maxima estimators can have good performances in describing species areal. When comparing the response models between species, we see that the majority of the single species models scored the lowest AICc when fitted on a quadratic or cubic spline. Due to this relatively low degree, most fitted models had a general appearance resembling a Gaussian response model. The relative advantage of having a flexible non-parametric form for the response curve was limited, as was the relative advantage of having all percentiles fitted. However, it is reassuring that the shape and the similarity between quantiles followed from the fitting procedure itself and were not imposed a priori. Thus, there is a perspective of simplifying the fitted models without much loss of information; the presently fitted, more complicated models, could form an excellent basis for the choice of a simpler model with fewer parameters.

2.4.2 Community responses across basins

Benthic community distributions were found very different across the basins, with higher biomass, density, richness and diversity characterizing the Oosterschelde. This was partly caused by higher peaks (for biomass, species richness and diversity), but mainly by a more skewed distribution along the d50 gradient in the Westerschelde (Figure 2.8). In the latter basin high community index values are realized only at muddy sites. All measures of biological richness dropped suddenly in coarser sediments, between 100 and 250 μm. This pattern can be interpreted as the result of stronger limitations at the right side of the d50 gradient. Tidal variability in salinity at a particular place is responsible for a considerable part of the brackish-water depression in diversity [Attrill, 2002]. The high and stable salinity in the Oosterschelde might partially explain the higher species richness and diversity compared to the Westerschelde [Ysebaert et al., 2003]. Higher salinity in the Oosterschelde may also explain the absence, in that system, of species that have clear preference for brackish conditions, such as *H. diversicolor*. However, sediment composition in the Westerschelde has been observed to be homogeneously distributed along the salinity gradient. Salinity variations by themselves are therefore not a sufficient explanation for the absence of sandy substrates with high biological richness (either in abundance, biomass or species number). In the Oosterschelde the probability to realize high community performances is maximal in fine sand substrates (Figure 2.9). Hydrodynamic stress in these sediments is lower compared to the Westerschelde (Figure 2.5), most likely explaining the higher values observed. When comparing the responses of total biomass and total abundance (Figure refCom2) between the two systems, it is noticeable that they differ. While predicted biomass in Westerschelde is lower than in Oosterschelde over almost the entire sediment gradient, predicted abundance tends to be higher for Westerschelde in fine sediments. Especially in these muddy sediments, the fauna is mainly composed of small organisms (*e.g. H. filiformis* average per capita biomass 0.9 mg, *S. shrubsolii* 0.1 mg) that become superabundant in fine, organic rich sediments [Nilsson and Rosenberg, 2000, Norkko et al., 2006, Pearson and Rosenberg, 1978]. In the Oosterschelde the maximal biomass and abundance were realized at finer granulometry (respectively at d50 of 147 and 126 μm) than the maximal species number and diversity (d50 of 187 and 252 μm). This behavior is in agreement with the Intermediate Disturbance Hypothesis: the highest diversity is reached at intermediate level of disturbance while the community is dominated by a few opportunistic species at high disturbance, and by a limited number of powerful competitors at low disturbance [Dial and Roughgarden, 1998]. The differences in individuals body size and life cycle suggests that it would be interesting to repeat this analysis on a trait-based approach [Statzner et al., 2004].

2.4.3 Individual taxa responses across basins

The 25 taxa analyzed in detail generally showed well-defined and differentiated responses to sediment grain size, with very different height but similar position of the optimum. The different correlation structure between granulometry and other environmental factors leads to a replacement of mud-preferring species by sand-preferring species when going from the Westerschelde to the Oosterschelde, rather than to a drastic shift in the sediment type occupied by a particular species. Therefore, although sediment granulometry does function as a proxy for other variables (hydrodynamic conditions in particular), it appears that sediment per se is also important, and for some species, such as *A. marina*, even predominant. While the taxa largely conserve their qualitative response to sediment texture, the quantitative response is strongly dependent on subsidiary factors. The higher abundance of low-salinity tolerant species (*e.g. H. filiformis*, *H. diversicolor*, *M. balthica*) in the Westerschelde can be partially explained by the presence of a gradient from brackish to saltwater [Ysebaert et al., 2002]. The same argument, however, cannot be used to explain the absence of sand-preferring species, since sandy sites are available at both low and high salinity also in the Westerschelde. These patterns are more likely related to the high hydrodynamic stress typically experienced by coarser sediments in this basin. Sandy sites are not available at low current velocities, as shown in Figure 2.5. It is likely that sand-preferring species cannot establish in their favorite environment due to this enhanced stress. We conclude that benthic organisms adapt their optimum with respect to granulometry only over a limited range and adapt to limitation by subsidiary factors by a drastic decrease in abundance. The representation of the different quantiles instead of a single parameter of distributions allows clearer insights on the observed patterns. In this respect it is interesting to compare the form of the expected distributions between species or, within the same species, between basins. Observing the distributions of *H. filiformis*, *M. balthica*, and *H. diversicolor* in the Westerschelde (Figure 2.9), it is clear that the latter species is way less abundant than the previous two although the higher 10% of the observations falls in a similar range. *A. marina*, *C. edule* and *Ensis spec.*, *i.e.*, taxa with high per capita biomass, have very skewed quantile distributions because rarely more than a few individuals are found at the scale of the sampling unit. Within species but between basins, it is instructive to compare the distributions of *Nepthys hombergii* and *N. cirrosa*. The upper boundary is similar or even higher in the Westerschelde than in the Oosterschelde, but the quantiles following below the maximum are much higher in the Oosterschelde. This means that a few sites have high biomass, sometimes even higher than the maximum in the Oosterschelde, but apart from these there are hardly any sites with sub-optimal conditions and sub-maximum biomass (Figure 2.8). The systematic shift of optima towards coarser sediment in the Oosterschelde (Figure 2.10) is indicative of conditions that can be considered as an emergent property of the local covariance structure of environmental variables. Biotic components are involved as well in determining the local combination of relevant environmental variables, and they can co-explain part of the observed variation between basins. As example, *H. filiformis* is a subsurface deposit feeding Polychaeta well adapted to muddy and organic-rich (oxygen-poor) sediment thanks to high oxygen-affinity hemoglobin. This species exhibits exceptionally high densities in the muddiest bottoms of some estuaries while it is generally scarce in others (Thrush et al. 2005, Figure 2.7). The abundance of *H. filiformis* has been found to be mostly controlled by predation from *N. hombergii* [Beukema et al., 2000]. High biomass of the latter species is exceptional in the Westerschelde, and much rare than in the Oosterschelde (Figure 2.9). The combination of physical (low salinity in part of the estuary, hydrodynamic stress also relevant to muddy sites) and biological conditions (intense predation only a few sites) in the Westerschelde leads to a striking dominance of *H. filiformis*.

2.4.4 Management considerations

To our knowledge, the recent coastal engineering works in the Oosterschelde are the main cause of the decoupling of the association between stronger hydrodynamics and coarse sediment [Louters et al., 1998], while the deepening of the Westerschelde channels had probably the opposite effect. Our analysis suggests that the benthic community composition and structure were affected by these human interventions. Anthropogenic alterations of the Oosterschelde, although leading to management problems in conservation of the eroding intertidal flats, have also probably led to improved species richness and biomass of the benthos. Anthropogenic alteration of the Westerschelde may have restricted benthic life in sandy sediments due to enhanced hydrodynamic stress [De Vriend et al., 2011]. Further analyses, including historical data, should confirm these observations and reveal proper management strategies for both basins.

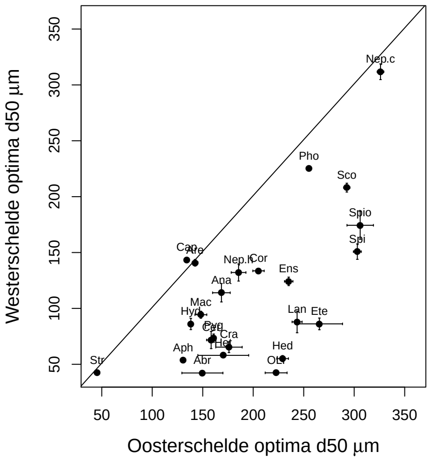

Figure 2.10: **Relationship between the sediment d50 optima detected separately for the two basins.** Optima are calculated as average of the optimal d50 values detected for each quantile of the forecasted distributions (from τ=0.01 to τ=0.99). The line shows the 1:1 ratio. Error bars are representative of the standard error of optima distribution around the mean value. Abbreviations refer to the first three letter of the generic name of the species. For species belonging to the same genus, also the first letter of the specific name is reported

2.5 Conclusions

Population responses to an environmental gradient (in the present case sediment granulometry) are not absolute, but they depend from the context in which they are expressed. Shifts in community compositions across different ecosystems can be ascribed to the different covariance structure between the sediment structure and other environmental factors. Additional knowledge about the covariance structure of environmental variables within the observed systems is then required in the interpretation of univariate models prediction. A multi-quantile regression approach is better suited to keep track of the environmental context because it shows the variation in responses as it is modulated from the subsidiary factors.

Acknowledgements

We thank the Monitoring taskforce (NIOZ-Yerseke) and Rijkswaterstaat for sample collection and processing, Wil Sistermans and Vincent Escavarge for the help in managing the dataset, Menno Eelkema for the DELFT3D modeling and three anonymous reviewer for their constructive criticisms. This work was founded from the Ecoshape/Building with Nature project. At the time of starting this project, NIOZ-Yerseke belonged to the Netherlands Institute of Ecology.

CHAPTER 3

A mixed modeling approach to predict the effect of environmental modification on species distributions

Francesco Cozzoli, Menno Eelkema, Tjeerd J. Bouma, Tom Ysebaert,
Vincent Escaravage and Peter M. J. Herman

Published as: Cozzoli, F., Eelkema, M., Bouma, T.J., Ysebaert, T., Escaravage, V. and Herman, P.M.J. (2014). A mixed modeling approach to predict the effect of environmental modification on species distributions. PLOS ONE 9

Abstract

Human infrastructures can modify ecosystems, thereby affecting the occurrence and spatial distribution of organisms, as well as ecosystem functionality. Sustainable development requires the ability to predict responses of species to anthropogenic pressures. We investigated the large scale, long term effect of important human alterations of benthic habitats with an integrated approach combining engineering and ecological modeling. We focused our analysis on the Oosterschelde basin (The Netherlands), which was partially embanked by a storm surge barrier (Oosterscheldekering, 1986). We made use of 1) a prognostic (numerical) environmental (hydrodynamic) model and 2) a novel application of quantile regression to Species Distribution Modeling to simulate both the realized and potential (habitat suitability) abundance of four macrozoobenthic species: *Scoloplos armiger*, *Peringia ulvae*, *Cerastoderma edule* and

Lanice conchilega. The analysis shows that part of the fluctuations in macrozoobenthic biomass stocks during the last decades is related to the effect of the coastal defense infrastructures on the basin morphology and hydrodynamics. The methodological framework we propose is particularly suitable for the analysis of large abundance datasets combined with high-resolution environmental data. Our analysis provides useful information on future changes in ecosystem functionality induced by human activities.

3.1 Introduction

The influence of human activities on Earth's ecosystems has caused changes in global and local scale species distributions [Parmesan, 2006]. With the recognition of the value of ecosystem services for human communities and the role of biodiversity in delivering these services [Costanza et al., 1997], there is an increasing demand to produce reliable projections of the effects of human interventions on species habitats and distributions. Models able to relate species abundances and environmental conditions (species distribution models) are being intensively used in ecological research and conservation planning [Syfert et al., 2013].

Advances in remote sensing and environmental modeling are greatly contributing to the development of species distribution models by supplying detailed descriptions of the environment. However, when reliable descriptions of (some) environmental variables are available, several conceptual and analytical issues still need to be investigated in order to increase confidence in the results of species distribution models [Araujo and Guisan, 2006, Kamino et al., 2012]. Species abundances are often the product of different constraints acting at different scales [Thrush et al., 2005]. Even when one (known, measured or modeled) environmental factor is favorable for the species, other (unknown) factors may not, and the species can be absent or limited to a low abundance (Liebig's law of the minimum). As a result, observed species abundances commonly show complex distributional patterns with respect to the known variables. Given the asymmetric distribution of the residuals, such patterns are difficult to interpret with central estimators (*e.g.*, Ordinary Least Square) [Blackburn et al., 1992, Cade et al., 2005, Thomson et al., 1996]. In addition, sampling stochasticity will contribute to variability in the response of the individual sample densities. Species distribution models usually focus on the 'true' responses to the known explanatory variable(s), excluding the variability induced by subsidiary factors. For this reason, they often have been restricted to a partial description of the distribution only, such as modeling of the maximum or binary modeling of presence/absence. This approach expresses species distributions in terms of potential niche or habitat suitability [Franklin, 2010]. Habitat suitability fluctuates less in time than realized abundances and it is generally preferred as a reference parameter for spatial management strategies [Degraer et al., 2008]. However, several applications of ecological forecasts require a quantification of the realized abundances rather than just a measure of habitat suitability. There is a need for forecasting models that represent the entire probability distribution of abundance (density, biomass) values at a particular combination of environmental factors [Thrush et al., 2003].

Quantile regression [Koenker and Bassett, 1978, Koenker and Hallock, 2001] is a statistical technique suitable for the analysis of complex distributional responses [Austin, 2007, Cade and Noon, 2003, Downes, 2010, Franklin, 2010]. The method can be used to predict the complete quantile (τ) distribution of the response variable Y when conditioned by one or more explanatory variables X^{1-n}: $Q_Y(\tau|X^{1-n})$. Therefore, regression quantile estimates can be used to construct predictions without specifying how variance heterogeneity is linked to changes in means. Quantile regression models have high performance in explaining the observed variance also in the presence of spatial autocorrelation of environmental variables [Cade et al., 2005].

Most studies have limited the use of quantile regression to determine the functional relationship between a stressor and the response variable at a limited number of high quantiles (*e.g.*, Anderson [2008]). Models of the higher quantiles estimate the maximum possible abundance given the known explanatory variables, thus providing estimate of the species potential niche theoretically founded on Liebig's Law. Sub-optimal components of the distribution can be investigated by extending the quantile regression model to the complete range of quantiles [Cade and Noon, 2003]. Multiple quantile models have been used to make inferences about the role of the different environmental factors in limiting the different values of the responses [Schmidt et al., 2012] or to accurately describe and compare species distributions along single gradients [Cozzoli et al., 2013].

In this paper we propose a novel integration of numerical hydrodynamic models and species distribution models to investigate the response of four common macrozoobenthic species to anthropogenic modifications of their habitat. We chose as study area a temperate coastal embayment in the south - west of The Netherlands: the Oosterschelde (Figure 3.1). This basin was recently subjected to major human interventions (the realization of coastal defence mega-infrastructures) that deeply affected the basin morphology and hydrology [Louters et al., 1998]. We estimate the consequences on an important component of coastal food webs: the macrozoobenthos [Borja et al., 2011].

Our study uses a combination of extensive empirical data sets and different types of models. Hydrodynamic variables are known to be among the most important in determining the macrozoobenthic species spatial distribution [Allen, 1985, Snelgrove and Butman, 1994], but they are rarely measured with full spatial coverage, such that they are known for all sample locations. Hydrodynamic and morphodynamic models can fill the gap as they can describe water motion, sediment transport and bed-level changes by numerically solving a coupled set of mathematical equations [De Vriend et al., 1993]. Thus, as a first step to investigate the effect of dike building on benthic habitats, we simulated several past, present and future hydrological scenarios of the Oosterschelde by using a numeric hydrodynamic model (DELFT3D). The scenarios are representative of different stages of the recent basin evolution and they can also explore alternative management options, in this case the extreme option of removal of the main storm surge barrier.

Extensive monitoring programmes of macrobenthic fauna have been executed in the Oosterschelde over the past 50 years, with most efforts concentrated in the last 20 years. We combine this information with the results of hydrological models to construct quantile regression species distribution models. Upper boundary models emphasize the role of the known variables in determining the species abundance, thus they were used to describe the species potential niche and to produce habitat suitability maps. To express our forecast in realized rather than potential biomass stocks, we account for the complete conditional response distribution forecast by fitting the model on all quantiles. In this way it is possible to reproduce the realistic scattering induced by subsidiary factors with no required assumption about the distributional form (*e.g.*, normal or lognormal) or about the role of the environmental factors (limitation *vs.* facilitation). While the majority of existent studies focus on local/short term disturbances (*e.g.*, bottom disruption, increase turbidity, resuspension of pollutants, look at Short and Wyllie-Echeverria 1996), the use of prognostic environmental models allow us to investigate the effects of morphological/hydrological alterations on a whole-basin scale and over a time span that is relevant compared to intrinsic morphodynamic time scales.

3.2 Material and methods

3.2.1 Study area

The Oosterschelde (Figure 3.1) is an enclosed sea arm located in the south of The Netherlands. It was formerly part of a complex delta of the rivers Scheldt, Rhine and Meuse. In 1986, it was partly separated from the North Sea by a storm surge barrier, that can be closed during storm floods. After the realization of the storm surge barrier, the tidal prism (volume of water flowing into or out of an inlet between mean high tide and mean low tide) has been reduced by approximately 30%. Current velocities have declined by 20-40% in the tidal channels and by over 40% around the tidal shoals and salt-marshes [Louters et al., 1998]. The import of sediment from the coastal sea has been cut off. The availability of suspended sediment for deposition on the flats has decreased considerably, with present suspended particulate matter concentrations being only half those of the pre-barrier situation (on average <20 mg l^{-1}) [Louters et al., 1998]. The decreased tide-induced sediment transport towards the tidal flats relative to the erosion of the flats caused by wind-waves is causing a net erosion of the intertidal area [De Vriend et al., 1989]. As a consequence, the channels tend to fill up using sediment eroding from the tidal flats. The erosion mostly affects on the upper intertidal, lowers the mudflats, and is expected to lead to a drastic decrease of the intertidal area ([Jongeling, 2007], Table 3.1). The loss of intertidal area is in itself a threat for coastal safety, as the mud and sand flats damp wave energy and protect the dikes behind. It also jeopardizes environmental quality. The Oosterschelde was designated a national park in 2002 and its primary importance as bird feeding area, especially for waders, is recognized in the framework of NATURA2000.

Table 3.1: **Areas of the total, subtidal and intertidal surface for the different scenarios.** Values are in km^2. NDW (No Delta Works) indicates the results of the scenarios simulated removing the major coastal defense infrastructures

	1968	1983	1993	2001	2010	2010 (NDW)	2100	2100 (NDW)
Intertidal	171	149	143	147	142	144	65	98
Subtidal	236	234	226	225	227	225	304	271
Total	407	382	370	372	369	369	369	369

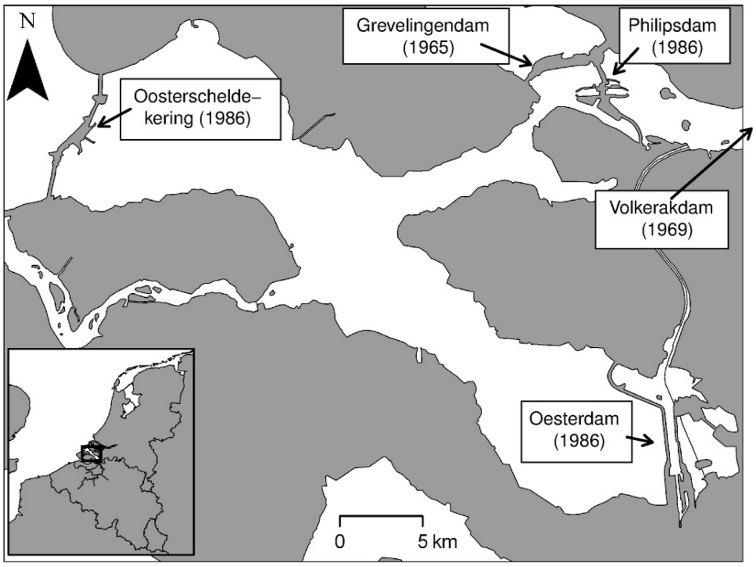

Figure 3.1: **The Oosterschelde basin.** In the boxes are reported the name and the realization date of the major dikes

3.2.2 Environmental variables

In order to reconstruct the impact of the Delta Works on the macrozoobenthos, we focused on the induced variation in the maximal tidal current velocity (maximal values reached during a full tidal cycle, m sec^{-1}) and the inundation time (% of time for which the site is submerged during a full tidal cycle). The sediment composition, traditionally considered as an other important factor for macrozoobenthic species distribution [Gray, 1974], was not considered in this study because it was not possible to compute accurate future scenarios for this variable. The lack of a proper salinity gradient and the limited variation between years in the Oosterschelde [Haas, 2008] make this variable not useful for our purpose.

For this research the DELFT3D-Flow model (version 3.55.05.00) is used in two-dimensional depth-averaged mode. The DELFT3D-Flow model is discussed in detail in [Lesser et al., 2004]. For application in and around the Oosterschelde, a specific model application has been made, called the KustZuid-model. This model application and its calibration are described in detail in [Eelkema et al., 2012]. Historical changes in hydraulic parameters were deduced from seven different model runs, each with a bathymetry from a different year. Sufficient bathymetry data of the basin were available for the years 1968, 1983, 1988, 1993, 2001, 2007 and 2010. The Storm Surge Barrier, Philipsdam, and Oesterdam were excluded from the 1968 and 1983 simulations, and included in the simulations for the years after 1986. Also, the 1968 situation was modeled without the Volkerakdam, so the Volkerak channel is still open. The 2100 scenario was modeled assuming the present trend toward erosion of the intertidal areas / filling of the deepest gullies will linearly continue in future. Additionally, we investigated the effect of the removal of the Delta Works on the 2010 and the 2100 scenarios. Although this is currently not a realistic option for management, these scenarios explore the consequences for the natural morphodynamics (and ecology) of the system. For each of the simulations, the seaward boundary conditions were kept unaltered.

3.2.3 Biotic variables

Benthic dataset

The data used in the present study have been extracted from the Benthic Information System (BIS version 2.01.0) hosted by the NIOZ research center in Yerseke (NL). The BIS database contains about 500000 distribution records about more than 2500 species of all major benthic classes that were collected since 1960 mostly in the Delta region (SW Netherlands). It comprises data from several monitoring projects performed mostly under the authority of Rijkswaterstaat (Dutch Ministry for Public Works and Water Management) in the framework of baseline and impact studies related to the management of the Oosterschelde. A subset of 3342 sampling locations has been selected according to the availability of abiotic data. The 1968 hydrodynamic model was used to extract the environmental conditions for the samples collected between 1962 and 1968. The other scenarios were used to extract the environmental conditions for the samples collected from one year before to one year later than the modeled year (Table 3.2). When using a dataset combining various monitoring projects with different sampling methods over an extended period of time, metadata have to be carefully checked for different sampling methodologies in order to avoid undue effects of sampling on the observations. The intertidal locations (n=1372) were mostly sampled by using handcorers pushed 20 to 30 cm in the sediment with a total sampling area between 0.005 and 0.045 m^2 (on average 0.019 m^2). The subtidal locations (n=1970) were on some occasions (n=176) sampled by using Van Veen grabs with a sampling area of 0.1 or 0.2 m^2 and a penetration depth around 15 cm depending upon the nature of the sediment. In most other cases the subtidal samples consist of subsamples with an average sampling area of 0.023 m^2 that were taken by using handcorers pushed 20 to 30 cm in the sediment contained in the bucket of a boxcorer after landing on the ship deck. Whereas most (ca. 95%) of the samples have similar characteristics regarding the sediment penetration and the sampling area, the few Van Veen samples stand out due to a ten times larger sampling area and a smaller (ca. 50%) sediment penetration compared to the other samples. Slightly lower density (because of deep living organisms not caught with the Van Veen grab) in the Van Veen samples compared with the handcorer samples have not be taken into account within the present analysis.

Table 3.2: **Number of samples included into analysis**

	1962-1968	1985-1989	1992-1994	2000-2002	2006-2008	2008-2010
Intertidal	152	37	541	549	542	149
Subtidal	65	455	138	169	272	273
Total	217	492	679	718	814	422

Target response variables

From a preliminary data inspection (Appendix A, Figure A.1), we identified 4 main clusters in the biomass distributions (g m^{-2} Ash Free Dry Weight, AFDW) of the 10 most frequently observed species (relative number of occupied samples). We investigated more in detail the distribution of the most common (or the only) species for each cluster (Table 3.3):

- *Scoloplos armiger* (bristleworm): intermediate-small motile Polychaeta. It is an opportunistic species, inhabiting a wide range of sedimentary habitats. *S. armiger* is widespread throughout the northern hemisphere and it is the most common species in the Oosterschelde [Holtmann et al., 1996].

- *Peringia ulvae* (mudsnail, new name for genus *Hydrobia*): small epibenthic gastropod. This species is mainly distributed in the silty upper intertidal, where it can graze on the benthic diatom film [Fenchel et al., 1975]. Despite its small individual body size, it can reach locally a high biomass due to very dense aggregation of individuals.
- *Cerastoderma edule* (common cockle): large shallow burrowing bivalve. It constitutes a predominant portion of the Oosterschelde intertidal biomass [Coosen et al., 1994, Kater et al., 2006]. Cockles are a primary food source for avifauna like Oystercatcher and Knot [Holtmann et al., 1996].
- *Lanice conchilega* (sand mason): medium-sized sedentary Polychaeta living in tubes that protrude several centimetres from the sediment. Dense aggregates of *L. conchilega* can form sand-reefs that have a relevant influence on the sedimentation [Borsje et al., 2008, Carey, 1987] and on the ecology of the macrozoobenthic community [Degraer et al., 2006, Zuhlke, 2001]. The species can be used as a proxy in the management of marine resources and the conservation of marine biodiversity [Rabaut et al., 2009].

Table 3.3: **Target species characteristics**

Class	Species	Feeding behavior	Average Ind. mass (mg AFDW)
Polychaeta	*S. armiger*	Opportunistic deposit feeder	2.6
Gastropoda	*P. ulvae*	Intertidal grazer	0.5
Bivalvia	*C. edule*	Suspension feeder	132
Polychaeta	*L. conchilega*	Selective deposit feeder	15

3.2.4 Model fitting and validation

Quantile regression [Koenker and Bassett, 1978, Koenker and Hallock, 2001] is an extension of the linear model that aims at fitting any desired quantile of a response variable distribution to an independent variable. The τ-th sample quantile of any random variable Y, $Q(\tau)$, is that value splitting the distribution in a *tau* portion $Y \leq Q(\tau)$ and a $(1-tau)$ portion $Y > Q(\tau)$. It can be calculated by solving:

$$\underset{\xi \in \Re}{\operatorname{argmin}} \sum_{i=1}^{n} (\rho_\tau (y_i - \xi)) = \underset{\xi \in \Re}{\operatorname{argmin}} \left[(\tau - 1) \sum_{y_i \leq \xi} (y_i - \xi) + \tau \sum_{y_i > \xi} (y_i - \xi) \right] \quad (3.1)$$

with respect to $\xi(\tau)$ (Equation 3.1). By extension, the linear conditional quantile distribution function $Q_Y(\tau|X = x)$ can be estimated by solving:

$$\hat{\beta}(\tau) = \underset{\beta\in\Re^p}{\operatorname{argmin}} \sum \rho_\tau(y_i - x_i'\beta) \tag{3.2}$$

where $\hat{\beta}(\tau)$ is the unknown regression coefficient for the τ-th quantile and β are the possible solutions with respect to x (Equation 3.2). For each species, the full conditional quantile distribution (from the 0.01 to the 0.99 quantile, with intervals of 0.02) of their biomass (g m^{-2} AFDW) was modeled with respect to the maximal current velocity, the inundation time and their first-degree interaction terms (model selected as the most explicative, Table A.1 lists AIC scores for different model structures). To validate our forecast for each of the modeled quantiles, the whole dataset was sampled with replacement. Due to sampling with replacement, some observations are repeated and others remain unpicked. The model was fitted on the sampled observations (training dataset) and used to predict the unpicked ones (validation dataset). To obtain a sufficiently large data population, the procedure was iterated 5000 times. The predicted values (expressed as a distributional quantile) were discretized in 10 homogeneous classes, for which the corresponding sample quantile of the validation data was calculated. To finally asses the validity of the model, observed and predicted quantiles were plotted against each other and checked for linear correlation. Examples of four quantiles for each species are shown in Figure 3.2.

Given that the maximum can be a fairly volatile statistic due to the influence of outliers [Anderson, 2008], we considered a slightly sub-optimal quantile to model the upper boundary of the species responses ($\tau = 0.975$, Figure 3.3). The abiotic scenarios forecasted by the hydrodynamic model (Figure 3.4) were used to predict maps of potential biomass (habitat suitability) for different years. In the Results section we show the outputs for the years 1968, 2010 and 2100 (Figure 3.5).

To estimate the total biomass standing stock in each scenario grid cell we randomly sampled a biomass from the forecast conditional distribution (Figure 3.6). The total biomass stock T (Figure 3.7) were calculated as

$$T = \sum_{i=1}^{n} \left\{ y_i \in Q_{y_i}[\tau|(X^1 = x_i{}^1, X^2 = x_i{}^2)] \right\} * S \tag{3.3}$$

where S is the grid cell surface (Equation 3.3). Realized stock estimates can slightly differ across different simulations due to stochasticity in the sampling from the conditional quantile distribution. The large number of modeled cells (ca. one million) strongly buffers this uncertainty. In any case, we averaged the outputs of 5 simulations. The error bars are not visible on the scale of the barplots (Figure 3.7). The inundation time scenarios were used to distinguish between intertidal (inundation time <100%) and subtidal stocks.

All analyses were performed with `R` R Development Core Team [2011] mostly using the packages `quantreg` [Koenker, 2013] and `raster` [Hijmans and van Etten, 2013].

3.3 Results

The fitted models (summary tables and graphs in Appendix A, Tables A.2 - A.5, Figures A.2 - A.5) were able to forecast with great accuracy each conditional quantile of the observed distributions (Figure 3.2). While for *S. armiger*, *P. ulvae* and *C. edule* the ratio between observed and predicted values was very close to 1, the model tended to systematically overestimate the lower values and to underestimate the higher values of the *L. conchilega* realized biomasses (Figure 3.2). The good match between observed and predicted occurrences (Table 3.4) indicates that the data scatter below the upper limit is well represented until the threshold for occurrence, even if the predicted values tend to be slightly higher than the observed ones.

Table 3.4: **Target species occurrences.** Observed occurrence are expressed in percentage of occupied samples on the overall dataset. For each modeled scenarios, predicted occurrences were calculated as the percentage of cells for which the model forecast a biomass >= of the lowest value observed in nature. The predicted occurrence values reported in the table are the average of all the scenarios modeled between 1968 and 2010

Species	Occurrence (%)					
	Total		Intertidal		Subtidal	
	Observed	Predicted	Observed	Predicted	Observed	Predicted
S. armiger	64	65	73	77	58	58
P. ulvae	30	34	60	69	9	14
C. edule	25	29	55	63	4	9
L. conchilega	23	27	17	27	27	27

Upper boundary response surfaces (Figure 3.3) describe the species' potential niche. *P. ulvae* has a clear preference for the sheltered and elevated mudflats. *C. edule* and *S. armiger* share the same optimal habitat in the intertidal zone (intermediate inundation time and moderate hydrodynamic stress), but they diverge for subtidal habitats. While *C. edule* is scarce in permanently inundated sites, *S. armiger* finds a sub-optimal habitat there, especially at strong current velocity. *L. conchilega* preferred subtidal but sheltered habitats (Figure 3.3).

The analysis of the Oosterschelde abiotic scenarios (Figure 3.4) shows a decrease in intertidal and subtidal maximal current velocity between 1968 and

1983, due to the realization of the back-barrier dams, and a more consistent drop after 1983 with the realization of the storm surge barrier. Given the ongoing trend in erosion, only a small and shallow portion of the intertidal area will remain in 2100. The removal of the Delta Works could reset the current velocity to the 1968 levels.

Extrapolated on the basis of the abiotic scenarios, upper boundary models provided a clear spatial representation of the species habitat suitability (Figure 3.5). While *S. armiger* is widely distributed in the basin, the *P. ulvae* and *C. edule* are restricted to the intertidal flats. This implies that the first species, even upon losing its preferential habitat, will be able to cope with the future erosion of the intertidal areas, while the last two will face a drastic decline. High biomasses of *L. conchilega* in 1968 were mostly confined to the eastern part of the basin and to the edge of the mudflats. The reduction of tidal current velocity improved drastically the habitat suitability of the north-east section of the basin for *L. conchilega*. The suitable habitat surface for this species will further increase in future, when the present mudflats will turn to shallow and almost permanently inundated areas.

Maps obtained from sampling the complete conditional quantile distribution (Figure 3.6 A) show the scatter below (and above, in case of facilitative interaction) the upper boundary surfaces (Figure 3.6 B). They are more difficult to read than those obtained by modeling just a single quantile, but they represent a more realistic situation. Thus, they can be used to quantify the realized species biomass. The trends in biomass standing stock (Figure 3.7) show changes between the years 1968 - 1993 (period of the Delta Works realization) and a relatively stable situation during the last two decades. As shown by Figure 3.5, the large intertidal area lost between 1979 and 1986 in the eastern part of the basin due to the beginning of the works for the Oesterdam (Figures 3.1 & Table 3.1) was able to sustain high biomasses of all the analyzed species. *S. armiger* stock declined after the Delta Works especially in the subtidal habitat.

Markedly intertidal species were positively (*P. ulvae*) or fundamentally not (*C. edule*) affected by the changes in the system hydrodynamics (Figure 3.7), but these species will face a dramatic decline in future due to expected loss of intertidal habitat (Figure 3.4 & Table 3.1). For the year 2100 the *C. edule* standing stock is estimated to be ca. 30% (just 10% in the intertidal) of the present situation, while *P. ulvae* will almost disappear from the system. *S. armiger* will be able to partially compensate the decline in the intertidal biomass by establishing in the subtidal habitat. In contrast, *L. conchilega* took advantage from the dampening of current velocities in the channels and increased its biomass by ca. 15 % between 1968 and 2001. If the Delta Works are not removed, a further increase in *L. conchilega* is expected in future (Figure 3.7). Potential biomass standing stocks (from models using 0.975 quantile) are well correlated with the same-year estimations for the realized stocks (Figure 3.8). The ratio between the realized and the potential stocks varies from ca. 1:5 (*S. armiger*) to 1:10 (*L. conchilega*).

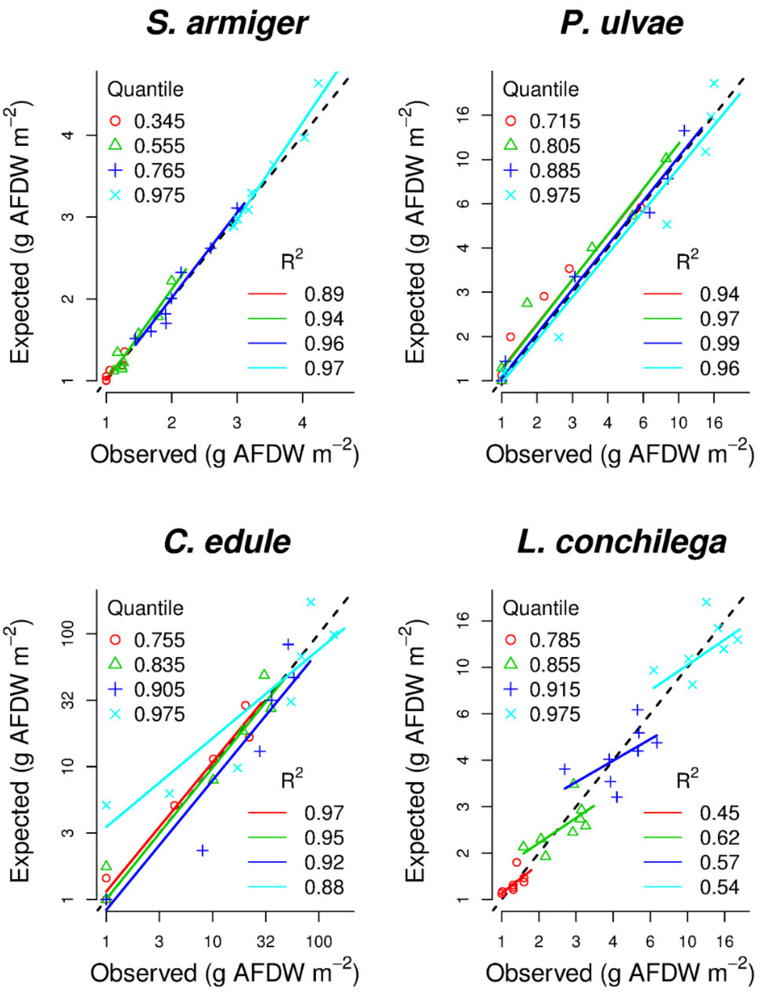

Figure 3.2: **Models validation. Ratio between observed and predicted values.** To validate our forecast for each of the modeled quantiles, the whole dataset was sampled with replacement. Due to sampling with replacement, some observations are repeated and others remain unpicked. The model was fitted on the sampled observation (training dataset) and used to predict the unpicked ones (validation dataset). The random sampling-fitting-predicting procedure was iterated 5000 times and repeated for each one of the forecast quantiles. To make predicted (quantiles) and realized values comparable each other, we discretized them in 10 homogeneous classes based on the predicted values. For each of the classes, the correspondent sample quantile of the observed data was calculated. To finally asses the validity of the model, observed and predicted quantiles were plotted against each other and checked for linear correlation. The four quantiles for species showed as examples in the graphs were selected among those predicting occurrence (*e.g.*, up to the 35th quantile for *S. armiger*, up to the 78th quantile for *L. conchilega* Table 3.4). The other quantiles generally follow the same trends. The black broken line represent the 1:1 ratio

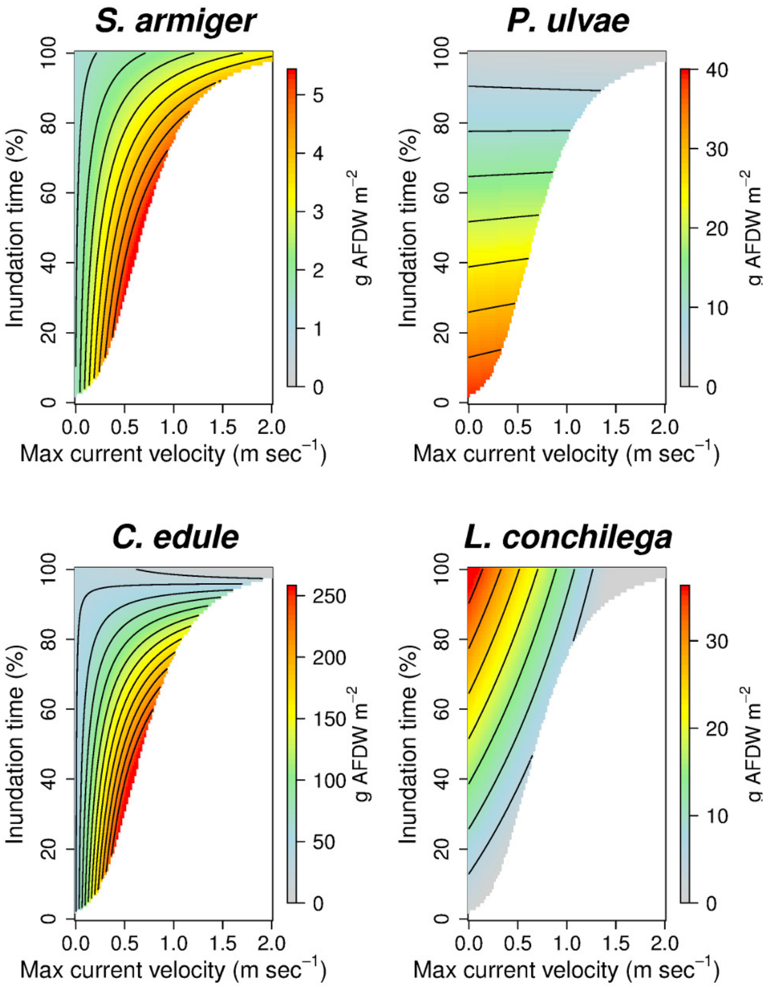

Figure 3.3: **Models of the 0.975th quantile, response surfaces.** Models of the maximal biomass, when extrapolated in the explanatory variable space, give a description of the species potential niche consistent with the Liebig's Law

3.4 Discussion

A major challenge in species distribution modeling is the clarification of the niche concept and the calculation of the influence of each predictor [Araujo and Guisan, 2006]. The methodology we present offers a contribution to this debate. It overcomes the dichotomy between 'potential' and 'realized' niche, in the sense that our forecast depends on the known environmental gradients but at the same time is fully able to reproduce the variance induced by subsidiary factors.

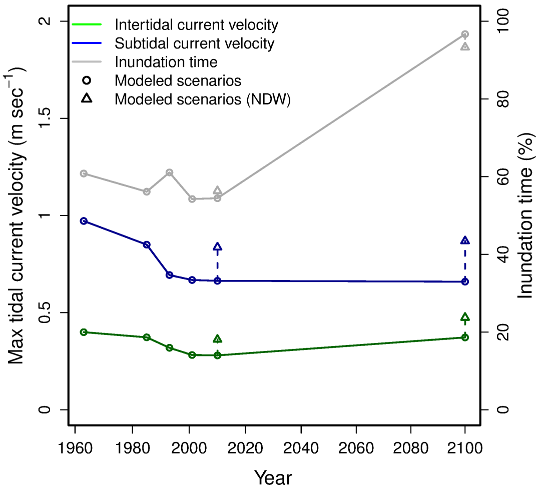

Figure 3.4: **Median values of the explanatory variables on different year-scenarios.** Circles represent the median values predicted for the available years-scenarios by the hydrodynamic model. Triangles represent the values predicted for the years 2010 and 2100 removing the Delta Works (NDW)

The upper boundary response surfaces offer a synthetic description of the species potential niche (Figure 3.3). They represent the 'true' species response to the known variables, in the sense that they exclude the influence of subsidiary factors on the basis of the Liebig's Law assumptions. This analysis is useful to depict the potentially important areas for the target species (Figure 3.5). On the other hand, maps obtained by sampling from the full conditional quantile distributions (Figure 3.6 A) give an image of the biomass values as they could be realistically observed in nature, taking into account the variance induced by subsidiary factors.

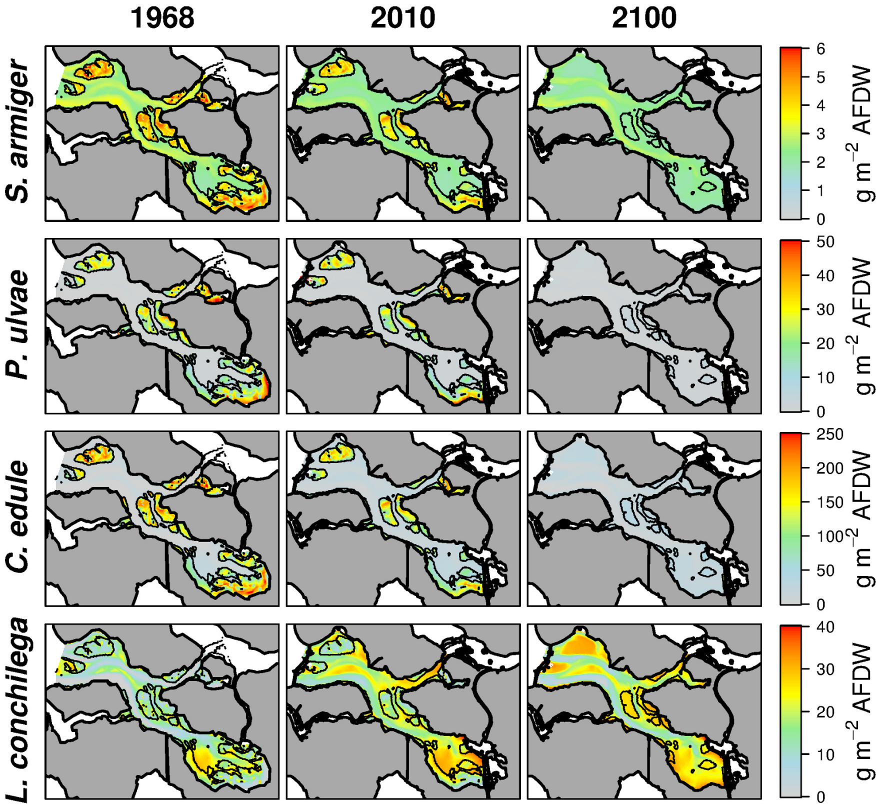

Figure 3.5: **Models of the 0.975^{th} quantile, habitat suitability.** Once extrapolated to realistic scenarios, the response surface shown in Figure 3.3 are useful to produce clearly interpretable habitat suitability maps. In the figure we show as example the output for the 1968, 2010 and 2100 scenarios

3.4.1 Considerations about the modeling methodology

Models of the full quantile distribution do not require assumptions about the role of the subsidiary factors (*e.g.*, models of the maxima assume that the effects of unmeasured variables will be further limiting rather than facilitative) or about the expected distributional shape (*e.g.*, He and Gaston [2007], Wenger and Freeman [2008]). While conventional species distribution models based on central estimators 1) assume constant error variance, regardless of the value of the predictor variable 2) may fail to distinguish real non-zero changes in zero-inflated distributions, the full quantile distribution model is 'adaptable' enough to describe the heterogeneous distributions of the analyzed species. However, phenomena generating endogenous autocorrelation and patchiness

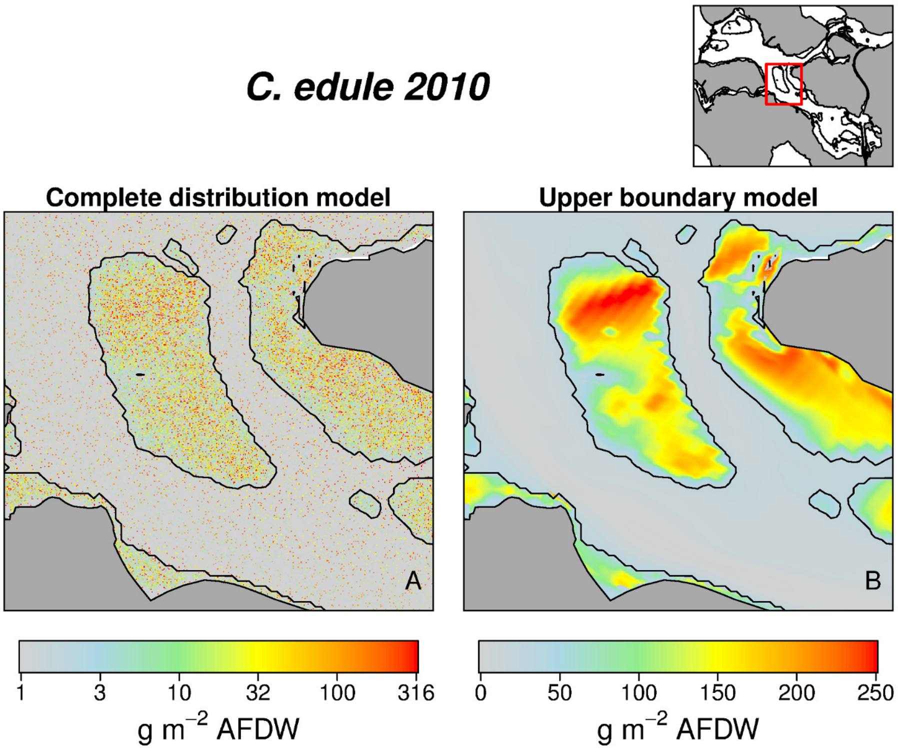

Figure 3.6: **Complete distribution model** *vs* **Model of the maxima.** Example for *C. edule*, year 2010. Map produced by sampling from the complete quantile distribution models (A) are able to represent the realistic scatter around (mainly below) the response surface shown in (B). To help the reader in appreciating the fine mosaic of points in (A) we restricted the map to a smaller portion of the basin and we used a logarithmic scale for plotting the estimated values

at a spatial scale smaller than that of the macrozoobenthos sampling grid (*i.e.*, propagation, aggregation, facilitation, competition) can lead the model to estimate an incorrect ratio between low and high biomass values. This is particularly the case for *L. conchilega* (Figure 3.2), characterized by a strong aggregational behavior [Degraer et al., 2006], while for the other species the effect is mostly limited to the lower quantiles and can lead to an overestimate of the realized occurrences (Table 3.4). The strong patchiness in the *L. conchilega* distribution is also evident from the fact that no overlaps are predicted between the values forecast from high and low quantiles (Figure 3.2).

The close relationship between the potential and the realized estimated stocks (Figure 3.8) can be explained by interactions and correlations between known and unknown environmental variables, that have the effect to increase the similitude of the responses obtained from different quantiles [Cade et al., 2005]. The implication is that models of the maxima constitute a good proxy for estimating other components of the distribution, as already shown earlier [VanDerWal et al., 2009]. However, the degree of scattering beyond the upper boundary (*i.e.*, the realized fraction of the potential stock, Figure 3.8) is species-specific and it is not possible to derive a generic 'rule of thumb' to directly convert potential biomass in realized stocks.

From a practical point of view, this kind of modeling needs a high number of samples to include the complete span of possible combinations between environmental conditions and biomass/abundance. In addition it needs high-resolution environmental layers. In our case we had approximately one million cells in each of the year scenarios, as the environmental layers were output by the hydrodynamic models. Other examples of similar environmental datasets are satellite images or interpolated surfaces from extensive spatially covering measurements. The use of prognostic environmental models creates the opportunity to extrapolate the results for (hypothetical) past and future conditions, but at the risk of generating error propagation between the environmental model and the species distribution models. In the present case, the limited accuracy of the hydrodynamic model in forecasting the environmental conditions at the edge of the mudflats can potentially lead to overestimation of the subtidal biomass of the mainly intertidal species. Moreover, the lower inundation time estimated for the year 1993 (Figure 3.4) is likely related to lack of resolution in the measured depths close to the shore rather than to effective variations in mudflat elevation or tidal amplitude.

Full quantile distribution models can be used, like in this paper, to quantify the overall effect of environmental changes on realized biomass (Figure 3.7), and can be useful for ecological applications that cannot rely only on habitat suitability estimations but require accurate information about the realized size of the populations. It should be noted, however, that this approach assumes that the nature of the distributions, and thereby the influence of non-measured subsidiary factors, will remain essentially unchanged. This assumption is difficult to assess in the case of future predictions.

3.4.2 Comparison with previous estimates

The response surfaces forecast by 0.975^{th} quantile regression are coherent with what is reported in literature for the analyzed species (*e.g.*, Degraer et al. [2006], Wolff [1983]). While our representation of the response of *C. edule* to inundation time and current velocity (Figure 3.3) closely matches with that reported for the Oosterschelde by [Kater et al., 2006] on the basis of stepwise backward logistic regression, the total biomass standing stock we estimated is approximately 3 times higher than that reported by these authors (27 vs 77 millions kg of wet biomass, assuming a loss of 96% from wet to dry weight [Ricciardi and

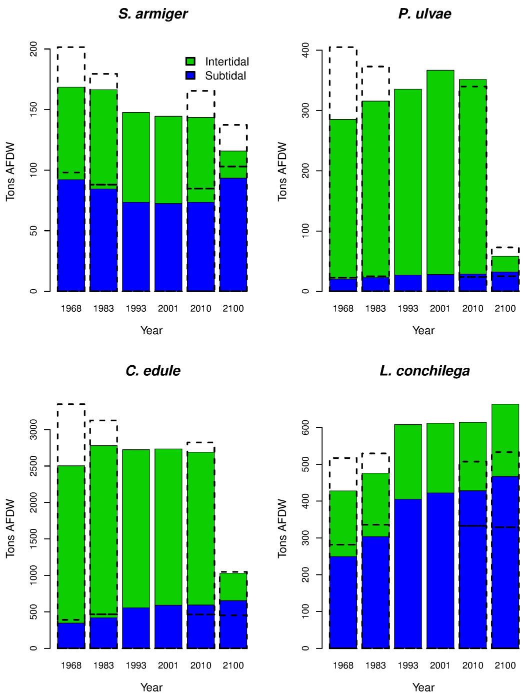

Figure 3.7: **Biomass standing stocks, time series.** Colored bar show the intertidal (green) and subtidal (blue) realized biomass stock estimated from the different scenarios for the present extension of the basin. Broken-line bars on the years 1968 and 1983 include the area that was cut-off from the beginning of the Oesterdam works in 1979 (25 km^2 between 1968 and 1983 and 12 km^2 between 1983 and 1986). Empty bars on the years 2010 and 2100 show the result of the scenarios simulated removing the Delta Works

Bourget, 1998]). This is related to the fact that logistic regression methods (more in general, occurrence models) are able to give an accurate description of the species presence but definitely underestimate the contribution to the standing stocks of patches with extremely high concentration of individuals.

Compared to previous estimates of *C. edule* standing stocks in the Oosterschelde from large surveys our results show less temporal variability (from 20000 tons AFDW in 1980 to 2000 tons AFDW in 1989 as estimated by Coosen et al. [1994]. This is related (in addition to large uncertainties and a potentially biased dataset in the analysis of Coosen et al. [1994]) to the fact that our models average the yearly and seasonal variability by uniformly ("neutrally") sampling the forecast conditional probability distributions. We made this choice to represent only the amount of variation in standing stocks that can be ascribed to

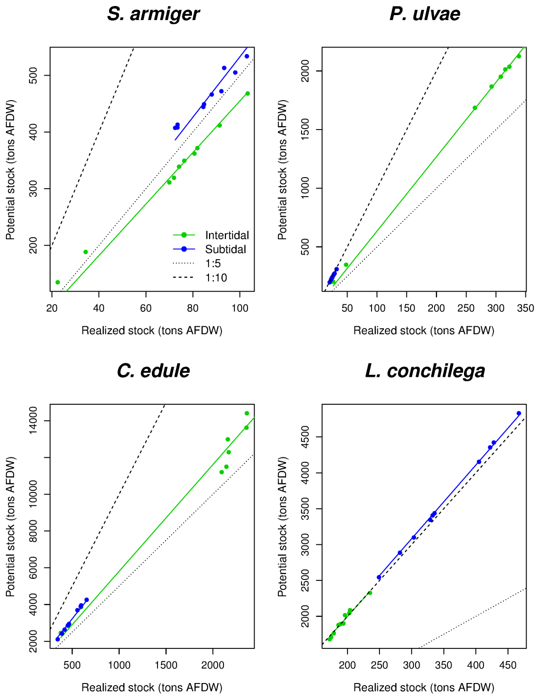

Figure 3.8: **Potential** *vs* **Realized stocks.** The graphs show the ratio between potential (τ=0.975) and realized (sampling from the complete cumulative distribution) intertidal (green) and subtidal (blue) biomass stocks estimated for different year/scenarios. The black dotted line represent the 1:5 ratio. The black broken line represent the 1:10 ratio

the target explanatory variables. Additional variability is still possible due to trends in large scale subsidiary factors [Thrush et al., 2005] that can restrict the realized output of the forecast distribution to particularly high or low values.

Previous studies applying univariate quantile regression to macrozoobenthic species distribution modeling (*e.g.*, Anderson [2008], Cozzoli et al. [2013]), have used non-linear regression techniques (*i.e.*, B-splines transformation of the explanatory variable). This was not necessary in our case: the interactions between the two explanatory variables made the models 'flexible' enough to accurately describe the species responses. More tests will be needed to see how general this conclusion is. In any case B-splines transformation could also be used in the multivariate statistical model if needed.

3.4.3 Temporal trends in the Oosterschelde

The comparison between the upper-boundary response surfaces and the realized biomass stocks allow us to make causal inferences about the fluctuations in species realized biomass across years. *P. ulvae* has maximum habitat suitability in sheltered and elevated sites (Figure 3.3). The positive trend in *P. ulvae* biomass stocks (Figure 3.7) from 1968 towards 2010 can be related to the decrease in intertidal tidal currents. For the same reason, species with preferences for intertidal environments with moderate current velocity, like *S. armiger* and *C. edule* (Figure 3.3) transited through an optimal condition in 1983 (reduction of the current velocity due to the realization of the back-barrier dams) followed by a decline in the following years (further reduction of the tidal currents, mainly due to the realization of the Oosterscheldekering). The effect of the dampening of tidal currents on the biomass of *S. armiger* and *C. edule* diverges in the subtidal environment: negative for *S. armiger* and positive for *C. edule* (Figure 3.7). Although the decline in the intertidal biomass of *C. edule* was partially compensated by the increase in the subtidal zone, the overall outcome suggests a decrease in the *C. edule* potential as food resource for the avifauna (especially waders like Oystercatcher).

L. conchilega prefers subtidal sites with weak currents (Figure 3.3). It was positively influenced (Figure 3.7) by the dampening of the tidal current velocity (Figure 3.4). In particular the realization of the Philipsdam and of the Volkerakdam induced a net increase in habitat suitability in the northern branch of the basin (Figure 3.5).

While in the last two decades the situation was rather stable for all the species (Figure 3.7), the future shrinking of the intertidal flats (Table 3.1, Figure 3.4) will induce a severe collapse of the standing stocks of *C. edule* and *P. ulvae*. Conversely, *L. conchilega* will reach the highest abundance in 2100, expanding its distribution on the shallow subtidal areas that will take the place of the present-time mudflats (Figure 3.5). *L. conchilega* is a powerful ecosystem engineer [Jones et al., 1994, 1997], able to stabilize the sediment and increase sedimentation [Borsje et al., 2008]. Therefore, colonizing of the lowering mudflat, *L. conchilega* can reduce the expected intertidal erosion. The decline in *C. edule* and *P. ulvae* biomass (both the species are believed to increase sediment erosion, either directly [Ciutat et al., 2007] or by disrupting the benthic diatoms film [Montserrat et al., 2008]) could have as well the effect to slow down the loss of intertidal areas.

At the present time, the removal of the Delta Works *per se* would not have an important positive effect on *C. edule* and *P. ulvae* (Figure 3.7), but it can be useful to slow down the erosion of the intertidal habitat. However, given that the realization of the Delta Works just amplified the pre-existent trend for sediment export Eelkema et al. [2012], some loss of habitat is always expected in the future. Once the erosion process will be very advanced (year 2100), the wider tidal range consequent to the removal of the dikes could increase the intertidal surface (Table 3.1), helping in preserving a (small) part of *C. edule* and *P.*

ulvae habitat. On the other hand, the removal of the coastal defense system would reduce the biomass stock of *L. conchilega* to just a slightly higher value than in the pre-Delta Works state. The only species that could substantially benefit from the removal of the Delta Works is *S. armiger* (Figure 3.7), that usually is not considered as a target for management strategies.

Retracing the past evolution of the Oosterschelde has given us the opportunity to build and validate models predicting macrozoobenthic community responses to environmental conditions as well as the anthropogenic modification of those conditions. However, in considering these forecasts, it should not be forgotten that they assume that the influence of non-measured subsidiary factors will remain constant through time. This assumption is difficult to assess in the case of future predictions.

At the time of constructing the storm surge barrier, it was already foreseen that tidal currents in the Oosterschelde would decrease in intensity (Figure 3.4) and that this would lead to enhanced erosion of intertidal flats [Van den Berg, 1982]. This increased erosion is effectively observed [Bijker, 2002], and different measures are taken to mitigate the effect. After a first trial, it is planned to regularly use dredge spoil dumped onto the tidal flats as nourishment [Jongeling, 2007]. Softer defense measures include artificially constructed oyster banks [Ysebaert et al., 2012] and saltmarsh restoration [Suykerbuyk et al., 2012]. The emphasis placed on these measures is related to the conservation goals, as legally fixed *e.g.*, in Natura2000 objectives.

What was not foreseen at the time of embankment, was the striking improvement in quality of the subtidal benthic habitat (Figures 3.5 & 3.7). The dampening of current stress allowed a vast portion of the subtidal Oosterschelde to be colonized by large macrozoobenthic organisms, which were confined to the inner and sheltered part of the estuary before the embankments. This change in habitats has created opportunities for touristic (diving) activities, in particular in combination with the increased transparency of the water. The evolution demonstrates that natural values of the original system, such as intertidal productivity and food provision for birds, are intrinsically incompatible with the management option for coastal safety that was chosen, but that other natural values such as subtidal benthic habitat quality do have the potential to be compatible with this option. A public debate is needed on whether nature conservation goals can and should be brought closer in line with other management objectives, or whether natural values should be constraining other management options.

3.5 Conclusion

The methodology we presented allows a realistic representation of species abundances on the basis of known environmental variables. The estimation of realized abundance rather than just habitat suitability revealed extra information on the sensitivity of species to environmental factors [Cade and Noon, 2003, Cade et al., 2005, Schmidt et al., 2012] and on their population dynamics and energetics [Blackburn et al., 1993, Marquet et al., 1995]. Quantile regression requires limited assumptions about the expected distributional shape and the interactions between explanatory variables. Therefore, it can be applied to a broad range of environments and organisms. The integration between numerical and statistical models is a versatile method for summarizing and simulating the response of species to environmental gradients. This study emphasize the importance of large and long term environmental monitoring programs, as they provide an useful source of information to forecast future ecosystem developments.

Ecological forecast must be included into dynamic infrastructure design to maintain operational efficiency and reduce the ecological impacts [Matthews et al., 2011]. Model extrapolations of the biological and physical environment are a fundamental step to explicitly integrate nature into infrastructure development and to forecast the future availability of ecosystem services Chan et al. [2006]. We showed that the realization of surge barriers has mixed and depth-dependent responses that also include improvement of environmental quality. Under this perspective, the analysis of Oosterschelde basins is a precious source of information to understand (and communicate) the future ecological consequences of global trends in human coastal development. The proposed framework can be applied to plan human interventions in a way to minimize their impact or, more optimistically, to maximize their benefits for target species.

Acknowledgments

This work was mainly funded by the Ecoshape/Building with Nature project. The NIOZ Monitor Taskforce was for a large part responsible for the fieldwork and the taxonomic analysis of the macrofauna samples. Rijkswaterstaat (executive body of the Dutch Ministry of Infrastructure and the Environment) was responsible for the funding of these activities in the framework of different national monitoring projects such as MWTL.

CHAPTER 4

Coastal defense *vs.* Enhanced navigability: how management affects benthic habitat quality.

Francesco Cozzoli, Sven Smolders, Menno Eelkema, Tjeerd J. Bouma, Tom Ysebaert, Vincent Escaravage, Stijn Temmerman, Patrick Meire and Peter M. J. Herman

Abstract

We aim to identify the ecological consequences of two main anthropogenic impacts on estuaries: intensification of global maritime trades and need of coastal defense. For this purpose, the Westerschelde and Oosterschelde estuaries (Dutch Delta, SW Netherlands) are an ideal model system because they were subjected, during the last 50 years, to contrasting management strategies: deepening of estuarine channels to enhance navigability *vs.* realization of a storm surge barrier to enhance coastal safety.

By multidisciplinary integration of empirical data and modeling of estuarine morphology, hydrodynamics and benthic ecology, we investigated the effects of habitat alterations on a whole-basin scale and over a time span that is relevant compared to intrinsic morphodynamic time scales. The use of general community descriptors instead of specific responses contributes to the robustness and ubiquitous applicability of the present ecosystem model.

We demonstrate opposite shifts in habitat quality in the two systems. Spatial divergence of consequences, *e.g.* between intertidal and subtidal habitats, also depends on management strategy. The realization of a storm surge barrier

leads to deterioration of intertidal habitat quality, but has positive consequences for subtidal habitats. Hydrological alterations following deepening have negative implications for benthic life throughout the estuary. With this study we show that a single set of ecological responses can equally describe the effects of completely different management measures on environmental targets.

4.1 Introduction

Estuaries and coastal embayments are a preferential habitat for humans [Small and Nicholls, 2003]. The expansion of coastal populations, in combination with sea level rise and increasing intensity of extreme storms, is bringing a large part of the world's human population under the threat of coastal storm surges [McMichael et al., 2006]. This has led to the still ongoing realization of a high number of dams, embankments and storm surge barriers in the richest countries (Figure 4.1). With the growing prosperity of developing countries (where the majority of the endangered population lives) these measures will likely be more commonly adopted worldwide [Temmerman et al., 2013].

Waterways play an important role in trade, especially in countries that have direct access to the sea. The handling capacity of estuarine ports is a crucial factor for the economic development [Halpern et al., 2008]. The continuously growing global trade network and the ongoing increase of the commercial ships are pushing toward a more intensive dredging of the waterways to the harbors (Figure 4.1). The global dredging market increased by nearly threefold over the past decade from \$ 5.3 bn in 2000 to \$ 14.7 bn in 2011, according to the International Association of Dredging Companies.

Both responses to global change in the 'Anthropocene' [Crutzen, 2002] have different consequences for coastal ecosystems. Dams, embankments and storm surge barriers provide coastal protection. In contrast, the deepening of estuarine beds often facilitate the inland penetration of seawater, leading to a landwards increase of the tidal energy [Stive and Wang, 2003]. In both cases, the ecological implications can be large, and should be taken into account for development plans [Nienhuis and Smaal, 1994, Swanson et al., 2012]. It is well known in general that hydrodynamic forces and their morphodynamic consequences structure estuarine life [Snelgrove and Butman, 1994, Ysebaert et al., 2003]. Alterations of the eco-hydro-morphological environment can have negative, or even catastrophic, social consequences when they affect essential ecological services [Adger et al., 2005, Danielsen et al., 2005, Diaz et al., 2006]. Yet there are several problems associated with the study and prediction of these complex alterations. One problem is related to the long intrinsic time scale and limited predictability of morphodynamic processes [De Vriend et al., 2011]. Secondly, it is not an easy task to translate morphodynamic conditions into habitat suitability. Thirdly, estuaries are diverse environments characterized by strong gradients in depth, salinity, current velocity, sediment composition and other factors. A management strategy at the scale of the system may lead

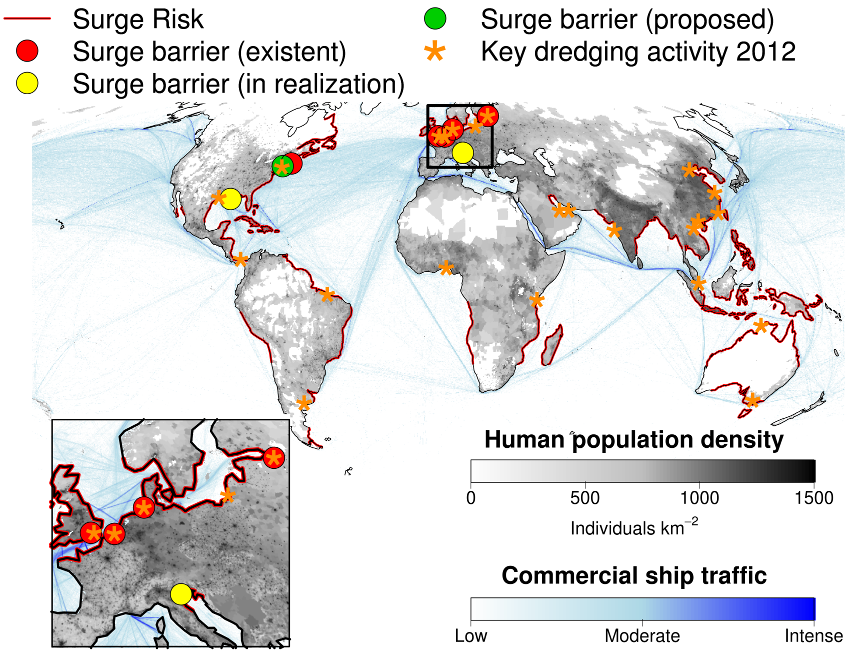
Surge Risk
Surge barrier (existent)
Surge barrier (in realization)
Surge barrier (proposed)
Key dredging activity 2012
Human population density
0
500
1000
1500
Individuals km^{-2}
Commercial ship traffic
Low
Moderate
Intense

Figure 4.1: **Coastal Anthropocene.** A large part of the human populations is nowadays endangered by storm surge risks (coastlines enlighten in red). In the northern hemisphere (particularly in Europe) this led to the construction of coastal defense infrastructures like open surge barriers. In the map we show the largest existent (red circles), under construction (yellow circles) or proposed (green circle) storm surge barriers. Other smaller storm surge barriers exist, mostly on tributaries rivers (*e.g.* along the Elbe, the Humber, the Hull). Contextually, the increasing exchange of goods through sea routes is pushing to a more extensive dredging of the waterways to harbors (main dredging operations in estuaries, embayments or straits are reported on the map with orange asterisks). Sources for flood risk: World Bank; ship transit: NCEAS , population density: FAO; key dredging projects 2012 in estuaries, lagoons, embayments or straits: International Dredger Association and China Dredger Association (representative of ca. 70% of the global dredging market)

to strong spatial divergence in response, where different subhabitats are affected in very different ways. The study of existing anthropogenically modified ecosystems is a precious source of information to support adaptive management and future decisions [Folke et al., 2004, Matthews et al., 2011].

In this paper we focus on the ecological effects of contrasting hydrological modifications of two adjacent estuarine habitats subject to large-scale infrastructural works. For this purpose, the neighboring Westerschelde and Oosterschelde basin (The Netherlands, Figure 4.2) are an ideal model system. The two basins share a common location, origin and regional pool of macrozoobenthic species [Cozzoli et al., 2013]. To a large extent, they had similar physical characteristics until approximately 50 years ago, but in the meantime they have undergone very different anthropogenic modifications. Coastal safety is a prominent issue in both sites, but, due to different navigability requirements, two radically different approaches were followed to achieve this goal. The Oosterschelde was partially embanked by a storm surge barrier. The Westerschelde, due of its importance as shipping route to the port of Antwerp, kept an open connection with the sea. In this basin, coastal safety is ensured by heightening and strengthening the dikes along the estuary. Flood control areas were created upstream to buffer the water mass at extreme storm tides [Beauchard et al., 2013a,b]. During the last decades the Westerschelde was extensively dredged to allow the transit of bigger vessels (Figure 4.2).

Our study uses a combination of extensive empirical data sets and different types of models. Empirical reconstructions of bathymetry and hydrological forcing for a situation before major anthropogenic changes are available for both systems. Similar datasets exist for present-day situations. Well-calibrated hydrodynamic models have been made for both systems and are the basis for our predictions of benthic habitat suitability. Extensive monitoring programmes of macrobenthic fauna have been executed over the past 50 years, with most effort concentrated in the last 20 years. We combine this information with the results of hydrological models to construct species distribution models that can predict changes in species distribution as response to environmental changes [Franklin, 2010, Pearson and Dawson, 2003, Sinclair et al., 2010]. In particular, we investigated the long-term effect of the habitat alterations for an important part of the estuarine natural community: the macrozoobenthos. Macrozoobenthic organisms are central component of the estuarine food webs [Herman et al., 1999] and they can affect biogeochemical cycles on a global scale [Heip et al., 1995]. Species distribution models of macrozoobenthos communities are useful tools to detect anthropogenic impacts at the ecosystem level [Borja et al., 2011]. We compared the benthic habitat suitability before (1960) and after (2010) the major infrastructural works. While the majority of existent studies focus on local/short term disturbances (*e.g.* bottom disruption, increase turbidity, resuspension of pollutants, look at Short and Wyllie-Echeverria 1996), the integration of hydrological and ecological modeling allow us to investigate the effects of morphological/hydrological alterations on a whole-basin scale and over a time span that is relevant compared to intrinsic morphodynamic time scales.

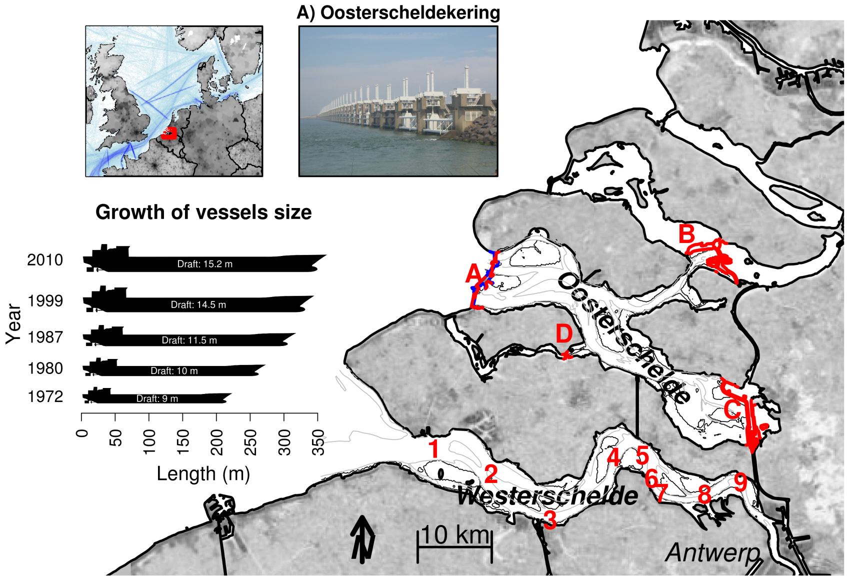
A) Oosterscheldekering
Growth of vessels size
2010
Draft: 15.2 m
1999
Draft: 14.5 m
Year
1987
Draft: 11.5 m
1980
Draft: 10 m
1972
Draft: 9 m
0
50
100
150
200
250
300
350
Length (m)
A
B
C
C
D
Oosterschelde
1
2
3
4
5
6
7
8
9
Westerschelde
10 km
Antwerp

Figure 4.2: **The Oosterschelde and Westerschelde basins.** A-D: main dams in the Oosterschelde; 1-9: main dredging sites in the Westerschelde. Intertidal areas are marked with a black line. Channels deeper than 10 m are enclosed by a with a gray line (bathymetry of 2010). Global trends in coastal development are well represented in the SW Delta of The Netherlands. On the one hand, the Oosterschelde was disconnected from the previous freshwater network (dams B & C) and embanked from the seaside by a storm surge barrier (Oostercheldekering, A). During the last decades,the maximal size of commercial vessels almost doubled. As consequence, channels in the Westerschelde were locally deepened (1-9) to enhance the shipping route capacity to the port of Antwerp (bottom right)

4.2 Material and methods

4.2.1 Study area

The present-day geomorphology of the SW Netherlands is the result of the interplay between natural processes and large-scale human interference that dates back at least two millennia. From the Middle Ages onwards, land reclamation led to a gradual separation between the Oosterschelde and the Westerschelde. The Oosterschelde was definitively cut off from the Schelde river in 1897. Following a disastrous flood in 1953, a massive system of coastal defense was implemented (Delta Works, 1959-1987). The Oosterschelde was isolated from the other connecting basins by the construction of two back-barrier dams in 1965 and 1969. This reduced freshwater input from the river Rhine from 70 m^3 sec^{-1} to 25 m^3 sec^{-1} [Nienhuis and Smaal, 1994]. In the subsequent years, the basin was partially closed off from the sea by a storm surge barrier, the Oosterscheldekering, finalized in 1986 (Figure 4.2). It is placed between the islands Schouwen-Duiveland and Noord-Beveland, is the largest (9 km of total length) of the 13 ambitious Delta Works series of dams and storm surge barriers. The construction of the Delta Works was in response to the widespread damage and loss of life due to the North Sea Flood of 1953. In normal conditions, the Oosterscheldekering is kept open and therefore allows tidal exchange and preserve marine life and shellfisheries, but it can be closed to prevent storm surges to flood the hinterland. Despite its relatively open nature, the barrier has reduced the tidal prism (i.e. the water volumes exchanged by the tide) of the Oosterschelde by approximately 30%. Current velocities have declined by 20-40% [Louters et al., 1998]. Sand exchange with the North Sea through the barrier is not possible due to the development of secondary currents. The new situation is thus characterized by channels that are too large for the tidal prism, which show a tendency to fill in. As this filling cannot be fed with sand from outside the tidal basin, sand is eroded from the tidal flats inside the basin and deposited in the channels. The new condition has amplified a pre-existent erosive trend in the tidal flats [Eelkema et al., 2012], to a degree where total disappearance of tidal flats in the system is predicted within less than one century [Jongeling, 2007].

The Westerschelde kept an open connection to the sea and to the Schelde river, and still has a full salinity gradient. Dredging in the Westerschelde started at the beginning of the past century, but has strongly intensified after the 1960's as a consequence of the growth of ship transit and draft. Nowadays, from 6.5 to 7 Mm^3 of sediment are annually dredged to maintain the shipping lane (Figure 4.2). The Netherlands and Belgium agreed in 2005 to further dredge the Westerschelde to allow container ships with a draft of up to 13.1 m to reach the port of Antwerp. Sediment extraction is very limited and by far most dredged sediments are disposed again within the estuary. Enlargement of the channels and amplified tidal range generated an increase in tidal currents of ca. 30% (since 1955) and altered the mixing patterns between fresh and salt water [Smolders et al., 2013, 2012].

4.2.2 Hydrodynamic variables

In order to reconstruct the impact of the last 50 years of basin hydrological management on the macrozoobenthos, we considered the induced changes in (yearly averaged) maximal tidal current velocity (maximal values reached during a full tidal cycle, m s^{-1}), inundation time (% of time for which the site is submerged during a full tidal cycle), average salinity (Practical Salinity Unit, PSU) and salinity range (Δ_{day} PSU). These variables are known to be among the most important hydrological variables in determining the benthos distribution in estuaries [Ysebaert et al., 2003, 2002], but they are rarely measured with full spatial coverage, such that they are known for all sample locations. Hydrodynamic models can fill these gaps as they can describe water motion and salt transport, given a bathymetry and appropriate boundary conditions. In this study, we used recently validated hydrodynamic models to simulate the Oosterschelde and Westerschelde present and past hydrological scenarios (Figure 4.3).

For the Oosterschelde, two scenarios, one for 1968 and one for 2010, are used in this study. These scenarios were modeled with a specific application of DELFT3D [Lesser et al., 2004] called the KustZuid-model. The resolution of the grid varies from more than 2000 m at the seaward boundary to around 100 m at the Westerschelde inlet. This model application and its calibration are thoroughly described in Eelkema et al. [2012]. The Westerschelde scenarios for 1955 and 2010 were modeled with 2Dh TELEMAC [Moulinec et al., 2011]. This model has a resolution up to 40 m in the intertidal zone. It accounts for salt transport, making it particularly appropriate for distribution modeling of estuarine species [Smolders et al., 2013]. In all modeled scenarios, wave forcing was omitted because we primarily focused on areas that are tide-dominated. The scenarios for the Westerschelde in 1955 and the Oosterschelde in 1968 represent the hydrological characteristics of the basins before the recent major anthropogenic alterations by dredging, embanking and damming. Salinity models for the Oosterschelde basin are not available; we neglected the role of the (limited) freshwater input from the Volkerak in the Oosterschelde 1968 scenarios. Both Oosterschelde scenarios were modeled with a constant salinity (30 PSU) and no salinity range. For simplicity, in the rest of the paper we will refer to the Westerschelde 1955 and the Oosterschelde 1968 scenarios as 1960 scenarios.

4.2.3 Ecological variables

Benthic community response to altered hydrodynamics was expressed in term of changes in potential macrozoobenthic biomass (g Ash Free Dry Weight (AFDW) m^{-2}), abundance (N. of individuals m^{-2}), per capita body size (biomass divided by the abundance of individuals, mg AFDW) and Shannon's species diversity index (H). The data used in the present study have been extracted from the Benthic Information System (BIS version 2.01.0) hosted by the NIOZ research center in Yerseke (NL). The BIS database contains about 500000 distribution records about more than 2500 species of all major benthic classes that were collected since 1960 mostly in the Delta region (SW Netherlands). For this study, a subset of 5510 (2272 Westerschelde; 3238 Oosterschelde) samples collected from 1962 to 2011 was selected in accordance to the availability of environmental data. Data collection was mainly carried out in spring and autumn. In the Westerschelde samples were randomly collected within four depth strata mainly from 2007 (Appendix B Table B.1). A longer sampling series is available for the Oosterschelde, where the large majority of data were collected by repeated sampling of the same sites across years in similar depth strata as used for the Westerschelde sampling (Table B.1). In both basins, 25% of the records come from intertidal sites, 50% of the records were collected above a depth of 5 m NAP (Normaal Amsterdams Peil, the Dutch height datum, 0 m NAP = mean sea level in Amsterdam) and 95% above 20 m NAP. The intertidal locations were mostly sampled by using handcorers pushed 20 to 30 cm in the sediment with a total sampling area between 0.005 and 0.045 m^{-2} (on average 0.019 m^{-2}). The subtidal locations were on some occasions sampled by using Van Veen grabs with a sampling area of 0.1 or 0.2 m^{2} and a penetration depth around 15 cm depending upon the nature of the sediment. In most other cases the subtidal samples consist of subsamples with an average sampling area of 0.023 m^{-2} that were taken by using handcorers pushed 20 to 30 cm in the sediment contained in the bucket of a boxcorer after landing on the ship deck. Whereas most (ca. 95%) of the samples have similar characteristics regarding the sediment penetration and the sampling area, the few Van Veen samples stand out due to a ten times larger sampling area and a smaller sediment penetration compared to the other samples.

4.2.4 Predicting benthic communities: upper boundary regression models

We describe changes in habitat suitability in term of changes in potential/maximal macrozoobenthic community parameters. Spatial distributions of organisms are often the product of different constraints acting at different scales [Thrush et al., 2005]. Even when one or more (known) environmental factors are not limiting, other (unknown) factors might be and organisms could be absent or limited to a low density. As a result, observed distributions tend to be scattered below an upper boundary rather than around a central, average value. Such patterns are difficult to interpret via central estimators (*e.g.* Ordinary Least Square) [Blackburn et al., 1992, Cade et al., 2005, Thomson et al., 1996]. Models of the upper boundary of the distribution are a better alternative to describe organisms' response to environmental constrains. They represent the maximal response in the absence of other, more limiting, factors [Anderson, 2008, Cade and Noon, 2003]. Models of the upper boundary forecast the habitat potential for the organism, rather than its realized performance. Thus, they give an estimation of habitat suitability [Cade and Noon, 2003, Downes, 2010]. In nature conservation and management, habitat suitability is often preferred as a descriptor over realized performances, because it fluctuates less in time [Degraer et al., 2008].

Quantile regression [Koenker and Hallock, 2001] can be used to predict any desired distribution quantile of the response when conditioned by one [Anderson, 2008] or more [Cozzoli et al., 2014] explanatory variables. We used multivariate linear quantile regression to describe the upper boundary of observed benthic community parameters as a function of the modeled hydrological variables, until their third-degree interaction terms. The use of a large and long-term dataset, as in our case, allows estimating the conditional quantiles of benthic community distribution with respect to a large number of environmental variables and their interactions. Given that the maximum can be a fairly volatile statistic due to the influence of outliers [Anderson, 2008], we considered a slightly sub-optimal quantile to model the upper boundary of the species responses (95^{th} quantile). The so obtained species distribution models were validated (procedure and results in Appendix B) and used to produce whole basin habitat suitability maps for the years 1960 and 2010. Differences between the predicted scenarios (Appendix B, Figures B.3 & B.4) were expressed in terms of absolute change in potential benthic communities performances. All analyses were performed with `R` [R Development Core Team, 2011].

4.3 Results

The fitted models were able to forecast with great accuracy the 95^{th} conditional quantile of the observed distributions (see Appendix B for models' summary and validation). In the Westerschelde, the tidal current velocities increased in most places (Figure 4.3) following the widening and deepening of the channels, and this was a strong limiting factor for benthic communities. We predict that subtidal benthic communities responded to increased current velocity and salinity range (Figure 4.3) by reducing their potential biomass, density, individual body size and species diversity in almost the whole basin (Figure 4.4). The strongest decrease in species diversity (Figure 4.4 D) was predicted in association with reduced salinity in the marine part of the estuary (Figure 4.3 C). Large parts of the intertidal strongly increased in height (Figure 4.3 B) and thereby current velocity remained relatively low there or even decreased (Figure 4.3 A). Reduced inundation time became the strongest limiting factor for the macrobenthos in the intertidal. The result was that the macrobenthos evolved towards smaller individual size and increased abundance (Figure 4.4 B & C).

In the 1960 scenario, the Oosterschelde current velocities were in the range of the Westerschelde ones (Figure 4.4 A). The Oosterschelde was however a potentially more suitable environment than the Westerschelde (Figure 4.4). We modeled that the dampening of tidal current velocities in the Oosterschelde (Figure 4.4 A) had a strong positive effect on the subtidal potential biomass (Figure 4.4 A). Our forecasts also show that the increase in biomass was related to larger individual body sizes (Figure 4.4 C), rather than increased abundance (Figure 4.4 B). The potential subtidal species diversity remained unchanged (Figure 4.4 D). At present, the inundation time of the Oosterschelde intertidal flats is just slightly higher than in the 1960's (Figure 4.3 B), inducing a limited decrease in abundance. The effects are most pronounced at the edges of the tidal flats. (Figure 4.4 B).

Observed trends in benthic community descriptors confirm model outputs for the Oosterschelde (Figure B.2). Not enough early observations are available for the Westerschelde to be directly compared with model predictions

(Table B.1). However, records from [Wolff, 1973], coherent with our forecasts, suggest that benthic organisms were more widely distributed in the subtidal than in later years.

4.4 Discussion

The management of coastal and estuarine areas is considered a critical issue as these ecosystems are among the most valuable [Costanza et al., 1997], but at the same time, also most impacted environments in the world [Barbier et al., 2011]. In this study we show that fundamental alternative management options entail long-term morphological and hydrological alterations of the ecosystem. We predict that hydrological alterations following deepening have negative implications for benthic life, while the realization of a storm surge barriers, has mixed and habitat-dependent responses, that also include improvement of environmental quality. The multidisciplinary integration of hydrodynamic and ecological models allows to investigate the long-term effect of these alterations for an important part of the natural community. Our findings for the SW Netherlands can be generalized to analogous management cases worldwide because: 1) they are based on general community descriptors, relatively more independent from local biogeographical features than species responses [Thrush et al., 2005]; 2) they account for the upper boundary of the distribution, hence excluding the influence of (local, particular) subsidiary factors [Blackburn et al., 1992, Cade et al., 2005, Thomson et al., 1996] and focusing on the response to those hydrological factors (tidal current velocity, inundation time, salinity) that are a direct consequence of the human infrastructures.

Macrozoobenthic body-size - abundance distributions reveal disturbance pressures through individual energetics, population dynamics, interspecific interactions and species coexistence responses [Basset et al., 2004]. Because of the importance of the individual body size for many individual and community traits, [Brown et al., 2004, Marquet, 2002], the predicted changes in potential per capita size of benthic organisms (Figure 4.4 C) can have profound effects across multiple scales of biological organization. The decrease in potential species diversity and body size, as predicted for the Westerschelde, can be detrimental for ecosystem functioning. In the intertidal, this pattern indicates an increase in reductive stress [Pearson and Rosenberg, 1978]. The lack of large macrozoobenthic organisms could result in a reduction of the bioturbation potential [Solan et al., 2004], with negative effects on nutrient cycling and sediment oxygen concentration [Heip et al., 1995]. On the other hand, a higher potential for bigger individuals, like predicted for the subtidal habitats in the Oosterschelde, is indicative of higher complexity in species trophic [Woodward et al., 2005] and non-trophic (*e.g.* ecosystem engineering, habitat forming [Kefi et al., 2012]) interactions. Communities composed of bigger individuals are generally more functional, productive and stable, and they can support more biomass at higher trophic levels [Brown et al., 2004]. In the case of subtidal macrozoobenthos in the Oosterschelde, the latter point could imply positive effects on macrofauna through the benthic-pelagic food chain [Rinne and Miller, 2006].

On the other hand, the striking improvement in quality of the subtidal benthic habitat (Figure 4.4) is an unexpected consequences of the Oosterschelde embankment. The dampening of current stress allowed a vast portion of the subtidal Oosterschelde to be colonized by large macrozoobenthic organisms, which were confined to the inner and sheltered part of the estuary before the embankments [Cozzoli et al., 2014]. This change in habitats has created opportunities for tourism (diving) activities, in particular in combination with the increased transparency of the water. While natural values of the original system (*e.g.*, intertidal productivity, food provision for birds) are intrinsically incompatible with the management option that was chosen, other natural values such as subtidal benthic habitat quality do have the potential to be compatible with this option.

It is evident that the realization of societal objectives such as transport and safety must also include ecological goals [Leschine et al., 2003]. The divergent human pressures on the Oosterschelde and Westerschelde (Figure 4.2) are exemplary of what the Anthropocene will imply in a near future for many of the world's coastal ecosystems (Figure 4.1). While the management regimes of the systems discussed in this paper show local effects on the scale of the impacted water body, the actual or expected diffusion of such types of management [Small and Nicholls, 2003] increases their relevance at a global scale. A public debate is needed on whether nature conservation goals can and should be brought closer in line with other management objectives, or whether natural values should be constraining other management options. Our analysis suggest that static management goals should be carefully considered in environmental planning, as ecosystems develop and new and unexpected features can emerge. Ecological forecast must be included into dynamic infrastructure design to maintain operational efficiency and reduce the ecological impacts [Matthews et al., 2011]. Model extrapolations of the biological and physical environment are a fundamental step to explicitly integrate nature into infrastructure development ("Building with nature", see at van Slobbe et al. 2013) and to forecast the future availability of ecosystem services [Chan et al., 2006]. In this perspective, the comparative analysis of the Westerschelde and Oosterschelde basins is a precious source of information to understand (and communicate) the future ecological consequences of global trends in human coastal development.

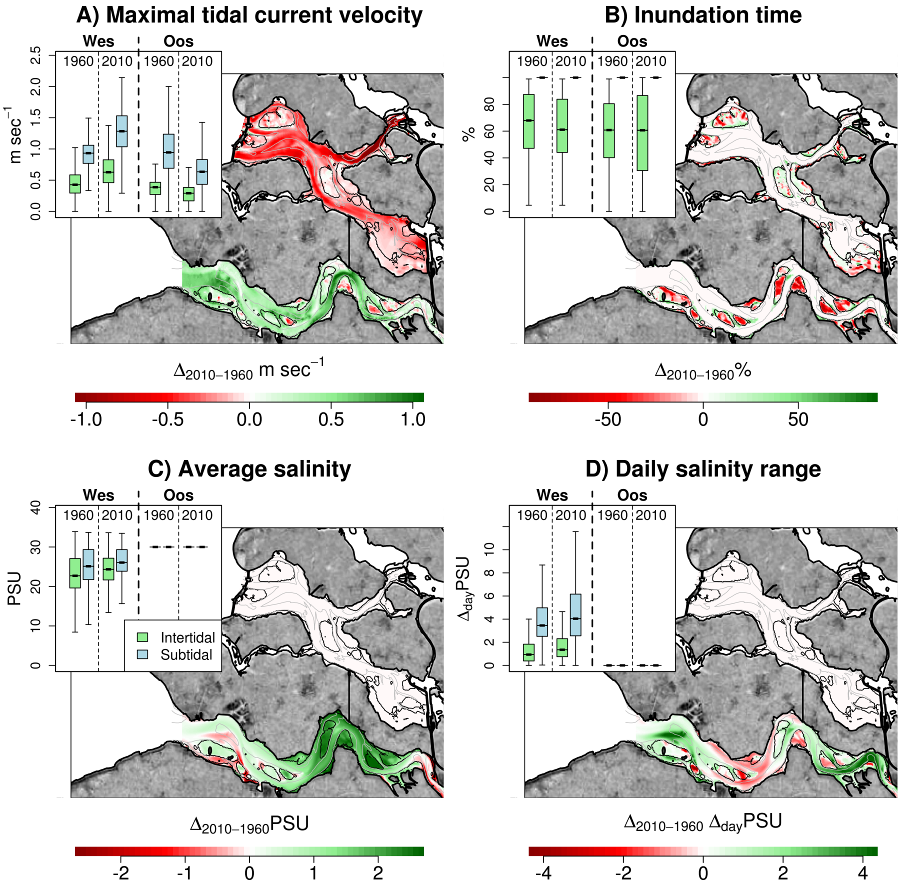
A) Maximal tidal current velocity
Wes
Oos
1960
2010
1960
2010
m sec−1
0.0
0.5
1.0
1.5
2.0
2.5
Δ2010–1960 m sec−1
-1.0
-0.5
0.0
0.5
1.0
B) Inundation time
Wes
Oos
1960
2010
1960
2010
%
0
20
40
60
80
Δ2010–1960%
-50
0
50
C) Average salinity
Wes
Oos
1960
2010
1960
2010
PSU
0
10
20
30
40
Intertidal
Subtidal
Δ2010–1960PSU
-2
-1
0
1
2
D) Daily salinity range
Wes
Oos
1960
2010
1960
2010
ΔdayPSU
0
2
4
6
8
10
Δ2010–1960 ΔdayPSU
-4
-2
0
2
4

Figure 4.3: **Changes in abiotic variables between 1960 and 2010.** Maps show the absolute changes in hydrodynamic variables, as predicted from the hydrodynamic models. Intertidal areas are marked with a black line. Boxplots show the distribution of the variables in 1960 and 2010 for the Westerschelde (Wes) and Oosterschelde (Oos). Intertidal (green) and subtidal (blue) data are presented separately in the box plots. The realization of the Oosterscheldkering in 1986 strongly dampened the tidal currents in the Oosterschelde, while deepening of the Westerschelde had the opposite effect, especially in the subtidal (A). Local decreases in intertidal current strength and high suspended sediment loads are promoting sedimentation on the Westerschelde intertidal mudflats. In the Oosterschelde some signs of intertidal erosion are visible on the edges of the mudflats (B). The increased tidal flux in the Westerschelde led to a deeper penetration of the saltwater in the estuary (C) and, in general, to wider daily salinity fluctuations (D)

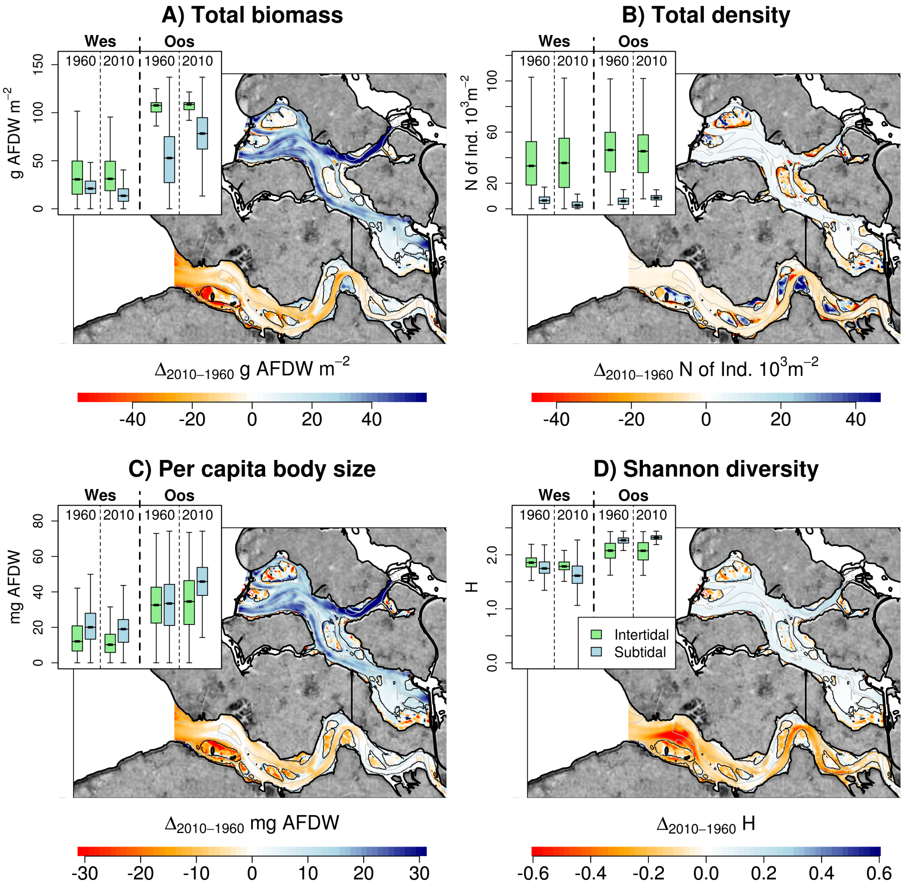
A) Total biomass
Wes
Oos
1960
2010
1960
2010
g AFDW m^-2
0
50
100
150
Δ2010–1960 g AFDW m^-2
-40
-20
0
20
40
B) Total density
N of Ind. 10^3m^-2
0
20
60
100
Δ2010–1960 N of Ind. 10^3m^-2
C) Per capita body size
mg AFDW
0
20
40
60
80
Δ2010–1960 mg AFDW
-30
-20
-10
0
10
20
30
D) Shannon diversity
H
0.0
1.0
2.0
Intertidal
Subtidal
Δ2010–1960 H
-0.6
-0.4
-0.2
0.0
0.2
0.4
0.6

Figure 4.4: **Changes in habitat suitability between 1960 and 2010.** Maps show the absolute changes in potential benthic communities responses, as predicted from the 95th quantile regression models. Intertidal areas are marked with a black line. Boxplots show the distribution of the predicted variables in 1960 and 2010 for the Westerschelde (Wes) and Oosterschelde (Oos). Prediction for the intertidal (green) and subtidal (blue) habitats are presented separately in the box plots. Compared to 1960, benthic habitat suitability has strongly improved in the subtidal part of the Oosterschelde, especially in terms of potential biomass (A), per capita body size (C) and species diversity (D). Changes are less relevant in the intertidal part of the basin, mostly involving a slightly decrease in individual density (B). For the Westerschelde, we modeled a generalized decrease in habitat suitability. Increases in intertidal potential density associated with decreases in potential per capita body size (B & C) are indicative of the proliferation of small sized opportunistic deposit feeders. Increased hydrodynamic and salinity stress had a detrimental effect on species richness, especially in the most marine part of the estuary (D)

Acknowledgments

This work was mainly funded by the Ecoshape/Building with Nature project. The NIOZ Monitor Taskforce was for a large part responsible for the fieldwork and the taxonomic analysis of the macrofauna samples. Rijkswaterstaat (executive body of the Dutch Ministry of Infrastructure and the Environment) was responsible for the funding of these activities in the framework of different national monitoring projects such as MWTL. The hydrodynamic modeling for the Westerschelde was funded by the Antwerp Port Authority.

CHAPTER 5

Modeling benthic habitat suitability to evaluate ecological benefits of a new sediment disposal strategy in shallow tidal waters

---

Sven Smolders, Francesco Cozzoli, Yves Plancke, Tom Ysebaert, Stefaan Ides, Tjeerd J. Bouma, Patrick Meire, Peter M. J. Herman and Stijn Temmerman

Abstract

Preserving estuarine functioning is a great challenge that demands a holistic approach. Estuarine morphological management should consider to steer the bed morphology in such a way to improve human safety and economical activities (*e.g.* transportation, fishery) while minimizing impacts on ecosystem functionality. We present an evaluation method to reconcile the disposal of dredged sediment with the preservation or improvement of benthic habitat suitability (essential for the ecological functioning). Using a numerical hydrodynamic model, we assessed changes in benthic habitat conditions after the nourishment of an intertidal shoal (Walsoorden, Westerschelde, The Netherlands). The physical scenarios were used to fit species distribution models of the macrozoobenthic community and to evaluate the ecological impacts of sediment disposal. We predict a general increase in benthic habitat suitability of the shallow subtidal zone after the implementation of the nourishment. Intertidally, a limited increase in habitat suitability is noted, as the intertidal flat heightened and the sediment become finer, but at the highest places the macrozoobenthic community is replaced by saltmarsh. Based on our forecast,

we also propose an additional, small intervention on the nourishment to further increase the benthic habitat conditions. The presented approach proves it usefulness not only for the impact assessment for morphological changes, but also in the design of these changes.

5.1 Introduction

Estuaries are naturally highly dynamic, productive and among the most valuable ecosystems in the world [Costanza et al., 1997]. They are a preferential habitat for large number of species and they are home of important ecosystem processes [Gray, 1997, Kennish et al., 2002]. Moreover, estuaries have also a major economical and social importance for human communities [Small and Nicholls, 2003]. The estuarine morphology is the common denominator influencing and steering both ecosystem performances and human usage. In estuaries worldwide the natural benthic morphology is often severely altered by human interventions like embankments, shipping and dredging [Gray, 1997, Kennish et al., 2002]. Some of the most relevant goals for the morphological management of estuaries are:

- **Flood defense**: In many cases the shorelines of estuaries are densely populated. Coastal populations need to be protected from flood risks especially caused by storm surges [Temmerman et al., 2013]. The estuarine morphology exerts friction on the landward propagation of tides and storm surges. Hence the morphology determines the balance between set up or attenuation of tidal and storm surge levels [Dronkers, 1986, Wang et al., 2002].

- **Port accessibility**: The world's largest ports are typically located along estuaries. Capital or maintenance dredging is often needed to allow access of the ever larger seagoing ships access to the inland ports. Depending on the natural morphology, channels with high self-eroding capacity diminish the need for maintenance dredging.

- **Ecological status**: The estuarine ecosystem functionality is highly responsive to natural and anthropogenic changes in the bed morphology [Roy et al., 2001]. The morphology determines spatial patterns of abiotic factors like water depth, salinity and flow velocity and is therefore a key parameter for the spatial patterns of benthic animal and plant communities [Herman et al., 1999, Ysebaert et al., 1998, 2002]. A good ecological status of estuaries is essential for the ecosystem services provided to human society, such as fishery and the conservation of marine and coastal biodiversity, including global assets such as migrating birds.

Preserving all three functions listed above is a great challenge that demands a holistic management approach, able to reduce frictions between different activities and needs [Folke et al., 2004, Leschine et al., 2003]. As an example, dredging is usually considered an activity with high environmental impact, both on the short [Short and Wyllie-Echeverria, 1996] and on the long term [Cozzoli et al., 2013, 2015c]. However, dredged material could be regarded as a potential resource, useful for shoreline protection, beach nourishment and for the creation or restoration of habitats, like mudflats or salt marshes [Bolam and Whomersley, 2005, Ray, 2000, Temmerman et al., 2013, Yozzo et al., 2004]. Up till now only small-scale experiments have been tested due to concerns about the subsequent movement of material by tidal current and wave action [Widdows et al., 2006]. This paper focuses on an evaluation method to reconcile the disposal of dredged sediment with the preservation or improvement of benthic habitat suitability.

The macrozoobenthos plays an essential role in the estuarine food chain, which means that changes in the macrozoobenthic community will translate into functional changes into the ecosystem [Pearson and Rosenberg, 1978, Warwick, 1986, Ysebaert et al., 2005, 1998, 2002]. It offers one of the best ways to assess the ecological status of an estuary because it responds to changes in an integrated set of environmental conditions (*e.g.* Gray [1974], Ysebaert et al. [1998]). Additionally, macrozoobenthos is relatively easy to monitor and reacts quickly on (local) disturbances by changing species composition and abundance (either expressed as numerical or biomass abundance). In previous studies macrozoobenthos has been used to estimate the ecological impact of dredging and disposal activities [Borja et al., 2000, Roberts et al., 1998, van der Wal et al., 2011].

Even in systems where the macrozoobenthic spatial distribution is relatively well-known, it is usually restricted to point observations at the sampling stations. There is however an increasing need for full coverage spatial distribution maps [Young, 2007]. One way to gain full coverage distribution maps is to spatially interpolate between all sampling points (*e.g.* Holtmann et al. [1996]). But community structures might change over short distances making the quality of the interpolation highly dependent on the number or spatial resolution of sampling points [Degraer et al., 2002]. Spatial interpolation produces a rather static map and does not allow to account for environmental changes without repeating the whole interpolation. A second way to obtain full coverage maps is to develop habitat suitability models that predict the presence of macrozoobenthos based on the suitability of the physical habitat. This method is limited by the availability and resolution of the environmental data, but these are generally less costly to gather, compared to the collection of the labor-intensive macrozoobenthos data.

A third way, offering the additional advantage of providing prognostic tools, is the combination of models predicting biotic responses to environmental conditions (species distribution models) and prognostic environmental models, such as hydrodynamic models. This combination of models allows us to investigate the effect of (natural or anthropogenic) morphological changes on benthic species and community distributions, and by extension the ecological status of the estuary.

This paper will use habitat suitability models for macrozoobenthos to evaluate the ecological impact of morphological changes. We will show that the model is not only used for evaluation but can also be used for optimization of the morphological changes. It can simultaneously consider both the effects on navigability and on the ecology of the estuary. Modelers and engineers can use this model already in the design phase of a project, where different scenarios can be simulated and evaluated for their ecological impact.

5.2 Material and methods

5.2.1 Study area

The Westerschelde is located at the border between The Netherlands and Belgium and is one of the longest estuaries in NW Europe with still a complete salinity gradient (Figure 5.1 A & B). It is funnel shaped and reaches from Vlissingen (km 0), with a tidal range of 3.8 m, to Ghent (km 160) where the tidal penetration is stopped by sluices and weirs. Flood enters the estuary twice a day with an average volume at the mouth of 1.04 Gm^3 [Baeyens et al., 1998]. The discharges of the Schelde and tributaries are very small (*i.e.* 104 m^3 sec^{-1} as long yearly average) compared to the tidal volume [Meire et al., 2005]. It is a well mixed estuary with small or negligible vertical salinity gradients [Baeyens et al., 1998]. The Westerschelde consists of a complex morphology, with different ebb and flood channels surrounding large intertidal flats and salt marshes. The tidal flats occupy 35% of the total surface area of the Westerschelde (310 km^2) [Ysebaert et al., 2002]. The Westerschelde is the main shipping route for seagoing ships to the port of Antwerp. Maintenance dredging (8 to 12 million m^3 of sediment per year), to keep the navigation channel deep enough for the largest ships, is one of the major anthropogenic stressors. The shoal of Walsoorden, our study area, is one of the intertidal shoals in the Westerschelde (most downstream part, km 55, Figure 5.1 B).

5.2.2 Evaluating a new disposal strategy aiming at ecological benefits

Until 2004, dredged material was disposed in the secondary channels, from where it returned, at least partly, to the navigation channel. This practice might destabilize the multi-channel estuarine system, if the disposed volumes become too large [Wang and Winterwerp, 2001]. Collapse of the multi-channel system into a single channel system is generally regarded as detrimental for the system's ecological state , as it leads to the loss of the complex of habitats constituted by the intertidal flats that develop in between flood and ebb channels and their surrounding low-dynamic shallow subtidal habitats. In a single-channel estuary, the banks at either side of the channel will increase in height and

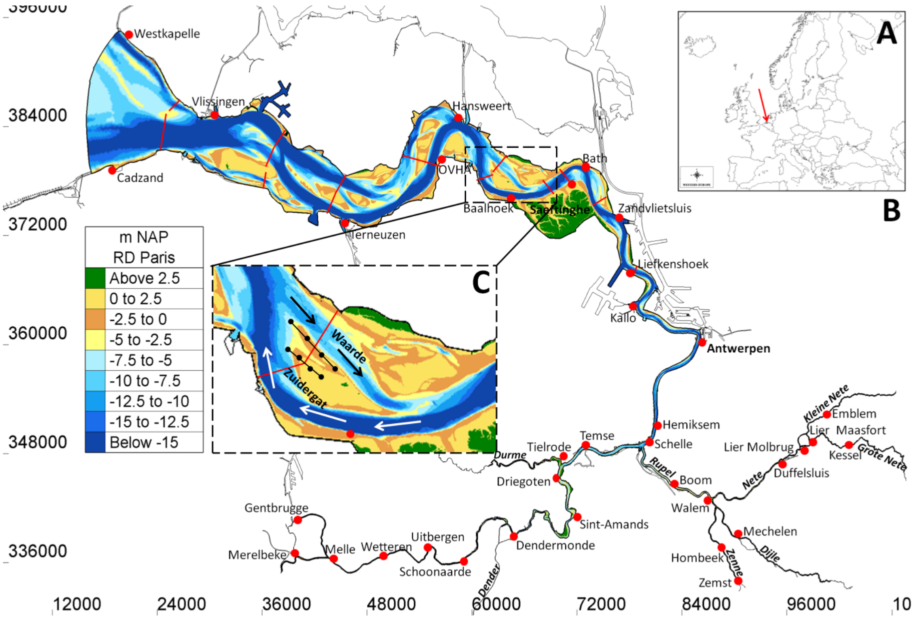
396000
384000
372000
360000
348000
336000
12000
24000
36000
48000
60000
72000
84000
96000
10
A
B
C
m NAP
RD Paris
Above 2.5
0 to 2.5
-2.5 to 0
-5 to -2.5
-7.5 to -5
-10 to -7.5
-12.5 to -10
-15 to -12.5
Below -15
Westkapelle
Vlissingen
Cadzand
Terneuzen
Hansweert
OVHA
Baalhoek
Saeftinghe
Bath
Zandvlietsluis
Liefkenshoek
Kallo
Antwerpen
Waarde
Zuidergat
Hemiksem
Schelle
Temse
Tielrode
Durme
Driegoten
Rupel
Boom
Walem
Lier Molbrug
Kleine Nete
Emblem
Lier
Maasfort
Kessel
Grote Nete
Nete
Duffelsluis
Mechelen
Hombeek
Zenne
Dijle
Zemst
Sint-Amands
Dendermonde
Dender
Gentbrugge
Merelbeke
Melle
Wetteren
Uitbergen
Schoonaarde

Figure 5.1: **The Schelde Estuary.** A) Location of the Westerschelde in Europe. B) The Westerschelde with tide gauges (red dots), discharge transects (red lines). C) Detail of shoal of Walsoorden with discharge transects (red lines) and locations of ADCP flow velocity measurements (black dots). The black arrows indicate the flood channel, the white arrows the ebb channel

become vegetated salt marshes, that are only flooded at the highest tidal levels and exert very little resistance to the tidal wave as it penetrates the estuary.

An alternative disposal strategy for dredged sediment in the Westerschelde was proposed to make beneficial use of dredge spoil material [Peters et al., 2001]. The new alternative disposal strategy is to put the material near the (eroding) edges of tidal flats, after which the material is expected to move slowly towards the flats by the natural forces of tidal currents and waves. The objective is to reshape the tidal flats in such a way that the ebb and flood currents are more effectively distributed between the different multiple channels. By doing this the multiple channel system is sustained. Moreover, dredging efforts could be reduced in the long-term, as dredge spoil material will move towards the navigation channel at slower rates because it is more stable along the shoal edges. In order to test this scenario, two small scale tests were executed moving each time 500.000 m^3 of dredged sand near the intertidal flat of Walsoorden (Figure 5.1 B & C). Another small scale test added another 900.000 m^3. The success of the small scale experiments granted the full scale disposal of 4 to 5 million m^3, representing more than half of the volume dredged yearly in the

Westerschelde [Plancke et al., 2006, 2012, Vos et al., 2009].

We will look at four different situations in time. The first one is the situation before any test disposal was made at the tip of the Walsoorden shoal. We used the bathymetry of 2003 for this case. The second situation uses the bathymetry after the test disposals (2009), but before the full scale disposal. The third situation is after the full scale disposal. Therefore we added the disposed sediments measured in 2012 at the tip of the shoal of Walsoorden to the bathymetry of 2009. Finally we added a fictitious scenario, which we will call the extra scenario in this paper, where we added extra sediment (340000 m^3) in the downstream tip of the shoal. This extra scenario wants to test if an *ad hoc* disposal of dredged sediments will not only better bifurcate the flow, but can also be more beneficial for the local benthos community. The detailed bathymetry of these four scenarios is given in Figure 5.2.

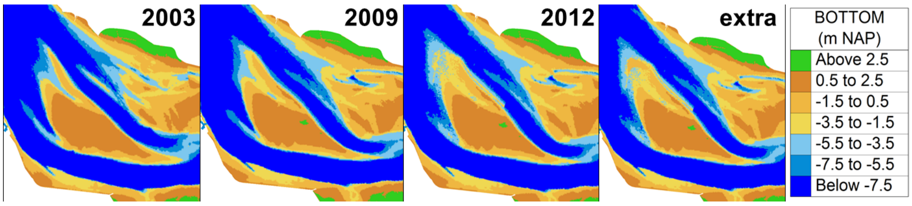

Figure 5.2: **Walsoorden nourishment.** Bathymetry of the tip of the shoal of Walsoorden (more detailed than Figure 5.1 C) for 2003, 2009, 2012 and an hypothetical scenario (addition of 340000 m^3 of sediment in the downstream tip of the shoal)

5.2.3 TELEMAC model

The hydrodynamic parameters for the benthos habitat suitability model are gathered by the simulation of the four above described scenarios in a 2D hydrodynamic TELEMAC model [Desombre, 2013] of the entire Westerschelde (Figure 5.1 B). The overall mesh resolution in the study area was 30 m. The mesh consisted of 494406 nodes in total. A tidal water level fluctuation was imposed at the seaward boundary. Discharges were imposed at the upstream river boundaries. The hydrodynamic model was stepwise calibrated against measurements of water levels in the whole estuary, discharge measurements through the subtidal channels near the intertidal shoal of Walsoorden, the focus of this study, and tidal current measurements on the intertidal shoal.

Calibration of water levels: 22 tidal gauge stations (red dots in Figure 5.1 B) were used for water level calibration. The Manning bottom friction coefficient, used as calibration parameter, was adapted between consecutive tide gauge stations, depending on the difference between the modeled and measured water level. A higher coefficient would slow down a flood flow, decreasing the high water levels upstream, and would slow down the ebb flow, increasing the low water levels upstream and decreasing the low water levels downstream. A cost function was used to evaluate the improvement of the calibration steps. Weight factors were assigned to all tidal measurement posts according to their importance: the closer to the study area the more important. The cost function added the average differences between measured and modeled water levels of the tide gauge stations (Equation 5.1).

$$Avg(WL) = \frac{\sum_{j=1}^{n} WL_{measured} - WL_{modeled}(J)}{n} \tag{5.1}$$

where WL is the Water level and n the number of tides considered (number of high or low water levels). The same was done for the phase of the tides. The cost function was calculated for the average differences in measured and modeled water level (Equation 5.2), and similarly for the average phase differences and for the standard deviations on water level and phase differences.

$$Cost = \sum_{i=1}^{m} \sigma_i Avg(WL)_i \tag{5.2}$$

where σ is a weight factor and m is the total number of tidal stations. The simulation with the lowest cost functions is kept as the best calibrated one. The cost function results for the water levels are shown in Figure 5.3. The lowest cost function value for the water levels (high and low water level together) for calibration run 7 equals 0.053 m and is comparable with the cost function value for the final calibration of the Westerschelde model described in Smolders et al. 2012, *i.e.* 0.047 m. For the phase difference the cost function equals 3.7 minutes for simulation 7.

Calibration of discharges: Discharges in the ebb and flood channels can be affected in the model by changing the local bottom friction coefficient. The main purpose of calibrating the discharges is to get the distribution of the total flow into the ebb and flood channel in the right proportions. If the ebb channel for example is getting too much flow and the flood channel not enough, the bottom friction coefficient can be locally increased in the ebb channel and decreased in the flood channel. Discharge measurements in the Westerschelde are scarce; a transect (locations are given as red line in Figure 5.1 B) is measured every four to five years. To tackle this, different techniques to compare model results with measurements are described in Smolders et al. 2012. For this model we focused on the total ebb and flood volumes of different tides in a spring neap tidal cycle plotted against their occurring tidal amplitude (difference between high and low water level). The measurements were plotted in the same figure. The distance of the measurement to the fitted linear regression line gives an estimate of how good the model represents the discharges in each transect. In Figure 5.3 an example is given for the 'Schaar van Waarde', which is the flood channel north of the shoal of Walsoorden. Slight changes were made in the

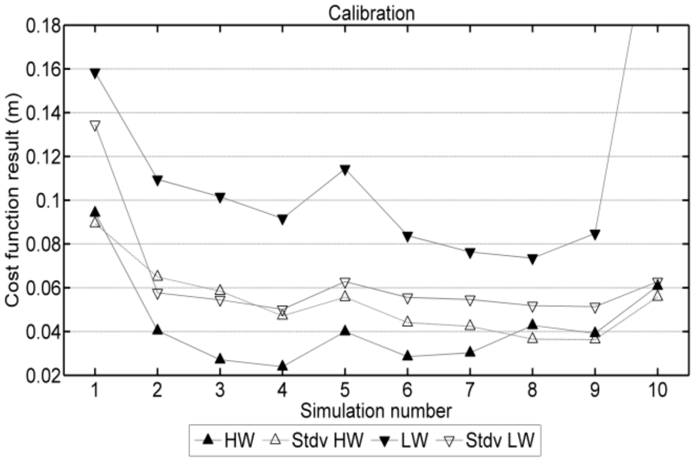

Figure 5.3: **Cost function.** The cost function results of different calibration steps (1-10) for high water levels (HW), the standard deviation on HW, low water levels (LW), standard deviation on LW

models bottom friction map to improve the discharges after which the water levels were checked again. This resulted in simulation 8 (Figure 5.4) being the new best calibrated model.

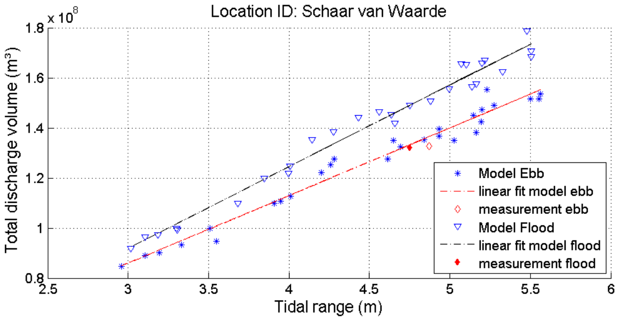

Figure 5.4: **Calibration of discharges.** For a neap spring tidal cycle the total discharge volumes over the transect 'Schaar van Waarde' are given in function of their respective tidal range. The distance between the measured total discharge volume and the models linear regression line evaluates the calibration effort

Calibration of flow velocities on shoals: For several shoals ADCP point measurements were available (for shoal of Walsoorden the measurement locations are given by the small black dots in Figure 5.1 C). Calibration was done by changing the Manning bottom friction coefficient for the entire shoal. This could only affect the magnitude of the flow velocity and not its direction. Maximum flow velocities were plotted as a function of the corresponding high water level. Model simulations and measurements are plotted for a neap-spring tidal cycle (Figure 5.5). The distance between the linear regression lines of model results and measurements indicates the quality of the model. For the shoal of Walsoorden a Manning coefficient of 0.024 proved to give the best overall results. Changing the bottom friction coefficient on the intertidal flats does not affect the water levels in the estuary.

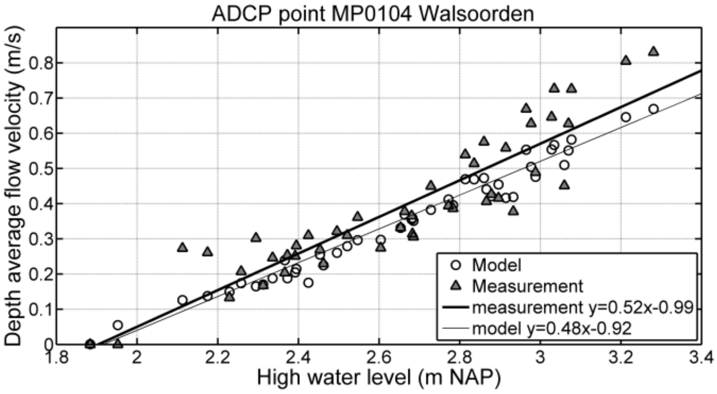

Figure 5.5: **Calibration of flow velocities.** For a neap-spring tidal cycle the maximum flow velocity is given as a function of the high water level (dots) for an ADCP measurement location on the shoal of Walsoorden. Measurements are shown as dark symbols and trend line, simulations as light symbols and trend line

Salinity: Salinity values were taken from a Westerschelde model with a coarser grid resolution (model described in Smolders et al. 2012). Calibrating salinity as a passive tracer needs long simulations at the cost of computation time. In that model the tracer was calibrated using the tracer diffusivity parameter. Modeled salinity values were compared with measured ones at two locations: Overloop van Hansweert (OVHA) and Baalhoek (Figure 5.1 B). For the tracer diffusivity parameter a value of 0.8 m^2 sec^{-1} gave the best results. This value does not compare with real salt diffusion values due to the added numerical diffusion in the model. For OVHA the model is not able to estimate the lowest salinity values every tide (Figure 5.6). For the location Baalhoek the model results were in better agreement with the measurements (Figure 5.6).

5.2.4 Macrozoobenthos habitat suitability model

The macrozoobenthos habitat suitability model we used is an upper boundary model. Spatial distributions of organisms are often the product of different constraints acting at different scales [Thrush et al., 2005]. Even when one or more (known) environmental factors are not limiting, other (unknown) factors

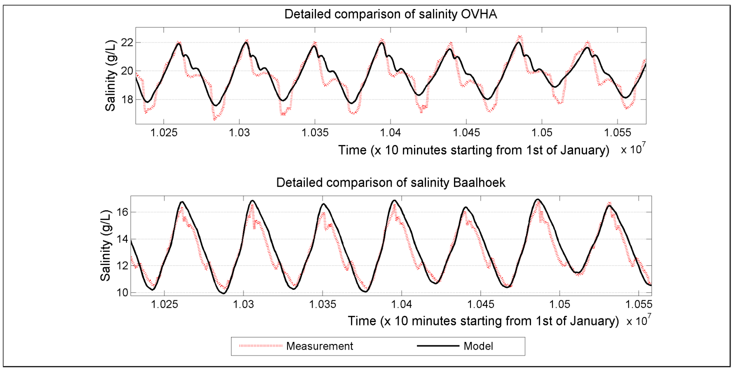

Figure 5.6: **Calibration of salinity level.** Comparison of measured and modeled salinity values (g L^{-1}) for the locations Overloop van Hansweert (OVHA) and Baalhoek (locations see Figure 5.1 B)

might be and organisms could be absent or limited to a low abundance. Models of the upper boundary represent the maximal response in the absence of other, more limiting, factors [Anderson, 2008, Cade and Noon, 2003]. They forecast the habitat potential for the organism, rather than its realized performance. Thus, upper boundary regression models can be used to give an estimation of habitat suitability [Cade and Noon, 2003, Downes, 2010]. In nature conservation and management, habitat suitability is often preferred as a descriptor over realized performances, because it fluctuates less in time [Degraer et al., 2008]. The model we used describes changes in habitat suitability in term of changes in potential of the macrozoobenthic community parameters distributions. To focus on the upper boundary rather than on the central trend of the distribution, we adopt a quantile regression approach [Koenker and Hallock, 2001]. Because the maximum can be a fairly volatile statistic due to the influence of outliers [Anderson, 2008], a slightly sub-optimal quantile is considered to model the upper boundary of the species responses (95^{th} quantile). Further insights about model fitting and validation can be found in Cozzoli et al. [2013] and Cozzoli et al. [2014].

Our habitat suitability model uses four physical variables that all can be simulated in the hydrodynamic model described above: maximal flow velocity (maximum of a full tidal cycle, m sec^{-1}), inundation time (% of time submerged during a full tidal cycle), daily averaged salinity (Practical Salinity Unit, PSU) and salinity range (Δ_{day} PSU). These variables are known to be among the most important hydrological variables in determining coastal and estuarine benthos distribution [Snelgrove and Butman, 1994, Snelgrove et al., 1994, Ysebaert et al., 2002]. While other variables have proven to contribute to the prediction of benthic community distribution (*e.g.* turbidity [Akoumianaki and Nicolaidou, 2007], primary production [Smith et al., 2006], organic matter [Verneaux et al., 2004], mean sediment grain size and mud content [de la

Huz et al., 2002, Degraer et al., 2008, Snelgrove and Butman, 1994, Snelgrove et al., 1994, van der Wal et al., 2011]), they are often well correlated with those accounted into analysis, so they do not increase significantly the explanatory power of the model [Cozzoli et al., 2013].

Benthic community responses to different environmental variable values were expressed in term of changes in potential macrozoobenthic biomass (g Ash Free Dry Weight (AFDW) m^{-2}), abundance of individuals (N. of individuals m^{-2}), per capita body mass (mg AFDW) and Shannon species diversity index (H). Apart from the community parameters we consider the total biomass (g m^{-2}) of five different species known to be common in our area of interest: *Cerastoderma edule*, *Macoma balthica*, *Hediste diversicolor*, *Heteromastus filiformis* and *Bathyporeia pilosa*. These species are among the most abundant in the brackish part of the Westerschelde (except for *B. pilosa*, but this species was taken into account because it has a specific preference for coarse sediment and relatively strong currents [Degraer et al., 2006]). The comparative analysis of their distributional response to human impacts is an ideal system investigate ecological impacts on a local/short time scale because: 1) they share a common habitat (muddy intertidal flats) but they are known to have slightly different preferences for habitat parameters like current velocity, reductive stress and sediment composition [Degraer et al., 2006] 2) they are mostly characterized by opportunistic behavior and fast population dynamics, thus they quickly adapt to the new environmental conditions [Degraer et al., 2006].

The data used to fit the SDMs have been extracted from the Benthic Information System (BIS version 2.01.0) hosted by the NIOZ research center in Yerseke (NL). For this study, a subset of 2272 samples collected from 1962 to 2011 was selected in accordance to the availability of environmental data. The use of such a large and long term dataset allows to extrapolate the upper boundary of the response distribution above a large span of different combination of subsidiary factors, thus increasing the generality and the reliability of our forecast. All the benthic parameters listed above will be investigated for the intertidal (>-2.5 m NAP) and subtidal (<-2.5 m NAP) area separately. Because of autonomous evolution of the morphology in the estuary it is difficult to separate the effects of the disposal strategy from the ongoing large scale morphological evolution. Therefore we focus only on the area directly near the new disposal strategy. Both the intertidal (red line) and subtidal (blue line) area investigated here are given in Figure 5.7.

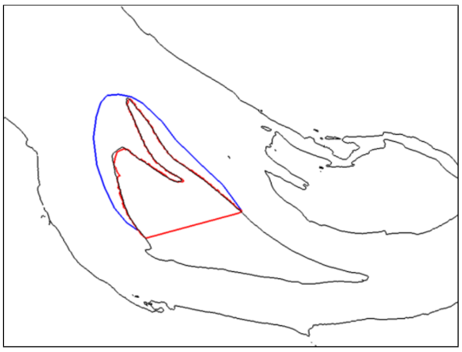

Figure 5.7: **Modeled area.** The subtidal area investigated for benthos at shoal of Walsoorden is comprised between between blue and red line. The intertidal area is inside the red polygon

5.3 Results

5.3.1 Physical variables

The morphological changes resulting from the different sediment disposal scenarios are relatively small compared to the scale of the estuary. As a consequence there was no or little change in the simulated salinity parameters. Daily averaged salinity was around 20 PSU and the salinity range was 3 PSU. The intertidal area of the shoal (full black line in Figure 5.8) increased by the sediment disposal and thus for these locations the inundation time drastically reduced. A larger change in maximum flow velocities for the shoal area is only seen after the full disposal of sediments (2012 scenario) and for the extra scenario (Figure 5.8). We notice a pronounced increase in flow velocity for the flood channel (Figure 5.1 C), although the total discharge volumes over transects through the ebb channel (Figure 5.1 C) increased every scenario but not significantly ($p - value > 0.05$).

5.3.2 Benthic community responses

For the benthic parameters we differentiate between the subtidal and intertidal zone. The subtidal habitat suitability increases, moderately at first in 2009, but then in a more pronounced way for the 2012 and extra scenario (Figure 5.11). Areas of potential increases in subtidal habitat suitability are localized both on the nourishment itself and in the sheltered parts of the channels (Figure 5.11), where the current velocity decreased (Figure 5.8). The increase in flow velocity across the main channel is related to a decrease in potential habitat suitability (Figure 5.11). The maximal per capita body mass on average decreases at first in the 2009 scenario for the subtidal zone (Figure 5.9 & 5.11), but recovers in 2012 and the extra scenario.

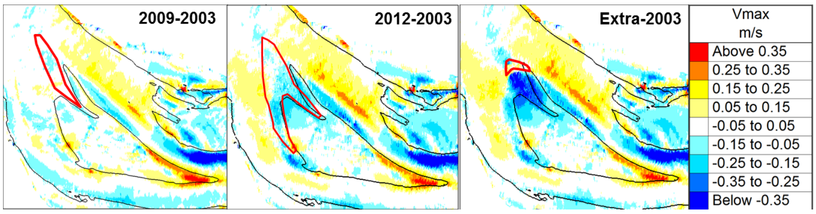

Figure 5.8: **Changes in maximum flow velocity.** The year 2003, before the sediment disposal, is taken as the reference for all scenarios. Positive values denote an increase and negative values a decrease in maximum flow velocities (m sec^{-1}). The full line indicates the border of the intertidal area. The thick red line indicates where sediment was disposed

The intertidal habitat suitability decreases over all scenarios (Figure 5.10). The decrease in potential for community performances (except for individual density) is more pronounced in two alternative situations: the central, upper part of the mudflat (Figure 5.11), in areas characterized by decreasing current velocity (Figure 5.8) and sediment accretion (Figure 5.2), and the southern tip of the mudflat, a low area characterized by increasing current velocity (Figure 5.8) and sediment erosion (Figure 5.2). Decreases in current velocity in the intermediate portion of the mudflat (Figure 5.8) and on the north-east tip (in accretion, Figure 5.2) are generally associated with increases in potential habitat suitability (Figure 5.11). Changes in potential intertidal individual density show an opposite spatial distributions of the other community parameters: they are positive on the upper mudflat and on the southern tip of the mudflat and negative in the intermediate portion (Figure 5.11).

5.3.3 Specific responses

In the subtidal zone habitat suitability for all *C. edule*, *M. balthica*, *H. diversicolor*, *H. filiformis* and *B. pilosa* significantly ($p - value < 0.05$) increases over all scenarios (Figure 5.12; *B. pilosa* not shown). Only *M. balthica* habitat suitability shows first a decrease in 2009 (Figure 5.12 & 5.14).

In the intertidal zone the typical species, *H. diversicolor* and *H. filiformis* show a significant ($p - value < 0.05$) increase in habitat suitability after 2009 (Figure 5.13). For *C. edule* there is no significant ($p - value > 0.05$) difference between the scenarios. In 2009 *M. balthica* density decreases significantly ($p - value < 0.05$) but it recovers in 2012 and remains in the extra scenario (Figure 5.13). *B. pilosa* has the same trend as *M. balthica*: a significant decrease in 2009 and a recovery afterwards (not shown). For the intertidal zone we notice especially the increase of *H. diversicolor* and *H. filiformis* for all scenarios (Figure 5.14).

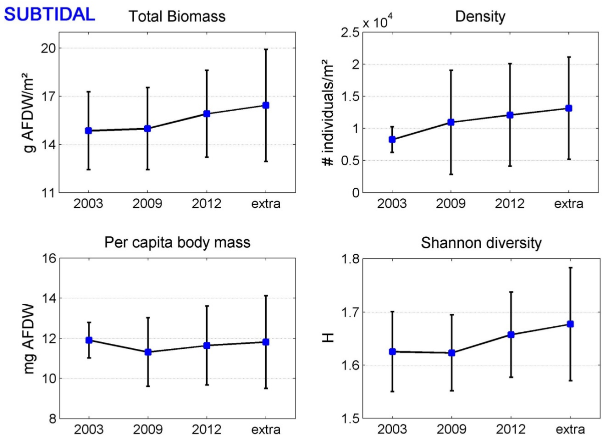

Figure 5.9: **Subtidal community responses.** Averages of benthic community maximal parameters (Biomass, Abundance, Per capita body mass and Shannon diversity) for the four scenarios for the subtidal zone around the downstream tip of the shoal of Walsoorden. Error bars indicate standard deviation

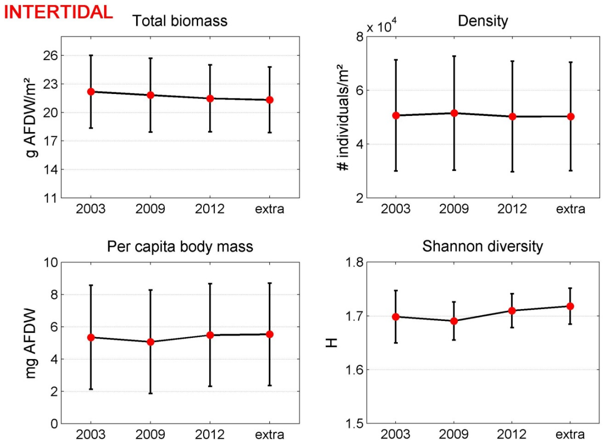

Figure 5.10: **Intertidal community.** Averages of benthic community maximal parameters (Biomass, Abundance, Per capita body mass and Shannon diversity) for the four scenarios for the intertidal zone around the downstream tip of the shoal of Walsoorden. Error bars indicate standard deviation

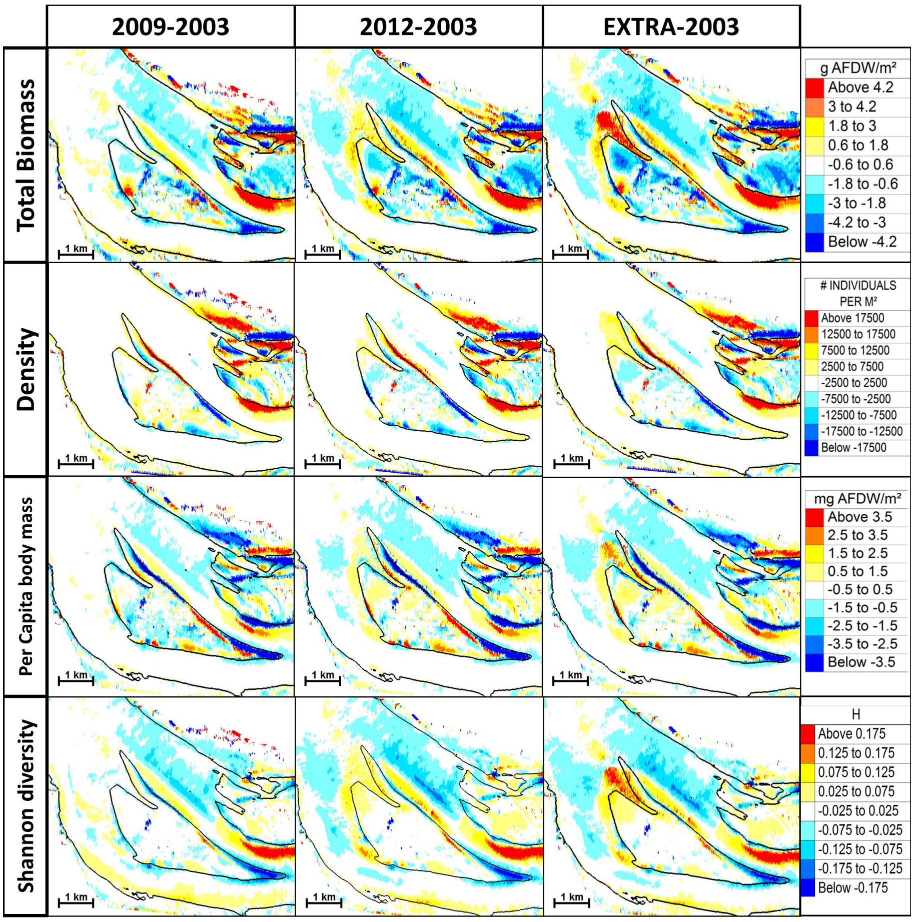
2009-2003
2012-2003
EXTRA-2003
Total Biomass
Density
Per Capita body mass
Shannon diversity
1 km
g AFDW/m²
Above 4.2
3 to 4.2
1.8 to 3
0.6 to 1.8
-0.6 to 0.6
-1.8 to -0.6
-3 to -1.8
-4.2 to -3
Below -4.2
# INDIVIDUALS PER M²
Above 17500
12500 to 17500
7500 to 12500
2500 to 7500
-2500 to 2500
-7500 to -2500
-12500 to -7500
-17500 to -12500
Below -17500
mg AFDW/m²
Above 3.5
2.5 to 3.5
1.5 to 2.5
0.5 to 1.5
-0.5 to 0.5
-1.5 to -0.5
-2.5 to -1.5
-3.5 to -2.5
Below -3.5
H
Above 0.175
0.125 to 0.175
0.075 to 0.125
0.025 to 0.075
-0.025 to 0.025
-0.075 to -0.025
-0.125 to -0.075
-0.175 to -0.125
Below -0.175

Figure 5.11: **Community responses.** Difference maps for the benthic community maximal parameters: Total biomass, Abundance, Per capita body mass and Shannon diversity

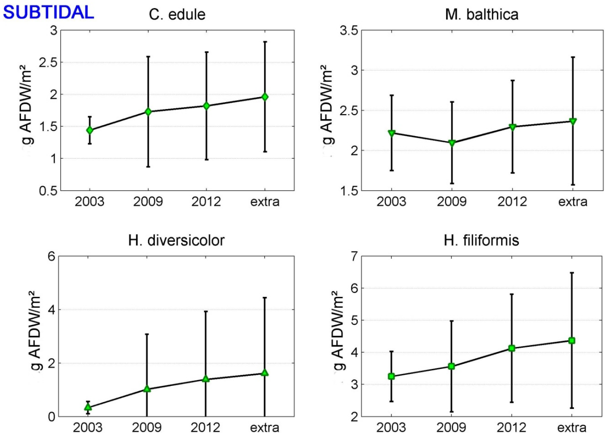

Figure 5.12: **Specific subtidal responses.** Averages of four benthic species maximal biomass (*C. edule*, *M. balthica*, *H. diversicolor*, *H. filiformis*) for the four scenarios for the subtidal zone around the downstream tip of the shoal of Walsoorden. Error bars indicate standard deviation.

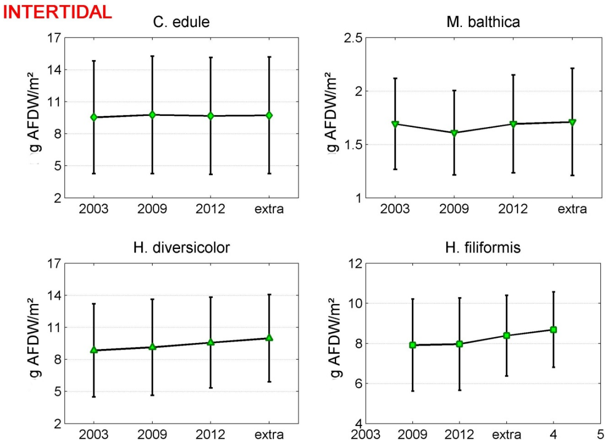

Figure 5.13: **Specific intertidal responses.** Averages of four benthic species maximal biomass (*C. edule*, *M. balthica*, *H. diversicolor*, *H. filiformis*) for the four scenarios for the intertidal zone around the downstream tip of the shoal of Walsoorden. Error bars indicate standard deviation

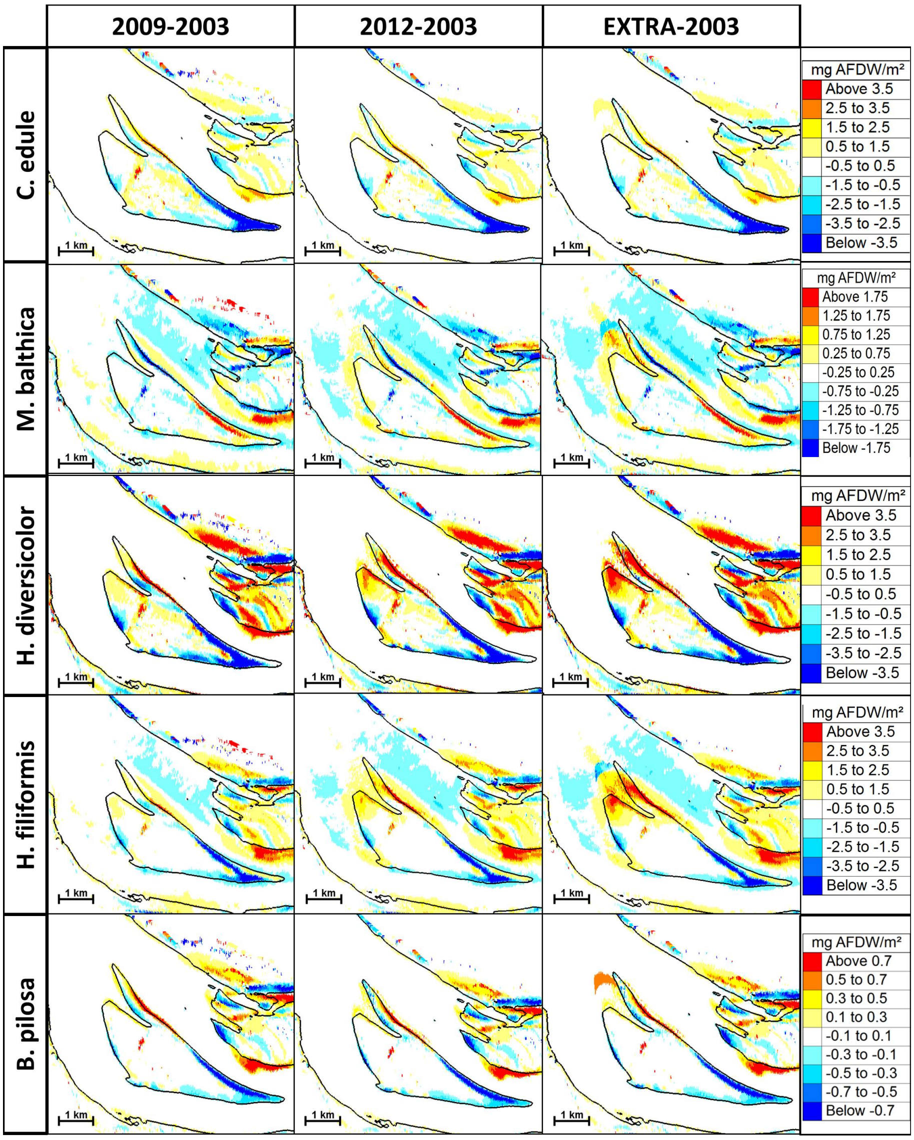
2009-2003
2012-2003
EXTRA-2003
C. edule
M. balthica
H. diversicolor
H. filiformis
B. pilosa
1 km
mg AFDW/m²
Above 3.5
2.5 to 3.5
1.5 to 2.5
0.5 to 1.5
-0.5 to 0.5
-1.5 to -0.5
-2.5 to -1.5
-3.5 to -2.5
Below -3.5
mg AFDW/m²
Above 1.75
1.25 to 1.75
0.75 to 1.25
0.25 to 0.75
-0.25 to 0.25
-0.75 to -0.25
-1.25 to -0.75
-1.75 to -1.25
Below -1.75
mg AFDW/m²
Above 0.7
0.5 to 0.7
0.3 to 0.5
0.1 to 0.3
-0.1 to 0.1
-0.3 to -0.1
-0.5 to -0.3
-0.7 to -0.5
Below -0.7

Figure 5.14: **Specific responses.** Difference maps for the benthic species maximal biomass: *C. edule*, *M. balthica*, *H. diversicolor*, *H. filiformis* and *B. pilosa*.

5.4 Discussion

In this paper we show that an integrated modeling approach can be useful for the ecological evaluation and optimization of sediment disposal strategies. Dredging is usually considered an activity with high environmental impact [Cozzoli et al., 2015c, Short and Wyllie-Echeverria, 1996], but necessary to keep and improve port accessibility [Halpern et al., 2008]. However, dredged material could be regarded as a potential resource for creation or restoration of habitats, like mudflats, or salt marshes [Bolam and Whomersley, 2005, Ray, 2000, Temmerman et al., 2013, Yozzo et al., 2004]. A new dredged sediment disposal strategy for the Westerschelde was tested. This disposal strategy is to put the material near the (eroding) edges of tidal flats, rather than to dump it in lateral channels. The main aim is to stabilize the multi-channel structure of the estuary and reduce dredging efforts on the long term. A secondary but very important goal is to dispose sediment in such a way as to minimize ecological impacts or even improve the benthic habitat quality [Peters et al., 2001]. First, three small scale tests were executed moving each relatively small amounts of dredged sand near the intertidal flat of Walsoorden (Figure 5.1 B & C). The first experiments for the new disposal strategy were monitored for changes in benthic fauna from 2004 until 2009. Given that no negative effects on the benthic community were monitored between 2004 and 2009, the full scale disposal in 2010 was carried out [van der Wal et al., 2011]. The monitoring of changes in benthic fauna is a necessary but essentially *a posteriori* approach to evaluate the environmental impact of the nourishments. Differently, the coupled hydrodynamic-species distribution modeling technique used in this paper enables to extrapolate, reconstruct and even foresee the ecosystem responses.

Reconstructing past changes is an important step to assess the validity of our forecast. However, a one-to-one comparison between the monitored results and the predictions is not realistic given the nature of our model. Habitat suitability indicates the specific ecological potentials of a habitat rather than the realized community composition. Our simulations show the habitat potential as it would be fully recovered directly after the disposal of sediments, while in nature the duration of impact, the re-adjustment time for the recovery of complex communities after morphological changes depends from case to case [Bolam and Whomersley, 2005, van der Wal et al., 2011]. The predicted suitable habitats for a macrobenthic community might be colonized by specific species, but might also lack them because of other environmental or anthropogenic stressors or just because of natural temporal variability [Cade and Noon, 2003]. Despite these confounding factors, model predictions are generally in agreement with field observation reported in van der Wal et al. [2011] and, for different study cases, by Ray [2000] and Bolam and Whomersley [2005].

For the three past scenarios examined in this paper (2003,2009 and 2012), we found that the maximum flow velocity, the expansion of the intertidal zone and the heightening of the intertidal flat are the variables determining change in benthic community parameters. The first disposal of sediments (scenario 2009) does not affect these variables much in the hydrodynamic model. The final disposal of 5 million m^3 in 2010 (scenario 2012) causes bigger changes: a decrease in maximum flow velocity, expansion of the flat and an increase of height of the intertidal area (Figure 5.8). This led the species distribution model to predict a significant increase in subtidal benthic habitat suitability between 2009 and 2012 (Figure 5.9 & 5.11). Intertidally, the total average biomass and density do not change much, but the spatial distribution shows considerable changes. The central (highest) part of the flat loses its macrobenthic community because of saltmarsh development, whereas zones of intermediate height gain biomass and density, as do the newly developing marginal areas of the flat. The southern tip becomes less favorable due to increased current velocity.

By modelling disposal of an extra volume of sediment (340.000 m^3) in the downstream point of the shoal, we simulated a weak current zone behind it ('extra' scenario, Figure 5.8), leading to a further, substantial increase in subtidal benthic habitat suitability (Figure 5.9 & 5.11). This last example shows that even a relatively small amount of sediment can have a relatively large effect on the mudflat ecology. Predictive physics-biota models like those presented in this paper can be an important tool to optimize sediment disposal, accounting both the effects on navigability and on the ecology of the estuary.

Decreases in flow velocity, as observed in the intertidal part of the study area, are often associated with the reduction in median grain size [Allen, 1985]. A gradual fining of the sediment was indeed monitored up the intertidal zone [van der Wal et al., 2011]. Coherent with these observations, our species distribution models (even if not explicitly accounting for sediment granulometry as explanatory variable) forecast an increase in habitat suitability for species with preference for fine sediment, like *H. filiformis* and *H. diversicolor*, and a decrease in species typically occurring in coarser sediment, like *B. pilosa*. This forecast is fully confirmed by field observations [van der Wal et al., 2011]. It must be noted that the increase in mud content was monitored already before the disposals [van der Wal et al., 2008] and is considered as consequence of processes already going on and not specifically induced by the disposal of sediments. Fining can be a point of concern, given that failure of created communities to converge to those of reference sites can be partly explained by differences in sediment characteristics between created and natural habitats [Levin et al., 1996, Ray, 2000]. The sediment fining monitored on the Waalsoorden can be interpreted as transient effects on the way to a tidal flat that supports less macrobenthos in the end. Indeed, heightening of the tidal flats in the Westerschelde has already been observed over the past decades [De Vriend et al., 2011]. It has led to the development of saltmarsh areas on the higher parts of many tidal flats and is considered to be a consequence of the dredging operations [De Vriend et al., 2011, Jeuken and Wang, 2010]. Saltmarshes, while *per se* considered as highly valuable habitats, are less suitable habitats for macrozoobenthos and have a lower importance as birds feeding areas [Kennish et al., 2002]. In our forecast, based on abiotic factors, the upper intertidal remains suitable for the individual species (Figure 5.13). However, forecast on the total macrozoobenthic biomass shows that beginning with a certain height the macrobenthos community disappears (Figure 5.11). These observations indicate that *per se* the environment has not became unfavourable but that a shift occurs at the community (competition) level: the salt marsh vegetion spatially outcompetes the macrozoobenthos in the higher intertidal.

5.5 Conclusions

The present study presents a methodology allowing the prediction of ecological consequences of changed dredge disposal strategies. Intensive monitoring of the bathymetry revealed that most of the disposed sediments remained at their disposal location, slowly moving (by the flood flow) towards the intertidal zone of the shoal. This entails restoration of the eroded part of the shoal of Walsoorden, as was originally planned [Vos et al., 2009]. It also contributes to heightening of the tidal flat, which changes its relative value as a habitat, by shifting from dynamic low-lying sands, over less dynamic more muddy conditions, to high-lying saltmarshes in the highest part. The spatial distribution of macrofauna closely follows these abiotic changes, as was also observed in the field [van der Wal et al., 2011]. The desirability of the changes in the habitat can thus be better evaluated when planning new management strategies. As shown by our extra scenario, future, relatively small interventions on the mudflat morphology could further accentuate these evolutions with relatively small effort. Our results highlight the fact that the interpretation of the results achieved by morphological management of mudflat is related to the time frame of observation, as ecosystems develop and new features can emerge.

Beneficial uses of dredged material include construction of artificial reefs, oyster reef restoration, intertidal wetland and mudflat creation, bathymetric recontouring, filling dead-end canals/basins, creation of bird/wildlife islands [Yozzo et al., 2004]. These applications would require a demonstration project, including post-construction environmental monitoring, before a full-scale implementation plan could be developed. In this paper we show that, while *a posteriori* monitoring remains crucial in evaluating morphological changes, different scenarios can be simulated on the base of *a priori* knowledge on the hydrology and the biology of the system. The geographical resolution can be determined by the mesh resolution of the hydrodynamic model and results can be eventually extrapolated for different contexts. The proposed modeling methodology offers the opportunity to assess beforehand induced changes in benthic habitats, offering to coastal zone managers the possibility to evaluate ecological impacts already in the design phase of a project.

Acknowledgements

The authors like to thank the Antwerp Port Authority and the Dehousse scholarship of the Antwerp University for the financial support. We like to acknowledge the technical support of the Flanders Hydraulics Research institute. We like to thank Rijkswaterstaat for all measurements and data sharing. We would like to thank the developers of the Telemac system and Blue Kenue software.

CHAPTER 6

Ecosystem Engineering, aiming to generalization

Francesco Cozzoli, Pauline Ottolander, Maria Salvador Lluch, Tjeerd J. Bouma, Tom Ysebaert, Peter M. J. Herman

Abstract

Ecosystem engineering is a biological process with a strong influence on ecosystem structure and functioning. Despite the generally accepted importance of ecosystem engineering in ecology, there is still a lack of insight on how this process can be compared across species and ecosystems. We propose an empirical framework to scale ecosystem engineers activity in terms of fundamental individuals and populations descriptors: individual body size and abundance of individuals. To test this framework, we performed a series of experiments to measure and compare the body-size and abundance scaling of the ecosystem engineering activity performed by different types of marine soft-sediment ecosystem engineers. We found a significant and positive relationship with both explanatory variables, which was homogeneous across different species and functional groups, indicating that ecosystem engineering-effects can be generalized across species using allometric relationship. The proposed framework can be used to scale and compare ecosystem engineering activity at ecosystem scale.

6.1 Introduction

The Ecosystem engineering concept focuses on how organisms physically change the abiotic environment, either by their structures (*i.e.*, autogenic ecosystem engineering) or by their activity (*i.e.*, allogenic ecosystem engineering) and how this feeds back to the biota [Jones et al., 1994, 1997]. Ecosystem engineering happens almost ubiquitously on earth, performed by different organisms, with different modalities, at different scales [Hastings et al., 2007]. It influences biogeomorphic landscape development [Raynaud et al., 2013] as well as the structure and the fate of entire communities [Bruno et al., 2003, Jones et al., 1994, 1997]. Descriptions of ecosystem engineering are important to the understanding of the patterns and dynamics of diverse species interactions in nature [Kefi et al., 2012]. Despite the major importance of ecosystem engineering in ecology, descriptions of the process often remain anecdotical and idiosyncratic, thus hampering comparisons and generalizations across species and ecosystems.

We aim at identifying a general method to scale ecosystem engineering across a broad range of functional diversity, either as a function of body size alone, or as a function of the combination of body size and individual abundance. Although ecosystem engineering-body size and abundance dependencies are commonly observed (*e.g.* Cammen [1980], Gallaway et al. [2009], Solan et al. [2004]) and have already been proposed as descriptors of the ecosystem engineers activities on a landscape level (*e.g.* Moore [2006]), to our knowledge comparative studies are not available. In this paper we present a simple conceptual framework to quantify, scale and compare ecosystem engineers activity, based on a large empirical dataset encompassing a broad range of functional diversity, individual densities and body sizes.

6.1.1 Conceptual framework: allometry in ecosystem engineering

Generalizations in ecology (and ecosystem engineering studies) need to be derived from fundamental biological laws, virtually valid for all (a wide range of) organisms and environmental contexts. Ecological scaling laws have often been based on body size allometries, since almost all the characteristic of organisms vary predictably with their size [Brown et al., 2004, Brown, 1995, De Roos et al., 2003, Gaston and Blackburn, 2000, Marquet, 2002]. Autogenic engineers modify the environment by their physical structures. It is conceivable that their individual impact is positively related to their body size by geometric constrains. This contention is supported by observations showing that tree age and tree size was a key factor for the magnitude of ecosystem engineering in terms of sediment transport through woodlands [Gallaway et al., 2009]. A positive scaling of performed ecosystem engineering with individual size can also be assumed in the allogenic case *via* the positive scaling of the individual metabolic rate [Kleiber, 1932]. The metabolisms is the fueling processes of the majority of biological activities [Brown et al., 2004] and it is directly reflected in organisms activities [Savage et al., 2004]. Along this line, we hypothesize that the impact of an allogenic engineer is related to the metabolic rate, so that it increases with the individual body mass. Supporting this idea, body size was found to be a strong predictor of the individual bioturbation potential [Solan et al., 2004].

Because of the relevance of body size for individual characteristics, the relationship between body size and abundance is an essential link between individual and population traits [Brown, 1995, De Roos et al., 2003, Schmid et al., 2002]. The expected link between individual body-size and performed ecosystem engineering effect may not be transferable to the population level purely on the base of body size - abundance relationships, as ecosystem engineering effects of individuals may have overlapping areas of influence. As an example, the amount of biodeposited sediment from blue mussels (*Mytilus edulis*) and the amount of bioturbated sediment from Baltic clams (*Macoma balthica*) both increased with individuals density until an upper asymptote was reached [Widdows et al., 1998].

Body size allometry is often expressed in the form of a power function, by means of a normalization constant a and an allometric exponent b: $Y = aX^b$. Power functions imply that percentage increases in the explanatory variable lead to constant percentage changes in the response. Despite some controversy about the correct application of power laws in biology [Xiao et al., 2011], they provide a first-order approach useful for exploration and generalization. The amount of ecosystem engineering performed by a homogeneous population (EE_{pop}) could be expressed as a combination of power functions of the individual body size M and the population abundance (number of individuals per unit surface) A:

$$EE_{pop} = aM^b A^c \tag{6.1}$$

where b is the allometric exponent relating the body size to the individual ecosystem engineers activity and c is the exponent relating the abundance to population activity EE_{pop}. The normalization constant a accounts for the different organisms functional behavior, that mediates the efficiency of ecosystem engineering. The value of b is expected to be positive, based on the geometric (autogenic engineers) or energetic (allogenic engineers) positive scaling of individual attributes and performances. A value of $c < 1$ is expected when individuals decrease each others' activities (negative interference), whereas $c > 1$ could be observed when individual activities reinforce each other (positive interference). Equation 6.1 establishes a quantitative link between EE_{pop} and the fundamental scaling principles at the individual and population levels.

6.1.2 Model system: bioturbation

Bioturbating macrobenthos that dominate tidal flats offer an ideal model system to test if ecosystem engineering can be scaled as a function of the per capita body size and population abundance, and if the same scaling rules are shared by different archetypes of engineers. Endobenthic macrobenthos that live inside the sediment are ecosystem engineers in the sense that they typically decrease sediment stability and increase the erodability by their bioturbating activities [Le Hir et al., 2007, van Prooijen et al., 2011, Willows et al., 1998]. These bioturbating effects are so strong that these ecosystem engineers can influence the development of these intertidal flats as a whole [Orvain et al., 2012]. There is a large number of endobenthic macrobenthic species, with variable body size, occurring in different abundances and manifesting different functional behaviors [Degraer et al., 2006, Holtmann et al., 1996]. Their ecosystem engineering effect can be easily quantified in terms of enhanced erodability, using simple laboratory flumes [Willows et al., 1998]. We collected a multi-species dataset on macrozoobenthic bioturbators effect of sediment erosion, using the suspended sediment concentration as quantitative measure of ecosystem engineering-activity. Our measurements span over a range of body sizes (10 to 1136 mg Ash Free Dry Weight per individual, AFDW) and natural abundances (13 to 382 Ind. m^{-2}). They are representing three qualitatively different types of bioturbation activity [Lee and Swartz, 1980] and have different effect on near-bed hydrodynamics [Friedrichs et al., 2009]. We specifically test the hypothesis that there is a body-size and abundance effect on performed ecosystem engineering when looking (1) within a species/bioturbator archetype and (2) between different bioturbator archetypes.

6.2 Material and methods

6.2.1 Target organisms

The ecosystem engineers used for this experiment were the bivalves *Cerastoderma edule*, *M. balthica*, *Abra alba*, *Venerupsis philippinarum*, *Scrobicularia plana*, and the Polychaeta *Arenicola marina* (Figure 6.1). These organisms share a common habitat (mainly muddy intertidal flats), but they live in the sediment at different depths: from very shallow (*C. edule*, shells usually emerge from the sediment surface) to intermediate (other bivalves, from 3 to 10 cm) and relatively deep (*A. marina*, below 10 cm) [Degraer et al., 2006, Holtmann et al., 1996]. In association, their feeding mode varies from obligatory suspension feeding (*C. edule*) to a mixture of suspension and deposit feeding (other bivalves) to obliged deposit feeding (*A. marina*) [Degraer et al., 2006, Holtmann et al., 1996]. *C. edule* reworking of sediment is mostly related to biodeposition, vertical and horizontal movements and valves adduction [Flach, 1996]. The other species of bivalves are generally less motile than *C. edule*, but they can disrupt the sediment surface by inhaling the sediment with their siphons to graze on benthic diatoms [Zwarts et al., 1994]. *A. marina* swallow surface sediment through a feeding funnel and expel it in the form of pseudofaeces, forming characteristic feeding pits and pseudofaeces casts [Zebe and Schiedek, 1996].

The animals were collected on intertidal flats of the Oosterschelde and Westerschelde between September 2011 and May 2012. After collection they were held in aerated containers with sediment and filtered Oosterschelde water at a constant temperature of 18 ^{o} C and allowed to acclimatize for 1 week. For each species different densities of homogeneous-sized individuals were tested (Table 6.1). Densities and body sizes were selected in way to represent the natural range of each of the analyzed species. The numbers of experimental runs was partially conditioned from the availability of model organisms. Only for *C. edule* and *A. marina* a full set of body sizes and densities was compared (Table 6.1). Consequently, *M. balthica*, *Abra alba*, *Venerupsis philippinarum* and *Scrobicularia plana* were grouped together on the base of their similar functional behavior.

6.2.2 Experimental devices

The annular flumes used are a variation of the design described by [Widdows et al., 1998] (Appendix C Figure C.1 - C.3). For experiments, homogeneous, wet, fine-sand sediment (median grain size = 120 μm) was put in a flume, mixed to a smooth mass and let consolidate. The excess of water was drained through a pebbled bed placed in the bottom of the flumes. After 48 hours, the flumes were filled with 31.4 L of filtered seawater. To prevent that the sediment surface got damaged, a sheet of bubble plastic was placed on top of it before gently spraying water into the flume. A current of 30 cm sec^{-1} (sufficient to fully resuspend the bioturbated sediment [Widdows et al., 1998]) was created with a smooth, adjustable rotating disk, which is driven by a microprocessor-controlled engine. An Acustic Doppler Velocimetry probe was used to calibrate water velocity as a function of the the engines rotation speed. Water turbidity, as a proxy of the bioturbating effect, was measured using an optical backscatter sensor (OBS 3+, Campbell scientific) and converted in Suspended Sediment Concentration, (SSC, g L^{-1}) based on calibration by gravitometric analysis. Previous studies [van Prooijen et al., 2011, Widdows et al., 1998] showed that in this kind of experiments mostly Type I erosion occurs: after a step increase in current velocity, the SSC increases to an equilibrium value due to limitation of erodible material [Mehta and Partheniades, 1982]. In our experiments, the equilibrium SSC was usually reached after ca. 5 minutes.

6.2.3 Experimental protocol

To be able to use the SSC as quantitative measure of ecosystem engineering activity by benthic animals, every experiment (2 replicates) consisted of a preliminary run without added animals (abiotic control) and an experimental run with benthic animals. Both runs lasted 20 min. The aim of the first run is to provide an independent control for each of the experimental run. Animals were introduced the flumes and evenly distributed on the sediment surface after the

Table 6.1: **Table of treatments.** According to the availability of experimental organisms, we tested several combinations of individual abundances and individual body sizes of different bioturbators.

Species	Individual body size (mg AFDW)	Abundance (N of ind. m^{-2})	Biomass (g AFDW m^{-2})
Cerastoderma edule	11	95	10
	11	191	21
	11	382	41
	101	32	32
	101	64	64
	101	127	129
	101	255	257
	616	13	78
	616	32	196
	616	64	392
Abra alba	14	45	6
	14	95	13
Scrobicularia plana	15	64	9
	15	382	55
Macoma balthica	30	32	9
	30	64	19
	30	191	57
	30	382	114
Venerupsis philippinarum	128	32	41
Scrobicularia plana	171	64	109
Arenicola marina	23	32	7
	23	64	15
	23	95	22
	23	127	29
	213	32	68
	213	64	136
	213	95	202
	213	127	270
	1136	32	36
	1136	64	73
	1136	95	108

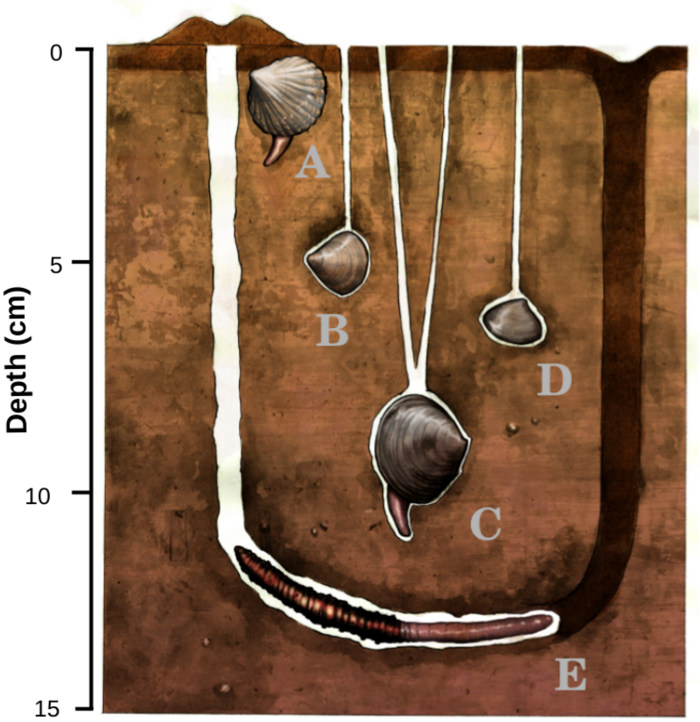

Figure 6.1: **Target organisms.** Three different archetypes of bioturbators were used in our experiments: shallow (A, *Cerastoderma edule*), intermediate (B *Macoma balthica*, C *Scrobicularia plana*, D *Abra alba*, *Venerupsis philippinarum*) and deep burrowers (E, *Arenicola marina*). *C. edule* reworking of sediment is mostly related to biodeposition, vertical and horizontal movements and valves adduction . The other species of bivalves are generally less motile than *C. edule*, but they can disrupt the sediment surface by inhaling the sediment with their siphons to graze on benthic diatoms [Zwarts et al., 1994]. *A. marina* swallow sediment from the surface and expel it in form of pseudo-faeces, forming characteristics feeding funnels and pseudofaeces casts [Zebe and Schiedek, 1996]. *Illustration cured by Fabrizio De Tommaso*

first run. They were allowed to settle for 48 hours before the second run. The vast majority of the animals buried within a few minutes after being placed in the flume. *A. marina* generally did not move from the initial settlement point and produced a single feeding pit and pseudofaeces cast for individual. Some individuals of *C. edule* and 'Other bivalves' crawled on and below the sediment surface, leaving evident tracks.

6.2.4 Data analysis

Taking the log of both the sides of Equation 6.1, it can be rearranged in suitable form for multivariate log-log regression analysis:

$$EE_{pop} = aM^bA^c \Rightarrow \log(EE_{pop}) = \log(a) + b\log(M) + c\log(A) \qquad (6.2)$$

We consider as proxy for EE_{pop} the (stable) SSC reached after 15 min of application of a 30 cm sec^{-1} water current. To focus solely on the amount of resuspended sediment due to the action of bioturbators, the SSC values measured during the first experimental run (abiotic control) where subtracted from those measured during the second experimental run (with bioturbators). Explanatory and response variables were log-transformed, centered and scaled. First - degree response surfaces were fitted separately for each of the three functional groups and on the overall dataset. Coefficients 95% CI were calculated by bootstrapping the dataset 50000 times.

In addition to testing the dependence of SSC on body size (M, mg AFDW per individual) and individuals abundance (A, Ind. m^{-2}), we fit the relationship between SSC and the product of the two explanatory variables, *i.e.* the total biomass (B, g AFDW m^{-2}). Measurements of goodness of fitness like the R^2 cannot decrease with increasing number of parameters. Conversely, the Akaike Information Criterion [Akaike, 1980] offers a relative measurement of the goodness of fit based on the trade off between the accuracy and the complexity of the model. The performances of the bivariate ($EE_{pop} = aM^bA^c$) *vs.* the univariate ($EE_{pop} = aB^d$) models were evaluated by comparing the models AIC. All analyses were performed with `R` [R Development Core Team, 2011].

6.3 Results

We observed a clear increase in ecosystem engineering activity measured as SSC with the increase of both bioturbators body size and abundance (Table 6.2). The presence of bioturbators increased the SSC over 15 times (with respect to the abiotic control) for combinations of large body sizes and high abundance of individuals. Regression models based on the per capita body size and individuals abundance are able to explain from over 50 % (*A. marina* and *C. edule*) to 28 % (Other bivalves) of the observed variance in SSC. Forecast response surfaces are similar between functional groups. A single response surface can describe 49 % of the variance in SSC observed across the whole dataset (Table 6.2), regardless of the different modalities in which the bioturbation activity is performed.

Allometric exponents relating SSC to individual body size are in the order of 0.3-0.4 and are not significantly different among groups (Table 6.2). Allometric exponents for abundance vary between 0.54 and 0.98 (Table 6.2). 95% CI are relatively large. Especially the exponent for body size in the group of 'Other bivalves' is subject to large uncertainty, probably as a result of the small range of sizes tested. The overall model encompassing all groups has exponents of 0.33 for body size and 0.67 for abundance. This model has smaller confidence intervals.

Models based on the total bioturbator biomass (Table 6.3) have generally worse performances in explaining the observed variance (Table 6.4) than those based on individual body size and abundance (Table 6.2). The estimated allometric exponents for SSC scaling with total biomass are ~ 0.5 for all the fitted models (Table 6.3).

Table 6.2: **Summary table of the multivariate models $EE_{pop} = aM^bA^c$.** Explanatory and response variables were log-transformed, centered and scaled to make coefficients directly comparable. 95% CI were calculated by bootstrapping the dataset 50000 times. R^2 values were adjusted to account for the effect of multiple explanatory variables

Species	Parameter	Estimate	Lower 95% CI	Upper 95% CI	Std. error	t - value	p - value	Adjusted R^2
C. edule	Intercept	-6.88	-9.14	-4.91	0.87	-7.93	0	0.56
	Body Size	0.31	0.14	0.51	0.08	3.87	0	
	Abundance	0.71	0.42	1.04	0.13	5.36	0	
Other bivalves	Intercept	-6.69	-9.72	-3.87	1.29	-5.2	0	0.28
	Body Size	0.44	0.01	0.89	0.2	2.18	0.04	
	Abundance	0.54	0.1	1.01	0.2	2.73	0.01	
A. marina	Intercept	-8.24	-11.3	-5.23	1.3	-6.32	0	0.53
	Body Size	0.33	0.13	0.54	0.08	4.2	0	
	Abundance	0.98	0.45	1.52	0.25	3.87	0	
Total	Intercept	-6.87	-8.26	-5.55	0.57	-12.05	0	0.49
	Body Size	0.33	0.21	0.45	0.05	6.44	0	
	Abundance	0.67	0.46	0.9	0.1	6.86	0	

Table 6.3: **Summary table of the univariate models $EE_{pop} = aB^d$.** Explanatory and response variables were log-transformed, centered and scaled to make coefficients directly comparable. 95% CI were calculated by bootstrapping the dataset 50000 times

Species	Parameter	Estimate	Lower 95% CI	Upper 95% CI	Std. error	t - value	p - value	R^2
C. edule	Intercept	-5.28	-7.39	-3.44	0.94	-5.6	0	0.31
	Biomass	0.33	0.12	0.57	0.1	3.24	0	
Other bivalves	Intercept	-6.65	-9.4	-3.9	1.25	-5.3	0	0.31
	Biomass	0.49	0.15	0.83	0.16	3.11	0.01	
A. marina	Intercept	-5.31	-7.28	-3.37	0.88	-6.01	0	0.36
	Biomass	0.32	0.1	0.54	0.09	3.43	0	
Total	Intercept	-5.57	-6.73	-4.46	0.51	-11.03	0	0.39
	Biomass	0.35	0.23	0.49	0.06	6.27	0	

Table 6.4: **Model comparison.** The AIC-scores of the different models are shown in the first and the second line. The p-values in the third line result from analysis of variance between the multivariate and the univariate model

	C. edule	Other bivalves	*A. marina*	Total
$EE_{pop} = aM^b A^c$	36.93	48.99	33.51	111.78
$EE_{pop} = aB^d$	46.39	47.2	38.91	123.37
p-value	0	0.68	0.01	0

6.4 Discussion

In this paper we derived across species relationships to describe ecosystem engineering, using soft-sediment macrobenthic bioturbators as model system. We based our formulation on fundamental biological principles governing the scale of individual activities and population abundances. Body size dependencies allow relating individual activities to the individual metabolism or to the individual physical structure, thus to the first principles of geometry, chemistry, and biology [Brown et al., 2004, Sousa et al., 2008]. Body size-abundance relationships can be used to link individual and population traits [Brown, 1995, De Roos et al., 2003, Schmid et al., 2002]. Along this line, we hypothesized that the amount of ecosystem engineering performed at population level can in general be quantified as a function (*i.e.* combination of power functions) of the individual per capita body size and abundance. We tested and confirmed this hypothesis by measuring the effect of different archetypes of bioturbators on sediment erodability.

Results show that a major portion of variance in SSC (as a proxy for EE_{pop} bioturbating effect) can be explained by the per capita body size and abundance of the inhabiting bioturbators (Table 6.2). Although the estimated coefficients are significant, the analysis suffers of large uncertainties, as indicated by the large 95 % CI in Table 6.2). It is difficult to asses if those uncertainties derived by intrinsic stochasticity in the abiotic matrix (*i.e.* sediment consolidation and structure), size and abundance-independent heterogeneity in bioturbators behavior, experimental errors or approximation related to the power function structure underpinning our models. The better performances (Table 6.4) of the bivariate models ($EE_{pop} = aM^b A^c$) respect to the univariate ones ($EE_{pop} = aB^d$) are indicative of emergent properties of the size/density ratio. While the total biomass remains a useful proxy for EE_{pop} (from 31 to 39 % of explained variance), neglecting these properties could lead to underestimate the effect of high concentration of individuals. The lower significance and the larger CIs of the model fitted for the 'Other bivalves' (Table 6.2) are likely related to the narrower range of tested body sizes (Table 6.1) rather than to the taxonomic diversity of the group. This conjecture is supported from the observation that the model encompassing the larger span of diversity (overall dataset) is also that one presenting the narrowest CIs.

Shifts in the intercept of the body size / metabolic-rate relationships are typically related to the different use of energy by different organisms groups [Ernest et al., 2003, Marquet, 2002]. Analogously, shifts in the intercept of the body size/ecosystem engineering relationships, a, may be expected for different functional groups. This was however not observed in our experiments. We conclude that, at the level of accuracy provided by our experiments, all the analyzed species are likely to belong to an homogeneous group with respect to the investigated process.

The abundance of *A. marina* is isometrically correlated with the EE_{pop}

(scale exponent ~ 1), from which we conclude that *A. marina* individuals simply cumulate their individual work, without interfering each others. Scale exponents for the abundance of *C. edule* and 'Other bivalves' are < 1 in the 97.25% of the bootstrap simulation (Table 6.2), implying that the per capita effect of sediment erodability decrease at the increase of individuals abundance. A possible explanation is that, in a finite amount of space, spatial overlapping in individual influence areas [van Prooijen et al., 2011] is more likely to happen for the (relatively) more motile 'Other bivalves' and *C. edule* rather than for the sedentary *A. marina*.

While EE_{pop} - abundance relationships are more likely to reflect species-specific behavior related to individuals aggregations rules or, as we suppose for our case, motility, EE_{pop} - body size scale exponents should be the results of universal metabolic/geometric constrains. Coherently with this expectation, we found a full overlap in the body size scale exponents of *C. edule* and *A. marina* (respectively 0.31 and 0.33) and, with larger CI, also for 'Other bivalves' (0.44). Our estimates for the body size scaling exponent of EE_{pop}, b, are < 0.75, which value typically expected for the scaling of individual metabolic rate and individuals activity, [Kleiber, 1932]) (Table 6.2). This implies a disproportional use of metabolic energy between size classes: smaller individuals invest relatively more energy in ecosystem engineering, or they do it with higher efficiency. Estimated exponents are also lower respect previously found for bioturbators sediment ingestion/egestion rate (0.77, Cammen 1980, 0.66, Cross et al. 2008), *C. edule* excretion rates (0.7, Smaal et al. 1997) or bioturbation potential accounting for species body size, abundance, mobility and mode of sediment mixing (0.98, Solan et al. 2004). These discrepancies can be explained from the facts that 1) bigger animals spend their energy to rework sediment also in deeper sediment strata, not directly exposed to erosion and 2) increasing the bottom roughness with their physical shape (protruding shells of *C. edule*) or with the structures they produce (feeding funnels, pseudofaeces casts), bigger animals could have a stronger effect than smaller animals in dampening the near-bottom water flux and reducing the bed shear stress. Overall, this suggests that inner dependences in data structure can have a major relevance for the realized outcome of ecosystem engineering activities.

Ecosystem engineering is a dynamic link between physical and biological phenomena [Jones et al., 1994, 1997]. By mean of ecosystem engineering, changes in organisms distribution (*e.g.* shift in areas, invasion, local extinction) can exacerbate or dampen ongoing physical trends [Crooks, 2002]. Semi-empirical descriptions of the behavior of organisms (like the one we present here) are needed for integrated modeling of biota-mediated physical processes [van Prooijen et al., 2011]. For example, it has been proposed that global warming will imply a shrinking of individuals body size [Lurgi et al., 2012]. Range limits of large-bodied species of bivalves are more sensitive to climate changes than the limits of small-bodied species [Roy et al., 2001]. Between different archetypes of bioturbators, body-size related extinctions could led to the preferential loss of big body sized species and thereby drastically reduce the bioturbation potential, potentially causing a negative relapse on global biogeochemical cycles [Solan et al., 2004]. Our results suggest that, within similar archetypes of engineers, body size shrinking can have the opposite effect: given a fixed amount of total biomass, each percent unit of decrease in per capita body size of bioturbators should increase the EE_{pop} of $\sim 0.3\%$ (Table 6.2). It follows that body size shrinking, if not associated with the extinction of the biggest body-sized species, could even boost ecosystem functionality due to the higher activity per unit of mass of smaller individuals.

On a global scale, the average individual body size is related to the individuals abundances by energetic constrains (*e.g.* Damuth [1981], White et al. [2007]). Once the EE_{pop} scale coefficients for body size c and abundance d have been determined by means of factorial experiments, Equation 6.2 can be extended to include body-size abundance dependencies:

$$EE_{pop} = aM^{c+e*d} \tag{6.3}$$

where e is the scale exponent relating the mean body size of a species/functional group of ecosystem engineers with its abundances in realized community (Local size-density relationship, in the terminology of [White et al., 2007]). Equation 6.3 allows broad quantifications of ecosystem engineering influence on ecosystems structure and functionality, fully based on the energetic principles governing the scale of individual activities and population abundances.

Ecosystem engineering can originate from very diverse interactions and activities [Hastings et al., 2007], which may also depend on external conditions. Thus, scale exponents for ecosystem engineering are not expected to be 'universal' in the sense that they rely on a basic and universally shared core of reactions, as is the case for individual metabolism. It is possible, therefore, that other relations result when the study is extended to other functional types of bioturbators (*e.g.* epibehtic grazers, burrowing bivalves, and burrowing Polychaeta not inducing advective fluxes [de Lucas Pardo et al., 2013, Kristensen et al., 2013]). However, independent of the type of bioturbation, metabolic energy will be spent on sediment reworking, in order to obtain food. This will result in sediment mixing, and the exposure of fine particles to the surface, where they can be resuspended. The ability to spend this energy will scale with metabolism, and therefore it is natural to expect a scaling of ecosystem engineering with body size and abundance. For autogenic engineers, where constraints are geometrical rather than energetic, qualitatively different scalings may be found, but this remains to be investigated. More experimental work is needed to further constrain the scaling of ecosystem engineering as proposed here. This systematic investigation of the variation of ecosystem engineering scaling coefficients across taxonomic and functional diversity gradients is important to forecast how change in biodiversity can affect ecosystem functioning and ecosystem evolution as affected by ecosystem engineering.

Acknowledgments

We gratefully thanks: Conrad Pilditch for providing insights on the flumes realization; Lowie Haazen, Bert Sinke, Jos van Soelen for their fundamental technical support and for their patience; Nilmawati, for her contribution during the experiments; Maestro Fabrizio de Tommaso for gently providing Figure 6.1. This work was funded by the Ecoshape/Building with Nature project. At the time of starting this project, NIOZ-Yerseke belonged to the Netherlands Institute of Ecology.

CHAPTER 7

Ecosystem engineering, extrapolation to a realistic context

Francesco Cozzoli, Pauline Ottolander, Maria Salvador Lluch, Sven Smolders, Menno Eelkema, Tjeerd J. Bouma, Tom Ysebaert, Vincent Escaravage, Stijn Temmerman, Patrick Meire and Peter M. J. Herman

Abstract

Ecosystem engineering is a fundamental ecological process that can potentially modify the landscape and its use by human communities. Explicit inclusion of ecosystem engineering in ecosystem modeling has both ecological and social relevance. It is important to identify a general method that can be used to scale the effect of ecosystem engineering from single individuals to population and landscape levels, accounting for the physical conditions in which ecosystem engineering is performed.

In this study we present and apply a four steps procedure to upscale ecosystem engineering observations to whole-ecosystem level. Prognostic models of the physical environment can be used to reconstruct the environmental context in which the ecosystem engineering activity is performed (Step 1). Species distribution models can estimate the spatial distribution of the ecosystem engineers (Step 2). Factorial experiments allow to parametrize the effect of the ecosystem engineers on the base of fundamental biological and physical descriptors (Step 3). The three steps can be integrated to extrapolate static maps about how the ecosystem engineering activity is distributed in space and time

(Step 4).

The recognition that organisms' responses to anthropogenic habitat alterations can induce (or, as we predict, buffer) further changes in the landscape is a fundamental step to explicitly integrate nature into human development. The integration of ecological insights in physical landscape models we present in this paper has the double advantage to provide simultaneous forecasts about the ecological and morphological landscape evolution and to account for the biotic-induced deviations from purely physical expectations.

7.1 Introduction

Technological developments during the last centuries led the human species to be one of the major sources of change in landscape ecomorphology. Given the magnitude, diffusion, extension and pervasivity of human interventions, the name 'Anthropocene' was proposed for the present geological era [Crutzen, 2002]. However, many other species are able to modify their environment. The ecosystem engineering framework focuses on how organisms change the physical environment, either by their structures (*i.e.*, autogenic engineers) or by their activity (*i.e.*, allogenic engineers) and how this feedbacks on their fitness [Jones et al., 1994, 1997]. Ecosystem engineering happens almost ubiquitously on Earth, performed by different organisms, with different modalities, at different scales [Hastings et al., 2007]. Descriptions of ecosystem engineering have a particular relevance in predicting changes in landscape evolution [Pearce, 2011]. On the one side, the ecosystem engineers (like any other organism) react to (natural or anthropogenic) environmental modifications, with ecological consequences that should be *per se* evaluated in ecosystem management. On the other side, changes in the ecosystem engineers distribution will inevitably affect their engineering activity at a population level. This could result in a different landscape evolution with respect to expectations from purely physical basis. Static management goals should be carefully considered in environmental planning, as new and unexpected features can emerge due to these processes. Explicit inclusion of ecosystem engineering in ecosystem modeling has both ecological [Kefi et al., 2012] and social relevance [Sanders et al., 2014]. It is important to identify a general method that can be used to scale the effect of ecosystem engineering from single individuals to population and landscape levels, accounting for the physical conditions in which ecosystem engineering is performed.

The feedback between abiotic and biotic elements has a particular relevance in sedimentary environments, where the physical processes involved in landscape formation (mainly sediment erosion, transport and deposition) act on energetic, temporal and spatial scales that are compatible with those of biological processes [Le Hir et al., 2007, McLusky, 2004]. Bioturbating macrozoobenthos offers an optimal model system to investigate the reciprocal dependence of biotic and abiotic/environmental factors in ecosystem engineering and landscape evolution. On the one hand, the environmental factors involved in sediment dynamics are important drivers for the spatial distribution of macrozoobenthic species. For example, high bed shear stress can inhibit the majority of benthic organisms to establish [Snelgrove and Butman, 1994], or the sediment composition can drive the species distribution on intertidal flats [Gray, 1974]. On the other hand, many benthic organisms act as ecosystem engineers in the sense that they typically modify the interactions between physical elements in sediment dynamics. While sediment dynamics are mainly driven by physical (hydrodynamic) forcings [Allen, 1985], benthic organisms generally increase the bottom roughness, changing the bottom boundary layer locally, and increasing the small-scale variability in bottom shear stress [Friedrichs et al., 2000]. In particular, endobenthic macrozoobenthos generally decreases sediment stability and increases the erodability by bioturbating activities [Le Hir et al., 2007, van Prooijen et al., 2011, Willows et al., 1998].

In this study we examined separately the two aspects of the sediment-biota feedback interactions by comparing the effect of two bioturbators species: *Cerastoderma edule* and *Arenicola marina*. The multidisciplinary integration of ecological and hydraulic engineering modeling techniques allowed us to extrapolate our predictions and estimate the effect of the bioturbators on real environments: the neighboring Westerschelde and Oosterschelde basins (The Netherlands, Figure 7.1). The recent divergence in hydrodynamic characteristics and benthic community composition between the two basins and the major ecological and socio-economical importance of sediment budget issues make their compared analysis very interesting to understand the bio-physical landscape organization and its response to human alterations. While the management regimes discussed in this paper show local effects on the scale of the impacted water body, the actual or expected diffusion of such types of management [Cozzoli et al., 2015c, Small and Nicholls, 2003] increases their relevance at a global scale.

7.2 Material & Methods

7.2.1 Study area

The Westerschelde and Oosterschelde basins are located at the boundary between The Netherlands and Belgium (Figure 7.1). To a large extent, they had similar physical characteristics until approximately 50 years ago, but in the meantime they have undergone very different anthropogenic modifications. Coastal safety is a prominent issue in both sites, but, due to different navigability requirements, two radically different approaches were followed to achieve this goal. The Oosterschelde was partially embanked by a storm surge barrier. The Westerschelde, due to its importance as shipping route to the port of Antwerp, kept an open connection with the sea. In this basin, coastal safety is ensured by heightening and strengthening the dikes along the estuary. Flood control areas were created upstream to buffer the water mass at extreme storm tides [Beauchard et al., 2013a,b]. During the last decades the Westerschelde was extensively dredged to allow the transit of bigger vessels (Figure 7.1).

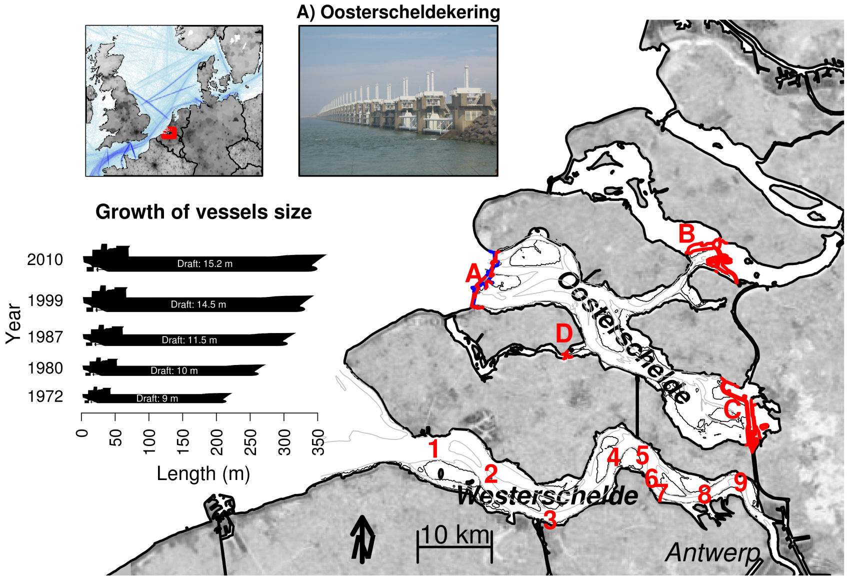
A) Oosterscheldekering
Growth of vessels size
Year
2010
1999
1987
1980
1972
Draft: 15.2 m
Draft: 14.5 m
Draft: 11.5 m
Draft: 10 m
Draft: 9 m
0
50
100
150
200
250
300
350
Length (m)
A
B
C
D
Oosterschelde
Westerschelde
1
2
3
4
5
6
7
8
9
10 km
Antwerp

Figure 7.1: **The Oosterschelde and Westerschelde basins.** A-D: main dams in the Oosterschelde; 1-9: main dredging sites in the Westerschelde. Intertidal areas are marked with a black line. Channels deeper than 10 m are enclosed by a with a gray line (bathymetry of 2010). Global trends in coastal development are well represented in the SW Delta of The Netherlands. On the one hand, the Oosterschelde was disconnected from the previous freshwater network (dams B & C) and embanked from the seaside by a storm surge barrier (Oostercheldekering, A). During the last decades,the maximal size of commercial vessels almost doubled. As consequence, channels in the Westerschelde were locally deepened (1-9) to enhance the shipping route capacity to the port of Antwerp (bottom right)

In both cases, human interventions had a relevant effect on the benthic habitats quality [Cozzoli et al., 2015c] and on the geomorphological equilibrium of the basins. The reduction of hydrodynamic energy due to the dike realization led the Oosterschelde to face a severe and (possibly) irreversible erosion of the intertidal areas [Jongeling, 2007, Louters et al., 1998], but also implied a strong improvement in subtidal benthic habitat suitability [Cozzoli et al., 2013, 2015c]. Dredging of the Westerschelde compromised the stability of the multi-channel system [Peters et al., 2001] and had detrimental effect on both intertidal and subtidal benthic habitats [Cozzoli et al., 2015c].

7.2.2 Target organisms

The species on which we focused in this case are the bivalve *C. edule* and the Polychaeta *A. marina*. They are widely distributed in temperate estuaries, where they often constitute a dominant portion of the intertidal macrozoobenthic biomass [Degraer et al., 2006]. The two species live in the sediment at different depth and they are representative of two different modalities of bioturbation. While their bioturbation effect has been widely investigated both in the field and the laboratory, comparative studies and body size and abundance dependencies are not available to our knowledge.

- *C. edule* are very shallow burrowers (shells sometimes emerge from the sediment surface). Their influence on sediment resuspension is mostly related to superficial sediment destabilization due to vertical and horizontal movements and valves adduction [Flach, 1996]. Sediment erosion can increase up to 10-fold with increasing *C. edule* abundance [Ciutat et al., 2007].
- *A. marina* are deposit feeders living in vertical J-shaped tubes (the adults usually live below 10 cm from the sediment surface.), from where they swallow sediment from the surface. By doing so, they form a characteristic feeding funnel and fecal casts [Zebe and Schiedek, 1996]. It has been observed that *A. marina* bioturbation activity increases mostly the erosion of fine (muddy) sediment, thus it can have a relevant role in keeping the intertidal sandy [Volkenborn et al., 2007].

7.3 Modeling sediment-biota interactions

7.3.1 Step 1: Prognostic model of the physical environment

Simulated scenarios of the estuarine hydrology/morphology can be used to predict the distribution of benthic bioturbators and their reaction to anthropogenic habitat alterations [Cozzoli et al., 2013, 2014, 2015c, Smolders et al., 2015]. In order to predict the biomass distribution of the examined bioturbators (*C. edule* and *A. marina*) in the Westerschelde and Oosterschelde, we modeled as environmental variables the maximal tidal current velocity (maximal values reached during a full tidal cycle, m sec^{-1}), inundation time (% of time for which the site is submerged during a full tidal cycle), average salinity (Practical Salinity Unit, PSU) and salinity range (Δ_{day} PSU) (Figure 7.2). In this study, we used recently validated hydrodynamic models to simulate the Oosterschelde and Westerschelde present and past hydrological scenarios (Figure 7.2).

For the Oosterschelde, two scenarios, one for 1968 and one for 2010, are used in this study. These scenarios were modeled with a specific application of DELFT3D [Lesser et al., 2004] called the KustZuid-model. The resolution of the grid varies from more than 2000 m at the seaward boundary to around 100 m at the Eastern Schelde Inlet. This model application and its calibration are thoroughly described in Eelkema et al. [2012]. The Westerschelde scenarios for 1955 and 2010 were modeled with 2Dh TELEMAC [Moulinec et al., 2011]. This model has a resolution up to 40 m in the intertidal zone. It accounts for salt transport, making it particularly appropriate for distribution modeling of estuarine species [Smolders et al., 2013, 2015]. In all modeled scenarios, wave forcing was omitted because we primarily focused on areas that are tide-dominated. The scenarios for the Westerschelde in 1955 and the Oosterschelde in 1968 represent the hydrological characteristics of the basins before the recent major anthropogenic alterations by dredging, embanking and damming. Salinity models for the Oosterschelde basin are not available; we neglected the role of the (limited) freshwater input from the Volkerak in the Oosterschelde 1968 scenarios. Both Oosterschelde scenarios were modeled with a constant salinity (30 PSU) and no salinity range. For simplicity, in the rest of the paper we will refer to the Westerschelde 1955 and the Oosterschelde 1968 scenarios as 1960 scenarios.

7.3.2 Step 2: Ecosystem engineers distribution model

Spatial distributions of organisms are often the product of different constraints acting at different scales [Thrush et al., 2005]. Even when one or more (known) environmental factors are not limiting, other (unknown) factors might be and organisms could be absent or limited to a low abundance. Thus, central estimators are not able to account for the variance-mean relationship. In a regime of limitation by subsidiary factors (high prevalence of zero observations along the entire gradient), they are not representative of the higher densities and they may fail to distinguish real non-zero changes [Cade and Noon, 2003, Terrell et al., 1996]. The quantile regression model [Koenker and Bassett, 1978, Koenker and Hallock, 2001, Koenker and Machado, 1999] can solve this problem. This method aims at fitting any desired quantile of a response variable distribution to an independent variable. Regression quantile estimates can be used to construct predictions without assuming any parametric error distribution and without specifying how variance heterogeneity is linked to changes in means. Predictions from the full quantile-range species distribution model are in the form:

$$\hat{y}_i \in Q_{Y_i}[\tau|(x_{1(i)}, x_{2(i)}, x_{3(i)}, \dots)] \tag{7.1}$$

where $\hat{y}_i$ is the response value (bioturbators biomass in our case) predicted for the $i-$point. $\hat{y}_i$ belong to the quantile distribution of possible biomass values Q_{Y_i}, which is modeled as a (linear, in our case) function of the local explanatory

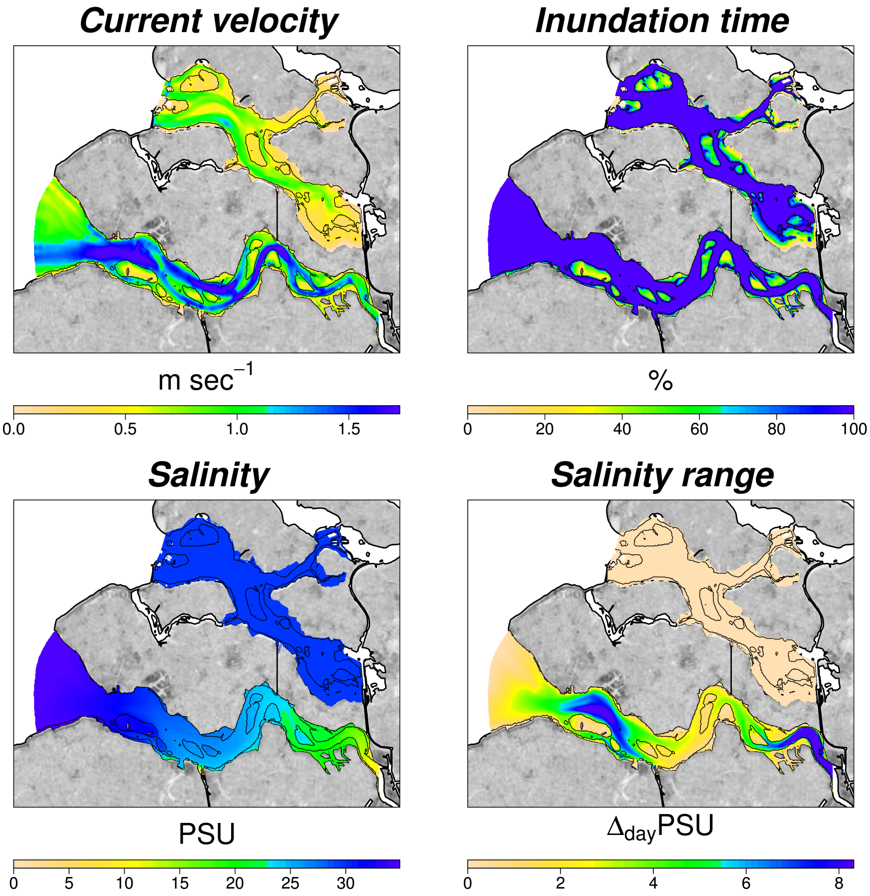
Current velocity
m sec^{-1}
0.0
0.5
1.0
1.5
Inundation time
%
0
20
40
60
80
100
Salinity
PSU
0
5
10
15
20
25
30
Salinity range
Δ_{day}PSU
0
2
4
6
8

Figure 7.2: **Physical variables.** The 2010 scenario is shown as example

variables $x_{1(i)}, x_{2(i)}, x_{3(i)}, \ldots$ [Koenker and Bassett, 1978, Koenker and Hallock, 2001, Koenker and Machado, 1999]. In case of biomass or abundance distribution, $\hat{y}_i$ with $\tau = 1$ represents the expected response when (unmeasured) disturbance is at a minimum, or (unmeasured) facilitation at a maximum [Anderson, 2008, Cade and Noon, 2003]. The succession of the underlying quantiles represents the expected distribution of responses given the actual distribution in the habitat of the unmeasured facilitating or inhibiting variables. Estimates obtained by sampling from the full conditional quantile distributions give biomass values as they could be realistically observed in nature, taking into account the variance induced by subsidiary factors [Cozzoli et al., 2014].

Our habitat suitability models are based on four explanatory, physical variables that all can be simulated in the hydrodynamic models described above: maximal flow velocity (maximum of a full tidal cycle, m $\sec^{-1}$), inundation time (% of time submerged during a full tidal cycle), daily averaged salinity (Practical Salinity Unit, PSU) and salinity range (Δ_{day} PSU). These variables are known to be among the most important hydrological variables in determining coastal and estuarine benthos distribution [Snelgrove and Butman, 1994, Snelgrove et al., 1994, Ysebaert et al., 2002]. While other variables have proven to contribute to the prediction of benthic community distribution (*e.g.,* turbidity [Akoumianaki and Nicolaidou, 2007], primary production [Smith et al., 2006], organic matter [Verneaux et al., 2004], mean sediment grain size and mud content [de la Huz et al., 2002, Degraer et al., 2008, Snelgrove and Butman, 1994, Snelgrove et al., 1994, van der Wal et al., 2011]), they are often well correlated with those accounted into analysis [Cozzoli et al., 2013], so they were not considered in this study.

The data used to fit the benthic species distribution models have been extracted from the Benthic Information System (BIS version 2.01.0) hosted by the NIOZ research center in Yerseke (NL). For this study, a subset of 5510 samples collected from 1962 to 2011 was selected in accordance to the availability of environmental data. The use of a large and long-term dataset (described in Cozzoli et al. 2013), allows estimations of the benthic community distributions with respect to a large number of environmental variables and their interactions. Combinations of individual body size and individuals abundance have been proven to be more efficient in describing the ecosystem engineering activity of a population than their product alone (*i.e.* the total biomass). However, our species distribution model, while having good performances in predicting both the individual body size than the individual abundance [Cozzoli et al., 2014, 2015c], does not allow to explicitly couple the two variables. Thus, we modeled only the total biomass distribution (g m^{-2} Ash Free Dry Weight) of *C. edule* and *A. marina*.

We used upper boundary regression to describe the potential (maximal) effect of the examined bioturbators and emphasize the relationships with the physical variables and models of the full quantile distribution to estimate the realized effect [Cozzoli et al., 2014]. Because the maximum can be a fairly volatile statistic due to the influence of outliers [Anderson, 2008] we considered to model the upper boundary of the species responses on a slightly sub-optimal quantile (90^{th} quantile). Quantile regression models have been proven to be able to accurately forecast the distribution of macrozoobenthic species [Anderson, 2008, Cozzoli et al., 2013, 2014, 2015c]. Further insights about model fitting and validation can be found in Cozzoli et al. [2013] and Cozzoli et al. [2015c].

7.3.3 Step 3: Allometric model of ecosystem engineers effect

In Cozzoli et al. [2015a] it was concluded that the population potential for ecosystem engineering (EE_{pop}) scales as a positive function of the individual body size and of the individuals abundance. A third element is needed to link the population potential for ecosystem engineering (EE_{pop}) to realized changes on a landscape level (EE_{lan}): a description of the context in which ecosystem engineering is performed. For example, wetland vegetation can have a relevant effect on sedimentation only in presence of a sufficient sediment input [Madsen and Hansen, 2001], or soil bioturbation could be limited by soil compaction and granulometry [Dashtgard et al., 2008]. Abiotic variables can be intrinsic components of the ecosystem engineering process, thus they can mediate the expression of the biological potential [Moore, 2006]. The allometric model presented in [Cozzoli et al., 2015a] can be extended to include the role of the environmental context:

$$EE_{lan} = aM^{b}A^{c}X^{z} \tag{7.2}$$

where the normalization constant a accounts for the functional behavior of different organisms, that mediates the efficiency of energy use in changing the environment and b is the (positive) allometric exponent relating the increase of EE_{ind} to the increase in individual body size M, c is the exponent relating the abundance A to the population ecosystem engineering activity and z is the exponent relating the population engineering activity to (a proxy of) the environmental conditions X. While the terms $aM^{b}A^{c}$ express the biological potential for ecosystem engineering from EE_{ind} to EE_{pop}, the realized change in landscape due to EE_{pop}, EE_{lan}, is mediated by the environmental/physical term X^{z}. Scale exponents for body size and density have been observed to be consistent across a large span of diversity in engineers archetypes [Cozzoli et al., 2015a].

Experimental devices and protocol

Details of flumes structure and preparation are given in Cozzoli et al. [2015a] and Appendix C. In each experimental run, the current velocity was increased from 10 to 35 cm sec^{-1} in steps of 5 cm sec^{-1}. Each current step lasted 20 minutes. This sequence imitate the typical range in current velocities above intertidal sediments during the tidal cycle. An Acoustic Doppler Velocimetry probe was used to measure the free-stream velocity and to calibrate the engines' rotation speed. Water turbidity was measured using an optical backscatter sensor (OBS 3+, Campbell scientific) and converted in Suspended Sediment Concentration (SSC , g L^{-1}). The OBS sensors were calibrated by gravitometric analysis.

As often observed in these experiments (*e.g.* Willows et al. [1998]), at each current velocity step the suspended sediment concentration increases in the first minutes (ca. 5 minutes in our experiments) and reaches an equilibrium value at the end. This behavior is caused by the limitation of erodible sediment and is often referred to as Type I erosion or supply-limited erosion [Mehta and Partheniades, 1982]. This implies: 1) all the sediment resuspended at a certain current velocity (plus other sediment) will be resuspended at an higher current velocity 2) in absence of sediment consolidation, all the sediment eroded in a first run and let settled will be eroded in a second run at the same current velocity.

Different densities of homogeneously sized *C. edule* and *A. marina* individuals were separately tested (Table 7.1). Abundances and body sizes were selected in a way to represent the natural range of each of the analyzed species. Every experiment (2 replicates) consisted of a preliminary run without added animals and an experimental run. The aim of the first run is to provide an independent abiotic control for each of the experimental run with animals. Animals were introduced into the flumes suddenly after the first run and let settle for 48 hours before the second run.

Data analysis

We consider as proxy for EE_{lan} the (stable) SSC reached after 15 minutes of each current velocity step. Taking the log of both sides, Equation 7.2 can be rearranged in a suitable form for multivariate regression analysis:

$$SSC = aM^b D^c X^z \Rightarrow \log(SSC) = \log(a) + b\log(M) + c\log(A) + z\log(X) \quad (7.3)$$

where M and A are the individual body size (mg AFDW) and the abundance (N. of Ind. m^{-2}) of the examined bioturbators (Table 7.1) and X is the (progressively increasing) current velocity generated by the rotor. Allometric regression models were fitted separately for the two analyzed species of bioturbators and for abiotic controls (using current velocity only as explanatory variable, Table 7.4). This kind of models have been proven to have better performances when they use separately the individual body size and the individuals abundance as explanatory variables, rather than when they are fitted on the product of the two variables (*i.e.* the total biomass, Equation 7.4) [Cozzoli et al., 2015a].

$$\log(SSC) = \log(a) + d\log(M * A = B) + z\log(X) \quad (7.4)$$

where B is the total biomass (g AFDW m^{-2}) and d is the allometric exponent relating the increase of EE_{pop} to the increase in bioturbators biomass. As mentioned before, our species distribution model does not allow to explicitly couple the body size and the abundance of the forecast species. Thus, while we reported results for both the three (Equation 7.3) and the two explanatory variables (Equation 7.4) allometric models, only the latter version was used for the extrapolation of ecosystem engineering activity in realistic environment (see next section). In all cases, variables were log-transformed, centered and scaled. First - degree response surfaces were fitted separately for each of the three functional groups and on the overall dataset. 95 % CIs were calculated by bootstrapping the dataset 50000 times.

Experimental results

The amount of resuspended sediment due to bioturbation can be scaled as a positive allometric function of the current velocity and of the bioturbators' body size and individual abundance (Table 7.2), as well as for the total biomass (Table 7.3). Regression models based on these three variables are able to explain from 57 % (*A. marina*) to 66 % (*C. edule*) of the observed variance in SSC (Table 7.2). Allometric exponents relating the suspended sediment concentration to individual body size are estimated as 0.21 (*C. edule*) and 0.33 (*A. marina*) and are not significantly different among bioturbators (look at 95 % CI in Table 7.2). The estimated allometric exponent relating SSC to individual abundance is 0.52 for *C. edule* and significantly higher (1.12) for *A. marina* (Table 7.2). Models based on the total bioturbators biomass have good performances in explaining the observed variance. The estimated allometric exponents for SSC scaling with total biomass are ~ 0.22 for all the fitted models (Table 7.3).

The scale exponent of SSC with current velocity, in absence of bioturbators, is equal to 1.5 (Table 7.4). In presence of *C. edule* the scaling exponent (~ 1.68) is not significantly higher than in the abiotic control, while the SSC follows a significantly steeper increase with current velocity (scale exponent~ 2.35) in presence of *A. marina* (Tables 7.2 & 7.3).

Scaling exponents for body size, abundance and biomass dependency of suspended sediment concentration are consistent with those shown in Cozzoli et al. [2015a] for a single current velocity step (30 cm sec^{-1}). Exponents for body size scaling are not significantly different between bioturbators. This pattern could reflect the common scaling of metabolic and geometric individual features [Brown, 1995, De Roos et al., 2003, Schmid et al., 2002]. Scaling coefficients for abundance and current velocity are significantly higher for *A. marina* than for *C. edule*. The scaling coefficient for *A. marina* abundance is around 1 (Table 7.2). For *C. edule* it is around 0.5. This suggests that *A. marina* have no negative interference between individuals in their ecosystem engineering activity, while *C. edule* could overlap their influence areas, leading to a negative allometry between abundance and SSC. Finally, *C. edule* have a lower exponent than *A. marina* for the relationship with the current velocity (respectively 1.67 and 2.33) and a higher intercept (respectively -11 and -16.67). This is in accordance with our visual observation that a relatively high current velocity (> 15 cm sec^{-1}) is needed before a consistent erosion of *A. marina* fecal casts occurs. The regression coefficients suggest that erosion starts at lower current velocities in *C. edule*, but increases less with current velocity once started.

Table 7.1: **Table of treatments.** According to the availability of experimental organisms, we tested several combinations of individual abundances and individual body sizes of *C. edule* and *A. marina*

Species	Individual body size (mg AFDW)	Abundance (N of ind. m^{-2})	Biomass (g AFDW m^{-2})
C. edule	11	95	10
C. edule	11	191	21
C. edule	11	382	41
C. edule	101	32	32
C. edule	101	64	64
C. edule	101	127	129
C. edule	101	255	257
C. edule	616	13	78
C. edule	616	32	196
C. edule	616	64	392
A. marina	23	32	7
A. marina	23	64	15
A. marina	23	95	22
A. marina	23	127	29
A. marina	213	32	68
A. marina	213	64	136
A. marina	213	95	202
A. marina	213	127	270
A. marina	1136	32	36
A. marina	1136	64	73
A. marina	1136	95	108

Table 7.2: **Summary table of the multivariate models $EE_{lan} = aM^bA^cX^z$.** Explanatory and response variables were log-transformed, centered and scaled to make coefficients directly comparable. 95% CI were calculated by bootstrapping the dataset 50000 times.

Species	Parameter	Estimate	Lower 95% CI	Upper 95% CI	Std. error	t - value	p - value	Adjusted R^2
C. edule	Intercept	-11	-12.52	-9.54	0.67	-16.4	0	0.57
	Body Size	0.21	0.11	0.3	0.05	4.46	0	
	Abundance	0.52	0.35	0.69	0.08	6.79	0	
	Current Velocity	1.67	1.35	1.9	0.15	11.34	0	
A. marina	Intercept	-16.61	-18.79	-14.44	1.05	-15.77	0	0.66
	Body Size	0.33	0.22	0.44	0.06	6	0	
	Abundance	1.12	0.83	1.41	0.18	6.28	0	
	Current Velocity	2.33	1.9	2.77	0.19	12.4	0	

Table 7.3: **Summary table of the multivariate models $EE_{lan} = aB^dX^z$.** Explanatory and response variables were log-transformed, centered and scaled to make coefficients directly comparable. 95% CI were calculated by bootstrapping the dataset 50000 times

Species	Parameter	Estimate	Lower 95% CI	Upper 95% CI	Std. error	t - value	p - value	Adjusted R^2
C. edule	Intercept	-9.81	-11.21	-8.42	0.68	-14.48	0	0.5
	Biomass	0.22	0.13	0.32	0.05	4.43	0	
	Current Velocity	1.69	1.35	2.03	0.16	10.55	0	
A. marina	Intercept	-13.38	-15.32	-11.47	0.86	-15.53	0	0.6
	Biomass	0.34	0.22	0.46	0.06	5.57	0	
	Current Velocity	2.37	1.91	2.82	0.2	11.54	0	

Table 7.4: **Summary table of the abiotic model $SSC = aX^z$.** Explanatory and response variables were log-transformed, centered and scaled to make coefficients directly comparable. 95% CI were calculated by bootstrapping the dataset 50000 times

Species	Parameter	Estimate	Lower 95% CI	Upper 95% CI	Std. error	t - value	p - value	R^2
Control	Intercept	-6.9	-8.61	-5.29	0.61	-11.41	0	0.62
	Current Velocity	1.5	1	2.01	0.2	7.56	0	

7.3.4 Step 4: Integration

Once descriptions of 1) the environmental context in which ecosystem engineering is performed; 2) the engineers distribution; 3) the covariance structure between the previous two factors; are available, they can be integrated to give a static representation of ecosystem engineering influence on a real ecosystem. Prognostic models of the physical environment can be used to reconstruct the environmental context in which the ecosystem engineering activity is performed (Step 1). Species distribution models can estimate the spatial distribution of the ecosystem engineers (Step 2). Factorial experiments allows to parametrize the effect of the ecosystem engineers on the base of fundamental biological and physical descriptors (Step 3). The previous three steps can be integrated to extrapolate static maps about how the ecosystem engineering activity is distributed in space and time (Step 4). Several physical components may be involved in ecosystem engineering processes, and, in principle, they should be considered as separate variables. However, physical components are correlated with each other. For example, both the magnitude of the hydrodynamic stress and the sediment granulometry and composition are important physical variables to determine wet sediment erosion [McLusky, 2004]. In nature they are strongly correlated by a causal relationships (the hydrodynamic energy sorts the sediment grains, eroding and allowing the settling of finer sediment at lower energy), thus one can be used as proxy for the others [Allen, 1985]. For this reason, in this study we will consider current velocity only as proxy for all environmental conditions.

The 1960 and 2010 physical scenarios obtained from the hydrodynamic models were used to predict the maximal and the realized biomass distribution of *C. edule* and *A. marina*. The current velocity and the biomass scenarios were combined by using the scaling coefficients reported in Table 7.3. We considered as measure of performed ecosystem engineering the relative increase in sediment erosion predicted in the bioturbators-scenarios with respect to purely physical expectation (Equation 7.5).

$$EE_{lan} = \frac{a_{bio} \hat{B}^{d} X_{vel}^{z_{bio}}}{a_{contr} X_{vel}^{z_{contr}}} \tag{7.5}$$

where EE_{lan} is the change (increment) in sediment erodability due to the action of bioturbators, X is the maximal tidal current velocity as predicted from the hydrodynamic model (Step 1), $\hat{B}$ is the biomass density as predicted from the species distribution model (Step 2), a_{bio}, d, and z_{bio} are the estimated coefficients (Table 7.3) for the bioturbators biomass and current velocity scaling of the SSC and a_{contr} and z_{contr} are the estimated coefficients (Table 7.4) for the current velocity scaling of SSC in absence of bioturbation (Step 3). If $\hat{B}$ is an upper boundary estimation (90^{th} quantile in our case), Equation 7.5 allows to predict the potential effect of bioturbators and to emphasize the relationships with the physical (explanatory) variables. If $\hat{B}$ is obtained by stochastically sampling, for each $i-$point, the probabilistic function $Q_{B(i)}$, Equation 7.5 can be used to quantify the overall contribution of a realistic amount of bioturbators biomass. Given that 1) the examined bioturbators are very rare or completely absent subtidally and 2) the subtidal current velocities can largely overcome the range experimentally tested (0 to 35 cm sec^{-1}), we limited our analysis to intertidal sites. Differences between the 1960 and the 2010 scenarios were expressed in terms of absolute change in bioturbation potential.

7.4 Results

The distributions of *C. edule* and *A. marina* are largely overlapping (Figure 7.3 A & B). Both species reach the maximal habitat suitability on the high and intermediate intertidal and they have both preference for high (marine) salinity. However, the potential ecosystem engineering effect on sediment resuspension is higher on the exposed edges of the mudflats, where the habitat suitability for bioturbators is low, rather than on the inner part, where the bioturbators can reach a high biomass but current velocity is too low to lead to high bioturbation effect (Figure 7.3 C & D). Along the same line, the predicted potential for bioturbation is higher in more dynamic and limiting environments like the Westerschelde rather than in shallow and bioturbator-suitable environments like the Oosterschelde. The comparison between the 1960 and the 2010 scenarios (Figure 7.3 E & F) shows a net increase in ecosystem engineering potential in the Westerschelde (especially on the edges of the mudflats, where the increase in current velocities between 1960 and 2010 was higher) and a decrease in the Oosterschelde.

Increases in current velocity had a negative effect on bioturbator biomass and a positive relationship with the bioturbation potential. The equilibrium between the two interaction pathways led to changes in bioturbation potential over time which were independent from changes in the bioturbators' biomass (Figure 7.4).

Models of the full quantile distribution allow realistic quantifications of the bioturbators biomass [Cozzoli et al., 2014], thus they were used to provide a realistic quantification of the ecosystem engineering impact. In all scenarios, the predicted realized biomass of *C. edule* is ~ 4-5 times higher than the biomass of *A. marina* (Figure 7.5 B). The latter bioturbator has a stronger ecosystem engineering effect per unit of biomass (Figure 7.3), thus differences in realized ecosystem engineering are smaller than differences in realized biomass. In both the low-current scenarios (Westerschelde 1960 and Oosterschelde 2010) *A. marina* has a stronger ecosystem engineering effect than *C. edule*, while in the high-current scenarios (Westerschelde 1960 and Oosterschelde 2010) the contribution of *C. edule* is more relevant (Figure 7.5 B).

Using full quantile distribution models (rather than model of the maxima), we predict that, while the realized biomass of both *A. marina* and *C. edule* is much higher in the upper intertidal (Figure 7.5 B), their engineering effect is stronger in the intermediate and lower parts of the mudflat (Figure 7.5 C), where maximal current velocities are higher due to increased flow exposure (Figure 7.5 A). Although variations in the average current velocity between 1960 and 2010 (Figure 7.5 A) had a limited effect on the realized biomass of the two species (Figure 7.5 B), their average ecosystem engineering effect had strong variations (Figure 7.5 C). In the Westerschelde, in relation to an increment of the average intertidal current velocity of 40%, the increment in sediment resuspension due to ecosystem engineering (compared to abiotic conditions) passed from 12% (*A. marina*) and 9% (*C. edule*) in 1960 to 52% (*A. marina*) and 78% (*C. edule*) in 2010. At the opposite, in the Oosterschelde a 40% decrease of the average intertidal current velocity led to a decrease of the *A. marina* induced sediment resuspension from 37% to 18% of the physical erosion and from 42% to 8% for *C. edule*.

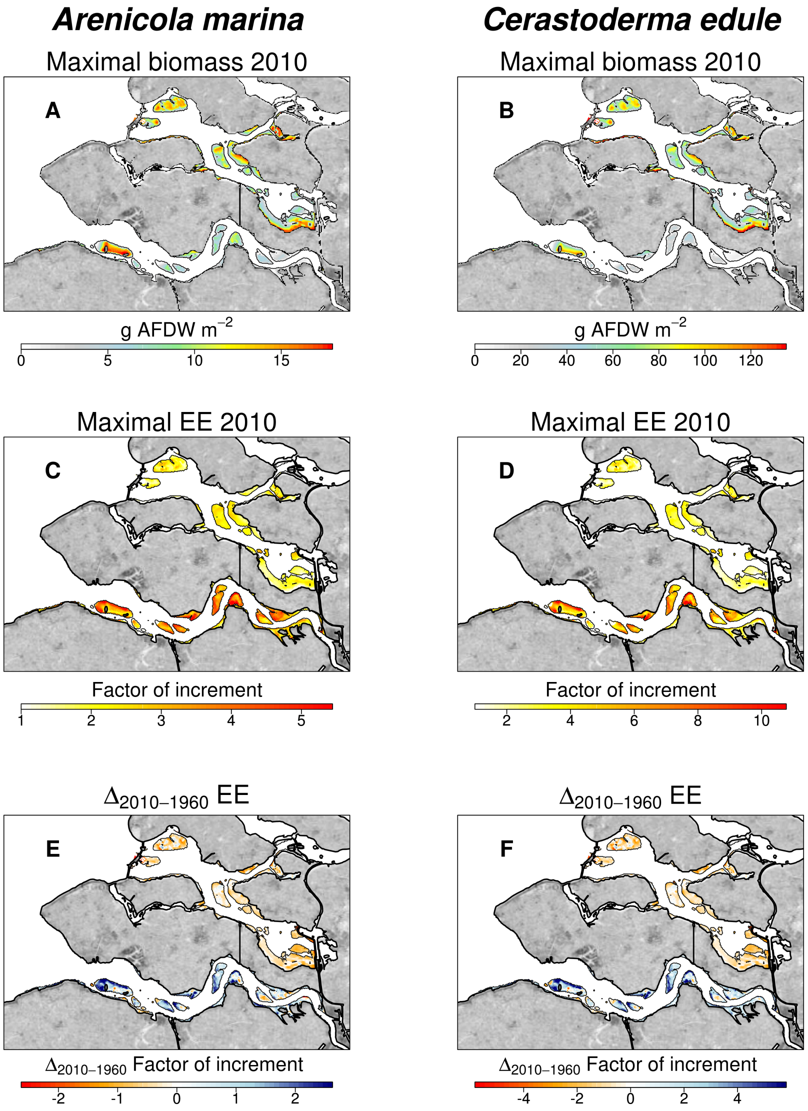
Arenicola marina
Cerastoderma edule
Maximal biomass 2010
Maximal biomass 2010
A
B
g AFDW m⁻²
0
5
10
15
g AFDW m⁻²
0
20
40
60
80
100
120
Maximal EE 2010
Maximal EE 2010
C
D
Factor of increment
1
2
3
4
5
Factor of increment
2
4
6
8
10
Δ2010–1960 EE
Δ2010–1960 EE
E
F
Δ2010–1960 Factor of increment
-2
-1
0
1
2
Δ2010–1960 Factor of increment
-4
-2
0
2
4

Figure 7.3: **Potential ecosystem engineering.** A-B) Maximal expected biomass of *C. edule* and *A. marina* (as estimated from a 0.9 quantile distribution model, [Cozzoli et al., 2014]; D-C) Maximal increase in sediment erodability due to *C. edule* and *A. marina* bioturbation. Estimates are expressed as factor of increment in sediment resuspension with respect to what predicted from the abiotic erosion model (Figure 7.3); E-F) Changes in maximal EE from 1960 to 2010

7.5 Discussion

7.5.1 Modeling sediment-biota interactions

This study constitutes a first approach to join ecological and morphological forecast in an holistic and multidisciplinary framework. Prognostic environmental scenarios were used to produce hydromorphological environmental scenarios (Figure 7.2). Quantile regression models of field data were applied to predict the ecosystem engineers distribution (Figure 7.3 A & B). The ecosystem engineers influence on physical processes was parametrized by means of factorial experiments (Table 7.2 & 7.3). These three steps were integrated in a final model able to forecast the potential and the realized increment in sediment resuspension due to the action of bioturbators (Figure 7.3 C & D). Simulated scenarios for the years 1960 and 2010 were compared to evaluate the impact of different estuarine management regimes on the bioturbation activity in the Westerschelde and Oosterschelde (Figure 7.3 E & F). The multidisciplinary integration of hydrodynamic and ecological models allows to investigate 1) the long-term effect of morphological and hydrological alterations for an important part of the natural community and 2) how the change in the benthic community could feed back the landscape evolution.

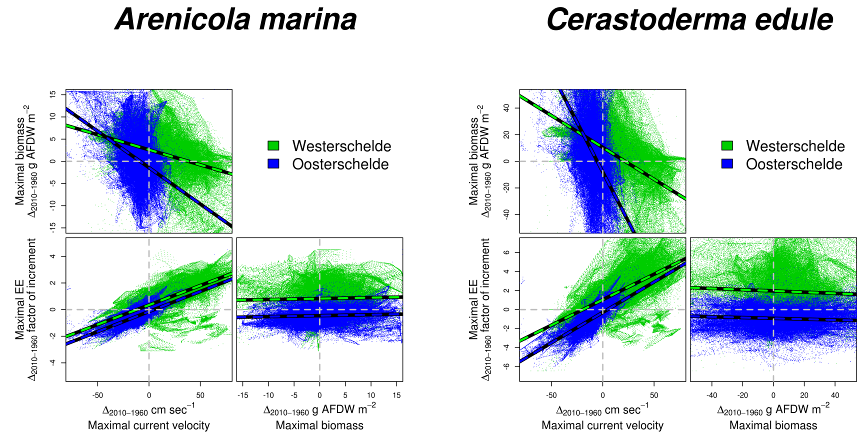

Figure 7.4: **Potential ecosystem engineering, changes between 1960 and 2010.** Correlation between changes in maximal current velocity, maximal bioturbators biomass and potential ecosystem engineering for the Westerschelde and Oosterschelde (one point each 400 m^2). Broken lines indicates the linear relationships between variables

Equation 7.5 can be used to extrapolate the ecosystem engineering effects and to express them in terms of induced variation in the underlying physical process (Figure 7.3 C & D). Most studies related to interactions between biota and sediment concluded that there was a strong dependence of erodability on the macrozoobenthos activity [Borsje et al., 2008, Orvain et al., 2012, van Prooijen et al., 2011, Willows et al., 1998, Wood and Widdows, 2002]. Conversely, our simulations show that even small biomasses (reduced activity) of bioturbators in dynamic current conditions can increase sediment resuspension significantly. Although both bioturbator biomass and current velocity are positively correlated with sediment resuspension (Table 7.3), the negative correlation between current velocity and bioturbators biomass (Figure 7.4) *de facto* led to an inverse relationship between bioturbator biomass and ecosystem engineering (Figure 7.4). This finding is in contrast with the hypothesis that ecosystem engineering can be more important at low hydrological energy and high ecosystem engineers biomasses [Moore, 2006].

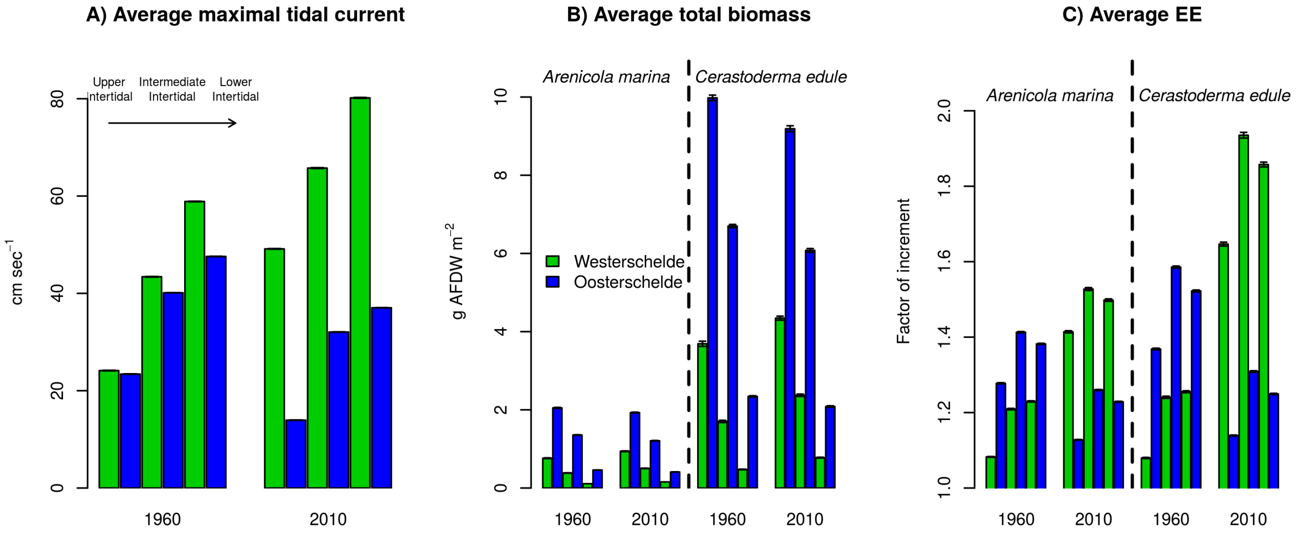

Figure 7.5: **Realized ecosystem engineering, summary of changes between 1960 and 2010.** Each block of bars shows (from left to right), for the Westerschelde (green) and Oosterschelde (blue) 1960 and 2010 scenarios, the average values predicted for the upper (submerged for less than the 50% of a tidal cycle), intermediate (submerged between 50% and 75% of a tidal cycle) and lower (submerged for more than the 75% of a tidal cycle) intertidal areas. Error bars represent standard errors. A) Average intertidal current velocity as estimated from the prognostic environmental model (Figure 7.2); B) Average realized intertidal biomass of *C. edule* and *A. marina* as estimated from a full quantile distribution model; C) Average realized increment of sediment resuspension due to bioturbation from *C. edule* and *A. marina*

We predict that, while the realized biomass of both *A. marina* and *C. edule* is much higher in the upper intertidal (Figure 7.5 B), their engineering effect is stronger in the intermediate and lower parts of the mudflat (Figure 7.5 C), where maximal current velocities are higher due to increased flow exposure (Figure 7.5 A). This finding is contrasting from what predicted from Orvain et al. [2012] for *Scrobicularia plana* (stronger effect in the upper intertidal) and more similar to what predicted from Wood and Widdows [2002] for *Macoma balthica*. The order of magnitude of influence in our forecast is comparable to what estimated from Orvain et al. [2012] and Wood and Widdows [2002]. By having a stronger engineering effect on the intermediate and lower part of the mudflat rather than on the upper one, benthic bioturbators can have the effect to make a mudflat 'steeper' than it would be when only physical sediment transport were considered. This trend could be further emphasized from the fact that the microphytobenthos (that has a main stabilizing effect on muddy sediment, [Stal, 2003]) is also more abundant on the high intertidal and at low current velocity. Reducing the elevation of the edges of the mudflat, bioturbators increase their exposure to strong currents, that is detrimental for their fitness. Thus, at least in the exterior part of the mudflat, bioturbation activities can induce a negative feedback with the environmental conditions. Given that the stronger is the current velocity the lower is the bioturbator biomass and, consequentially, the increase in erodability due to biotic influences, equilibrium conditions are likely to establish (Figure 7.4). The inverse correlation between mycrophytobenthos distribution and bioturbation potential can be relevant also to simulate the export of microphytobenthos to the water column [Ubertini et al., 2012].

Different combinations of bioturbators biomass and current velocity can have a similar overall effect. Despite the differences in average current velocity (Figure 7.5 A) and bioturbator biomass (Figure 7.5 B), both the low current velocity scenarios (Westerschelde 1960 and Oosterschelde 2010) and the high current velocity scenarios (Westerschelde 2010 and Oosterschelde 1960) are similar to each other in the predicted contribution of ecosystem engineering to sediment resuspension (Figure 7.5 C). In all the predicted species distribution scenarios, *A. marina* reaches ca. 25 % of the *C. edule* biomass (Figure 7.5 B). However, given the stronger interactions with the hydrodynamic stress (Table 7.3) and the preference for slightly higher current velocity (Figure 7.3 A & B), *A. marina* it is able to produce a just slightly lower engineering effect than *C. edule* in the high current velocity scenarios (Westerschelde 2010 and Oosterschelde 1960) or even a higher effect in the low current velocity scenarios (Westerschelde 1960 and Oosterschelde 2010). We can infer that the higher efficiency of *A. marina* (compared to *C. edule*) in inducing sediment resuspension derives from a lack of destructive interference between individuals and from a stronger interaction with the hydrodynamic stress rather than from a higher individual potential (Table 7.2).

We found that anthropogenic alterations of the hydrodynamic conditions (Figure 7.2) had a minor effect on the bioturbator biomass but induced large variations in the bioturbation potential (Figure 7.5). In 1960, the predicted effect of bioturbation was higher in the Oosterschelde than in the Westerschelde, while presently the situation is the reverse. However, our analysis also shows that physical trends can overwhelm the biotic influence. Despite the reduction (from 1960) in ecosystem engineering contribution to sediment resuspension (Figure 7.5 C), the Oosterschelde is currently facing a severe intertidal erosion due to change in the hydrological equilibrium and sediment input [Louters et al., 1998]. The Westerschelde mudflats are in accretion despite the strong increase in sediment destabilization and resuspension by bioturbators (Figure 7.5 C). Across both systems, ecological factors thus had a dampening effect on the influence of physical modifications of the habitats. Some of these features can be considered as negative consequences of habitat alterations (decrease in habitat suitability in the Westerschelde, erosion of Oosterschelde mudflats). Others have a positive connotation (both in the Oosterschelde, increasing in subtidal habitat suitability and decrease in intertidal sediment resuspension due to bioturbation). While the management regimes of the systems discussed in this paper show local effects on the scale of the impacted water body, the actual or expected diffusion of such types of management [Cozzoli et al., 2015c, Small and Nicholls, 2003] increases their relevance at a global scale.

7.5.2 Recommendations for future research

The model presented in this paper clearly represents a simplified system, which does not account for all relevant variables in the sediment erosion process. Our results should be carefully considered due to large extrapolations and model assumptions. Some important points to investigate and clarify to refine our predictions are:

- **Improvement of the environmental context characterization** by adding other physical (explanatory) variables. As an example, the covariance structure between current velocity and sediment granulometry is determinant for realized species abundances and it is also an important driver for sediment erosion [Winterwerp and van Kesteren, 2004]. While we used the current velocity as a proxy for sediment granulometry and other covarying environmental features, future and more accurate modeling of biotic influence on sediment erosion should consider sediment characteristics like granulometry and compaction as additional explanatory variables. Complexity arises from the fact that additional variables need to be implemented in each one of the four modeling steps described in this paper. Caution must be exerted, since the addition of more environmental factors will inevitably increase the fit of statistical models, but will not necessarily lead to robust models that perform better in extrapolation.

- **Investigation of the effect of species assemblages.** Interactions between different ecosystem engineers have not yet been explicitly considered in our framework. Often organisms with contrasting engineering behavior, like biostabilizer and bioturbators, are co-occurent. For example, areas with high densities of *C. edule* and *A. marina* are often rich in microphytobenthos [Montserrat et al., 2011]. Interactions between different engineers can affect their distribution (*i.e.* ecological interactions affecting the spatial range, the size or the abundance of a species) as well as their functional activity (*i.e.* cumulative or destructive interference in the ecosystem engineering activity). They can generate themselves feedback dynamics (*i.e.* if the ecosystem engineering activity of one engineer affect the fitness of the other one). The fine patchiness in species abundances and occurrences and the diversity of their ecosystem engineering effect should be carefully investigated for future applications.

- **Field validation:** Ideally, the results of the model should be compared to observations of erosion and deposition over an intertidal flat. However, on the one hand, there are very few data of this sort available. On the other hand, our models are still based on many assumptions and approximations (see the two points above) that can render the direct comparison of predictions with field data difficult. Both an improvement in the realism of the model and a large number of *in situ* observations and manipulation experiments are required to fully assess the validity of our predictions and their reliability as guidelines for estuarine management.

- **From a static to a dynamic representation of ecosystem engineering:** parameterization of numerical (dynamic) models. Current morphodynamic models simulate purely physical dynamics and are parameterized on the basis of field observations. Any ecosystem engineering effects are subsumed and may effectively have contributed to the calibrated values of the parameters. Once 'fueled' with semi-empirical descriptions of the ecological processes, numerical models of sediment transport can actively account for the biotic influence in landscape evolution [van Prooijen et al., 2011] and feed back the new environmental scenarios to the species distribution models. This has the double advantage of 1) increasing the morphodynamic model accuracy by considering the biota-mediated deviations separately from the expected physical trends and 2) producing simultaneous forecast on the morphological and ecological future state of estuaries.

7.6 Conclusion

The recognition that organism responses to the anthropogenic habitat alterations can induce (or, as we predict, buffer) further changes in the landscape is a fundamental step to explicitly integrate nature into human development [Ecoshape, 2014] and to forecast the future availability of ecosystem services [Chan et al., 2006]. The integration of ecological insights in physical landscape models presents the double advantage to provide simultaneous forecasts about the ecological and morphological landscape evolution and to account for the biotic-induced deviations from purely physical expectations. It allows generalization of interactions mediated by ecosystem engineering, thus providing a framework for extrapolation and application to a wide range of environments. Integrated physical-biotic models of sediment dynamics can be used to upscale the quantification of the interactions between biota and sediment transport to a whole-estuary context. While this work is specifically aimed to forecast estuarine geomorphological dynamics, the proposed framework can be generalized to quantify the realized impact of any kind of ecosystem engineering on landscape evolution and ecosystem functionality.

Acknowledgements

This work was mainly funded by the Ecoshape/Building with Nature project. The NIOZ Monitor Taskforce was for a large part responsible for the fieldwork and the taxonomic analysis of the macrofauna samples. Rijkswaterstaat (executive body of the Dutch Ministry of Infrastructure and the Environment) was responsible for the funding of these activities in the framework of different national monitoring projects such as MWTL. The hydrodynamic modeling for the Westerschelde was funded by the Antwerp Port Authority.

CHAPTER 8

Outlook

Estuaries are among the richest natural habitats in the world. They play a pivotal role in global ecological dynamics [McLusky, 2004] and produce important commercial and social assets for human communities [Costanza et al., 1997]. The physical and biological state of estuarine systems (bed morphology, hydrodynamics, nutrients, hydrology, . . .) is subject to continuous, natural changes. The natural evolution of estuaries is often severely influenced by human interventions [Gray, 1997, Kennish et al., 2002]. Preserving estuarine functioning in a regime of strong anthropogenic habitat alteration is a great challenge. Given the interactions between physical, ecological and social factors, a holistic approach is required for integrated ecosystem management [Ecoshape, 2014, Leschine et al., 2003, Temmerman et al., 2013].

The morphology is a common denominator of many ecological and social services and functions provided by the estuarine environment [Gray, 1997, Kennish et al., 2002]. On the one hand, anthropogenic alterations of the estuarine morphology should be planned in a way to minimize their ecological impact or to compensate it with the creation of new opportunities for nature and society (*e.g.* the Delfland Sand Engine [van Slobbe et al., 2013] or the Walsoorden nourishment [Smolders et al., 2015]). On the other hand, natural components can be regarded as an operational part of the infrastructure functional design (*e.g.* the use of oyster reefs to prevent intertidal erosion in the Oosterschelde [Ysebaert et al., 2012] or the design of ecosystem-based management of tropical coastlines [Gillis et al., 2014]). It is evident that ecological forecasts must be included into dynamic landscape management to maintain operational efficiency and reduce the ecological impacts [Matthews et al., 2011]. Given the complexity of the interactions between natural and anthropogenic components, accurate and dynamic forecasts about system eco-morphological responses are essential to guide estuarine management actions and plans.

This PhD thesis can be seen as a first step toward the inclusion of ecological elements in morphological forecasts. The multidisciplinary integration of hydrodynamic and ecological models allows to investigate 1) the effect of morphological and hydrological alterations for an important part of the natural community and 2) how the change in the benthic community could feed back the landscape evolution.

Integrated hydro-ecological models allows the introduction of better ecosystem management practices, both on the intermediate and long term. As an example, the historical analysis of the Westerschelde and Oosterschelde evolution can provide useful insights for future infrastructures realization. The decrease in potential species diversity and body size, as predicted for the 'dredged' Westerschelde [Cozzoli et al., 2013, 2015c], can be detrimental for ecosystem functioning. At the opposite, a higher potential for bigger individuals, like predicted for the subtidal habitats in the 'embanked' Oosterschelde [Cozzoli et al., 2013, 2014, 2015c], is indicative of higher complexity in species trophic [Woodward et al., 2005] and non-trophic (*e.g.* ecosystem engineering, habitat forming [Kefi et al., 2012]) interactions and could imply positive effects on macrofauna through the benthic-pelagic food chain [Rinne and Miller, 2006]. Thus, morphological alterations of estuaries implying an increase in hydrodynamic energy should be coupled, when possible, with habitat compensation measures to limit their negative ecological impact (*e.g.* the Walsoorden nourishment). Integrated models can be used to plan targeted interventions on the mudflat morphology that can increase the local benthic habitat suitability and, at the same time, offer a smart way to dispose dredged sediment [Smolders et al., 2015]. By doing so, the effects of a detrimental activity for the benthic habitat suitability like dredging [Cozzoli et al., 2015c] can be partially compensated by using a waste product of the activity itself (*i.e.* the dredged sediment). Morphological alterations implying a decrease in hydrodynamic energy can destabilize the morphological equilibrium of the system and lead to a shrinking of valuable habitats like intertidal flats. However, the decrease in current velocity should not be considered by itself as a threat for the benthic communities. Rather, it has the effect to strongly improve the subtidal habitat quality. We also predicted that decreases of hydrodynamic energy in the mesohaline part of the estuary could also lead to the proliferation of opportunistic species and could imply a decrease in habitat quality [Smolders et al., 2015].

The evaluation of ecological responses to habitat modifications must include a quantification of the induced changes in provided ecosystem services and functions. The complex covariance structure between biotic and abiotic factors involved in ecosystem functioning complicates the construction of forecasts directly from field observations. The integration of species distribution models and laboratory experiments allows the parametrization and extrapolation of semi-empirical models of organism behavior. These forecasts have a particular relevance when applied to ecosystem engineering activities, because they can be used to simulate the feedbacks between abiotic and biotic components. We showed that power laws can be efficiently used to describe the magnitude of ecosystem engineering processes [Cozzoli et al., 2015a], also accounting for the environmental context in which the ecosystem engineering activity is performed [Cozzoli et al., 2015b]. The resulting picture is that both general (body size dependencies) and species-specific (abundance, interaction with the environmental conditions) elements can be relevant for determining the final magnitude of ecosystem engineering. Most studies related to interactions between biota and sediment concluded that there was a strong dependence of erodability on the macrozoobenthos activity [Borsje et al., 2008, Orvain et al., 2012, van Prooijen et al., 2011, Willows et al., 1998, Wood and Widdows, 2002]. Conversely, our simulations show that even small biomasses (reduced activity) of bioturbators in dynamic current conditions can increase sediment resuspension significantly. Although both bioturbator biomass and current velocity are positively correlated with sediment resuspension (Figure 7.3), the negative correlation between current velocity and bioturbator biomass *de facto* led to an inverse relationship between bioturbator biomass and ecosystem engineering. This finding is in contrast with the hypothesis that ecosystem engineering can be more important at low hydrological energy and high engineers' biomass [Moore, 2006]. Given the inverse correlation between current velocity and bioturbator biomass and the positive correlation between current velocity and effectiveness of bioturbation, our predictions show that bioturbators population dynamics are more likely to buffer physical trends rather than to emphasize them [Cozzoli et al., 2015b]. We conclude that environmental changes related to alteration of the bioturbation activity should not be regarded as a major point of concern in the preliminary assessment of wet infrastructures impacts.

Descriptions of ecosystem engineering are important to understand the patterns and dynamics of landscape evolution [Pearce, 2011], diverse species interactions [Kefi et al., 2012], ecological succession [Bouma et al., 2005, Bruno, 2000] and many other ecosystem processes (*e.g.*, Dangerfield et al. [1998], Gutiérrez and Jones [2006], Lavelle et al. [2006]). Explicit inclusion of ecosystem engineering in ecosystem modeling can have both ecological [Kefi et al., 2012] and social relevance [Sanders et al., 2014]. While in this thesis we focus on a specific case study, the approach we developed can have broader applications in ecology because of:

- The use of prognostic environmental models and quantile regression species distribution models can be applied to describe the distribution of any kind of organisms;
- One of the most characteristic traits of organisms is body size, and generalizations in ecology are often based on scaling of body size to organisms' rates and activities. Thus, our observations can be easily framed within broader ecological theories (*e.g.* the Metabolic Theory of Ecology) and allow macro-ecological generalizations of the ecosystem engineering concept;

- Our models describe ecological processes but are based on physical parameters. They are fully compatible with the existent physical descriptions of sediment transport and can, therefore, be used to parametrize large scale semi-empirical models of biotic-mediated sediment dynamics.

- While we specifically focus on ecosystem engineering, our approach can be generalized to other ecological performances and activities related to organisms' spatial distribution.

Appendices

Appendix A: A mixed modeling approach to predict the effect of environmental modification on species distributions

Table A.1: **AIC scores for different models (average of the AIC scores of all the fitted quantiles)**

Species	Current velocity	Inundation time	Both (no interaction)	Both (interaction)
S. armiger	6373	6080	6055	6017
P. ulvae	13725	13165	13146	13090
C. edule	26590	26834	26586	26521
L. conchilega	15977	15937	15915	15915

Table A.2: ***S. armiger*, summary of the 0.975 quantile (upper boundary) model**

	Value	Std. Error	t value	Pr
(Intercept)	1.2436	0.0028	450.6048	0
vel	13.0383	1.427	9.1371	0
em	-0.0015	0.0025	-0.5996	0.5488
vel:em	-0.1181	0.0144	-8.2059	0

Table A.3: ***P. ulvae*, summary of the 0.975 quantile (upper boundary) model**

	Value	Std. Error	t value	Pr
(Intercept)	26.8086	5.6075	4.7808	0
vel	41.5138	18.3858	2.2579	0.024
em	-0.2625	0.0564	-4.658	0
vel:em	-0.4193	0.1834	-2.2859	0.0223

Table A.4: ***C. edule*, summary of the 0.975 quantile (upper boundary) model**

	Value	Std. Error	t value	Pr
(Intercept)	0.6862	4.4632	0.1537	0.8778
vel	862.6848	200.3753	4.3053	0
em	0.2352	0.0738	3.1853	0.0015
vel:em	-8.8116	1.9921	-4.4233	0

Table A.5: ***L. conchilega*, summary of the 0.975 quantile (upper boundary) model**

	Value	Std. Error	t value	Pr
(Intercept)	0	0.7372	0	1
vel	-15.1511	7.9585	-1.9038	0.057
em	0.3855	0.0511	7.5379	0
vel:em	-0.114	0.0789	-1.4448	0.1486

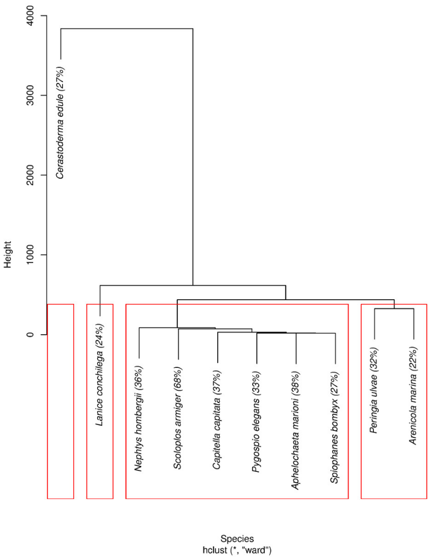

Figure A.1: **Cluster analysis** on biomass distributions (g AFDW m^{-2}) of the 10 most common species in the Oosterschelde between 1963 and 2010

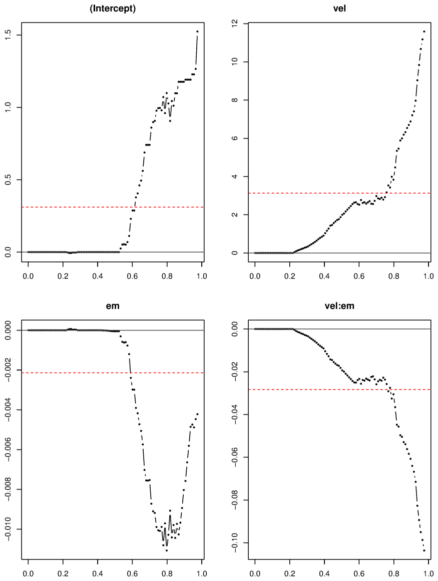

Figure A.2: **Variations of the coefficients with respect to modeled quantile for *S. armiger*.** vel = current velocity, em = emersion time

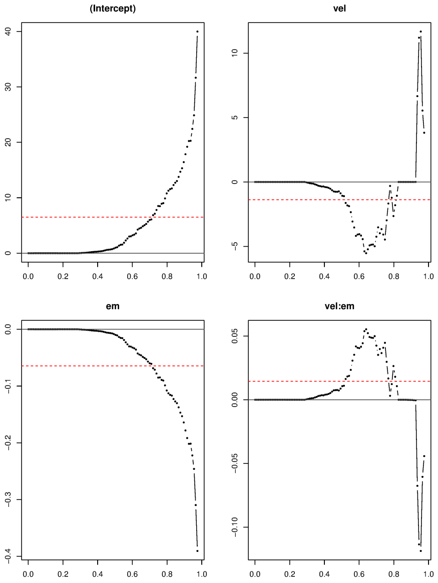

Figure A.3: **Variations of the coefficients with respect to modeled quantile for *P. ulvae*.** vel = current velocity, em = emersion time

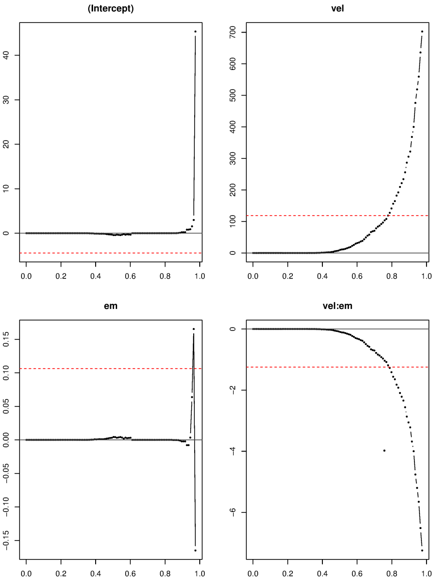

Figure A.4: **Variations of the coefficients with respect to modeled quantile for *C. edule*.** vel = current velocity, em = emersion time

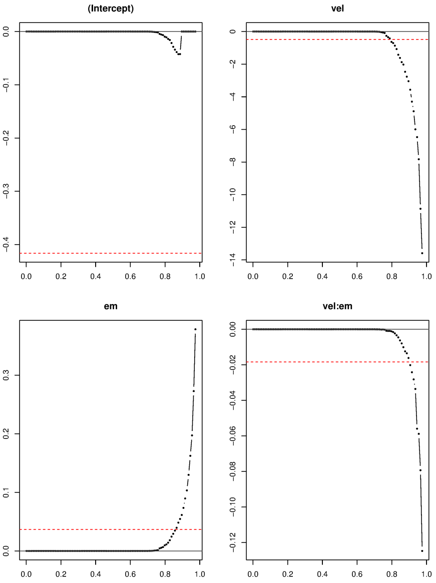

Figure A.5: **Variations of the coefficients with respect to modeled quantile for *L. conchilega*.** vel = current velocity, em = emersion time

Appendix B: Coastal defense *vs.* Enhanced navigability: how management affects benthic habitat quality.

Models validation

To validate our forecast for each of the modeled quantiles, the whole dataset was sampled with replacement. Due to sampling with replacement, some observations are repeated and others remain unpicked. The model was fitted on the sampled observation (training dataset) and used to predict the unpicked ones (validation dataset). The random sampling-fitting-predicting procedure was iterated 10000 times to obtain a large dataset of predicted (potential, 95^{th} quantile) and correspondent observed (realized) values. To make potential and realized values comparable each other, we discretized them in 20 homogeneous classes based on the predicted values. For each of the classes, the 95^{th} sample quantile of the observed data was calculated. To finally asses the validity of the model, observed and predicted quantiles were plotted against each other (for each class, empirical 95^{th} quantile of observed data vs. median point of the predicted values) and checked for linear correlation. All models show a great accuracy in reproducing the upper boundary of the observed data (Figure B.1).

Table B.1: **Summary of the analyzed benthic dataset.** For the Westerschelde only the present time scenarios can be used to extrapolate the abiotic condition for a larger number of benthic samples. For the Oosterschelde, several intermediate year-scenario were modeled, thus it was possible to include in the analysis a large number of observation collected in the past. The use of a large and long-term dataset allow to include the complete span of possible combinations between environmental conditions and biomasses/densities.

year	Oosterschelde		Westerschelde	
	Intertidal	Subtidal	Intertidal	Subtidal
1962	2	13	0	0
1963	19	23	30	0
1964	34	76	0	0
1965	0	0	10	0
1985	336	23	0	0
1988	1	0	0	0
1989	118	14	0	0
1992	48	176	0	0
1993	47	178	0	0
1994	43	173	0	0
2000	56	180	0	0
2001	56	181	0	0
2002	57	179	0	0
2006	59	168	0	0
2007	58	170	326	456
2008	155	179	319	385
2009	94	53	114	67
2010	95	47	99	77
2011	83	44	121	268

Table B.2: **Total biomass, summary of the 95th quantile regression model.** Standard errors were calculated by an inverted rank test. *vel= current velocity; salmean = average salinity, salrange= daily salinity range, em=inundation time*

	Value	Std. Error	t value	Pr
(Intercept)	-5.17	57.254	-0.09	0.928
vel	-802.039	204.602	-3.92	0
salmean	0.997	2.031	0.491	0.623
salrange	289.288	55.164	5.244	0
em	-1.758	0.712	-2.47	0.014
vel:salmean	36.311	8.379	4.333	0
vel:salrange	-20.353	20.525	-0.992	0.321
vel:em	9.444	2.005	4.71	0
salmean:salrange	-13.299	2.228	-5.968	0
salmean:em	0.096	0.026	3.617	0
salrange:em	-2.655	0.561	-4.734	0
vel:salmean:salrange	1.035	0.288	3.587	0
vel:salmean:em	-0.44	0.081	-5.426	0
vel:salrange:em	0.012	0.197	0.063	0.949
salmean:salrange:em	0.12	0.023	5.223	0

Table B.3: **Density of inidividuals, summary of the 95th quantile regression model.** Standard errors were calculated by an inverted rank test. *vel= current velocity; salmean = average salinity, salrange= daily salinity range, em=inundation time*

	Value	Std. Error	t value	Pr
(Intercept)	-11.032	13.48	-0.818	0.413
vel	55.075	42.362	1.3	0.194
salmean	0.598	0.534	1.119	0.263
salrange	20.121	10.195	1.974	0.048
em	-1.083	0.319	-3.394	0.001
vel:salmean	-3.092	1.736	-1.781	0.075
vel:salrange	-4.206	6.391	-0.658	0.51
vel:em	0.241	0.542	0.444	0.657
salmean:salrange	-1.157	0.499	-2.32	0.02
salmean:em	0.059	0.013	4.408	0
salrange:em	-0.044	0.106	-0.411	0.681
vel:salmean:salrange	0.661	0.224	2.956	0.003
vel:salmean:em	-0.01	0.022	-0.471	0.638
vel:salrange:em	-0.093	0.05	-1.85	0.064
salmean:salrange:em	0.004	0.006	0.736	0.462

Table B.4: **Per capita body mass, summary of the 95th quantile regression model.** Standard errors were calculated by an inverted rank test. *vel= current velocity; salmean = average salinity, salrange= daily salinity range, em=inundation time*

	Value	Std. Error	t value	Pr
(Intercept)	-11.03	15.93	-0.69	0.49
vel	55.07	39.92	1.38	0.17
salmean	0.6	0.63	0.95	0.34
salrange	20.12	10.32	1.95	0.05
em	-1.08	0.35	-3.11	0
vel:salmean	-3.09	1.56	-1.98	0.05
vel:salrange	-4.21	7.92	-0.53	0.6
vel:em	0.24	0.52	0.46	0.65
salmean:salrange	-1.16	0.49	-2.37	0.02
salmean:em	0.06	0.01	3.94	0
salrange:em	-0.04	0.11	-0.39	0.7
vel:salmean:salrange	0.66	0.24	2.81	0
vel:salmean:em	-0.01	0.02	-0.5	0.62
vel:salrange:em	-0.09	0.07	-1.38	0.17
salmean:salrange:em	0	0.01	0.72	0.47

Table B.5: **Shannon diversity, summary of the 95th quantile regression model.** Standard errors were calculated by an inverted rank test. *vel= current velocity; salmean = average salinity, salrange= daily salinity range, em=inundation time*

	Value	Std. Error	t value	Pr
(Intercept)	-0.518	1.186	-0.437	0.662
vel	4.365	2.52	1.732	0.083
salmean	0.074	0.041	1.822	0.068
salrange	0.072	0.298	0.242	0.809
em	0.024	0.015	1.624	0.104
vel:salmean	-0.157	0.087	-1.793	0.073
vel:salrange	-0.134	0.395	-0.339	0.735
vel:em	-0.058	0.026	-2.272	0.023
salmean:salrange	0.003	0.011	0.302	0.763
salmean:em	-0.001	0.001	-1.1	0.271
salrange:em	-0.001	0.004	-0.274	0.784
vel:salmean:salrange	-0.006	0.008	-0.751	0.452
vel:salmean:em	0.002	0.001	2.239	0.025
vel:salrange:em	0.003	0.003	0.91	0.363
salmean:salrange:em	0	0	-0.281	0.779

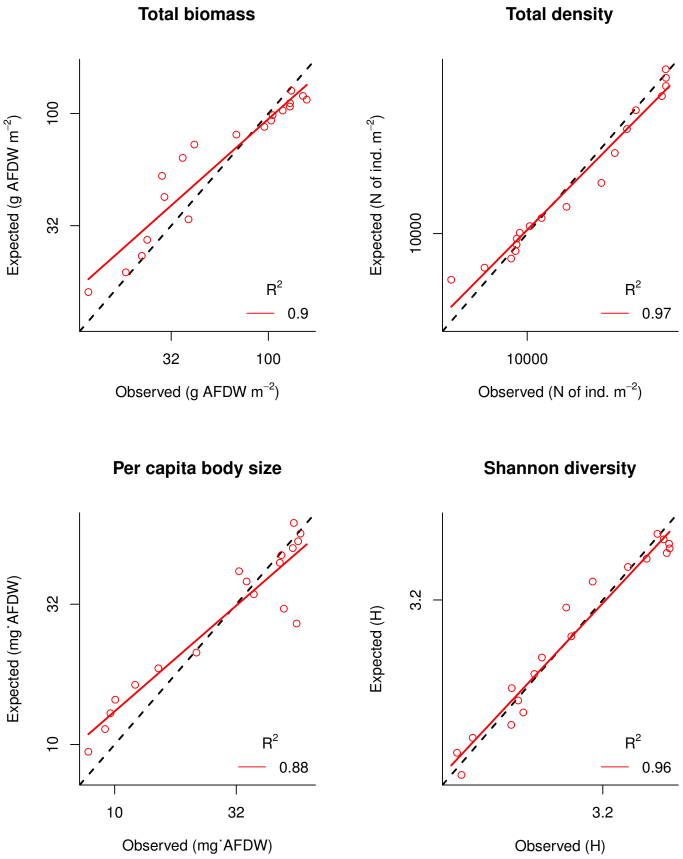

Figure B.1: **Validation, Observed vs Predicted values.** Red lines and R^2 coeffiecnts were obtained by linear regression. Dashed lines indicates the 1:1 ratio

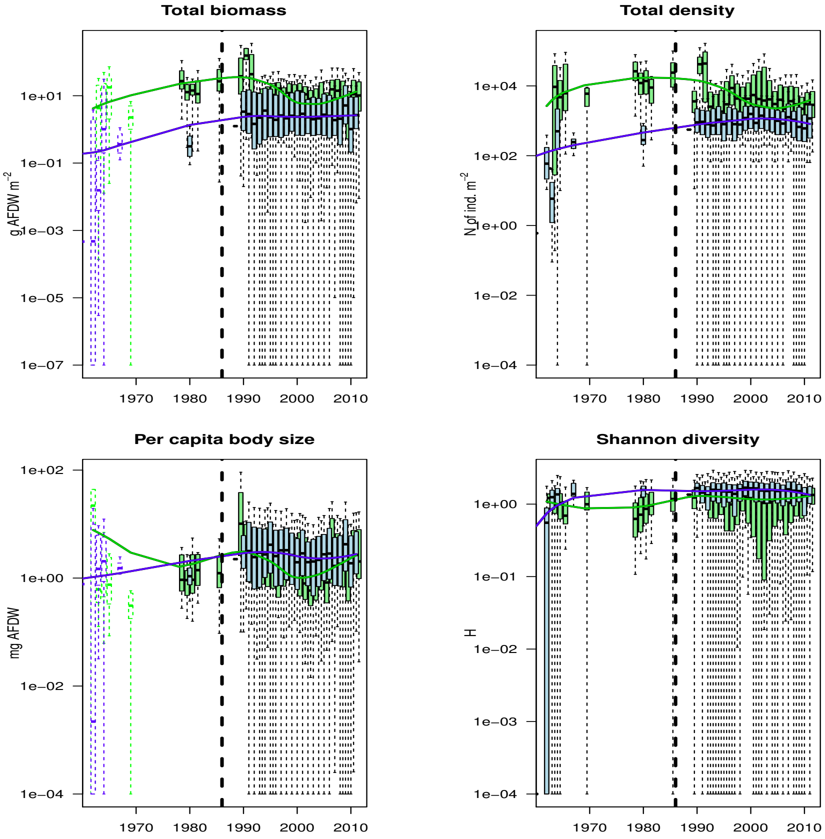

Figure B.2: **Oosterschelde, benthic observations**. The black vertical dashed line marked the finalization year of the Oosterscheldekering (1986). Before than 1975, only individuals density and taxonomical records were take. Average body size and total biomass values were obtained by multiplying the numerical density of each species for the average body size registered in later years (dahsed boxes). Coherently with our forecast, observed data show a decrease in intertidal habitat suitability and an increase in subtidal habitat suitability after the realization of the Oosterscheldekering. Not enough observation are available for plotting a similar time series for the Westerschelde (Table B.1)

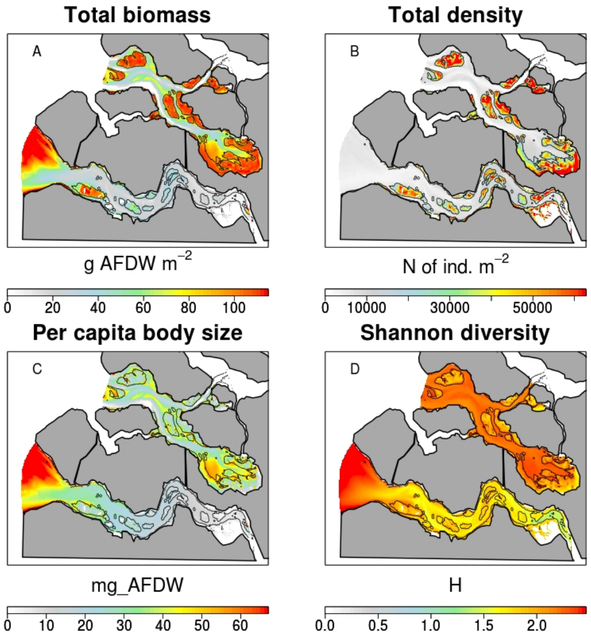
Total biomass
A
g AFDW m^{-2}
0
20
40
60
80
100
Total density
B
N of ind. m^{-2}
0
10000
30000
50000
Per capita body size
C
mg_AFDW
0
10
20
30
40
50
60
Shannon diversity
D
H
0.0
0.5
1.0
1.5
2.0

Figure B.3: **Potential community parameters distribution in 1960.**

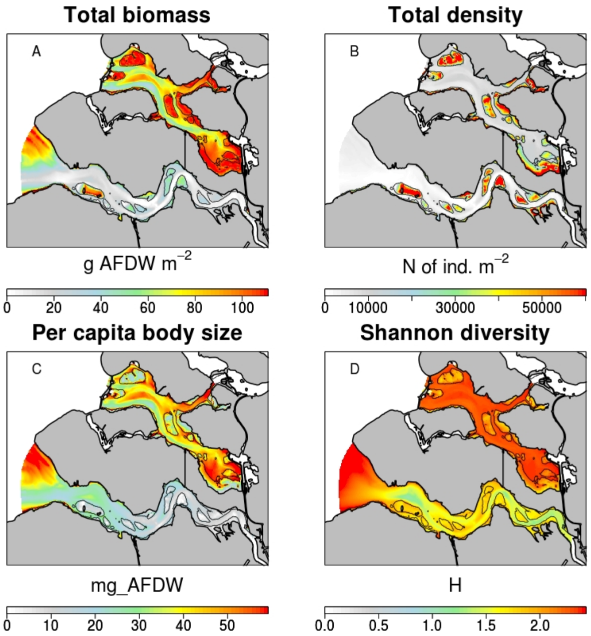
Total biomass
A
g AFDW m^{-2}
0
20
40
60
80
100
Total density
B
N of ind. m^{-2}
0
10000
30000
50000
Per capita body size
C
mg_AFDW
0
10
20
30
40
50
Shannon diversity
D
H
0.0
0.5
1.0
1.5
2.0

Figure B.4: **Potential community parameters distribution in 2010.**

Appendix C: Ecosystem Engineering, aiming to generalization

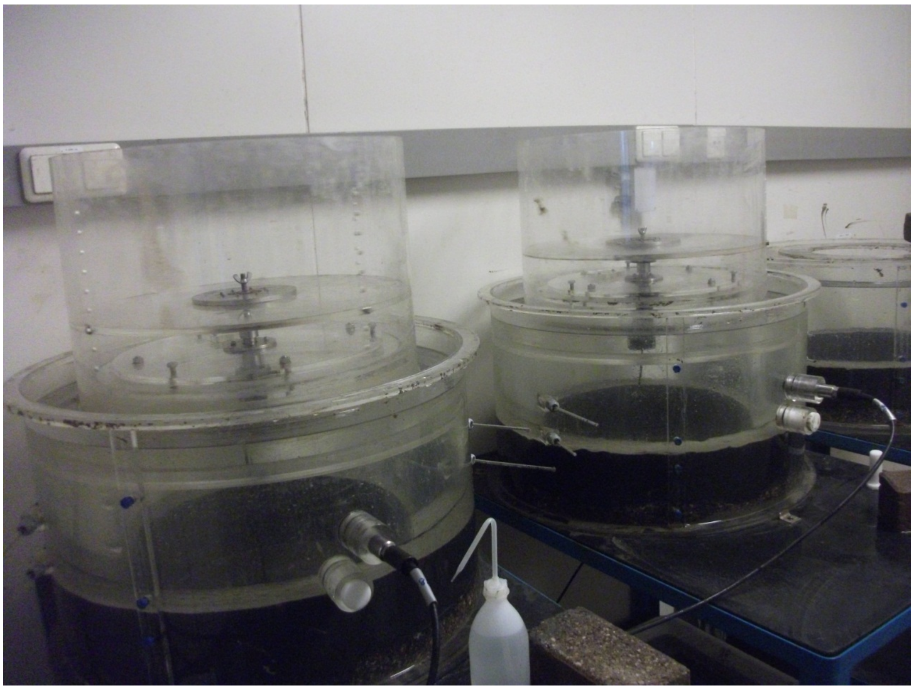

Figure C.1: **Experimental devices**. The annular flumes used are a variation of the design described by [Widdows et al., 1998]. For each experiment, we used standard, wet, fine-sand sediment (median grain size = 120 μm).

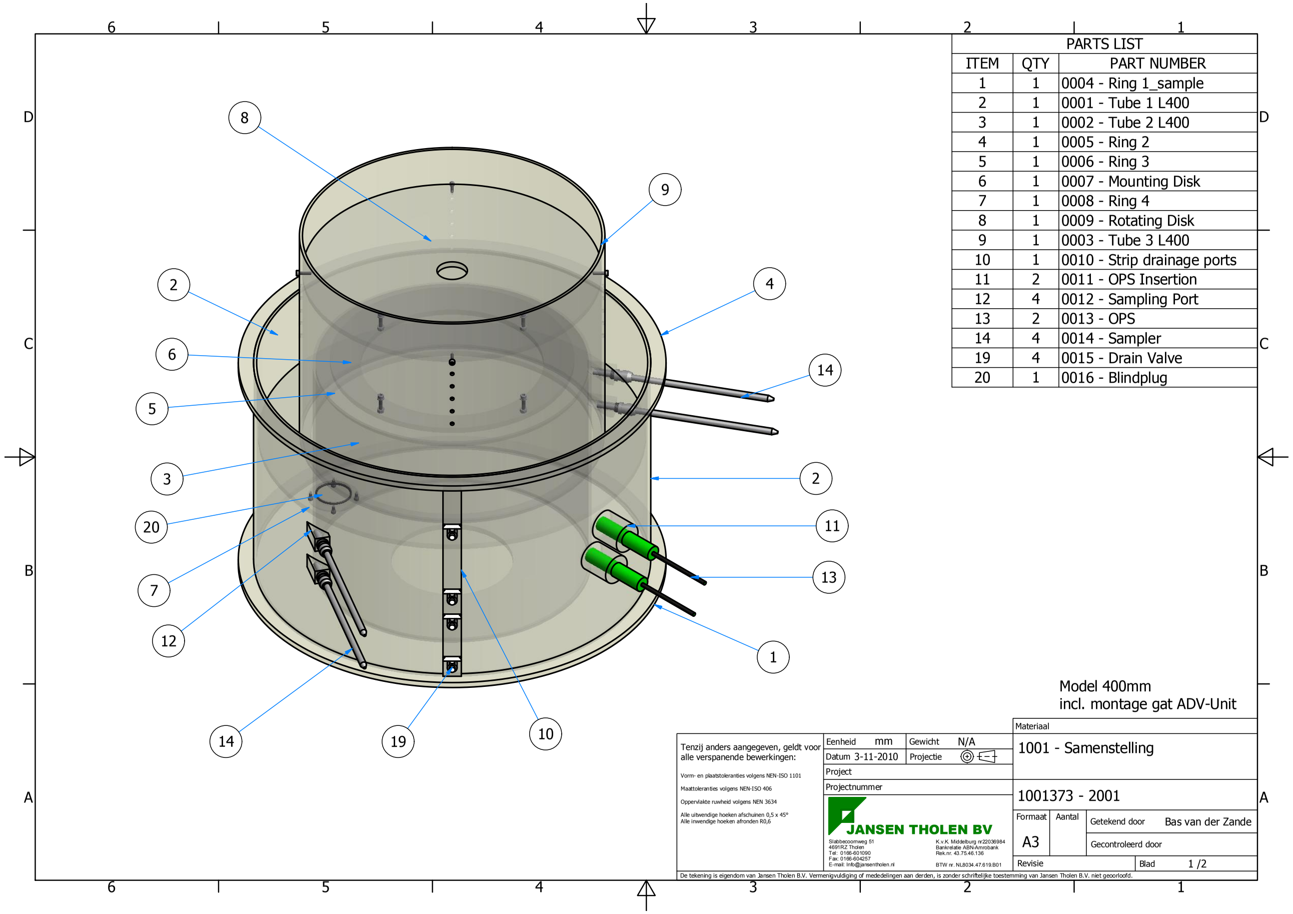

PARTS LIST

ITEM	QTY	PART NUMBER
1	1	0004 - Ring 1_sample
2	1	0001 - Tube 1 L400
3	1	0002 - Tube 2 L400
4	1	0005 - Ring 2
5	1	0006 - Ring 3
6	1	0007 - Mounting Disk
7	1	0008 - Ring 4
8	1	0009 - Rotating Disk
9	1	0003 - Tube 3 L400
10	1	0010 - Strip drainage ports
11	2	0011 - OPS Insertion
12	4	0012 - Sampling Port
13	2	0013 - OPS
14	4	0014 - Sampler
19	4	0015 - Drain Valve
20	1	0016 - Blindplug

6
5
4
3
2
1
D
C
B
A
8
9
2
4
6
14
5
3
2
20
11
7
13
12
1
14
19
10
Model 400mm
incl. montage gat ADV-Unit
Materiaal
Tenzij anders aangegeven, geldt voor alle verspanende bewerkingen:
Vorm- en plaatstoleranties volgens NEN-ISO 1101
Maattoleranties volgens NEN-ISO 406
Oppervlakte ruwheid volgens NEN 3634
Alle uitwendige hoeken afschuinen 0,5 x 45°
Alle inwendige hoeken afronden R0,6
Eenheid mm
Gewicht N/A
Datum 3-11-2010
Projectie
Project
Projectnummer
1001 - Samenstelling
1001373 - 2001
JANSEN THOLEN BV
Slabbecoornweg 51
4691RZ Tholen
Tel: 0166-601090
Fax: 0166-604257
E-mail: Info@jansentholen.nl
K.v.K. Middelburg nr22036984
Bankrelatie ABN-Amrobank
Rek.nr. 43.75.46.136
BTW nr. NL8034.47.619.B01
Formaat A3
Aantal
Getekend door Bas van der Zande
Gecontroleerd door
Revisie
Blad 1 /2
De tekening is eigendom van Jansen Tholen B.V. Vermenigvuldiging of mededelingen aan derden, is zonder schriftelijke toestemming van Jansen Tholen B.V. niet geoorloofd.

Figure C.2: Annular flumes, 40 cm height model

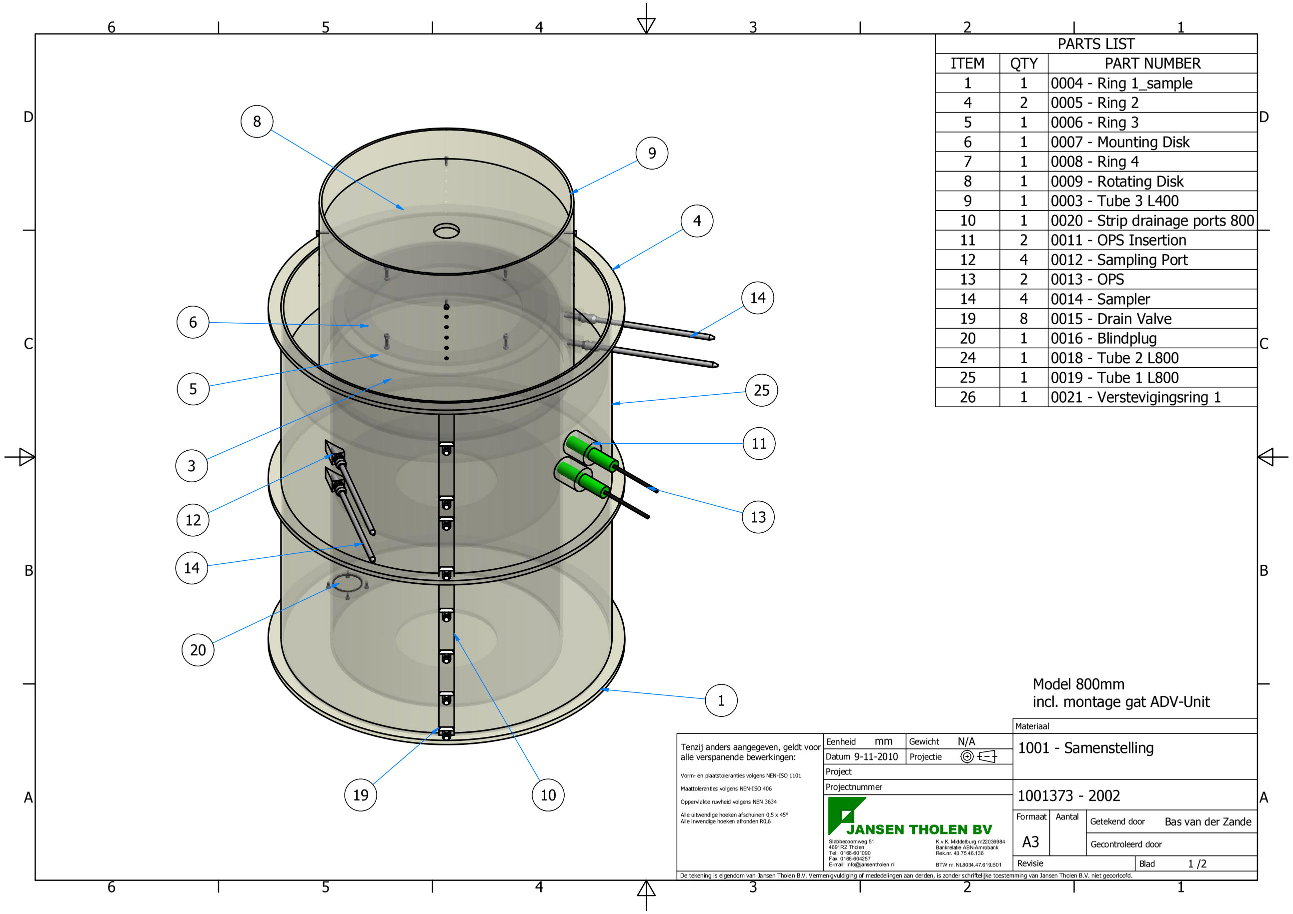

PARTS LIST		
ITEM	QTY	PART NUMBER
1	1	0004 - Ring 1_sample
4	2	0005 - Ring 2
5	1	0006 - Ring 3
6	1	0007 - Mounting Disk
7	1	0008 - Ring 4
8	1	0009 - Rotating Disk
9	1	0003 - Tube 3 L400
10	1	0020 - Strip drainage ports 800
11	2	0011 - OPS Insertion
12	4	0012 - Sampling Port
13	2	0013 - OPS
14	4	0014 - Sampler
19	8	0015 - Drain Valve
20	1	0016 - Blindplug
24	1	0018 - Tube 2 L800
25	1	0019 - Tube 1 L800
26	1	0021 - Verstevigingsring 1

Model 800mm
incl. montage gat ADV-Unit

Tenzij anders aangegeven, geldt voor alle verspanende bewerkingen:

Vorm- en plaatstoleranties volgens NEN-ISO 1101

Maattoleranties volgens NEN-ISO 406

Oppervlakte ruwheid volgens NEN 3634

Alle uitwendige hoeken afschuinen 0,5 x 45°
Alle inwendige hoeken afronden R0,6

Eenheid mm
Gewicht N/A
Datum 9-11-2010
Projectie
Project
Projectnummer

JANSEN THOLEN BV
Slabbecoornweg 51
4691RZ Tholen
Tel: 0166-601090
Fax: 0166-604257
E-mail: Info@jansentholen.nl

K.v.K. Middelburg nr22036984
Bankrelatie ABN-Amrobank
Rek.nr. 43.75.46.136
BTW nr. NL8034.47.619.B01

Materiaal
1001 - Samenstelling
1001373 - 2002
Formaat A3
Aantal
Getekend door Bas van der Zande
Gecontroleerd door
Revisie
Blad 1 /2

De tekening is eigendom van Jansen Tholen B.V. Vermenigvuldiging of mededelingen aan derden, is zonder schriftelijke toestemming van Jansen Tholen B.V. niet geoorloofd.

Figure C.3: Annular flumes, 80 cm height model

Summary

The feedback between abiotic and biotic elements has a strong importance in shaping the landscape. This is particularity true in sedimentary environments, where the physical processes involved in landscape formation (mainly sediment erosion, transport and deposition) act on energetic, temporal and spatial scales that are compatible with those of biological processes. While complex numerical models are available for simulating sediment transport on physical basis, biologic elements are still hard to predict. The macrozoobenthos potentially constitutes an hinge point between the morphological and the ecological state of the estuarine environments. On the one hand the distribution of the macrozoobenthos is dependent on physical constrains. On the other hand, benthic organisms ecosystem engineering of the sediment transport dynamics can modify the physical state of the habitat. Ecosystem engineers are often able to modify the same environmental conditions (niche axes) that are relevant for their fitness or for that of co-occurring species. By doing so, ecosystem engineers can induce changes in their population structure and abundance, that in turn are reflected in their potential to modify the environment.

During this PhD project we investigated both the sides of the sediment-biota feedback interaction. On one side we modelled the macrozoobenthic species spatial distribution in estuarine environments as function of those environmental variables that are relevant for sediment transport. On the other side, we measured in laboratory conditions the effect of several macrozoobenthic species on sediment erodability. Finally, we integrate these two points in a unitary framework able to forecast the potential effect of macrozoobenthos on sediment erosion in a realistic context: the Westerschelde and Oosterschelde basins (The Netherlands).

Presence of ecosystems engineers: species distribution models. We presented a methodology to obtain accurate forecast about macrozoobenthos abundances on the basis of physical models outputs (DELFT3D and TELEMAC). This methodology allows estimation of the potential impacts on benthic habitats of natural or anthropic (*i.e.* land reclamation, dredging, em-

banking) modifications of the estuarine morphology. It can be used in a predictive way if applied on simulated future (simulated) physical scenarios, or it can be used to reconstruct the evolution of the benthic ecosystem on the basis of historical data. We applied our methodology to the analysis of the Westerschelde and Oosterschelde basins, showing that an increase in hydrodynamic energy (like in the Westerschelde) can have a detrimental effect on benthic habitat suitability, while a decrease in hydrodynamic energy (like in the Oosterschelde) can have a positive effect, especially on subtidal habitats.

Effect of the ecosystem engineers: laboratory experiments. The effect of common bioturbators on sediment erosion was quantified at the variation of several biotic (individual body size, abundance, total biomass) and abiotic (current velocity) factors. We observed that, while some of these factors (abundance, interaction with hydrodynamic stress) act in species-specific way, different types of bioturbators showed the same scaling exponent for the relationships between ecosystem engineering effect (increase in sediment resuspension) and individual body size. The body size is one of the most characteristic traits of organisms, and generalization in ecology are often based on body size scaling of organisms' rates and activities. Thus, our observations can be easily framed in broader ecological theories (*e.g.* the Metabolic Theory of Ecology) and allow macro-ecological generalizations of the ecosystem engineering concept. Our models describe ecological processes but are based on physical parameters. They can be used to parametrize semi-empirical models of biotic-mediated sediment dynamics.

Integration. Once 'fueled' with semi-empirical descriptions of the ecological processes, numerical models of sediment dynamics can be used to upscale the quantification of the interactions between biota and sediment transport to a whole-estuary contest. The integration of ecological insights in sediment transport models present the advantage to provide simultaneous forecasts about the ecological and morphological evolution of sedimentary basins. The explicit inclusion of macrozoobenthic influences in sediment dynamics modelling allow to account for the biotic-induced deviations from purely physical expectations. Applied to the recent (last 50 years) evolution of the Westerschelde and Oosterschelde basins, our analysis show the negative correlation between current velocity and bioturbator biomass *de facto* led to an inverse relationship between bioturbator biomass and realized ecosystem engineering. While we specifically focus on ecosystem engineering, our approach can be virtually applied to describe any kind of ecological performances and activities related to organisms distribution.

Samenvatting

De terugkoppeling tussen abiotische en biotische elementen is belangrijk bij het vormgeven van het landschap. Dit is met name het geval in het sedimentaire milieu, waar de fysische processen welke een rol spelen in landschapsvorming (voornamelijk erosie, transport en afzetting van sediment) hun invloed doen gelden op energie-, tijds- en ruimteschalen welke compatibel zijn met die van biologische processen. Terwijl complexe numerieke modellen voorhanden zijn om sedimenttransport gebaseerd op fysische parameters te simuleren, is het nog altijd moeilijk de invloed van biologische elementen te voorspellen. Het macrozoöbenthos vormt potentieel een scharnierpunt tussen de morfologische en de ecologische toestand van estuariene milieus. Aan de ene kant is de ruimtelijke verdeling van het macrozoöbenthos afhankelijk van fysische randvoorwaarden. Aan de andere kant kunnen bodemdieren via *ecosysteem engineering* van de dynamiek van het sedimenttransport de fysische toestand van hun leefomgeving aanpassen. Vaak zijn *ecosystem engineers* in staat om dezelfde omgevingsomstandigheden (zogenaamde niche-assen) te veranderen ten behoeve van hun eigen fitness, of die van andere soorten die samen met hen voorkomen. Door dit te doen, kunnen zij zo veranderingen in hun populatiestructuur en -dichtheid bewerkstelligen, welke op hun beurt weer de *ecosysteem engineering*-activiteit beïnvloeden.

Tijdens deze promotiestudie zijn de beide zijden van de sediment-biota terugkoppelingsinteractie onderzocht. Enerzijds hebben we de ruimtelijke verdeling van het macro- zoöbenthos in estuariene omgevingen gemodelleerd als functie van juist die milieu-variabelen die relevant worden geacht voor sedimenttransport. Anderzijds zijn er onder laboratoriumomstandigheden accurate metingen gedaan aan de effecten van verschillende soorten macrozoöbenthos op de erodeerbaarheid van het sediment. Tenslotte integreren we deze twee punten in een unitair kader wat in staat is om het potentiële effect van macrozoöbenthos op sedimenterosie in een realistische context te voorspellen: de Westerschelde en Oosterschelde bekkens in zuid-west Nederland).

Aanwezigheid van *ecosystem engineers*: soortverspreidingsmodellen. In dit proefschrift presenteren we een methodologie om accurate voorspellingen over dichtheden van macrozoöbenthos op basis van fysische modeloutputs (DELFT3D en TELEMAC) te verkrijgen. Deze methode maakt het mogelijk een schatting te maken van de potentiële effecten op de zeebodem, als gevolg van natuurlijke of antropogene modificaties van de bodemmorfologie in estuariene milieus. De methode kan voorspellend worden gebruikt indien zij wordt toegepast op simulaties van eventueel toekomstige fysische scenarios, of ze kan worden gebruikt om de ontwikkeling van het bodemecosysteem te reconstrueren op basis van historische gegevens. Onze methodologie is toegepast voor de analyse van zowel het Westerschelde- als het Oosterschelde-bekken, waaruit blijkt dat een verhoging van hydrodynamische energie (zoals in de Westerschelde) nadelige gevolgen voor de benthische habitatgeschiktheid kan hebben, terwijl juist een afname in hydrodynamische energie (zoals in de Oosterschelde) een positief effect kan hebben, en dan met name in subtidale habitats.

Effecten van *ecosystem engineers*: laboratoriumexperimenten. Het effect van algemeen voorkomende bioturbatoren op sedimenterosie is gekwantificeerd aan de hand van de variatie van verschillende biotische (individuele lichaamsgrootte, dichtheid, totale biomassa) en abiotische (stroomsnelheid) factoren. We vonden dat, terwijl de invloed van sommige van deze factoren (overvloed, interactie met hydrodynamische stress) zeer soortsspecifiek zijn, de verschillende onderzochte bioturbatoren juist dezelfde schalingsfactor vertoonden voor de relatie tussen individuele lichaamsgrootte en het ecosysteem engineering effect, namelijk de toename van sediment-resuspensie.

Een van de meest karakteristieke eigenschappen van organismen is hun lichaamsgrootte en generalisaties over processnelheden en/of activiteiten in de ecologie zijn vaak gebaseerd op een schalingsfactor van lichaamsgrootte van organismen. Op deze manier kunnen onze observaties gemakkelijk in een kader worden geplaatst voor ecologische theorieën in bredere zin (zoals bijv.de Metabolische Theorie voor Ecologie) en staan deze macro-ecologische generalisaties van het concept *ecosystem engineering* toe. Onze observaties beschrijven typisch ecologische processen, maar zijn gebaseerd op puur fysische parameters, en kunnen zo worden gebruikt om semi-empirische modellen te parametriseren van sedimentdynamiek welke wordt gemoduleerd door de activiteit van benthische macrobiota.

Integratie. Eenmaal 'gevoed' met semi-empirische beschrijvingen van de ecologische processen, kunnen numerieke, sediment-dynamische modellen worden gebruikt om de kwantificering van de interacties tussen biota en sedimenttransport naar de context van een heel estuarium op te schalen. De integratie van ecologische inzichten in sedimenttransport-modellen bieden het dubbele voordeel van gelijktijdige prognoses over de ecologische en morfologische evolutie van sedimentaire bekkens. Op deze wijze kan expliciet het effect van macrozoöbenthos op de sedimentdynamiek worden beschouwd, waarmee biotisch-geïnduceerde afwijkingen kunnen worden bepaald op basis van puur fysische model-verwachtingen. Toegepast op de recente (laatste 50 jaar) evolutie van de beide Westerschelde- en Oosterschelde-bekkens, toont onze analyse aan dat de negatieve correlatie tussen stroomsnelheid en bioturbator-biomassa *de facto* heeft geleid tot een omgekeerde relatie tussen bioturbator-biomassa en de uiteindelijk gerealiseerde *ecosysteem engineering*. Terwijl we specifiek richten op ecosysteem engineering, kan onze aanpak praktisch worden toegepast op elke vorm van ecologische prestaties en activiteiten met betrekking tot de distributie organismen beschrijven.

Sommario

L'interazione reciproca tra elementi biotici ed abiotici può avere un ruolo significativo nella formazione del paesaggio. Questo ruolo è particolarmente rilevante negli ambienti sedimentari, dove i processi fisici coinvolti nella formazione del paesaggio (principalmente erosione, trasporto e deposizione del sedimento) agiscono su scale energetiche, spaziali e temporali che sono compatibili con quelle dei processi biologici. Mentre è attualmente possibile simulare con buona approssimazione le dinamiche sedimentarie su base fisica, l'influenza degli elementi biologici è ancora difficili da predirre. Il macrozoobenthos costituisce un punto cardine tra lo stato ecologico e lo stato morfologico dell'ambiente estuarino. Da un lato la distribuzione del macrozoobenthos dipende da costrizioni fisiche. Dall'altro lato, l'alterazione delle dinamiche di trasporto del sedimento da parte degli ecosystem engineers bentonici può modificare lo stato fisico degli habitats. Spesso gli *ecosystem engineers* sono in grado di modificare le condizioni ambientali rilevanti per la loro fitness e per quella delle organismi che ne condividono l'habitat.

In questa tesi di dottorato sono stati investigati entrambi i lati della reciproca interazione tra sedimento e biota. Da un lato la distribuzione delle specie bentoniche è stata modellata sulla base delle variabili fisiche coinvolte nel trasporto del sedimento. Dall'altro lato, l'effetto di differenti specie benthoniche sull' erodibilità del sedimento è stato misurato sperimentalmente. Infine, i due punti sono stati integrati per modellare l'effetto potenziale del macrozoobenthos sull' erosione del sedimento in un contesto realistico: i bacini del Westerschelde e Oosterschelde (Paesi Bassi).

Presenza degli *ecosystem engineers*: modelli di distribuzione delle specie. In questa tesi è stat presentata una metodologia per predire accuratamente l'abbondanza delle specie macrozoobenthiche sulla base di modelli fisici (DELFT3D e TELEMAC). Questa metodologia permette di stimare il potenziale impatto di cambiamenti, naturali o antropiche, della morfologia estuarina. Può essere usata in maniera predittive se applicata a scenari fisici futuri (simulati) o puó essere applicata per ricostruire l'evoluzione dell'ecosistema ben-

tonico sulla base di dati storici. Applicando questa metodologia ai bacini del Westerschelde e Oosterschelde, abbiamo mostrato che un incremento in energia idrodinamica nel sistema può avere effeti negativi sulla qualitá degli habitats benthonici, mentre un decremento in energia idrodinamica (come nell'Oosterschelde) può avere effetti positivi, specialmente sugli habitat permanentemente sommersi.

Effetto degli *ecosystem engineers*: parametrizzazione empirica di modelli allometrici. L'effetto di alcune comuni specie di bioturbatori sull'erosione del sedimento è stato quantificato al variare di diversi parametri biologici (specie, comportamento, mole individuale, abbondanza) e fisici (velocità di corrente.). Abbiamo osservato che, mentre alcuni fattori (abbondanza, interazione con lo stress idrodinamico) agiscono in maniera specie-specifica, differenti tipologie di bioturbatori presentano un comune esponente di scala nella relazione tra il loro effetto ingegneristico (incremento della sospensione di sedimento) e loro mole individuale. La mole corporea è uno dei tratti più caratteristici degli organismi, al punto che differenti teorie macro-ecologiche sono basate sui tassi di scala delle attivitá individuali con la mole corporea. Di conseguenza, le nostre osservazioni possono essere facilmente interpretate nell'abito di teorie ecologiche piu vaste (*i.e.* The Metabolic Theory of Ecology) e permettono di generalizzare il concetto di *ecosystem engineering* su scala macroecologica. Le nostre osservazioni descrivono un processo ecologico ma sono basate su parametri fisici. Possono essere quindi utilizzate per parametrizzare modelli semi-empirici delle dinamiche sedimentarie sotto l'influenza di componenti biologiche.

Integrazione. Una volta che sono stati forniti di descrizione semi-empiriche dei processi ecologici, i modelli fisici delle dinamiche sedimentarie possono essere usati per estrapolare la quantificazione delle interazioni tra trasporto del sedimento e biota ad un contesto a larga scala (l'intero estuario). L'integrazione di conoscienze ecologiche nei modelli di trasporto del sedimento presenta il doppio vantaggio di 1) fornire previsioni simultanee sull'evouzione ecologica e morfologica dei bacini sedimentari e 2) includere esplicitamente l'effetto del macrozoobenthos sulle dinamiche sedimentarie. Applicata alla evoluzione recente (ultimi 50 anni) del Westerschelde e Oosterschelde, la nostra analisi mostra che la correlazione inversa tra velocità di corrente e biomassa dei bioturbatori di fatto porta ad una inversione della relazione (di per se positiva) tra biomassa dei bioturbaturbatori e effetto realizzato sull'erosione del sedimento. Mentre la nostra analisi e specificatamente orientata su processi di *ecosystem engineering*, l'approccio da noi sviluppato è virtualmente applicabile all quantificazione di ogni tipo di attività e prestazioni ecologiche legate alla distribuzione degli organismi.

Curriculum vitae

Francesco Cozzoli was born the 9^{th} of September 1985 in the coastal city of Brindisi, south of Italy. For some strange reason, he did not inherited the family talent for basketball. He was rather intersted in observing the nature around him. Following this passion, he chose scientifical studies and graduated at 'Liceo Scentifico E. Fermi' in 2004. The same year he started to study biology at University of Salento (Italy), where he specialized in ecology and he deepened its knowledge on coastal ecosystems and, mostly, on the energetic mechanisms underlying the biological organization (still his favorite research topic). Between 2009 and 2013, he carried out his PhD research that focused on feedback interactions between sediment dynamics and benthic biota, at the departments of Spatial Ecology at NIOZ Yerseke (The Netherlands). During this period he gained experience in statistical and spatial modeling and he performed many laboratory and field experiments on biotic-mediated sediment dynamics. His work was published in peer-reviewed international journals and presented at international conferences. At present, he is working on optimization of marine monitoring strategies (within the Marine Framework Strategy Directive context) as a post-doctoral researcher at the University of Salento. He remains actively involved in research on ecosystem management, ecosystem engineering, metabolic ecology and community organization.

Publications

- Basset, A., Cozzoli, F. and Paparella, F. (2012). A unifying approach to allometric scaling of resource ingestion rates under limiting conditions. ECOSPHERE 3 (1).

- Cozzoli, F., Bouma, T. J., Ysebaert, T. & Herman, P. M. J. (2013). Application of non-linear quantile regression to macrozoobenthic species distribution modelling: comparing two contrasting basins. MARINE ECOLOGY PROGRESS SERIES, 475, 119+.

- de Lucas Pardo, M. A., Bakker, M., van Kessel, T., Cozzoli, F. & Winterwerp, J. C. (2013). Erodibility of soft freshwater sediments in Markermeer: the role of bioturbation by meiobenthic fauna. OCEAN DYNAMICS, 63, 1137-1150.

- Cozzoli, F., Eelkema, M., Bouma, T. J., Ysebaert, T., Escaravage, V. & Herman, P. M. J. (2014). A mixed modeling approach to predict the effect of environmental modification on species distributions. PLOS ONE, 9.

- Zhu, Z., Cozzoli, F., Chu, N., Salvador Lluch, M., Ysebaert, T., Zhang, L., Herman, P. M. J. & Bouma, T. (2015). Interactive effects between physical forces and ecosystem engineering on seed burial in tidal flats. OIKOS

In preparation

- Cozzoli, F., Ottolander, P., Salvador Lluch, M., Bouma, T. J., Ysebaert, T. & Herman, P. M. J. General rules in bioturbation.

- Cozzoli, F., Smolders, S., Eelkema, M., Bouma, T., Ysebaert, T., Escaravage, V., Temmerman, S., Meire, P. & Herman, P. M. J. Coastal defense vs. Enhanced navigability: how management affects benthic habitat quality.

- Cozzoli, F., Ottolander, P., Salvador Lluch, M., Smolders, S., Eelkema, M., Bouma, T. J., Ysebaert, T., Escaravage, V., Temmerman, S., Meire, P. & Herman, P. M. J. Ecosystem engineering, extrapolation to a relistic context.

- Smolders, S., Cozzoli, F., Plancke, Y., Ysebaert, T., Ides, T., Bouma, T., Meire, P.,Herman, P. M. J. & Temmerman, S. Modelling benthic habitat suitability to evaluate ecological benefits of a new sediment disposal strategy in shallow tidal waters.

Acknowledgments

I would like to express my sincere gratitude to my promoter and co-promoters Prof. Dr. P.M.J. Herman, Prof. Dr. T.J. Bouma and Dr. T. Ysebaert, for the continuous support of my Ph.D study, for their patience, motivation, and immense knowledge. Their guidance helped me in all the time of research and writing of this thesis.

A very precious contribution for the realization of this work came from my students Paoline Ottolander, Maria Salvador Lluch and Nilmawati.

I would like to thank Miguel de Lucas Pardo, Sven Smolders, Vincent Escaravege, Stijin Temmerman, Menno Eelkema, Francesc Montserrat, Diana Vasquez, Lucy Gillis, Henk Bolhuis, Helene de Paoli, Daphne van der Wal, Jim van Belzen, Zhigang Ma, Loreta Cornacchia, Luciana Lippo, Olivier Beauchard, Dorina Seitaj, Sil Nieuwhof, Christian Schwarz, Samuele Tecchio, Fabio Bozzeda, Vanessa Gonzalez Ortiz, Serena Donadi, Zhan Hu, Wouter Suykerbuyk, Michele Grego, Silvia Hidalgo Martinez, Filip Meysman, Hui Cheng, Kris Giesen, Vincent Saderne, Laura Govers, Thorsten Balke, Nicolette Volp, Simeon Moons, Tadao Kunihiro, Marjolijn Christianen, Siti Yaakub, Greg Silsbe, Sairah Malkin, Cecile Cathalot, Maarteen de Jong, Bregje Van Wesenbeeck, Kelly Elschot, Stefanie Nolte, Martin Ubertini, Andrea D'Alpaos, Marco Sigovini, Carl Van Colen, Clive Jones, Bram van Prooijen, Francis Orvain, Zhenchang Zhu, Johan van den Koppel and Brenda Walles for all the insightful comments and the stimulating discussion we had.

My sincere thanks also goes to the members of NIOZ - Yerseke technical staff, and in particular to Bas Koutstaal, Jos van Soelen, Lowie Haazen, Bert Sinke, Lennart van Ijzerloo and Jeron van Dalen. Without they precious support and their teachings it would not be possible to conduct this research. I must also thank Jan Megens for the amazing way in which he takes care of everything.

Thank to the people that I met during my staying in The Netherlands, they were the most important thing I discover. Among them, I cannot avoid to mentionate Lucy, Michele and Silvia, I really don't know how I would have done without them.

Thank very much to my hard-core bunch of fellows from school and university, that make happier any moment of my life. In particular, thank to Fabrizio for realizing the cover of this thesis.

I would also like to extend my deepest gratitude to my aunts, uncles, cousins, brother, mom and dad. Without their love, example and encouragement, I would never be able to face this challenge.

Bibliography

Adger, W. N., T. P. Hughes, C. Folke, S. R. Carpenter, and J. Rockstrom. 2005. Social-ecological resilience to coastal disasters. *SCIENCE* 309:1036–1039.

Akaike, Hirotugu. 1980. Likelihood and the Bayes procedure. In *BAYESIAN STATISTICS*, ed. J.M Bernardo, 143–166. Valencia University Press.

Akoumianaki, I., and A. Nicolaidou. 2007. Spatial variability and dynamics of macrobenthos in a Mediterranean delta front area: the role of physical processes. *JOURNAL OF SEA RESEARCH* 57:47–64.

Allen, J. R. 1985. Field measurement of longshore sediment transport sandy hook, New Jersey, USA. *JOURNAL OF COASTAL RESEARCH* 1:231–240.

Anderson, Marti J. 2008. Animal-sediment relationships re-visited: Characterising species' distributions along an environmental gradient using canonical analysis and quantile regression splines. *JOURNAL OF EXPERIMENTAL MARINE BIOLOGY AND ECOLOGY* 366:16–27.

Araujo, Miguel B., and Antoine Guisan. 2006. Five (or so) challenges for species distribution modelling. *JOURNAL OF BIOGEOGRAPHY* 33:1677–1688. Workshop on Generalized Regression Analyses and Spatial Predictions, Riederalp, SWITZERLAND, AUG, 2004.

Attrill, M. J. 2002. A testable linear model for diversity trends in estuaries. *JOURNAL OF ANIMAL ECOLOGY* 71:262–269.

Austin, M. P. 2007. Species distribution models and ecological theory: A critical assessment and some possible new approaches. *ECOLOGICAL MODELLING* 200:1–19.

Baeyens, W., B. van Eck, C. Lambert, R. Wollast, and L. Goeyens. 1998. General description of the Scheldt estuary. *HYDROBIOLOGIA* 34:83–107.

Barbier, Edward B., Sally D. Hacker, Chris Kennedy, Evamaria W. Koch, Adrian C. Stier, and Brian R. Silliman. 2011. The value of estuarine and coastal ecosystem services. *ECOLOGICAL MONOGRAPHS* 81:169–193.

Barsky, B. A., and S. W. Thomas. 1981. Transpline - a system for representing curves using transformations among 4 spline formulations. *THE COMPUTER JOURNAL* 24:271–277.

Basset, A., F. Sangiorgio, and M. Pinna. 2004. Monitoring with benthic macroinvertebrates: advantages and disadvantages of body size descriptors. *AQUATIC CONSERVATION-MARINE AND FRESHWATER ECOSYSTEMS* 14:S43–S58.

Beauchard, Olivier, Sander Jacobs, Tom Ysebaert, and Patrick Meire. 2013a. Avian response to tidal freshwater habitat creation by controlled reduced tide system. *ESTUARINE COASTAL AND SHELF SCIENCE* 131:12–23.

Beauchard, Olivier, Sander Jacobs, Tom Ysebaert, and Patrick Meire. 2013b. Sediment macroinvertebrate community functioning in impacted and newly-created tidal freshwater habitats. *ESTUARINE COASTAL AND SHELF SCIENCE* 120:21–32.

Beukema, J. J., K. Essink, and R. Dekker. 2000. Long-term observations on the dynamics of three species of polychaetes living on tidal flats of the Wadden Sea: the role of weather and predator-prey interactions. *JOURNAL OF ANIMAL ECOLOGY* 69:31–44.

Bijker, W. E. 2002. The Oosterschelde storm surge barrier - A test case for Dutch water technology, management, and politics. *TECHNOLOGY AND CULTURE* 43:569–584.

Blackburn, T. M., V. K. Brown, B. M. Doube, J. J. D. Greenwood, J. H. Lawton, and N. E. Stork. 1993. The relationship between abundance and body-size in natural animal assembalges. *JOURNAL OF ANIMAL ECOLOGY* 62:519–528.

Blackburn, T. M., J. H. Lawton, and N. J. Perry. 1992. A method of estimating the slope of upper-bounds of plots of body size and abundance in natural animal assemblages. *OIKOS* 65:107–112.

Bolam, S.G., and P. Whomersley. 2005. Development of macrofaunal communities on dredged material used for mudflat enhancement: a comparison of three beneficial use schemes after one year. *MARINE POLLUTION BULLETIN* 50:40–47.

Borja, A., J. Franco, and V. Pérez. 2000. A marine Biotic Index to establish the ecological quality of soft-bottom benthos within european estuarine and coastal environments. *MARINE POLLUTION BULLETIN* 40:1110–1114.

Borja, Angel, Enrico Barbone, Alberto Basset, Gunhild Borgersen, Marijana Brkljacic, Michael Elliott, Joxe Mikel Garmendia, Joao Carlos Marques, Krysia Mazik, Inigo Muxika, Joao Magalhaes Neto, Karl Norling, J. German Rodriguez, Ilaria Rosati, Brage Rygg, Heliana Teixeira, and Antoaneta Trayanova. 2011. Response of single benthic metrics and multi-metric methods to anthropogenic pressure gradients, in five distinct European coastal and transitional ecosystems. *MARINE POLLUTION BULLETIN* 62:499–513.

Borsje, B. W., M. B. de Vries, S. J. M. H. Hulscher, and G. J. de Boer. 2008. Modeling large-scale cohesive sediment transport affected by small-scale biological activity. *ESTUARINE COASTAL AND SHELF SCIENCE* 78:468–480.

Bouma, T. J., M. B. De Vries, E. Low, G. Peralta, C. Tanczos, J. Van de Koppel, and P. M. J. Herman. 2005. Trade-offs related to ecosystem engineering: A case study on stiffness of emerging macrophytes. *ECOLOGY* 86:2187–2199.

Brown, J. H., J. F. Gillooly, A. P. Allen, V. M. Savage, and G. B. West. 2004. Toward a metabolic theory of ecology. *ECOLOGY* 85:1771–1789.

Brown, J.H. 1995. MACROECOLOGY. The University of Chicago Press.

Bruno, J.F. 2000. Facilitation of cobble beach plant communities through habitat modification by *Spartina alterniflora*. *ECOLOGY* 81:1179–1192.

Bruno, J.F., J.J. Stachowicz, and M.D. Bertness. 2003. Inclusion of facilitation into ecological theory. *TRENDS IN ECOLOGY & EVOLUTION* 18:119–125.

Bruschetti, Martin, Cielo Bazterrica, Eugenia Fanjul, Tomas Luppi, and Oscar Iribarne. 2011. Effect of biodeposition of an invasive polychaete on organic matter content and productivity of the sediment in a coastal lagoon. *JOURNAL OF SEA RESEARCH* 66:20–28.

Bulleri, Fabio, and Maura G. Chapman. 2010. The introduction of coastal infrastructure as a driver of change in marine environments. *JOURNAL OF APPLIED ECOLOGY* 47:26–35.

Butman, C. A. 1987. Larval settlement of soft-sediment invertebrates - the spatial scale of pattern explained by active habitat selection and the emerging role of hydrodynamical processes. *OCEANOGRAPHY AND MARINE BIOLOGY* 25:113–165.

Cade, B. S., J. W. Terrell, and R. L. Schroeder. 1999. Estimating effects of limiting factors with regression quantiles. *ECOLOGY* 80:311–323.

Cade, B.S., and B.R. Noon. 2003. A gentle introduction to quantile regression for ecologists. *FRONTIERS IN ECOLOGY AND THE ENVIRONMENT* 1:412–420.

Cade, B.S., B.R. Noon, and C.H. Flather. 2005. Quantile regression reveals hidden bias and uncertainty in habitat models. *ECOLOGY* 86:786–800.

Cammen, L. M. 1980. Ingestion rate - empirical model for acquatic deposit feedrs and detritivores. *OECOLOGIA* 44:303–310.

Carey, D. A. 1987. Sedimentological effects and palaeoecological implications of the tube-building polychaete *lanice conchilega* (pallas). *SEDIMENTOLOGY* 34:46–66.

Carlson, J. K., T. A. Randall, , and M. E. Mroczka. 1997. Feeding habits of winter ounder (pleuoronectes americanus) in a habitat exposed to anthropogenic disturbance. *JOURNAL OF NORTHWEST ATLANTIC FISHERY SOCIETY* 21:65 – 73.

Chan, K. M. A., M. R. Shaw, R. D. Cameron, E. C. Underwood, and G. C. Daily. 2006. Conservation planning for ecosystem services. *PLOS BIOLOGY* 4:2138–2152.

Chapman, M. G., T. J. Tolhurst, R. J. Murphy, and A. J. Underwood. 2010. Complex and inconsistent patterns of variation in benthos, micro-algae and sediment over multiple spatial scales. *MARINE ECOLOGY PROGRESS SERIES* 398:33–47.

Christensen, P. B., S. Rysgaard, N. P. Sloth, T. Dalsgaard, and S. Schwaerter. 2000. Sediment mineralization, nutrient fluxes, denitrification and dissimilatory nitrate reduction to ammonium in an estuarine fjord with sea cage trout farms. *AQUATIC MICROBIAL ECOLOGY* 21:73–84.

Ciutat, Aurelie, John Widdows, and Nick D. Pope. 2007. Effectof *Cerastoderma edule* density on near-bed hydrodynamics and stability of cohesive muddy sediment. *JOURNAL OF EXPERIMENTAL MARINE BIOLOGY AND ECOLOGY* 346:114–126.

Coosen, J., F. Twisk, M.W.M van der Tol, R.H.D Lambeck, M.R van Stralen, and P.M Meire. 1994. Variability in stock assessment of cockles (*Cerastoderma edule*, L.) in the Oosterschelde (in 1980-1990), in relation to environmental factors. *HYDROBIOLOGIA* 283:381–395.

Costanza, R., R d'Arge, R de Groot, S. Farber, M. Grasso, B. Hannon, K. Limburg, S. Naeem, R. V. O'Neill, J. Paruelo, R. G. Raskin, P. Sutton, and M. van den Belt. 1997. The value of the world's ecosystem services and natural capital. *NATURE* 387:253–260.

Cozzoli, F., T. J. Bouma, T. Ysebaert, and P. M. J. Herman. 2013. Application of non-linear quantile regression to macrozoobenthic species distribution modelling: comparing two contrasting basins. *MARINE ECOLOGY PROGRESS SERIES* 475:119+.

Cozzoli, F., M. Eelkema, T. J. Bouma, T. Ysebaert, V. Escaravage, and P. M. J. Herman. 2014. A mixed modeling approach to predict the effect of environmental modification on species distributions. *PLOS ONE* 9.

Cozzoli, F., P. Ottolander, M. Salvador Lluch, T. J. Bouma, T. Ysebaert, and P. M. J. Herman. 2015a. Ecosystem engineering, aiming to generalization. *In preparation, this thesis* .

Cozzoli, F., P. Ottolander, M. Salvador Lluch, S. Smolders, M. Eelkema, T. J. Bouma, T. Ysebaert, V. Escaravage, S. Temmerman, P. Meire, and P. M. J. Herman. 2015b. Ecosystem engineering, extrapolation to a relistic context. *In preparation, this thesis* .

Cozzoli, F., S. Smolders, M. Eelkema, T.J. Bouma, T. Ysebaert, V. Escaravage, S. Temmerman, P. Meire, and P. M. J. Herman. 2015c. Coastal defense *vs.* Enhanced navigability: how management affects benthic habitat quality. *In preparation, this thesis* .

Crooks, J. A. 2002. Characterizing ecosystem-level consequences of biological invasions: the role of ecosystem engineers. *OIKOS* 97:153–166.

Cross, Wyatt. F., A. Ramirez, A. Santana, and L. Silvestrini Santiago. 2008. Toward quantifying the relative importance of invertebrate consumption and bioturbation in Puerto Rican streams. *BIOTROPICA* 40:477–484.

Crutzen, P.J. 2002. The "anthropocene". *JOURNAL DE PHYSIQUE IV* 12:1–5. European Research Course on Atmospheres, GRENOBLE, FRANCE, 2002.

Cuddington, K., W. G. Wilson, and A. Hastings. 2009. Ecosystem engineers: Feedback and population dynamics. *AMERICAN NATURALIST* 173:488–498.

Curry, K. J., R. H. Bennett, L. M. Mayer, A. Curry, M. Abril, P. M. Biesiot, and M. H. Hulbert. 2007. Direct visualization of clay microfabric signatures driving organic matter preservation in fine-grained sediment. *GEOCHIMICA ET COSMOCHIMICA ACTA* 71:1709–1720.

Damuth, J. 1981. Population density and body size in mammals. *NATURE* 290:699–700.

Dangerfield, J. M., T. S. McCarthy, and W. N. Ellery. 1998. The mound-building termite *Macrotermes michaelseni* as an ecosystem engineer. *JOURNAL OF TROPICAL ECOLOGY* 14:507–520.

Danielsen, F., M. K. Sorensen, M. F. Olwig, V. Selvam, F. Parish, N. D. Burgess, T. Hiraishi, V. M. Karunagaran, M. S. Rasmussen, L. B. Hansen, A. Quarto, and N. Suryadiputra. 2005. The Asian tsunami: A protective role for coastal vegetation. *SCIENCE* 310:643.

Dashtgard, Shahin E., Murray K. Gingras, and S. George Pemberton. 2008. Grain-size controls on the occurrence of bioturbation. *PALAEOGEOGRAPHY PALAEOCLIMATOLOGY PALAEOECOLOGY* 257:224–243.

Day, J. W., C. A. S. Hall, W. M. Kemp, and A. Yanez-Arancibia. 1989. *ESTUARINE ECOLOGY*. Wiley, New York.

de la Huz, R., M. Lastra, and J. Lopez. 2002. The influence of sediment grain size on burrowing, growth and metabolism of *Donax trunculus* L. (Bivalvia: Donacidae). *JOURNAL OF SEA RESEARCH* 47.

de Lucas Pardo, Miguel Angel, Marieke Bakker, Thijs van Kessel, Francesco Cozzoli, and Johan Christian Winterwerp. 2013. Erodibility of soft freshwater sediments in Markermeer: the role of bioturbation by meiobenthic fauna. *OCEAN DYNAMICS* 63:1137–1150.

De Roos, A. M., L. Persson, and E. McCauley. 2003. The influence of size-dependent life-history traits on the structure and dynamics of populations and communities. *ECOLOGY LETTERS* 6:473–487.

De Vriend, H. J. 1991. Mathematical modelling and large-scale coastal behaviour. *JOURNAL OF HYDRAULIC RESEARCH* 29:727–740.

De Vriend, H. J. 2001. Long-term morphological prediction. In *RIVER, COASTAL AND ESTUARINE MORPHODYNAMICS*, ed. Seminara, G and Blondeaux, P, 163–190. IAHR, HEIDELBERGER PLATZ 3, D-14197 BERLIN, GERMANY: SPRINGER-VERLAG BERLIN. Symposium on River, Coastal and Estuarine Morphodynamics, GENOA, ITALY, SEP 06-10, 1999.

De Vriend, H. J, T. Louters, F. Berben, and R. C. Steijn. 1989. Hybrid prediction of a sandy shoal evolution in a mesotidal estuary. In *HYDRAULIC AND ENVIRONMENTAL MODELLING OF COASTAL, ESTUARINE AND RIVER WATERS*, ed. R A Falconer, P. Goodwin, and R G S Matthew, volume 14, 145–156. International Conference Bradford, England.

De Vriend, H. J., Z. B. Wang, T. Ysebaert, P. M. J. Herman, and P. Ding. 2011. Eco-Morphological Problems in the Yangtze Estuary and the Western Scheldt. *WETLANDS* 31:1033–1042.

De Vriend, H. J., J. Zyserman, J. Nicholson, J. A. Roelvink, P. Péchon, and H. N. Southgate. 1993. Medium-term 2DH coastal area modelling. *COASTAL ENGINEERING* 21:193–224.

Degraer, S., V. Van Lancker, G. Moerkerke, M. Van Hoey, G.and Vincx, and J.P. Jacobs, P.and Henriet. 2002. INTENSIVE EVALUATION OF THE

EVOLUTION OF A PREDICTED BENTHIC HABITAT: HABITAT REPORT. Technical report, Federal Office for Scientific, Technical and Cultural Affairs (OSTC), Brussels, Belgium.

Degraer, S., E. Verfaillie, W. Willems, E. Adriaens, M. Vincx, and V. Van Lancker. 2008. Habitat suitability modelling as a mapping tool for macrobenthic communities: An example from the Belgian part of the North Sea. *CONTINENTAL SHELF RESEARCH* 28:369–379.

Degraer, S., J. Wittoeck, Appeltans J., K. Cooreman, T. Deprez, H. Hillewaert, Hostens K., J. Mees, E. Van den Berghe, and M. Vincx. 2006. *THE MACROBENTHOS ATLAS OF THE BELGIAN PART OF THE NORTH SEA*. Belgian Science Policy.

Desombre, J. 2013. TELEMAC 2D SOFTWARE – REFERENCE MANUAL. Technical report, Release 6.2, p. 104.

Dial, R., and J. Roughgarden. 1998. Theory of marine communities: The intermediate disturbance hypothesis. *ECOLOGY* 79:1412–1424.

Diaz, Sandra, Joseph Fargione, F. Stuart Chapin, III, and David Tilman. 2006. Biodiversity loss threatens human well-being. *PLOS BIOLOGY* 4:1300–1305.

Downes, Barbara J. 2010. Back to the future: little-used tools and principles of scientific inference can help disentangle effects of multiple stressors on freshwater ecosystems. *FRESHWATER BIOLOGY* 55:60–79.

Dronkers, J. 1986. Tidal asymmetry and estuarine morphology. *NETHERLANDS JOURNAL OF SEA RESEARCH* 20:117–131.

Ecoshape. 2014. BUILDING WITH NATURE. URL `http://www.ecoshape.nl/overview-bwn.html`.

Eelkema, Menno, Zheng B. Wang, and Marcel J. F. Stive. 2012. Impact of back-barrier dams on the development of the ebb-tidal delta of theEastern Scheldt. *JOURNAL OF COASTAL RESEARCH* 28:1591–1605.

Elith, J., and J. Leathwick. 2007. Predicting species distributions from museum and herbarium records using multiresponse models fitted with multivariate adaptive regression splines. *DIVERSITY AND DISTRIBUTION* 13:265–275.

Ellis, J., T. Ysebaert, T. Hume, A. Norkko, T. Bult, P. M. J. Herman, S. F. Thrush, and J. Oldman. 2006. Predicting macrofaunal species distributions in estuarine gradients using logistic regression and classification systems. *MARINE ECOLOGY PROGRESS SERIES* 316:69–83.

Ernest, S. K. M., B. J. Enquist, J. H. Brown, E. L. Charnov, J. F. Gillooly, V. Savage, E. P. White, F. A. Smith, E. A. Hadly, J. P. Haskell, S. K. Lyons, B. A. Maurer, K. J. Niklas, and B. Tiffney. 2003. Thermodynamic and metabolic effects on the scaling of production and population energy use. *ECOLOGY LETTERS* 6:990–995.

Fairbridge, R. W. 1980. *CHEMISTRY AND BIOCHEMISTRY OF ESTUARIES*, chapter The estuary; its definition and geodynamic cycle., 1–35. Wiley.

Fenchel, T., L. H. Kofoed, and A. Lappalainen. 1975. Particle size-selection of two deposit feeders: the amphipod *Corophium volutator* and the prosobranch *Hydrobia ulvae*. *MARINE BIOLOGY* 30:119–128.

Flach, E. C. 1996. The influence of the cockle, *Cerastoderma edule*, on the macrozoobenthic community of tidal flats in the Wadden Sea. *MARINE ECOLOGY-PUBBLICAZIONI DELLA STAZIONE ZOOLOGICA DI NAPOLI I* 17:87–98. 29th European Marine Biology Symposium, UNIV VIENNA, BIOCENTRE, VIENNA, AUSTRIA, AUG 29-SEP 02, 1994.

Folke, C., S. Carpenter, B. Walker, M. Scheffer, T. Elmqvist, L. Gunderson, and C. S. Holling. 2004. Regime shifts, resilience, and biodiversity in ecosystem management. *ANNUAL REVIEW OF ECOLOGY EVOLUTION AND SYSTEMATICS* 35:557–581.

Franklin, Janet. 2010. Moving beyond static species distribution models in support of conservation biogeography. *DIVERSITY AND DISTRIBUTIONS* 16:321–330.

Friedrichs, M., G. Graf, and B. Springer. 2000. Skimming flow induced over a simulated polychaete tube lawn at low population densities. *MARINE ECOLOGY PROGRESS SERIES* 192:219–228.

Friedrichs, M., T. Leipe, F. Peine, and G. Graf. 2009. Impact of macrozoobenthic structures on near-bed sediment fluxes. *JOURNAL OF MARINE SYSTEMS* 75:336–347.

Gallaway, J. M., Y. E. Martin, and E. A. Johnson. 2009. Sediment transport due to tree root throw: integrating tree population dynamics, wildfire and geomorphic response. *EARTH SURFACE PROCESSES AND LANDFORMS* 34:1255–1269.

Gaston, K. J., and T. Blackburn. 2000. PATTERN AND PROCESS IN MACROECOLOGY. Blackwell Science.

Gillis, L. G., T. J. Bouma, C. G. Jones, M. M van Katwijk, I. Nagelkerken, C. J. L. Jeuken, Herman P. M. J., and Ziegler A. D. 2014. Potential for landscape-scale positive interactions among tropical marine ecosystems. *MARINE ECOLOGY PROGRESS SERIES* 503:289–303.

Gray, J. S. 1974. Animal-sediment relationships. *OCEANOGRAPHY AND MARINE BIOLOGY ANNUAL REVIEW* 12:223–261.

Gray, J. S. 1997. Marine biodiversity: Patterns, threats and conservation needs. *BIODIVERSITY AND CONSERVATION* 6:153–175.

Gutiérrez, J. L., and C. G. Jones. 2006. Physical ecosystem engineers as agents of biogeochemical heterogeneity. *BIOSCIENCE* 56:227–236.

Gutiérrez, Jorge L., and Clive G. Jones. 2008. *ECOSYSTEM ENGINEERS*. J. Wiley and Sons, Chichester, UK.

Haas, Herman. 2008. EFFECTEN VAN EEN ZOUT VOLKERAK-ZOOMMER OP DE OOSTER-EN DE WESTERSCHELDE. Technical report, Rijkwaterstaat.

Halpern, Benjamin S., Shaun Walbridge, Kimberly A. Selkoe, Carrie V. Kappel, Fiorenza Micheli, Caterina D'Agrosa, John F. Bruno, Kenneth S. Casey, Colin Ebert, Helen E. Fox, Rod Fujita, Dennis Heinemann, Hunter S. Lenihan, Elizabeth M. P. Madin, Matthew T. Perry, Elizabeth R. Selig, Mark Spalding, Robert Steneck, and Reg Watson. 2008. A global map of human impact on marine ecosystems. *SCIENCE* 319:948–952.

Hastings, Alan, James E. Byers, Jeffrey A. Crooks, Kim Cuddington, Clive G. Jones, John G. Lambrinos, Theresa S. Talley, and William G. Wilson. 2007. Ecosystem engineering in space and time. *ECOLOGY LETTERS* 10:153–164.

He, Fangliang, and Kevin J. Gaston. 2007. Estimating abundance from occurrence: An underdetermined problem. *AMERICAN NATURALIST* 170:655–659.

Heip, C. H. R., G. Duineveld, E. Flach, G. Graf, W. Helder, P. M. J. Herman, M. Lavaleye, J. J. Middelburg, O. Pfannkuche, K. Soetaert, T. Soltwedel, H. de Stigter, L. Thomsen, J. Vanaverbeke, and P. de Wilde. 2001. The role of the benthic biota in sedimentary metabolism and sediment-water exchange processes in the Goban Spur area (NE Atlantic). *DEEP SEA RESEARCH PART I* 48:3223–3243.

Heip, C. H. R., N. K. Goosen, P. M. J. Herman, J. Kromkamp, J. J. Middelburg, and K. Soetaert. 1995. Production and consumption of biological particles in temperate tidal estuaries. *OCEANOGRAPHY AND MARINE BIOLOGY ANNUAL REVIEW* 33:1–149.

Herman, P. M. J., J. J. Middelburg, and C. H. R. Heip. 2001. Benthic community structure and sediment processes on an intertidal flat: results from the ECOFLAT project. *CONTINENTAL SHELF RESEARCH* 21:2055–2071.

Herman, P. M. J., J. J. Middelburg, J. van de Koppel, and C. H. R. Heip. 1999. Ecology of estuarine macrobenthos. *ADVANCES IN ECOLOGICAL RESEARCH* 29:195–240.

Hijmans, R. J., and J. van Etten. 2013. *raster: Geographic data analysis and modeling*. URL `http://CRAN.R-project.org/package=raster`, r package version 2.1-37.

Holtmann, S.E., A. Groenewold, K.H.M. Schrader, J. Asjes, J.A. Craeymeersch, G.C.A. Duineveld, A.J. van Bostelen, and J. van der Meer. 1996. *ATLAS OF THE ZOOBENTHOS OF THE DUTCH CONTINENTAL SHELF*. Ministry of Transport, Public Works and Water Management: Rijswijk.

Huettel, M., and G. Gust. 1992. Impact of bioroughness on iterfacial solute exchange in permeable sediments. *MARINE ECOLOGY PROGRESS SERIES* 89:253–267.

Hutchinson, G. E. 1957. Concluding remarks. In *COLD SPRING HARBOR SYMPOSIA ON QUANTITATIVE BIOLOGY*, volume 22, 415–427.

Jackson, J. B. C., M. X. Kirby, W. H. Berger, K. A. Bjorndal, L. W. Botsford, B. J. Bourque, R. H. Bradbury, R. Cooke, J. Erlandson, J. A. Estes, T. P. Hughes, S. Kidwell, C. B. Lange, H. S. Lenihan, J. M. Pandolfi, C. H. Peterson, R. S. Steneck, M. J. Tegner, and R. R. Warner. 2001. Historical overfishing and the recent collapse of coastal ecosystems. *SCIENCE* 293:629–638.

Jeuken, M. C. J. L., and Z. B. Wang. 2010. Impact of dredging and dumping on the stability of ebb-flood channel systems. *COASTAL ENGINEERING* 57:553–566.

Jones, C. G., J. H. Lawton, and M. Shachak. 1994. Organisms as ecosystem engineers. *OIKOS* 69:373–386.

Jones, C. G., J. H. Lawton, and M. Shachak. 1997. Positive and negative effects of organisms as physical ecosystem engineers. *ECOLOGY* 78:1946–1957.

Jongeling, T. H. G. 2007. ZANDHONGER OOSTERSCHELDE: MAATRELEGEN TER VERGROTING VAN DOORSTROOMCAPACITEIT EN ZANDDOORVOER STORMVLOEDKERING OOSTERSCHELDE. Technical report, Deltares.

Kamino, Luciana H. Y., Joao Renato Stehmann, Silvana Amaral, Paulo De Marco, Jr., Thiago F. Rangel, Marinez F. de Siqueira, Renato De Giovanni, and Joaquin Hortal. 2012. Challenges and perspectives for species distribution modelling in the neotropics. *Biology Letters* 8:324–326.

Kater, B. J., A. J. M. Geurts van Kessel, and J. J. M. D. Baars. 2006. Distribution of cockles *Cerastoderma edule* in the Eastern Scheldt: habitat mapping with abiotic variability. *MARINE ECOLOGY PROGRESS SERIES* 318:221–227.

Kefi, Sonia, Eric L. Berlow, Evie A. Wieters, Sergio A. Navarrete, Owen L. Petchey, Spencer A. Wood, Alice Boit, Lucas N. Joppa, Kevin D. Lafferty, Richard J. Williams, Neo D. Martinez, Bruce A. Menge, Carol A. Blanchette, Alison C. Iles, and Ulrich Brose. 2012. More than a meal ... integrating non-feeding interactions into food webs. *ECOLOGY LETTERS* 15:291–300.

Kennish, R., K. D. P. Wilson, J. Lo, S. C. Clarke, and S. Laister. 2002. Selecting sites for large-scale deployment of artificial reefs in Hong Kong: constraint mapping and prioritization techniques. *ICES JOURNAL OF MARINE SCIENCE* 59:S164–S170. 7th International Conference on Artificial Reefs and related Aquatic Habitats, SAN REMO, ITALY, OCT 07-11, 1999.

Kleiber, M. 1932. Body size and metabolism. *HILGARDIA* 6:315:353.

Koenker, R. 1994. Quantile smoothing splines. *BIOMETRIKA* 81:673–680.

Koenker, R., and G. Bassett. 1978. Regression quantiles. *ECONOMETRICA* 46:33–50.

Koenker, R., and K. F. Hallock. 2001. Quantile regression. *JOURNAL OF ECONOMIC PERSPECTIVES* 15:143–156. Annual Meeting of the Allied-Social-Science-Association, NEW ORLEANS, LOUISIANA, JAN, 2001.

Koenker, R., and J. A. F. Machado. 1999. Goodness of fit and related inference processes for quantile regression. *JOURNAL OF THE AMERICAN STATISTICAL ASSOCIATION* 94:1296–1310.

Koenker, Roger. 2013. *quantreg: Quantile regression*. URL `http://CRAN.R-project.org/package=quantreg`, r package version 4.98.

Kraufvelin, P., B. Sinisalo, E. Leppakoski, J. Mattila, and E. Bonsdorff. 2001. Changes in zoobenthic community structure after pollution abatement from fish farms in the Archipelago Sea (N. Baltic Sea). *MARINE ENVIRONMENTAL RESEARCH* 51:229–245.

Kristensen, Erik, Joao Magalhaes Neto, Morten Lundkvist, Lars Frederiksen, Miguel Angelo Pardal, Thomas Valdemarsen, and Mogens Rene Flindt. 2013. Influence of benthic macroinvertebrates on the erodability of estuarine cohesive sediments: Density- and biomass-specific responses. *ESTUARINE COASTAL AND SHELF SCIENCE* 134:80–87.

Lammens, Eddy, Francien van Luijn, Yolanda Wessels, Harry Bouwhuis, Ruurd Noordhuis, Rob Portielje, and Diederik van der Molen. 2008. Towards ecological goals for the heavily modified lakes in the IJsselmeer area, The Netherlands. *HYDROBIOLOGIA* 599:239–247.

Lavelle, P., T. Decaens, M. Aubert, S. Barot, M. Blouin, F. Bureau, P. Margerie, P. Mora, and J. P. Rossi. 2006. Soil invertebrates and ecosystem services. *EUROPEAN JOURNAL OF SOIL BIOLOGY* 42:S3–S15. 14th International Colloquium on Soil Zoology - Soil Animals and Ecosystems Services, Univ Rouen, Mt St Aignan, FRANCE, AUG 30-SEP 03, 2004.

Le Hir, P., Y. Monbet, and F. Orvain. 2007. Sediment erodability in sediment transport modelling: Can we account for biota effects? *CONTINENTAL SHELF RESEARCH* 27:1116–1142. 3rd Workshop on the Comparison of Laboratory and in situ Measuring Devices, and the Extrapolation of Flume and Erosion Device Data to the Field, Venice Int Univ, Venice, ITALY, AUG, 2004.

Le Hir, P., W. Roberts, O. Cazaillet, M. Christie, P. Bassoullet, and C. Bacher. 2000. Characterization of intertidal flat hydrodynamics. *CONTINENTAL SHELF RESEARCH* 20:1433–1459.

Lee, H, and R. C. Swartz. 1980. Biological processes affecting the distribution of pollutants in marine sediments. part II. biodeposition and bioturbation. In *CONTAMINANTS AND SEDIMENT*, ed. RA Baker. Environmental Protection Agency.

Leschine, T. M., B. E. Ferriss, K. P. Bell, K. K. Bartz, S. MacWilliams, M. Pico, and A. K. Bennett. 2003. Challenges and strategies for better use of scientific information in the management of coastal estuaries. *ESTUARIES* 26:1189–1204.

Lesser, G. R., J. A. Roelvink, J. A. T. M. van Kester, and G. S. Stelling. 2004. Development and validation of a three-dimensional morphological model. *COASTAL ENGINEERING* 51:883–915.

Levin, L. A., D. Talley, and G. Thayer. 1996. Succession of macrobenthos in a created salt marsh. *MARINE ECOLOGY PROGRESS SERIES* 141:67–82.

Louters, T., J. H. van den Berg, and J. P. M. Mulder. 1998. Geomorphological changes of the Oosterschelde tidal system during and after the implementation of the delta project. *JOURNAL OF COASTAL RESEARCH* 14:1134–1151.

Lurgi, Miguel, Bernat C. Lopez, and Jose M. Montoya. 2012. Novel communities from climate change. *PHILOSOPHICAL TRANSACTIONS OF THE ROYAL SOCIETY B-BIOLOGICAL SCIENCES* 367:2913–2922.

Madsen, N., and K. E. Hansen. 2001. Danish experiments with a grid system tested in the North Sea shrimp fishery. *FISHERIES RESEARCH* 52:203–216.

Marquet, P. A. 2002. Of predators, prey and power laws. *SCIENCE* 295:2229–2230.

Marquet, P. A., S. A. Navarrete, and J. C. Castilla. 1995. Body-size, population-density, and the energetic equivalence rule. *JOURNAL OF ANIMAL ECOLOGY* 64:325–332.

Matthews, John H., Bart A. J. Wickel, and Sarah Freeman. 2011. Converging currents in climate-relevant conservation: Water, Infrastructure, and Institutions. *PLOS BIOLOGY* 9.

Mayer, L. M. 1994. Surface-area control of organic carbon accumulation in continental shelf sediments. *GEOCHIMICA ET COSMOCHIMICA ACTA* 58:1271–1284.

McLusky, D. S. 1993. Marine and estuarine gradients-an overview. *NETHERLANDS JOURNAL OF AQUATIC ECOLOGY* 27:489–493.

McLusky, Michael, Donald S.; Elliott. 2004. *THE ESTUARINE ECOSYSTEM: ECOLOGY, THREATS AND MANAGEMENT*. Oxford University Press; Oxford.

McMichael, A. J., R. E. Woodruff, and S. Hales. 2006. Climate change and human health: present and future risks. *LANCET* 367:859–869.

Mehta, A., and E. Partheniades. 1982. Resuspension of deposited cohesive sediment beds. In *18th CONFERENCE ON COASTAL ENGINEERING*.

Meire, P., T. Ysebaert, S. Van Damme, E. Van den Bergh, T. Maris, and E. Struyf. 2005. The Scheldt estuary: A description of a changing ecosystem. *HYDROBIOLOGIA* 540:1–11.

Montserrat, F., W. Suykerbuyk, R. Al-Busaidi, T. J. Bouma, D. van der Wal, and P. M. J. Herman. 2011. Effects of mud sedimentation on lugworm ecosystem engineering. *JOURNAL OF SEA RESEARCH* 65:170–181.

Montserrat, F., C. Van Colen, S. Degraer, T. Ysebaert, and P. M. J. Herman. 2008. Benthic community-mediated sediment dynamics. *MARINE ECOLOGY PROGRESS SERIES* 372:43–59.

Moore, J. W. 2006. Animal ecosystem engineers in streams. *BIOSCIENCE* 56:237–246.

Mouillot, D. 2007. Niche-assembly vs. dispersal-assembly rules in coastal fish metacommunities: implications for management of biodiversity in brackish lagoons. *JOURNAL OF APPLIED ECOLOGY* 44:760–767.

Moulinec, C., C. Denis, C. T. Pham, D. Rouge, J. M. Hervouet, E. Razafindrakoto, R. W. Barber, D. R. Emerson, and X. J. Gu. 2011. TELEMAC: An efficient hydrodynamics suite for massively parallel architectures. *COMPUTERS & FLUIDS* 51:30–34.

Newell, R. 1998. Ecological changes in Chesapeake Bay; are they a result of over-harvesting the American oyster *Crassostrea virginica*? In *UNDERSTANDING THE ESTUARY: ADVANCES IN CHESAPEAKE BAY RESEARCH*. Chesapeake Research Consortium Publication Baltimore 29.

Nienhuis, P. H., and A. C. Smaal. 1994. The Oosterschelde estuary, a case-study of a changing ecosystem - An introduction. *HYDROBIOLOGIA* 283:1–14.

Nilsson, H. C., and R. Rosenberg. 2000. Succession in marine benthic habitats and fauna in response to oxygen deficiency: analysed by sediment profile-imaging and by grab samples. *MARINE ECOLOGY PROGRESS SERIES* 197:139–149.

Norkko, A., R. Rosenberg, S. F. Thrush, and R. B. Whitlach. 2006. Scale- and intensity-dependent disturbance determines the magnitude of opportunistic response. *JOURNAL OF EXPERIMENTAL MARINE BIOLOGY AND ECOLOGY* 330:195–207.

Orvain, Francis, Pierre Le Hir, Pierre-Guy Sauriau, and Sebastien Lefebvre. 2012. Modelling the effects of macrofauna on sediment transport and bed elevation: Application over a cross-shore mudflat profile and model validation. *ESTUARINE COASTAL AND SHELF SCIENCE* 108:64–75. ECSA 46 International Conference on Wadden Sea - Changes and Challenges in a World Heritage Site, Alfred Wegener Inst Polar & Marine Res (AWI), List, GERMANY, MAY 03-06, 2010.

Parmesan, Camille. 2006. Ecological and evolutionary responses to recent climate change. *ANNUAL REVIEW OF ECOLOGY EVOLUTION AND SYSTEMATICS* 37:637–669.

Pearce, Trevor. 2011. Ecosystem engineering, experiment, and evolution. *BIOLOGY & PHILOSOPHY* 26:793–812.

Pearson, R. G., and T. P. Dawson. 2003. Predicting the impacts of climate change on the distribution of species: are bioclimate envelope models useful? *GLOBAL ECOLOGY AND BIOGEOGRAPHY* 12:361–371.

Pearson, T. H., and R. Rosenberg. 1978. Macrobenthic succession in relation to organic enrichment and pollution of the marine environment. *OCEANOGRAPHY AND MARINE BIOLOGY ANNUAL REVIEW* 5:229–311.

Peters, J. J., R. H. Maed, W. R. Parker, and M.A. Stevens. 2001. Improving navigation conditions in the westerschelde and managing its estuarine environment. how to harmonize accessibility, safety and naturalness? In *FINAL REPORT TO PROSES*.

Plancke, Y., J.J. Peters, and S. Ides. 2006. A new approach for managing the western scheldt's morphology and ecology. In *31*st *PIANC CONGERSS, PORTUGAL*.

Plancke, Y., D. Vertommen, K. Beirinckx, and G. Vos. 2012. High resolution topo-bathymetric and flow measurements and 2D-hydrodynamic numerical modelling to evaluate the effects of the deepening of the navigation channel in the Western Scheldt. In *TAKING CARE OF THE SEA*, volume 13-15, 215–221. Dorst, LL.

R Development Core Team. 2011. *R: A language and environment for statistical computing*. R Foundation for Statistical Computing, Vienna, Austria. URL `http://www.R-project.org/`, ISBN 3-900051-07-0.

Rabaut, Marijn, Magda Vincx, and Steven Degraer. 2009. Do *Lanice conchilega* (sandmason) aggregations classify as reefs? Quantifying habitat modifying effects. *Helgoland Marine Research* 63:37–46.

Ray, G. L. 2000. Infaunal assemblages on constructed intertidal mudflats at Jonesport, Maine (USA). *MARINE POLLUTION BULLETIN* 40:2286–2300.

Raynaud, Xavier, Clive G. Jones, and Sebastien Barot. 2013. Ecosystem engineering, environmental decay and environmental states of landscapes. *OIKOS* 122:591–600.

Rhoads, D. C., and D. K. Young. 1970. The influence of deposit-feeding organisms on sediment stability and community trophic structure. *JOURNAL OF MARINE RESEARCH* 28:150–178.

Ricciardi, A., and E. Bourget. 1998. Weight-to-weight conversion factors for marine benthic macroinvertebrates. *MARINE ECOLOGY PROGRESS SERIES* 163:246–251.

Rietkerk, M., S.C. Dekker, P.C. de Ruiter, and J. van de Koppel. 2004. Self-organized patchiness and catastrophic shifts in ecosystems. *SCIENCE* 305:1926–1929.

Rinne, J. N., and D. Miller. 2006. Hydrology, geomorphology and management: Implications for sustainability of native southwestern fishes. *REVIEWS IN FISHERIES SCIENCE* 14:91–110. Conference on Aquatic Resources in Arid Lands, Las Cruces, NM, APR 30-MAY 02, 2003.

Roberts, R. D., M. R. Gregory, and B. A. Forster. 1998. Developing an efficient macrofauna monitoring index from an impact study – a dredge spoil example. *MARINE POLLUTION BULLETIN* 36:231–235.

Roni, P., T. J. Beechie, R. E. Bilby, F. E. Leonetti, M. M. Pollock, and G. R. Pess. 2002. A review of stream restoration techniques and a hierarchical strategy for prioritizing restoration in Pacific northwest watersheds. *NORTH AMERICAN JOURNAL OF FISHERIES MANAGEMENT* 22:1–20.

Roy, K., D. Jablonski, and J. W. Valentine. 2001. Climate change, species range limits and body size in marine bivalves. *ECOLOGY LETTERS* 4:366–370.

Sanders, D., C. G. Jones, E. Thébault, T. J. Bouma, T. van der Heide, J van Belzen, and S. Barot. 2014. Integrating ecosystem engineering and food webs. *OIKOS* 1.

Savage, V. M., J. F. Gillooly, J. H. Brown, G. B. West, and E. L. Charnov. 2004. Effects of body size and temperature on population growth. *AMERICAN NATURALIST* 163:429–441.

Scheffer, M., and S. R. Carpenter. 2003. Catastrophic regime shifts in ecosystems: linking theory to observation. *TRENDS IN ECOLOGY & EVOLUTION* 18:648–656.

Schmid, P. E., M. Tokeshi, and J. M. Schmid-Araya. 2002. Scaling in stream communities. *PROCEEDINGS OF THE ROYAL SOCIETY B-BIOLOGICAL SCIENCES* 269:2587–2594.

Schmidt, T. S., W. H. Clements, and B. S. Cade. 2012. Estimating risks to aquatic life using quantile regression. *Freshwater Science* 31:709–723.

Shephard, F. P. 1954. Nomenclature based on sand-silt-sand ratios. *JOURNAL OF SEDIMENTARY PETROLOGY* 24:151–158.

Short, F. T., and S. Wyllie-Echeverria. 1996. Natural and human-induced disturbance of seagrasses. *ENVIRONMENTAL CONSERVATION* 23:17–27.

Sinclair, Steve J., Matthew D. White, and Graeme R. Newell. 2010. How Useful Are Species Distribution Models for Managing Biodiversity under Future Climates? *ECOLOGY AND SOCIETY* 15.

Smaal, C., A. P. M. A. Vonck, and M. Bakker. 1997. Seasonal variation in physiological energetics of *Mytilus edulis* and *Cerastoderma edule* of different size classes. *JOURNAL OF THE MARINE BIOLOGICAL ASSOCIATION OF THE UNITED KINGDOM* 77:817–838.

Small, C., and R. J. Nicholls. 2003. A global analysis of human settlement in coastal zones. *JOURNAL OF COASTAL RESEARCH* 19:584–599.

Smith, C. R., S. Mincks, and D. J. DeMaster. 2006. A synthesis of bentho–pelagic coupling on the antarctic shelf: food banks, ecosystem inertia and global climate change. *DEEP SEA RESEARCH PART II* 53.

Smolders, S., F. Cozzoli, S. Ides, Y. Plancke, and P. Meire. 2013. A 2Dh hydrodynamic model of the Scheldt estuary in 1955 to assess the ecological past of the estuary. In *20th TELEMAC-MASCARET USERS CONFERENCE*.

Smolders, S., F. Cozzoli, Y. Plancke, T. Ysebaert, T. Ides, T.J. Bouma, P. Meire, P. M. J. Herman, and S. Temmerman. 2015. Modelling benthic habitat suitability to evaluate ecological benefits of a new sediment disposal strategy in shallow tidal waters. *In preparation this thesis* .

Smolders, S., S. Ides, Y. Plancke, P. Meire, and S. Temmerman. 2012. Calibrating discharges in a 2d hydrodynamic model of the scheldt estuary : which parameters can be used and what is their sensitivity? In *PROCEEDINGS OF THE 10th INTERNATIONAL CONFERENCE ON HYDROINFORMATIC*.

Snelgrove, P. V. R. 1998. The biodiversity of macrofaunal organisms in marine sediments. *BIODIVERSITY AND CONSERVATION* 7:1123–1132.

Snelgrove, P.V.R., and C.A. Butman. 1994. Animal-Sediment relationships revisited - Cause vs Effect. *OCEANOGRAPHY AND MARINE BIOLOGY* 32:111–177.

Snelgrove, P.V.R., J.F. Grassle, and R.F. Petrecca. 1994. Macrofaunal response to artifical enrichments and depressions in a deep sea habitat. *JOURNAL OF MARINE RESEARCH* 52:345–369.

Solan, M., B. J. Cardinale, A. L. Downing, K. A. M. Engelhardt, J. L. Ruesink, and D. S. Srivastava. 2004. Extinction and ecosystem function in the marine benthos. *SCIENCE* 306:1177–1180.

Sousa, Tania, Tiago Domingos, and S. A. L. M. Kooijman. 2008. From empirical patterns to theory: a formal metabolic theory of life. *PHILOSOPHICAL TRANSACTIONS OF THE ROYAL SOCIETY B-BIOLOGICAL SCIENCES* 363:2453–2464.

Stal, L. J. 2003. Microphytobenthos, their extracellular polymeric substances, and the morphogenesis of intertidal sediments. *GEOMICROBIOLOGY JOURNAL* 20:463–478.

Statzner, B., S. Doledec, and B. Hugueny. 2004. Biological trait composition of European stream invertebrate communities: assessing the effects of various trait filter types. *ECOGRAPHY* 27:470–488.

Stive, M.J.F., and Z.B. Wang. 2003. *MORPHODYNAMIC MODELLING OF TIDAL BASINS AND COASTAL INLETS*, 367–392. ADVANCES IN COASTAL MODELLING. Oxford, UK: Elsevier.

Sutherland, T. F., C. L. Amos, and J. Grant. 1998. The effect of buoyant biofilms on the erodibility of sublittoral sediments of a temperate microtidal estuary. *LIMNOLOGY AND OCEANOGRAPHY* 43:225–235.

Suykerbuyk, Wouter, Tjeerd J. Bouma, Tjisse van der Heide, Cornelia Faust, Laura L. Govers, Wim B. J. T. Giesen, Dick J. de Jong, and Marieke M. van Katwijk. 2012. Suppressing antagonistic bioengineering feedbacks doubles restoration success. *ECOLOGICAL APPLICATIONS* 22:1224–1231.

Swanson, R., C. O'Connell, and R. Wilson. 2012. Storm surge barriers: Ecological and special concerns. In *STORM SURGE BARRIERS TO PROTECT NEW YORK CITY*, ed. D Hill, , MJ Bowman, and JS Khinda, 122–133. American Society of Civil Engineers.

Syfert, Mindy M., Matthew J. Smith, and David A. Coomes. 2013. The effects of sampling bias and model complexity on the predictive performance of MaxEnt species distribution models. *PLOS ONE* 8.

Temmerman, S., P. Meire, T. J. Bouma, P. M. J. Herman, T. Ysebaert, and H. J. De Vriend. 2013. Ecosystem-based coastal defence in the face of global change. *NATURE* 504:79–83.

Terrell, J. W., B. S. Cade, J. Carpenter, and J. M. Thompson. 1996. Modeling stream fish habitat limitations from wedge-shaped patterns of variation in standing stock. *TRANSACTIONS OF THE AMERICAN FISHERIES SOCIETY* 125:104–117.

Thompson, P., Y. Cai, R. Moyeed, D. Reeve, and J. Stander. 2010. Bayesian nonparametric quantile regression using splines. *COMPUTATIONAL STATISCS & DATA ANALYSIS* 54:1138–1150.

Thomson, J. D., G. Weiblen, B. A. Thomson, S. Alfaro, and P. Legendre. 1996. Untangling multiple factors in spatial distributions: Lilies, gophers, and rocks. *ECOLOGY* 77:1698–1715.

Thrush, S. F., J. E. Hewitt, and V. Cummings. 2004. Muddy waters: elevating sediment input to coastal and estuarine habitats. *FRONTIERS IN ECOLOGY AND ENVIRONMENT* 2:299–306.

Thrush, S. F., J. E. Hewitt, P. M. J. Herman, and T. Ysebaert. 2005. Multiscale analysis of species-environment relationships. *MARINE ECOLOGY PROGRESS SERIES* 302:13–26.

Thrush, S. F., J. E. Hewitt, A. Norkko, P. E. Nicholls, G. A. Funnell, and J. I. Ellis. 2003. Habitat change in estuaries: predicting broad-scale responses of intertidal macrofauna to sediment mud content. *MARINE ECOLOGY PROGRESS SERIES* 263:101–112.

Tibshirani, R. 1996. Regression shrinkage and selection via the lasso. *JOURNAL OF THE AMERICAN STATISTICAL SOCIETY B* 58:267–288.

Ubertini, Martin, Sebastien Lefebvre, Aline Gangnery, Karine Grangere, Romain Le Gendre, and Francis Orvain. 2012. Spatial variability of benthic-pelagic coupling in an estuary ecosystem: Consequences for microphytobenthos resuspension phenomenon. *PLOS ONE* 7.

Underwood, A.J., and J Kromkamp. 1999. Primary production by phytoplankton and microphytobenthos in estuaries. In *ADVANCES IN ECOLOGICAL RESEARCH, VOL 29: ESTUARIES*, ed. Nedwell, DB and Raffaelli, DG, volume 29 of *Advances in Ecological Research*, 93–153. 525 B STREET, SUITE 1900, SAN DIEGO, CA 92101-4495 USA: ELSEVIER ACADEMIC PRESS INC.

van de Koppel, J., P. M. J. Herman, P. Thoolen, and C. H. R. Heip. 2001. Do alternate stable states occur in natural ecosystems? Evidence from a tidal flat. *ECOLOGY* 82:3449–3461.

van de Koppel, J., M. Rietkerk, N. Dankers, and P. M. J. Herman. 2005. Scale-dependent feedback and regular spatial patterns in young mussel beds. *AMERICAN NATURALIST* 165:E66–E77.

Van den Berg, J. H. 1982. Migration of large-scale bedforms and preservation of crossbedded sets in highly accretional parts of tidal channles in the Oosterschelde, SW Netherlands. *GEOLOGIE EN MIJNBOUW* 61:253–263.

van der Wal, D., R. M. Forster, F. Rossi, H. Hummel, T. Ysebaert, F. Roose, and P. M. J. Herman. 2011. Ecological evaluation of an experimental beneficial use scheme for dredged sediment disposal in shallow tidal waters. *MARINE POLLUTION BULLETIN* 62:99–108.

van Ledden, M., W. M. G. van Kesteren, and J. C. Winterwerp. 2004. A conceptual framework for the erosion behaviour of sand-mud mixtures. *CONTINENTAL SHELF RESEARCH* 24:1–11.

van Prooijen, B., and J. C. Winterwerp. 2010. A stochastic formulation for erosion of cohesive sediments. *JOURNAL OF GEOPHYSICAL RESEARCH - OCEANS* 115:C01005.

van Prooijen, Bram C., Francesc Montserrat, and Peter M. J. Herman. 2011. A process-based model for erosion of *Macoma balthica*-affected mud beds. *CONTINENTAL SHELF RESEARCH* 31:527–538.

van Slobbe, E., H. J. de Vriend, S. Aarninkhof, K. Lulofs, M. de Vries, and P. Dircke. 2013. Building with Nature: in search of resilient storm surge protection strategies. *NATURAL HAZARDS* 66:1461–1480.

VanDerWal, J., L. P. Shoo, C. M. Johnson, and S. E. Williams. 2009. Abundance and the environmental niche: Environmental suitability estimated from niche models predicts the upper limit of local abundance. *THE AMERICAN NATURALIST* 174:282–291.

Verneaux, V., J. Verneaux, A. Schmitt, and J.C. Lambert. 2004. Relationships of macrobenthos with dissolved oxygen and organic matter at the sediment–water interface in ten French lakes. *ARCHIV FUR HYDROBILOGIE* 160.

Volkenborn, N., S. I. C. Hedtkamp, J. E. E. van Beusekom, and K. Reise. 2007. Effects of bioturbation and bioirrigation by lugworms (Arenicola marina) on physical and chemical sediment properties and implications for intertidal habitat succession. *ESTUARINE COASTAL AND SHELF SCIENCE* 74:331–343.

Vos, G., Y. Plancke, S. Ides, T. De Mulder, and F. Mostaert. 2009. ALTERNATIEVE STORTSTRATEGIE WESTERSCHELDE. PROEFSORTING WALSOORDEN: EINDEVALUATIE PROEFSTORTING. Technical report, Flanders Hydraulics Research, Antwerp, Belgium.

van der Wal, D., P. M. J. Herman, R. M. Forster, T. Ysebaert, F. Rossi, E. Knaeps, Y. M. G. Plancke, and S. J. Ides. 2008. Distribution and dynamics of intertidal macrobenthos predicted from remote sensing: response to microphytobenthos and environment. *MARINE ECOLOGY PROGRESS SERIES* 367:57–72.

Wang, Z. B., M. C. J. L. Jeuken, H. Gerritsen, H. J. De Vriend, and B. A. Kornman. 2002. Morphology and asymmetry of the vertical tide in the western scheldt estuary. *CONTINENTAL SHELF RESEARCH* 22:2599–2609.

Wang, Z. B., and J. C. Winterwerp. 2001. Impact of dredging and dumping on the stability of the ebb–flood channel systems. In *PROCEEDINGS OF THE 2^{nd} IAHR SYMPOSIUM ON RIVER, COASTAL AND ESTUARINE MORPHODYNAMICS*. Ikeda S.

Warwick, R. M. 1986. A new method for detecting pollution effects on macrobenthic communities. *MARINE BIOLOGY* 92:557–562.

Wenger, Seth J., and Mary C. Freeman. 2008. Estimating spe occurrence, abundance and detection proability using zero-inflated distributions. *ECOLOGY* 89:2953–2959.

White, Ethan P., S. K. Morgan Ernest, Andrew J. Kerkhoff, and Brian J. Enquist. 2007. Relationships between body size and abundance in ecology. *TRENDS IN ECOLOGY & EVOLUTION* 22:323–330.

Widdows, J., and M. Brinsley. 2002. Impact of biotic and abiotic processes on sediment dynamics and the consequences to the structure and functioning of the intertidal zone. *JOURNAL OF SEA RESEARCH* 48:143–156.

Widdows, J., M.D. Brinsley, N.D. Pope, F.J. Staff, S.G. Bolam, and P.J. Somerfield. 2006. Changes in biota and sediment erodability following the placement of fine dredged material on upper intertidal shores of estuaries. *MARINE ECOLOGY PROGRESS SERIES* 319:27–41.

Widdows, J., M.D. Brinsley, P.N. Salkeld, and M. Elliott. 1998. Use of annular flumes to determine the influence of current velocity and bivalves on material flux at the sediment-water interface. *ESTUARIES* 21:552–559.

Willows, R. I., J. Widdows, and R. G. Wood. 1998. Influence of an infaunal bivalve on the erosion of an intertidal cohesive sediment: A flume and modeling study. *LIMNOLOGY AND OCEONAGRAPHY* 43:1332–1343.

Winterwerp, J. C., and W. van Kesteren. 2004. Introduction to the physiscs of cohesive sediment in the marine environment. In *DEVELOPMENTS IN SEDIMENTOLOGY*, volume 56. Amsterdam, Elsevier, 1 edition.

Wolff, W. J. 1973. THE ESTUARY AS A HABITAT. An analysis of data on the soft-bottom macrofauna of the estuarine area of the rivers Rhine, Meuse, and Scheldt. Doctoral Dissertation, Zoöl. Verh., Leiden 126: 1-242.

Wolff, W. J. 1983. *ECOSYSTEMS OF THE WORLD, ESTUARIES AND ENCLOSED SEAS*, volume 26, 337–374. Elsevier, Amsterdam.

Wood, R., and J. Widdows. 2002. A model of sediment transport over an intertidal transect, comparing the influences of biological and physical factors. *LIMNOLOGY AND OCEANOGRAPHY* 47:848–855.

Woodward, G., B. Ebenman, M. Emmerson, J. M. Montoya, J. M. Olesen, A. Valido, and P. H. Warren. 2005. Body size in ecological networks. *TRENDS IN ECOLOGY & EVOLUTION* 20:402–409.

Xiao, Xiao, Ethan P. White, Mevin B. Hooten, and Susan L. Durham. 2011. On the use of log-transformation vs. nonlinear regression for analyzing biological power laws. *ECOLOGY* 92:1887–1894.

Young, A. 2007. MESH maps come online. A framework to support seabed habitat mapping. *HYDRO INTERNATIONAL* 11:6–9.

Yozzo, D. J., P. Wilber, and R. J. Will. 2004. Beneficial use of dredged material for habitat creation, enhancement, and restoration in new york–new jersey harbor. *JOURNAL OF ENVIRONMENTAL MANAGEMANT* 73:39–52.

Ysebaert, T., P. M. J. Herman, P. Meire, J. Craeymeersch, H. Verbeek, and C. H. R. Heip. 2003. Large-scale spatial patterns in estuaries: estuarine macrobenthic communities in the Schelde estuary, NW Europe. *ESTUARINE COASTAL AND SHELF SCIENCE* 57:335–355.

Ysebaert, T., Fettweis M., P. Meire, and M. Sas. 2005. Benthic variability in intertidal soft-sediments in the mesohaline part of the Schelde estuary. *HYDROBIOLOGIA* 540:197–216.

Ysebaert, T., P. Meire, J. Coosen, and K. Essink. 1998. Zonation of intertidal macrobenthos on estuaries of Schelde and Ems. *ACQUATIC ECOLOGY* 32:53–71.

Ysebaert, T., P. Meire, P. M. J. Herman, and H. Verbeek. 2002. Macrobenthic species response surfaces along estuarine gradients: prediction by logistic regression. *MARINE ECOLOGY PROGRESS SERIES* 225:75–95.

Ysebaert, Tom, Brenda Walles, Christian Dorsch, Jasper Dijkstra, Karin Troost, Nicolette Volp, Bram van Prooijen, Mindert De Vries, P. M. J. Herman, and Anneke Hibma. 2012. Ecodynamic solutions for the protection of intertidal habitats: the use of oyster reefs. *JOURNAL OF SHELLFISH RESEARCH* 31:362.

Zebe, E., and D. Schiedek. 1996. The lugworm *Arenicola marina*: A model of physiological adaptation to life in intertidal sediments. *HELGOLANDER MEERESUNTERSUCHUNGEN* 50:37–68.

Zobel, Martin. 1997. The relative of species pools in determining plant species richness: an alternative explanation of species coexistence? *TRENDS IN ECOLOGY & EVOLUTION* 12:266 – 269.

Zuhlke, R. 2001. Polychaete tubes create ephemeral community patterns: *Lanice conchilega* (Pallas, 1766) associations studied over six years. *JOURNAL OF SEA RESEARCH* 46:261–272.

Zwarts, L., A.M. Blomert, P. Spaak, and B. De Vries. 1994. Feeding radius, burying depth and siphon size of *Macoma balthica* and *Scrobicularia plana*. *JOURNAL OF EXPERIMENTAL MARINE BIOLOGY AND ECOLOGY* 183:193–212.